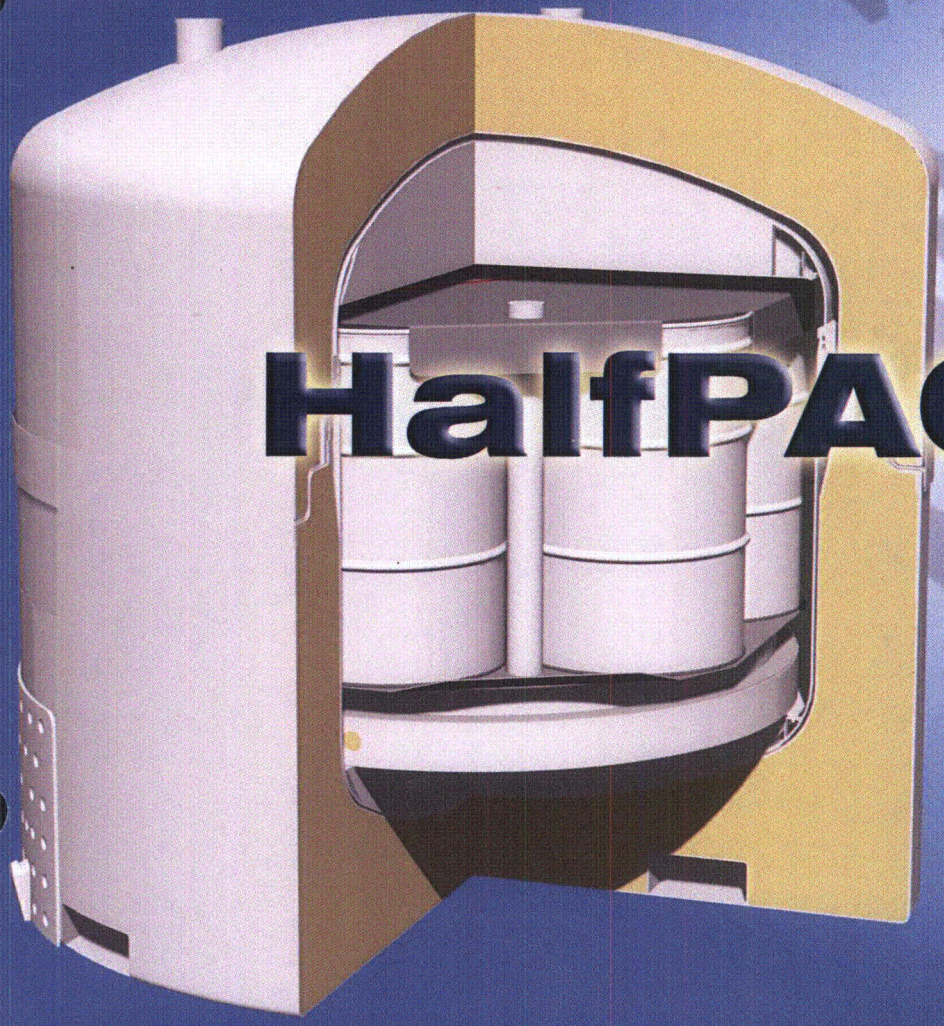

HalfPACT

Safety Analysis Report

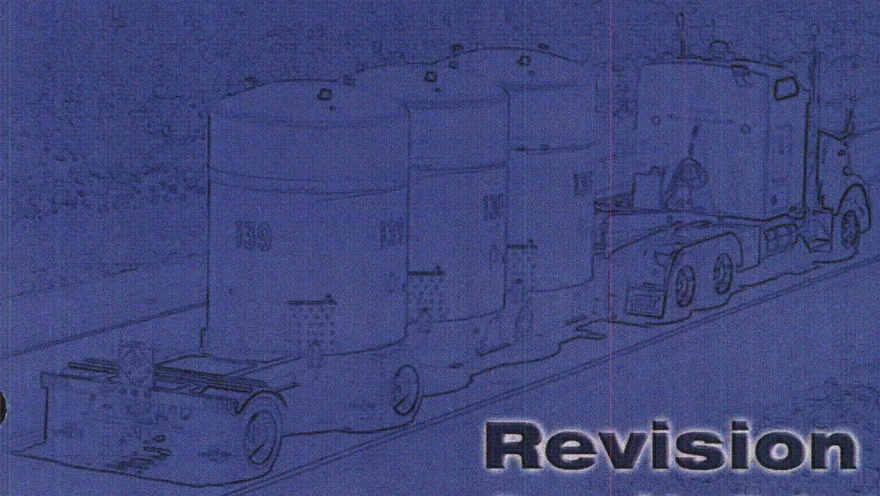

Revision 6
April 2012

TABLE OF CONTENTS

LIST OF TABLES

LIST OF FIGURES

1.0 GENERAL INFORMATION

This chapter of the Safety Analysis Report (SAR) presents a general introduction and description of the HalfPACT contact-handled transuranic waste (CH-TRU) package. The major components comprising the HalfPACT package are presented as Figure 1.1-1 and Figure 1.1-2. Figure 1.1-1 presents an exploded view of all major HalfPACT packaging components. Figure 1.1-2 presents a detailed view of the closure and seal region. Detailed drawings presenting the HalfPACT packaging design are presented in Appendix 1.3.1, *Packaging General Arrangement Drawings.* All details relating to payloads and payload preparation for shipment in a HalfPACT package are presented in the *Contact-Handled Transuranic Waste Authorized Methods for Payload Control* (CH-TRAMPAC)[1]. Descriptions of the standard, S100, S200, and S300 pipe overpack payload configurations are provided in Appendices 4.1, 4.2, 4.3, and 4.4, respectively, of the *CH-TRU Payload Appendices*[2]. A description of the shielded container payload configuration is provided in Appendix 4.5 of the *CH-TRU Payload Appendices.* A description of the criticality control overpack payload configuration is provided in Appendix 4.6 of the *CH-TRU Payload Appendices.* Terminology and acronyms used throughout this document are presented as Appendix 1.3.2, *Glossary of Terms and Acronyms.*

1.1 Introduction

The model HalfPACT package has been developed for the United States Department of Energy (DOE) as a safe means for transportation of CH-TRU materials and other authorized payloads. The packaging design is based very closely on the currently licensed TRUPACT-II package. The primary difference between the two packages is the body length. The TRUPACT-II packaging body length is shortened by 30 inches to create the HalfPACT packaging. Other minor differences are present, as described in subsequent sections.

The HalfPACT package is designed for truck transport. As many as three, loaded HalfPACT packages can be transported on a single semi-trailer. The rugged, lightweight design of the HalfPACT package allows the efficient transport of heavier-than-average payloads, thereby reducing the total number of radioactive shipments. The HalfPACT is also suitable for rail transport. As many as seven loaded HalfPACT packages can be transported per railcar.

The goals of maintaining public safety while achieving a lightweight design are satisfied by use of a deformable sealing region that can absorb both normal conditions of transport (NCT) and hypothetical accident condition (HAC) deformations without loss of leaktight capability[3]. This same design was extensively tested on the TRUPACT-II package, and the HalfPACT packaging program utilized the knowledge of the TRUPACT-II packaging program as background information. Nevertheless, both a full scale HalfPACT engineering test unit (ETU), and a certification test unit

---

[1] U.S. Department of Energy (DOE), *Contact-Handled Transuranic Waste Authorized Methods for Payload Control* (CH-TRAMPAC), U.S. Department of Energy, Carlsbad Field Office, Carlsbad, New Mexico.

[2] U.S. Department of Energy (DOE), *CH-TRU Payload Appendices*, U.S. Department of Energy, Carlsbad Field Office, Carlsbad, New Mexico.

[3] Leaktight is defined as 1×10^{-7} standard cubic centimeters per second (scc/s), or less, air leakage per the definition in ANSI N14.5-1997, *American National Standard for Radioactive Materials - Leakage Tests on Packages for Shipment,* American National Standards Institute, (ANSI), Inc.

(CTU) were subjected to a series of free drops and puncture drops, and a fully engulfing pool fire test. These tests conclusively demonstrated containment integrity of the HalfPACT package.

The payload within each HalfPACT package will be within 55-gallon drums, 85-gallon drums, 100-gallon drums, standard waste boxes (SWBs), or shielded containers (SCs). Hereafter, the term "85-gallon drum" is used to refer to 75- to 88-gallon drums that may, with the appropriate dimensions, overpack a single 55-gallon drum. Pipe overpacks and criticality control overpacks (CCO) utilize 55-gallon drums as overpacks. A single HalfPACT package can transport seven 55-gallon drums (with or without pipe components or criticality control containers), one SWB, four 85-gallon drums (with or without 55-gallon drums), three 100-gallon drums, or three SCs. Specifications for payload containers are provided in Section 2.0, *Container and Physical Properties Requirements*, of CH-TRAMPAC.

The HalfPACT packaging provides a single leakage rate testable level of containment for the payload during both normal conditions of transport (NCT) and hypothetical accident conditions (HAC). However, the HalfPACT package was originally designed, tested, and licensed prior to 2004 with two levels of containment. The 2004 NRC Rule change with regard to 10 CFR §71.63[4,5] eliminated the requirement for double containment in packages carrying in excess of 20 curies of plutonium in solid form. With only a single level of containment now required, the outer containment assembly (OCA) has been revised throughout this document to be the outer confinement assembly (still the OCA), and the outer containment vessel (OCV) has been revised throughout this document to be the outer confinement vessel (still the OCV). The use of O-ring seals (and corresponding pressure and leakage rate testing) is now optional for the OCV, and design and fabrication of the OCA (including the OCV) now falls under ASME Boiler and Pressure Vessel Code, Section III, Subsection NF[6]. For conservatism, structural calculations for the OCV presented in Chapter 2.0, *Structural Evaluation*, continue to use the requirements from ASME Boiler and Pressure Vessel Code, Section III, Subsection NB[7].

Based on the shielding and criticality assessments provided in Chapter 5.0, *Shielding Evaluation*, and Chapter 6.0, *Criticality Evaluation*, the Criticality Safety Index (CSI) for the HalfPACT package is zero (0.0), and the shielding Transport Index (TI) is determined at the time of shipment.

Authorization is sought for shipment of the HalfPACT package by truck or railcar as a Type B(U)F-96 package per the definition delineated in 10 CFR §71.4[4].

---

[4] Title 10, Code of Federal Regulations, Part 71 (10 CFR 71), *Packaging and Transportation of Radioactive Material*, 01-01-12 Edition.

[5] *Compatibility With IAEA Transportation Safety Standards (TS-R-1) and Other Transportation Safety Amendments, Federal Register*, 69 FR 3698, effective date October 1, 2004.

[6] American Society of Mechanical Engineers (ASME) Boiler and Pressure Vessel Code, Section III, *Rules for Construction of Nuclear Power Plant Components*, Subsection NF, *Supports*, 1995 Edition, 1997 Addenda.

[7] American Society of Mechanical Engineers (ASME) Boiler and Pressure Vessel Code, Section III, *Rules for Construction of Nuclear Power Plant Components*, Subsection NB, *Class 1 Components*, 1995 Edition, 1997 Addenda.

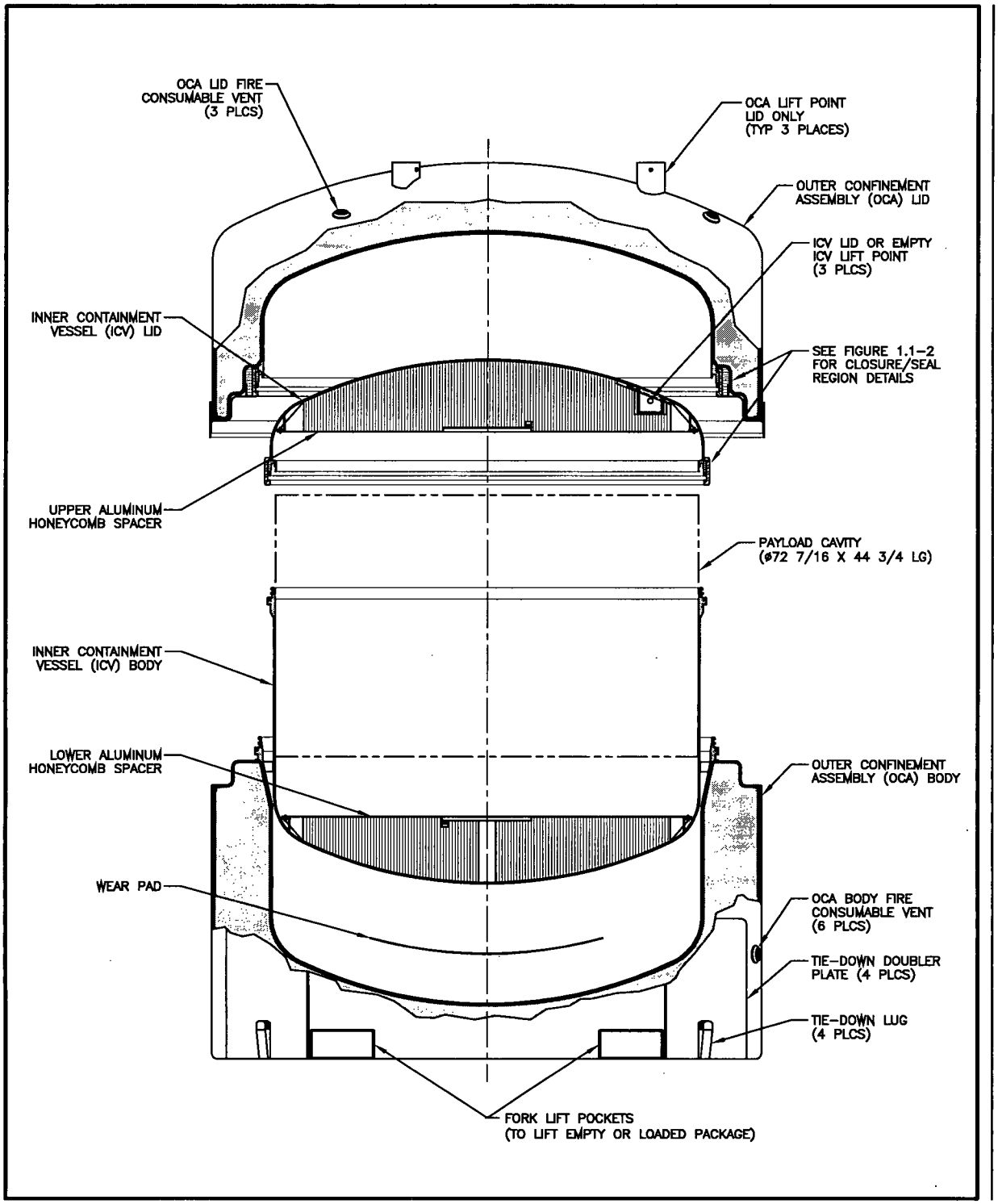

Figure 1.1-1 – HalfPACT Package Assembly

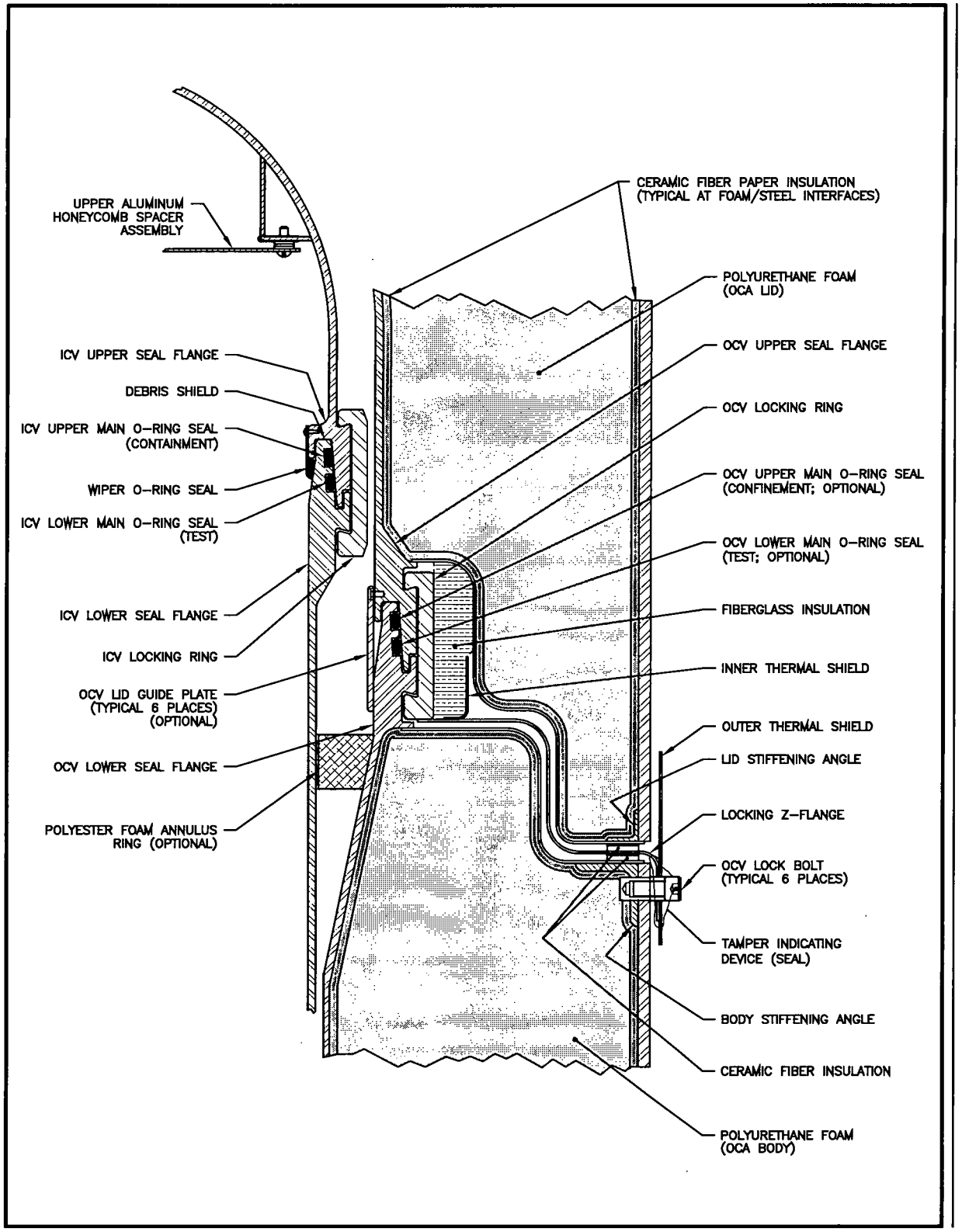

Figure 1.1-2 – HalfPACT Packaging Closure/Seal Region Details

1.2 Package Description

This section presents a basic description of the HalfPACT package. General arrangement drawings of the HalfPACT packaging are presented in Appendix 1.3.1, *Packaging General Arrangement Drawings*. Drawings illustrating payload assembly details are presented in the CH-TRAMPAC[1].

1.2.1 Packaging

1.2.1.1 Packaging Description

The HalfPACT packaging is comprised of an outer confinement assembly (OCA) that provides a secondary confinement boundary when its optional O-ring seals are utilized, and an inner containment vessel (ICV) that provides the primary containment boundary. Two aluminum honeycomb spacer assemblies are used within the ICV, one inside each ICV torispherical head. A silicone wear pad is utilized at the interface between the bottom exterior of the ICV and the bottom interior of the OCA. An optional polyester foam annulus ring may be used in the annulus between the ICV and OCV, just below the OCV lower seal flange to prevent debris from becoming entrapped between the vessels.

Inside the ICV, the payload will be within 55-gallon drums, 85-gallon drums, 100-gallon drums, standard waste boxes (SWBs), or shielded containers (SCs). The OCA, ICV, and the aluminum honeycomb spacer assemblies are fully described in the following subsections. The design details and overall arrangement of the HalfPACT packaging are presented in the Appendix 1.3.1, *Packaging General Arrangement Drawings*. Drawings illustrating payload assembly details are presented in the CH-TRAMPAC.

1.2.1.1.1 Outer Confinement Assembly (OCA)

The OCA consists of an OCA lid and OCA body, each primarily comprised of an inner stainless steel shell structure, a relatively thick layer of rigid polyurethane foam, and an external stainless steel shell structure. The inner OCA shell structure comprises the outer confinement vessel (OCV).

Not considering the seal flange region, the OCA lid has a nominal external diameter of 94⅜ inches and a nominal internal diameter of 76 13/16 inches. Likewise, not considering the seal flange region, the OCA body has a nominal external diameter of 94⅜ inches and a nominal internal diameter of 73⅝ inches, tapering outward to a nominal inside diameter of 76⅞ inches at the OCV lower seal flange. The nominal external diameter of the OCV seal region is 95 inches, and the nominal internal diameter of the OCV seal region is 76 7/16 inches. With the OCA lid installed onto the OCA body, the OCA has a nominal external length of 91½ inches, and a nominal internal height is 70 inches at the OCV cavity centerline.

The confinement boundary provided by the OCA consists of the inner stainless steel vessel formed by a mating lid and body, plus the uppermost of two optional main O-ring seals enclosed between an upper and lower seal flange. The main O-ring seals are polymer with a nominal

[1] U.S. Department of Energy (DOE), *Contact-Handled Transuranic Waste Authorized Methods for Payload Control* (CH-TRAMPAC), U.S. Department of Energy, Carlsbad Field Office, Carlsbad, New Mexico.

3/8±1/8-inch diameter cross-section. The purpose of the lower main O-ring seal is for establishing a vacuum on the exterior side of the upper main O-ring seal for optional helium and/or pressure rise leakage rate testing.

A vent port feature in the OCV body's lower seal flange is the only other confinement boundary penetration. A vent port coupling, a seal welded threaded fitting, and an OCV vent port plug with an optional O-ring seal defines the confinement boundary at the OCV vent port penetration. Access to the OCV vent port is gained through an external penetration in the OCA outer shell once an outer 1½ NPT plug and a foam or ceramic fiber material plug is removed. The connecting tube is fabricated of non-thermally conductive fiberglass.

Optional leakage rate testing of the OCV's optional upper main O-ring seal (confinement seal) is performed through an OCV seal test port that is located in the OCA lid. Similar in design to the OCV vent port, access to the OCV seal test port is gained through an external penetration in the OCA outer shell once an outer 1½ NPT plug and a foam or ceramic fiber material plug is removed. The connecting tube is fabricated of thin-walled stainless steel.

The cylindrical portion of the OCV body is 3/16-inch nominal thickness, Type 304, stainless steel. All other shells comprising the OCV are 1/4-inch nominal thickness, Type 304, stainless steel, including the lower and upper torispherical heads. The OCA outer shell varies between 1/4- and 3/8-inch nominal thickness, Type 304, stainless steel. The 3/8-inch nominal thickness material is used adjacent to the closure interface to ensure protection from HAC puncture bar penetration near the sealing regions. All other shells comprising the OCA exterior are 1/4-inch nominal thickness, Type 304, stainless steel, including the lower flat head and upper torispherical head. As illustrated in Figure 1.1-2, the inner and outer shell structures for both the OCA lid and OCA body are connected together via 14-gauge (0.075-inch thick), Type 304, stainless steel Z-flanges. Secure attachment of the 14-gauge Z-flanges to the 3/8-inch thick OCA outer shell is assured by the use of rolled angle reinforcements (2 × 2 × 1/4 inches for the OCA body junction, and 1 × 1 × 1/8 inches for the OCA lid junction). A locking Z-flange between the upper and lower (i.e., OCA lid and OCA body) Z-flanges allows rotation of the OCV locking ring from the HalfPACT package exterior. The Z-flanges serve the purpose of precluding direct flame impingement on the OCV seal flanges during the hypothetical accident condition (HAC) thermal event (fire). To further preclude flame and hot gas entry into the Z-flange channel, inner and outer thermal shields are included as part of the locking Z-flange assembly.

The OCA lid is secured to the OCA body via the OCV locking ring located at the outer diameter of the OCV upper and lower seal flanges. Closure design and operation for the ICV is illustrated in Figure 1.2-1 (the OCV is similar). The lower end of the OCV locking ring has 18 tabs that mate with a corresponding set of 18 tabs on the OCV lower seal flange. To install the OCA lid, the OCV locking ring is rotated to the "unlocked" position, using alignment marks on the OCA exterior for reference. The unlocked position aligns the tabs on the OCV locking ring with the cutouts between the tabs on the OCV lower seal flange. Next, install the OCA lid onto the OCA body, optionally evacuating the OCV cavity through the OCV vent port sufficiently to allow free movement of the OCV locking ring. Positive closure is attained by rotating the OCV locking ring to the "locked" position, again using the alignment marks on the OCA exterior for reference. In order to allow rotation of the OCV locking ring from the HalfPACT packaging exterior, a locking Z-flange extends radially outward to the OCA exterior. Six, 1/2-inch diameter, stainless steel socket head cap screws secure the locking Z-flange in the locked position. A single, localized cutout in the OCV locking ring is provided for access to the OCV seal test port feature.

Within the annular void between the OCV and the OCA outer shell structure is a relatively thick layer of thermally insulating and energy absorbing, rigid, polyurethane foam. Surrounding the periphery of the polyurethane foam cavity is a layer of 1/4-inch nominal thickness, ceramic fiber paper capable of resisting temperatures in excess of 2,000 °F. The combination of OCA exterior shell, fire resistant polyurethane foam, and insulating ceramic fiber paper is sufficient to protect the confinement boundary from the consequences of all regulatory defined tests.

Two fork lift pockets are incorporated into the base of the OCA body. These pockets provide the handling interface for lifting a HalfPACT package. Three sets of lifting straps are included in the OCA lid assembly for lifting of the OCA lid only, and are so appropriately identified. Four tie-down lugs with reinforcing doubler plates are also provided at the base of the OCA body.

Polymer materials used in the OCA include butyl, and ethylene propylene or neoprene, as applicable, for the main O-ring seals, silicone for the wear pad, and polyester foam for the optional annulus foam ring. Plastic is used for the polyurethane foam cavity, fire-consumable vent plugs, and optional guide plates. The OCA lid lift pockets, vent port access tube, and a portion of the seal test port access tube are made from fiberglass. Brass is used for the OCV vent and seal test port plugs. High alloy stainless steel is used for the OCV locking ring joint pins. Insulating materials such as ceramic fiber paper along the periphery of the polyurethane foam cavity, and fiberglass-type insulation for the inner thermal shield are also used. Finally, a variety of stainless steel fasteners, greases and lubricants, and adhesives are also utilized, as specified in Appendix 1.3.1, *Packaging General Arrangement Drawings.*

1.2.1.1.2 Inner Containment Vessel (ICV) Assembly

The inner containment vessel (ICV) assembly consists of an ICV lid and ICV body, each primarily comprised of a stainless steel shell structure. Not considering the seal flange region, the ICV lid has a nominal external diameter of 74⅜ inches and a nominal internal diameter of 73⅞ inches. Likewise, not considering the seal flange region, the ICV body has a nominal external diameter of 73⅛ inches and a nominal internal diameter of 72⅝ inches. The nominal external diameter of the ICV seal region is 76⅝ inches, and the nominal internal diameter of the ICV seal region is 72⅞ inches. With the ICV lid installed onto the ICV body, the ICV has a nominal external length of 69 inches, and a nominal internal height is 68½ inches at the ICV cavity centerline.

The containment boundary provided by the ICV consists of a stainless steel vessel formed by a mating lid and body, plus the uppermost of two main O-ring seals enclosed between an upper and lower seal flange. The upper main O-ring seal (containment) is butyl rubber with a nominal 0.400-inch diameter cross-section. The lower main O-ring seal (test) may be neoprene or ethylene propylene with a nominal 0.375-inch diameter cross-section. The purpose of the lower main O-ring seal is for establishing a vacuum on the exterior side of the upper main O-ring seal for helium and pressure rise leakage rate testing. To protect the main O-ring seals from debris that may be associated with some payloads, a wiper O-ring seal is used between the ICV upper and lower seal flanges. In addition to the wiper O-ring seal, a silicone debris shield, located at the top of the ICV lower seal flange, provides a secondary debris barrier to the upper main O-ring seal. To ensure that helium tracer gas reaches the region directly above the upper main O-ring seal (containment) during helium leakage rate testing, a helium fill port is integral to the ICV vent port configuration (see Appendix 1.3.1, *Packaging General Arrangement Drawings*). In addition, to allow for pressure equalization across the silicone debris shield during ICV lid

installation and removal, three, 1/8-inch nominal diameter holes are located in the top of the ICV lower seal flange.

A vent port feature in the ICV body's lower seal flange is the only other containment boundary penetration. A vent port insert and an outer ICV vent port plug with an O-ring seal define the containment boundary at the ICV vent port penetration.

Leakage rate testing of the ICV's upper main O-ring seal (containment seal) is performed through an ICV seal test port that is located in the ICV lid.

All shells comprising the ICV are 1/4-inch nominal thickness, Type 304, stainless steel, including the lower and upper torispherical heads.

The ICV lid is secured to the ICV body via the ICV locking ring located at the outer diameter of the ICV upper and lower seal flanges. Closure design and operation is illustrated in Figure 1.2-1. The lower end of the ICV locking ring has 18 tabs that mate with a corresponding set of 18 tabs on the ICV lower seal flange. To install the ICV lid, the ICV locking ring is rotated to the "unlocked" position, using alignment marks for reference. The unlocked position will align the tabs on the ICV locking ring with the cutouts between the tabs on the ICV lower seal flange. Next, the ICV lid is installed onto the ICV body, optionally evacuating the ICV cavity through the ICV vent port sufficiently to allow free movement of the ICV locking ring. Positive closure is attained by rotating the ICV locking ring to the "locked" position, using the alignment marks for reference. Three, 1/2-inch diameter, stainless steel socket head cap screws secure the ICV locking ring in the locked position.

Three lift sockets, each containing a lift pin, are integrated into the ICV lid for lifting the ICV lid or an empty ICV assembly. Any lifting of the loaded ICV is performed using the OCA forklift pockets with the ICV located within the OCA.

Polymer materials used in the ICV include butyl, ethylene propylene, neoprene, buna-N, flourosilicone or flourocarbon, as applicable, for the main and wiper O-ring seals, and silicone for the debris shield. Brass is used for the ICV vent and seal test port plugs. High alloy stainless steel is used for the ICV locking ring joint pins. Finally, a variety of stainless steel fasteners, and greases and lubricants are also utilized, as specified in Appendix 1.3.1, *Packaging General Arrangement Drawings*.

1.2.1.1.3 Aluminum Honeycomb Spacer Assemblies

Aluminum honeycomb spacer assemblies are designed to fit within the torispherical heads at each end of the ICV cavity. Each aluminum honeycomb spacer assembly includes an optional, 18-inch nominal diameter by 1½-inch nominal depth pocket that may be used in the future to accommodate a catalyst assembly. The lower spacer assembly also includes a 3-inch nominal diameter hole at the center that serves as an inspection port to check for water accumulation in the ICV lower head. With the spacer assemblies in place, the nominal ICV cavity height becomes 44¾ inches.

1.2.1.2 Gross Weight

The gross shipping weight of a HalfPACT package is 18,100 pounds maximum. A summary of overall component weights is delineated in Table 2.2-1 of Section 2.2, *Weights and Centers of Gravity*.

1.2.1.3 Neutron Moderation and Absorption

The HalfPACT package does not require specific design features to provide neutron moderation and absorption for criticality control. Fissile materials in the payload are limited to amounts that ensure safely subcritical packages for both NCT and HAC. The fissile material limits for a single HalfPACT package are based on optimally moderated and reflected fissile material. The structural materials in the HalfPACT packaging are sufficient to maintain reactivity between the fissile material in an infinite array of damaged HalfPACT packages at an acceptable level. Further discussion of neutron moderation and absorption is provided in Chapter 6.0, *Criticality Evaluation*.

1.2.1.4 Receptacles, Valves, Testing, and Sampling Ports

There are no receptacles or valves used on the HalfPACT packaging, however, the OCV and ICV each have a seal test port and a vent port (see Appendix 1.3.1, *Packaging General Arrangement Drawings*). For each containment/confinement vessel, a seal test port provides access to the region between the upper and lower (containment/confinement and test) main O-ring seals between the upper and lower (lid and body) seal flanges. The seal test ports are used to leakage rate test the upper main ICV seal and, if used, the optional upper main OCV seal to verify proper assembly of the HalfPACT package prior to shipment.

The vent port is used during loading and unloading to facilitate lid installation and removal, and to allow blowdown of internal vacuum or pressure prior to opening a loaded package. As an option, a low vacuum may be applied to the vent port to fully seat the lid and assure free rotation of the locking ring.

Two separate penetrations through the polyurethane foam within the OCA are provided to access the seal test port and vent port plugs. The access ports are capped at the OCA exterior surface with 1½-inch pipe plugs (NPT) within 3-inch diameter couplings. Reinforcing doubler plates are also included on the inner surface of the OCA exterior shell, adjacent to the couplings. In addition, removable foam or ceramic fiber plugs fill the region within the access hole tubes to provide a level of thermal protection from the HAC thermal event. The vent port access tube is comprised of a non-metallic fiberglass, and a fiberglass link is included with the stainless steel, seal test port access tube as a lining to reduce radial thermal conductivity. When the OCA lid is removed, the ICV vent and seal test port plugs are readily accessible.

The OCV seal test port and both the ICV seal test and vent port plugs are accessed through localized cutouts in the corresponding vessel locking rings. An elongated cutout in the ICV locking ring is utilized at the ICV vent port location to allow locking ring rotation while an optional vacuum pump is installed. Smaller cutouts are provided in the ICV and OCV locking rings at the seal test port locations since these ports are only used with the locking rings in the locked position. The OCV vent port feature is located in the OCA body, therefore a cutout in the OCV locking ring is not necessary.

Detailed drawings of the test and vent port features and the associated local cutouts in the locking rings are provided in Appendix 1.3.1, *Packaging General Arrangement Drawings*.

1.2.1.5 Heat Dissipation

The HalfPACT package design capacity is 30 thermal watts maximum. The HalfPACT package dissipates this relatively low internal heat load entirely by passive heat transfer for both NCT and

HAC. No special devices or features are needed or utilized to enhance the dissipation of heat. Features are included in the design to enhance thermal performance in the HAC thermal event. These include the use of a high temperature insulating material (ceramic fiber paper) at polyurethane foam-to-steel interfaces and the presence of an inner and outer thermal shield at the OCA lid-to-body interface. A more detailed discussion of the package thermal characteristics is provided in Chapter 3.0, *Thermal Evaluation.*

1.2.1.6 Coolants

Due to the passive design of the HalfPACT package with regard to heat transfer, there are no coolants utilized within the HalfPACT package.

1.2.1.7 Protrusions

The only significant protrusions on the HalfPACT package exterior are those associated with the lifting and tie-down features on the OCA exterior. The only significant external protrusions from the OCA lid are lift straps and corresponding guide pockets that extend from three equally spaced locations at the lid top. These lift features protrude above the OCA upper torispherical head, but are radially located such that they remain below torispherical head's crown and do not affect overall package height. The guide pockets are made of a fiberglass material that is designed to break away for lid-end impacts. The only significant external protrusions from the OCA body are the tie-down features at the bottom end of the package. Four tie-down lugs, with associated doubler plates, are used at locations corresponding with the main beams of the trailer. These tie-down protrusions extend a maximum of 2⅛ inches radially from the OCA body exterior shell.

The only significant protrusion on the ICV exterior is the ICV locking ring. The ICV locking ring extends radially outward approximately one inch from the outside surface of the upper ICV torispherical head. With its 3⅞-inch axial length directly backed and supported by the OCV (the nominal radial gap is 1/4 inch), this external protrusion is of little consequence for the package. The only significant protrusions on the ICV interior are the three lift pockets that penetrate the upper ICV torispherical head. These lift pockets are equally spaced on a 56-inch diameter, extending into the ICV cavity a maximum of 4½ inches from the inner surface of the upper ICV torispherical head. The ICV lift pockets are of little consequence as they are protected by the surrounding aluminum honeycomb spacer assembly. There are no significant internal or external protrusions associated with the ICV body.

1.2.1.8 Lifting and Tie-down Devices

Three sets of lift pins, lift straps and associated doubler plates used in the OCA lid are designed to handle the OCA lid only (including overcoming any resistance to lid removal associated with the presence of the main O-ring seals). The OCA lid lifting devices are not designed to lift a loaded package or empty OCA. Under excessive load, failure occurs in the region of the OCA lift pin locations (at the pin-to-strap welds), away from the OCA torispherical head. A loaded HalfPACT package or any portion thereof can be lifted via the pair of fork lift pockets that are located at the base of the OCA body. These pockets are sized to accommodate forks up to 10 inches wide and up to 4 inches thick. An overhead crane can also be used to lift the loaded package, utilizing lifting straps, through the fork lift pockets.

Lifting of the ICV is via the three lift pockets inset into the upper ICV torispherical head. These lift pockets, with their associated lift pins and adjacent doubler plates, are sized to lift an empty

ICV or handle the ICV lid (including overcoming any resistance to lid removal associated with the presence of the main O-ring seals). A loaded ICV must be fully supported with the OCA body and lifted via the OCA fork lift pockets. Under excessive load, the ICV lift pins are designed to fail in shear prior to compromising the ICV containment boundary.

Both the OCA and ICV lifting points are appropriately labeled to limit their use to the intended manner.

Four tie-down lugs, with associated doubler plates, are used at locations corresponding with the main beams of the trailer. At each tie-down location, one doubler is used on the outside surface of the OCA side wall and one on the inside surface of the OCA lower flanged head. At each tie-down lug location, an internal gusset plate is also used between the inside of the OCA exterior shell and the doubler in the lower head to stiffen the tie-down regions. The doubler plates are sized to adequately distribute the regulatory-defined tie-down loads (10 *g*s longitudinal, 5 *g*s lateral, and 2 *g*s vertical, applied simultaneously) outwardly into the 1/4-inch thick OCA exterior shell. Each tie-down lug is welded directly to the adjacent side doubler plate. In an excessive load condition, these tie-down lug welds are sized to shear from the corresponding doubler plate.

A detailed discussion of lifting and tie-down designs, with corresponding structural analyses, is provided in Section 2.5, *Lifting and Tie-down Standards for All Packages.*

1.2.1.9 Pressure Relief System

There are no pressure relief systems included in the HalfPACT package design to relieve pressure from within the ICV or OCV. Fire-consumable vents in the form of plastic pipe plugs are employed on the exterior surface of the OCA. These vents are included to release any gases generated by charring polyurethane foam in the HAC thermal event (fire). During the HAC fire, the plastic pipe plugs melt allowing the release of gasses generated by the foam as it flashes to a char. Three vents are used on the OCA lid and six on the OCA body, located at the center of foam mass in each component. For optimum performance, the vents are located uniformly around the circumference of the OCA lid and body.

1.2.1.10 Shielding

Due to the nature of the contact-handled transuranic (CH-TRU) payload, no biological shielding is necessary or provided by the HalfPACT packaging.

1.2.2 Operational Features

The HalfPACT package is not considered to be operationally complex. All operational features are readily apparent from an inspection of the drawings provided in Appendix 1.3.1, *Packaging General Arrangement Drawings*, and the previous discussions presented in Section 1.2.1, *Packaging*. Operational procedures and instructions for loading, unloading, and preparing an empty HalfPACT package for transport are provided in Chapter 7.0, *Operating Procedures*.

1.2.3 Contents of Packaging

The HalfPACT packaging is designed to transport contact-handled transuranic (CH-TRU) and other authorized payloads such as tritium-contaminated materials that do not exceed 10^5 A_2 quantities. The *Contact-Handled Transuranic Waste Authorized Methods for Payload Control* (CH-TRAMPAC)[1] is the governing document for shipments of solid or solidified CH-TRU and tritium-contaminated

wastes in the HalfPACT package. All users of the HalfPACT package shall comply with all payload requirements outlined in the CH-TRAMPAC, using one or more of the methods described in that document.

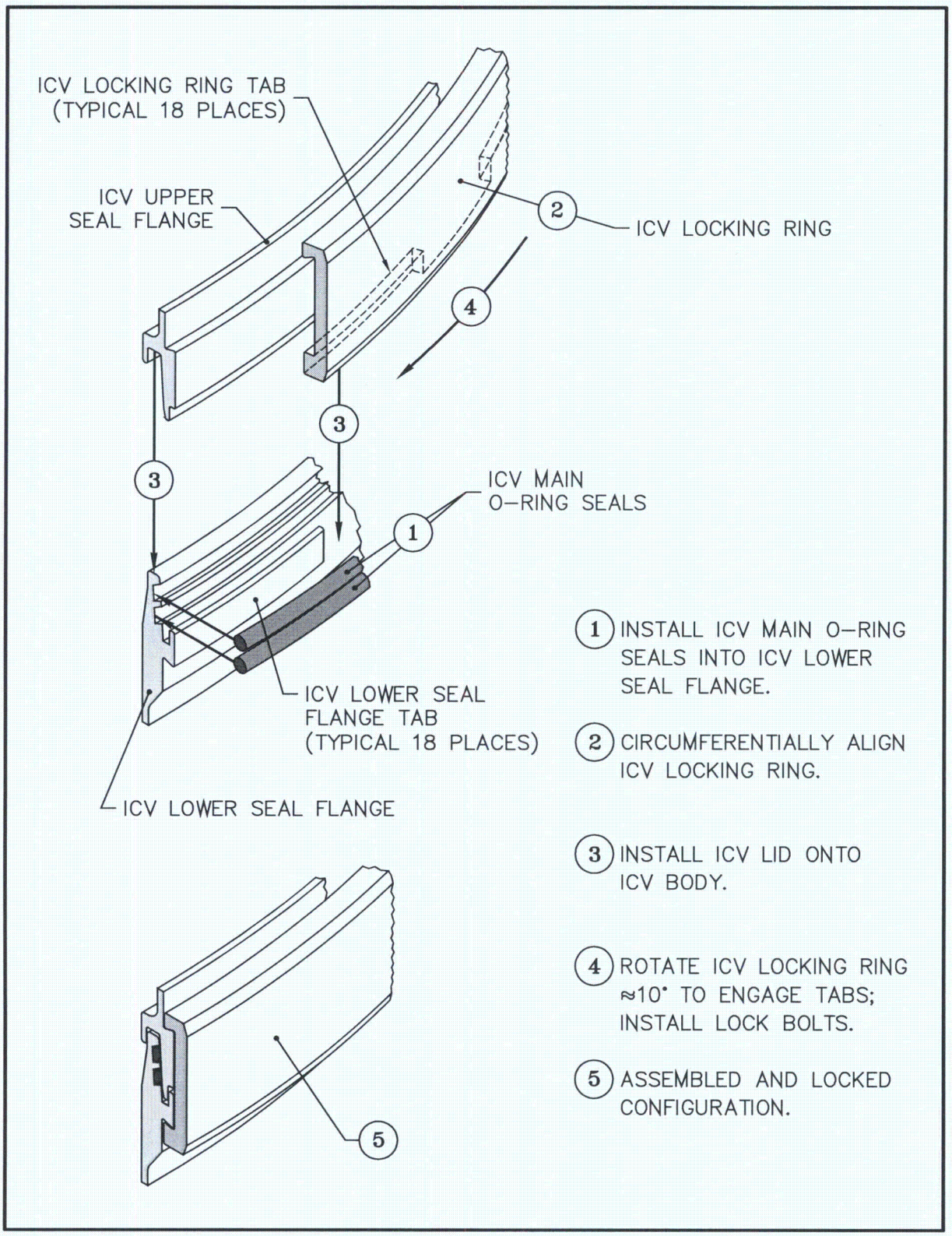

Figure 1.2-1 – ICV Closure Design (OCV closure is similar)

This page intentionally left blank.

1.3 Appendices

1.3.1 *Packaging General Arrangement Drawings*

1.3.2 *Glossary of Terms and Acronyms*

This page intentionally left blank.

1.3.1 Packaging General Arrangement Drawings

This section presents the HalfPACT packaging general arrangement drawing[1], consisting of 12 sheets entitled, *HalfPACT Packaging SAR Drawing, Drawing Number 707-SAR.* In addition, the standard pipe overpack general arrangement drawing, consisting of 3 sheets entitled, *Standard Pipe Overpack, Drawing Number 163-001*, is presented in this section. The S100 pipe overpack, the S200 pipe overpack, and the S300 pipe overpack are depicted in *Drawing Numbers 163-002, 163-003*, and *163-004*, respectively. The 55-gallon, 85-gallon, and 100-gallon compacted puck drum spacers are depicted in *Drawing Number 163-006.* The shielded containers and associated dunnage assemblies are depicted in *Drawing Number 163-008.* The criticality control overpack is depicted in *Drawing Number 163-009.*

Within the packaging general arrangement drawing, dimensions important to the packaging's safety are dimensioned and toleranced (e.g., structural shell thicknesses, polyurethane foam thicknesses, and the sealing regions on the seal flanges). All other dimensions are provided as a reference dimension, and are toleranced in accordance with the general tolerance block.

[1] The HalfPACT packaging, pipe overpack, compacted puck drum spacer, and shielded container general arrangement drawings utilize the uniform standard practices of ASME Y14.5M, *Dimensioning and Tolerancing*, American National Standards Institute, Inc. (ANSI).

This page intentionally left blank.

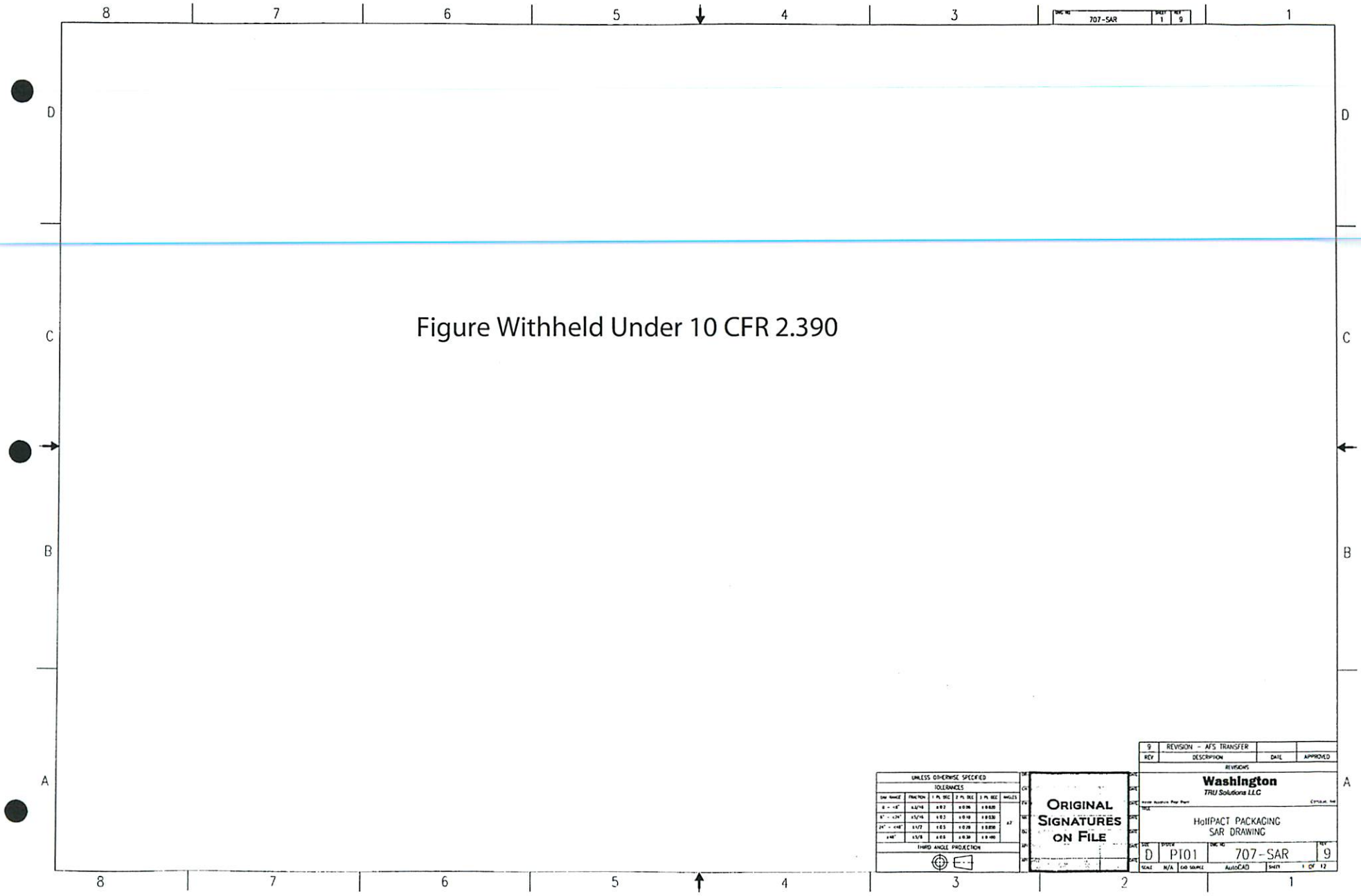
Figure Withheld Under 10 CFR 2.390
ORIGINAL SIGNATURES ON FILE
Washington
TRU Solutions LLC
HoltPACT PACKAGING
SAR DRAWING
707-SAR
REVISION - AFS TRANSFER

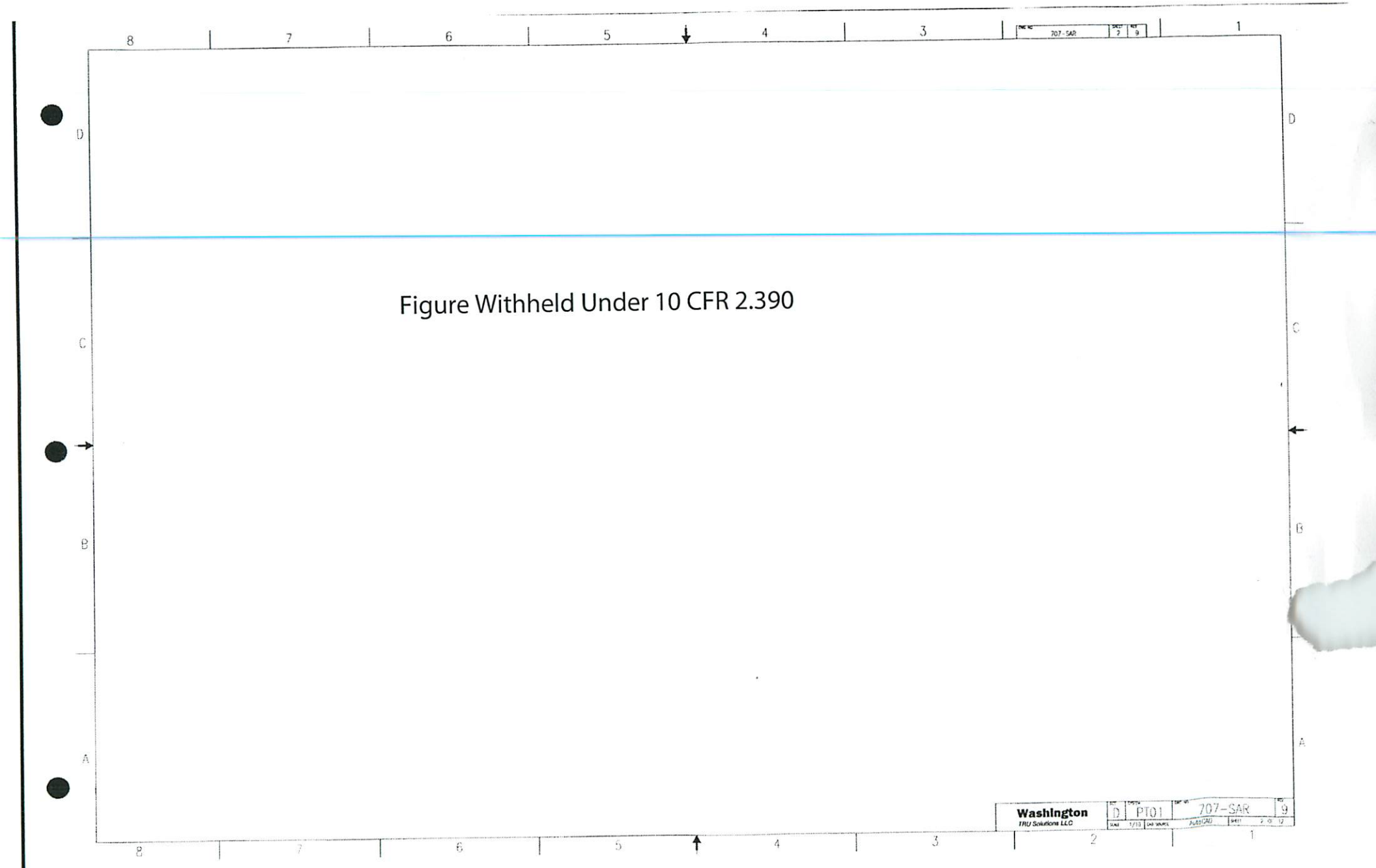
Figure Withheld Under 10 CFR 2.390
707 - SAR
Washington
TRU Solutions LLC
D
PT01
707-SAR
9
AutoCAD

Figure Withheld Under 10 CFR 2.390

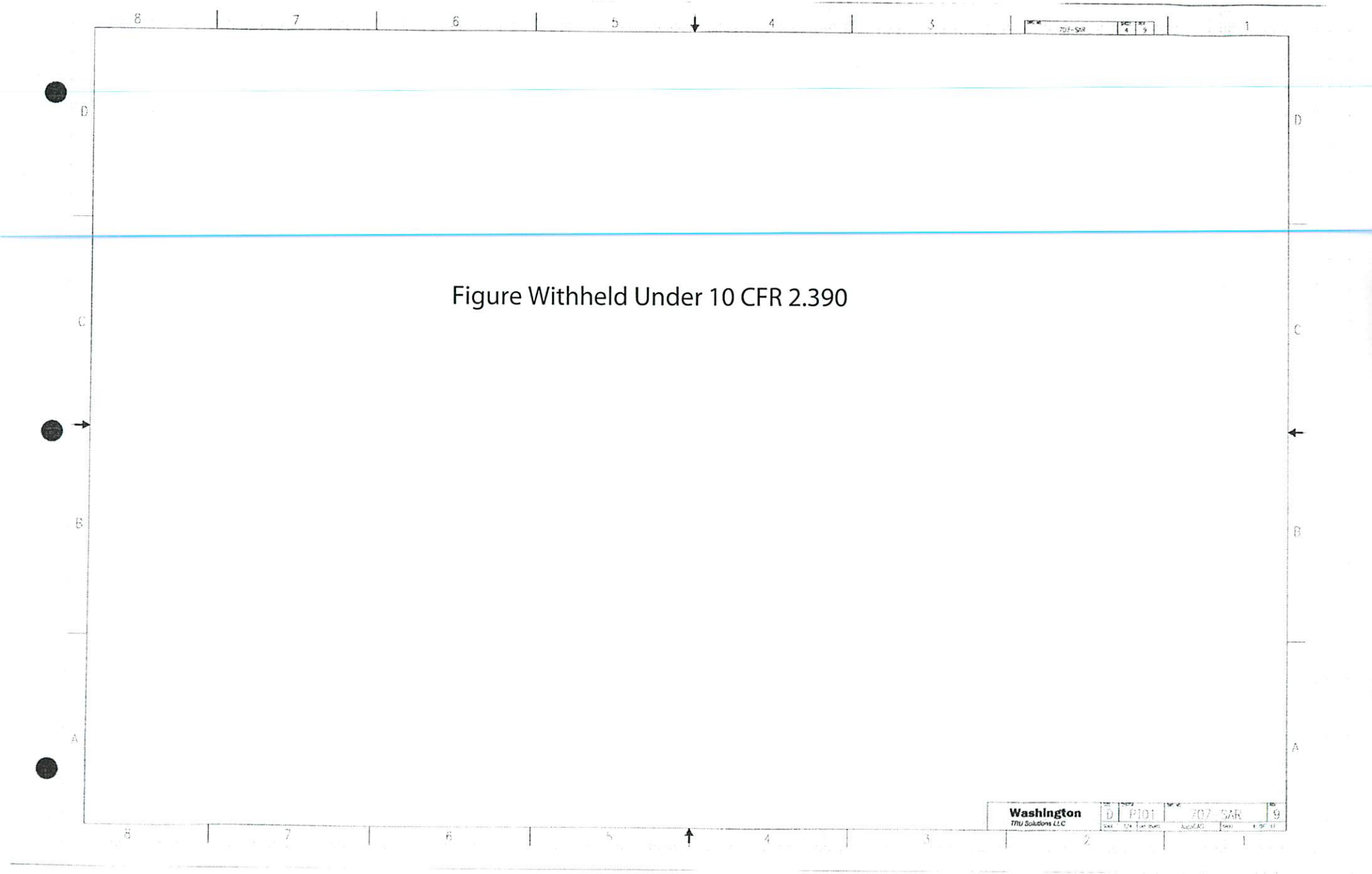
Figure Withheld Under 10 CFR 2.390

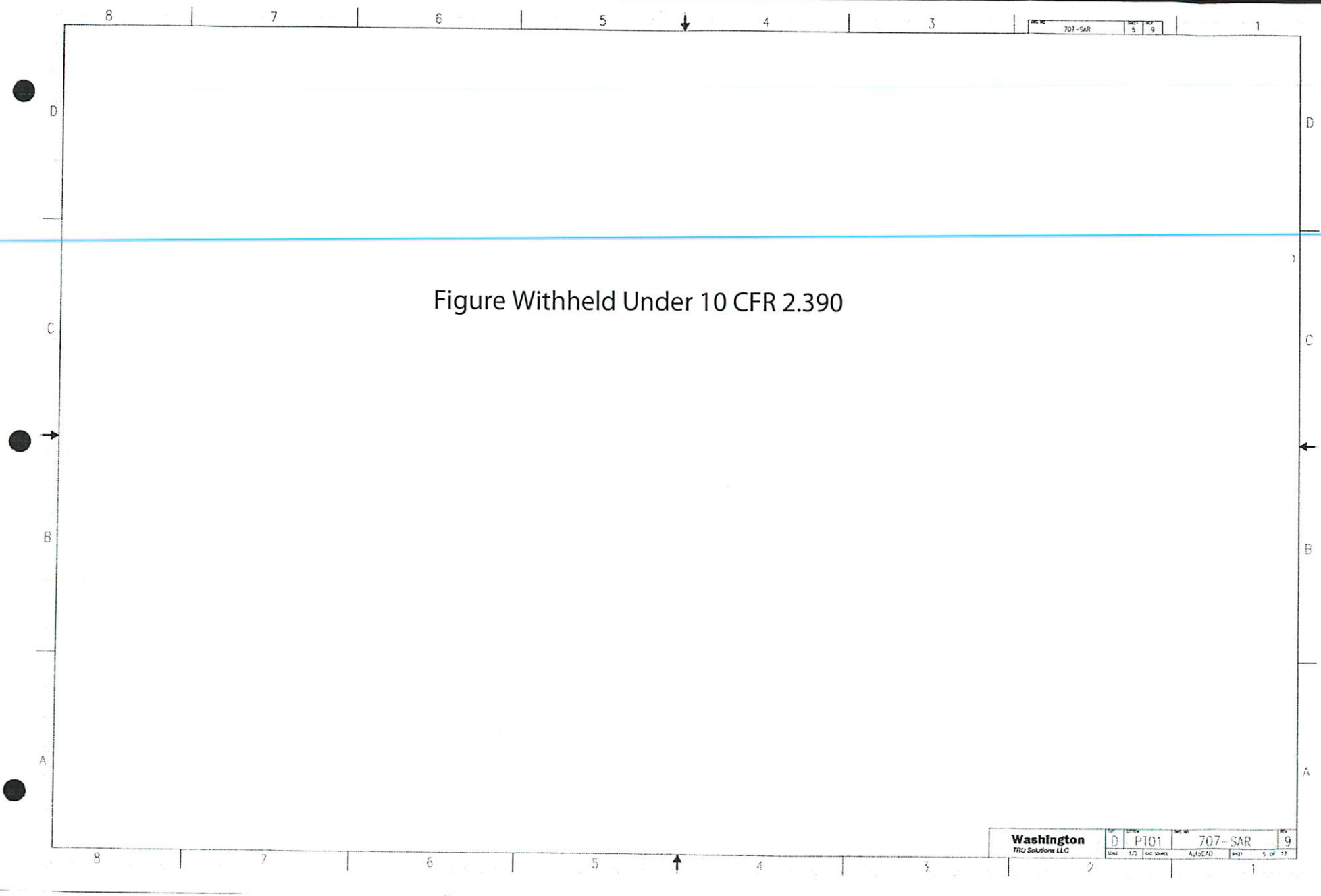
Figure Withheld Under 10 CFR 2.390

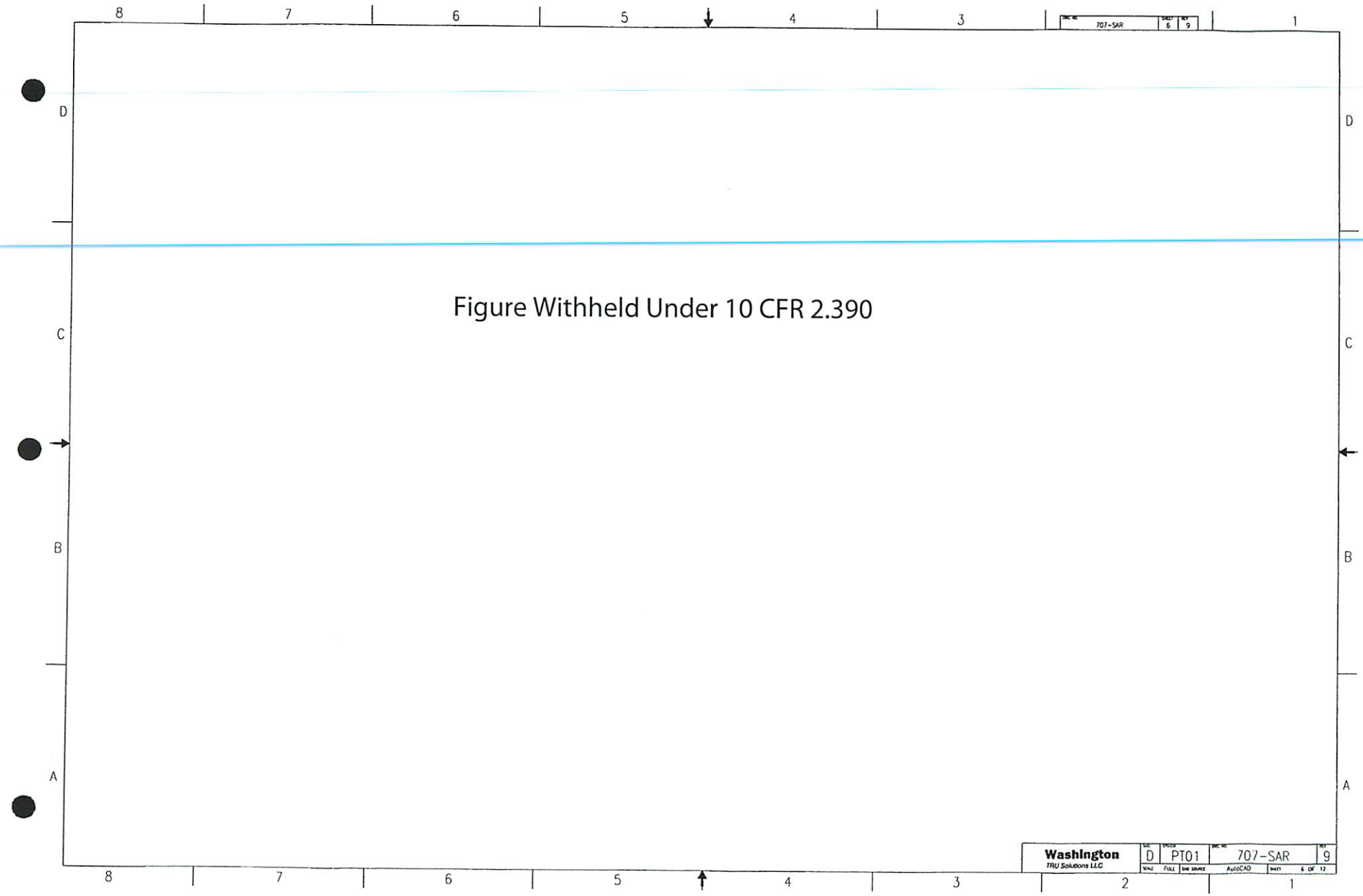
Figure Withheld Under 10 CFR 2.390
Washington
TRU Solutions LLC
PT01
707-SAR
AutoCAD

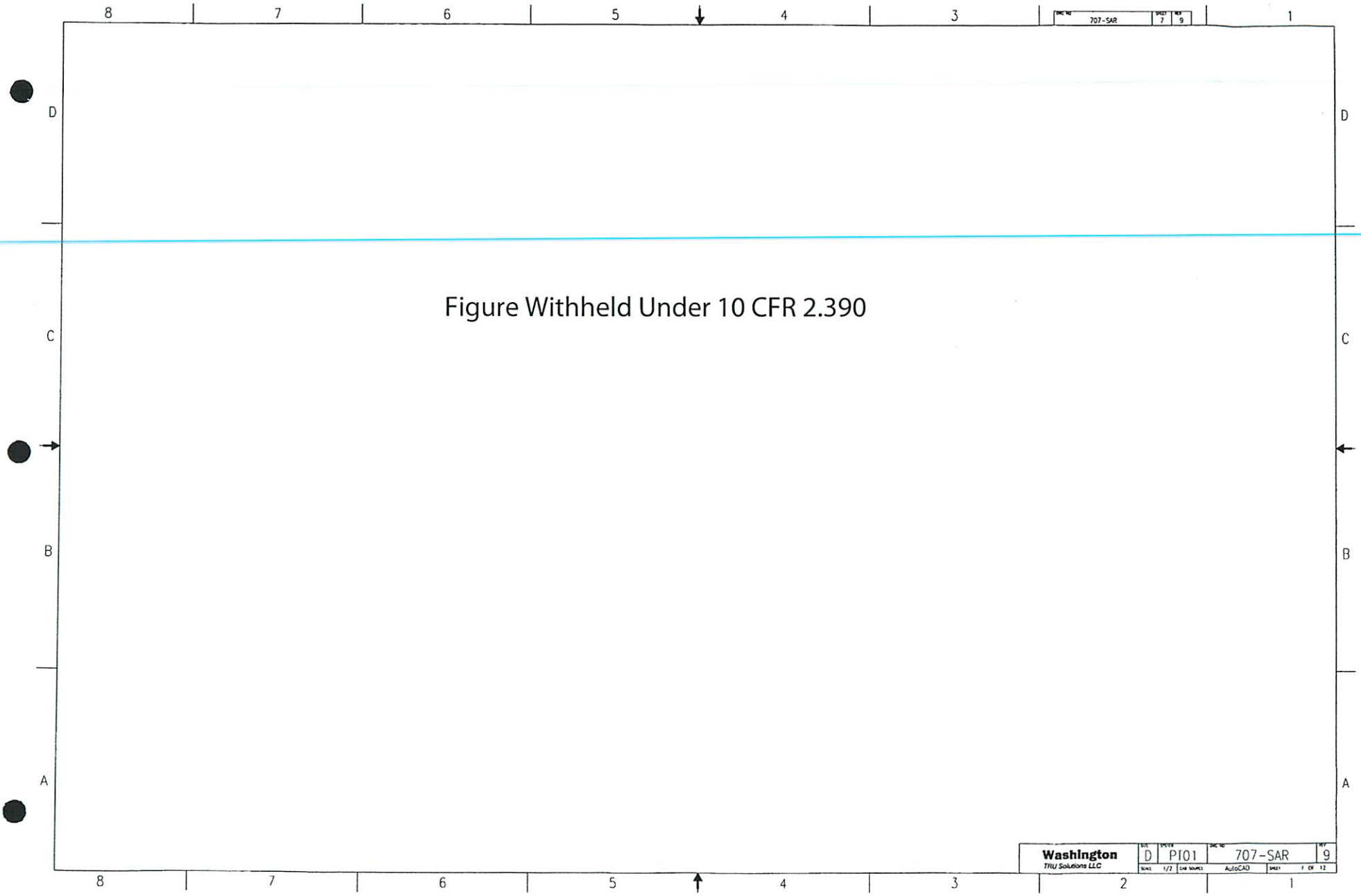
8
7
6
5
4
3
2
1
D
C
B
A
707-SAR
7
9
Figure Withheld Under 10 CFR 2.390
Washington
TRU Solutions LLC
D
P101
707-SAR
9
1/2
AutoCAD
1 OF 12

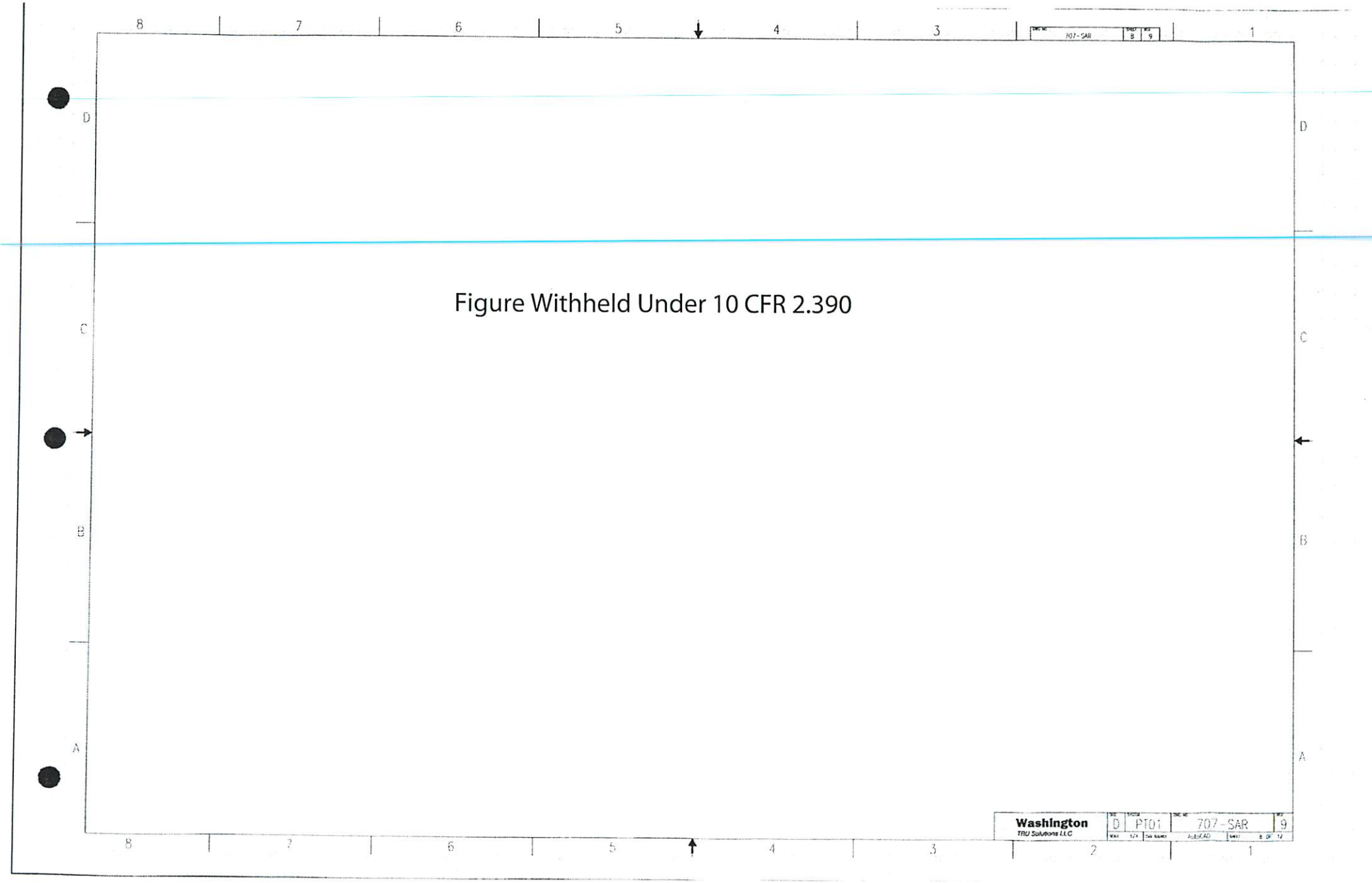
Figure Withheld Under 10 CFR 2.390
Washington
TRU Solutions LLC
PT01
707-SAR

Figure Withheld Under 10 CFR 2.390

Washington TRU Solutions LLC	SIZE D	SYSTEM PT01	DWG NO 707-SAR	REV 9
	SCALE 1/8	CAD SOURCE AutoCAD	SHEET 9 OF 12	

Figure Withheld Under 10 CFR 2.390

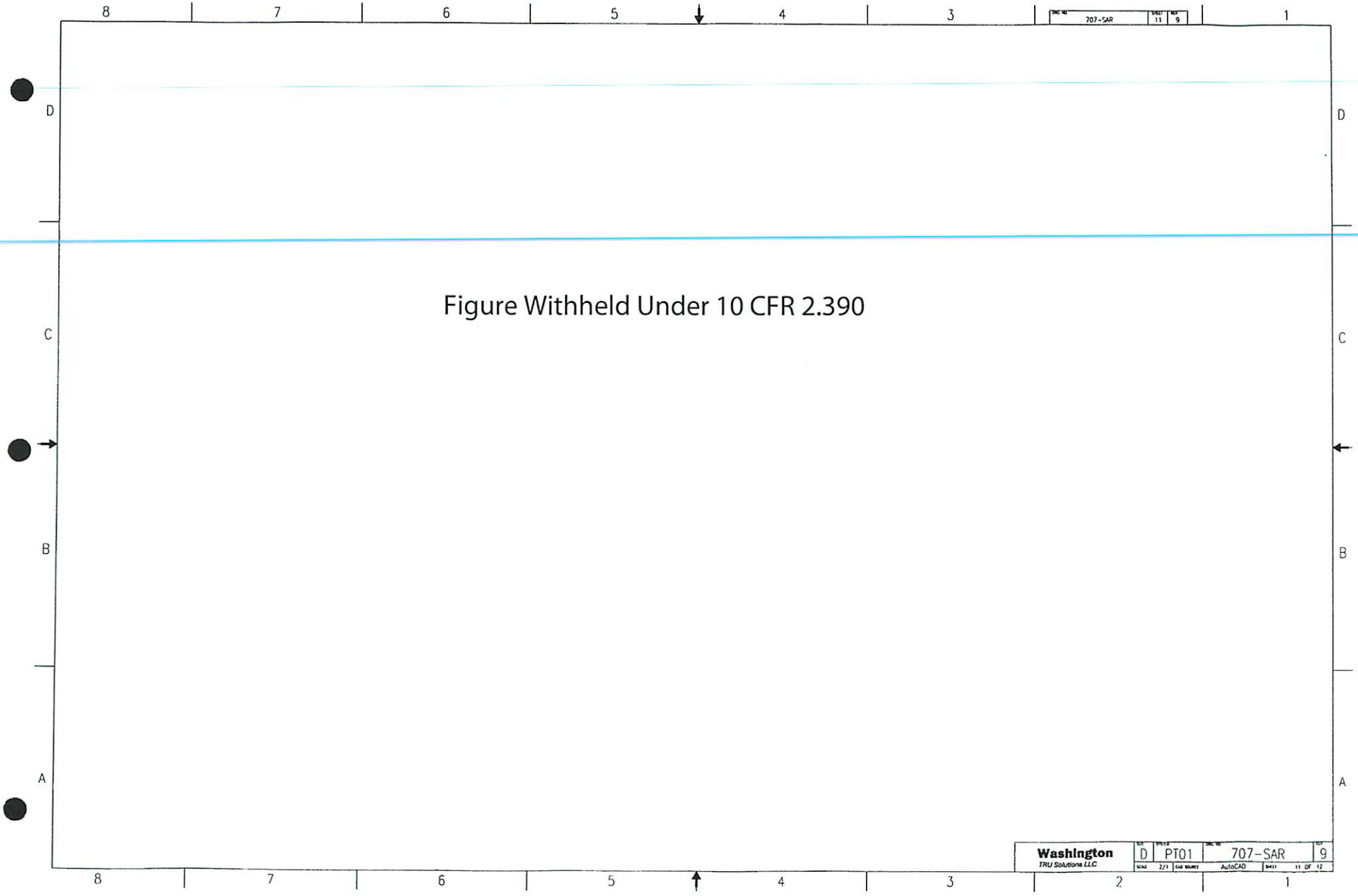
8
7
6
5
4
3
2
1
D
C
B
A
707-SAR
11
9
Figure Withheld Under 10 CFR 2.390
Washington
TRU Solutions LLC
D
PT01
707-SAR
9
2/1
AutoCAD
11 OF 12

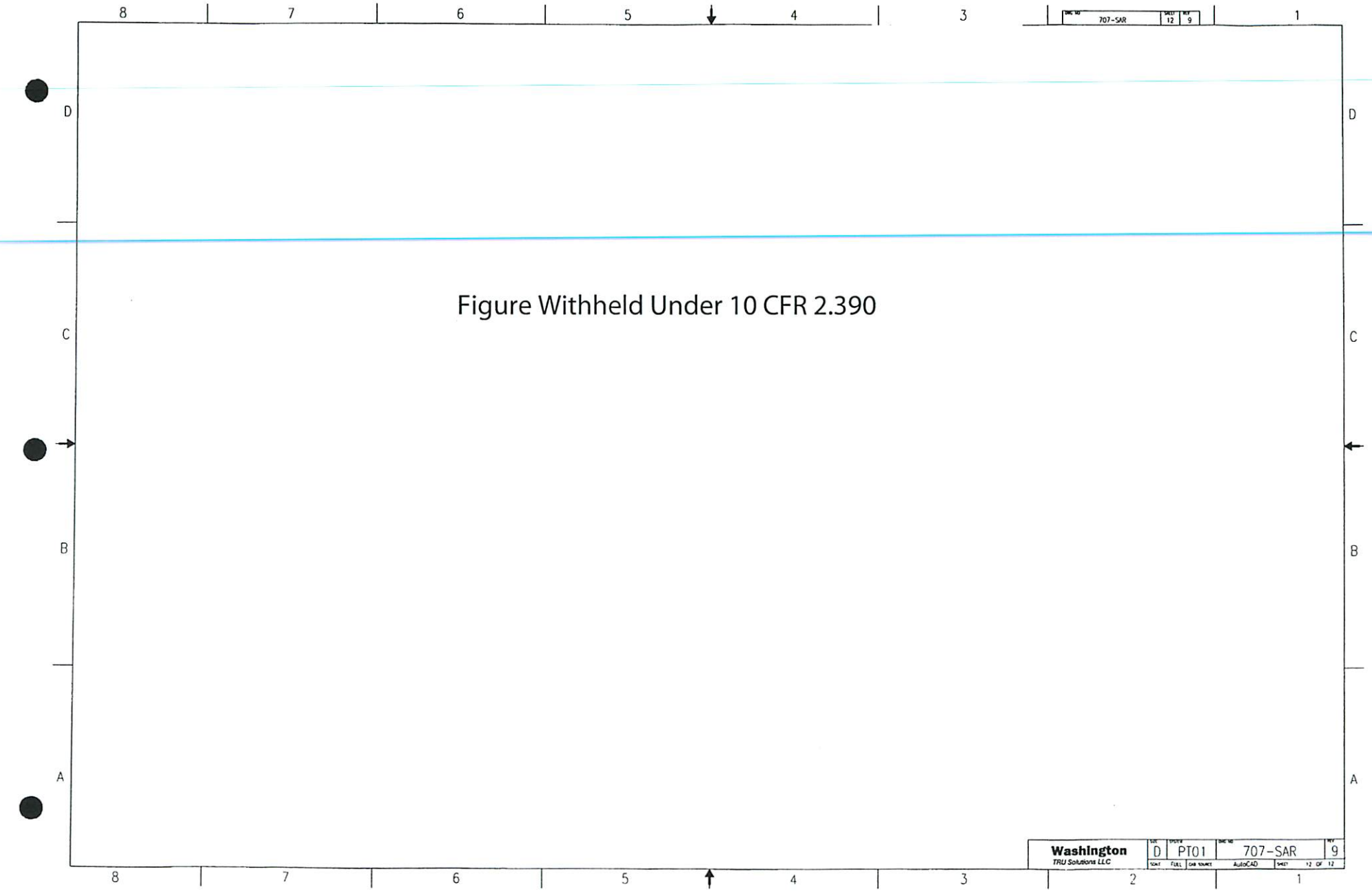
Figure Withheld Under 10 CFR 2.390
Washington
TRU Solutions LLC
D
PT01
707-SAR
9
AutoCAD
12 OF 12

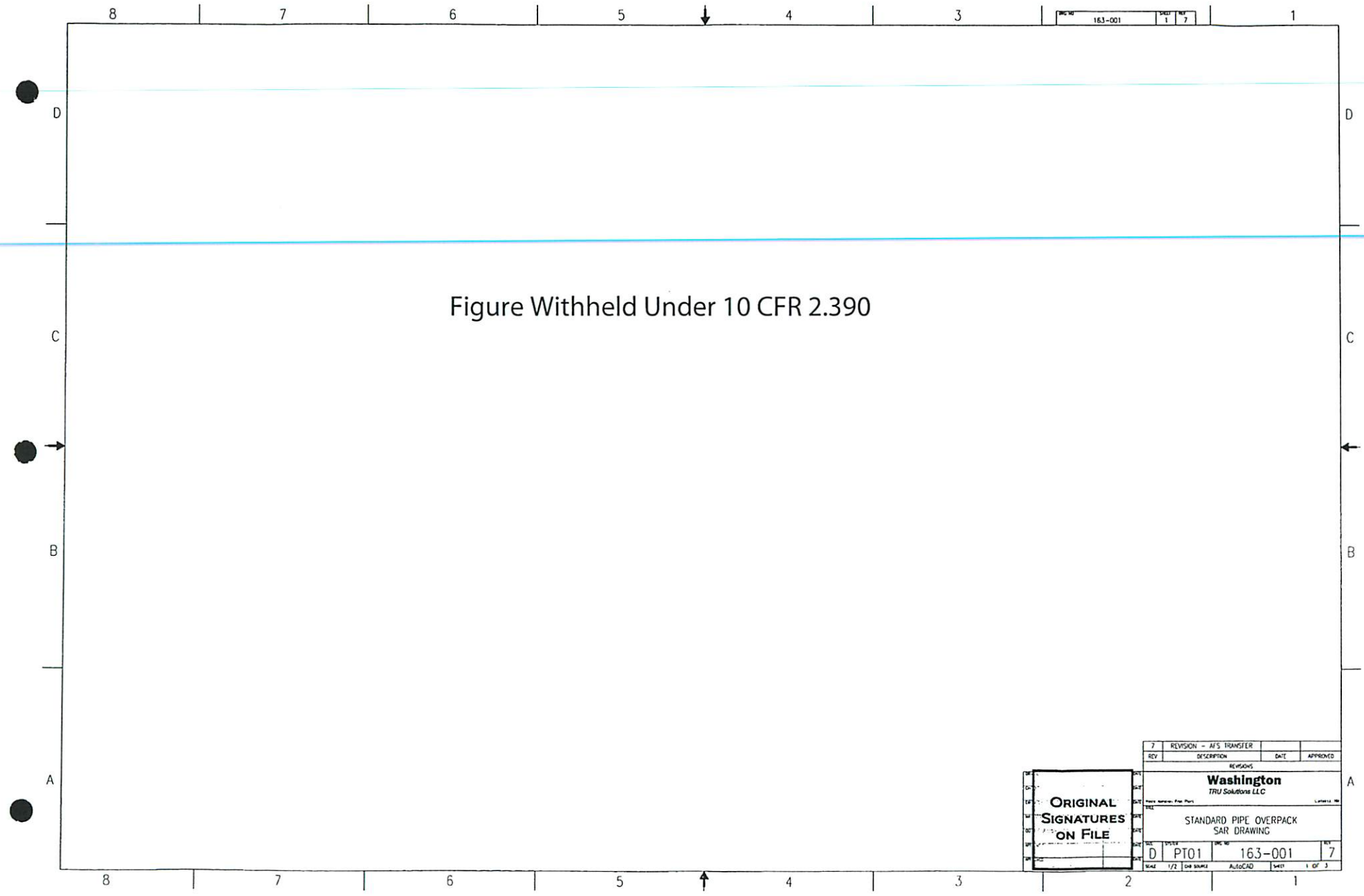
Figure Withheld Under 10 CFR 2.390
ORIGINAL SIGNATURES ON FILE
7 REVISION - AFS TRANSFER
REVISIONS
Washington
TRU Solutions LLC
STANDARD PIPE OVERPACK
SAR DRAWING
D PT01 163-001 7

Figure Withheld Under 10 CFR 2.390

Washington
TRU Solutions LLC
D | PT01 | 163-001 | 7

Figure Withheld Under 10 CFR 2.390

Washington
TRU Solutions LLC

D | PT01 | 163-001 | 7

AutoCAD | 3 OF 3

Figure Withheld Under 10 CFR 2.390

ORIGINAL SIGNATURES ON FILE

REV	DESCRIPTION	DATE	APPROVED
5	REVISION - AFS TRANSFER		

REVISIONS

Washington
TRU Solutions LLC

S100 PIPE OVERPACK
SAR DRAWING

SIZE	STYLE	DWG NO	REV
D	PT01	163-002	5

SCALE 1/2 | CAD SOURCE AutoCAD | SHEET 1 OF 2

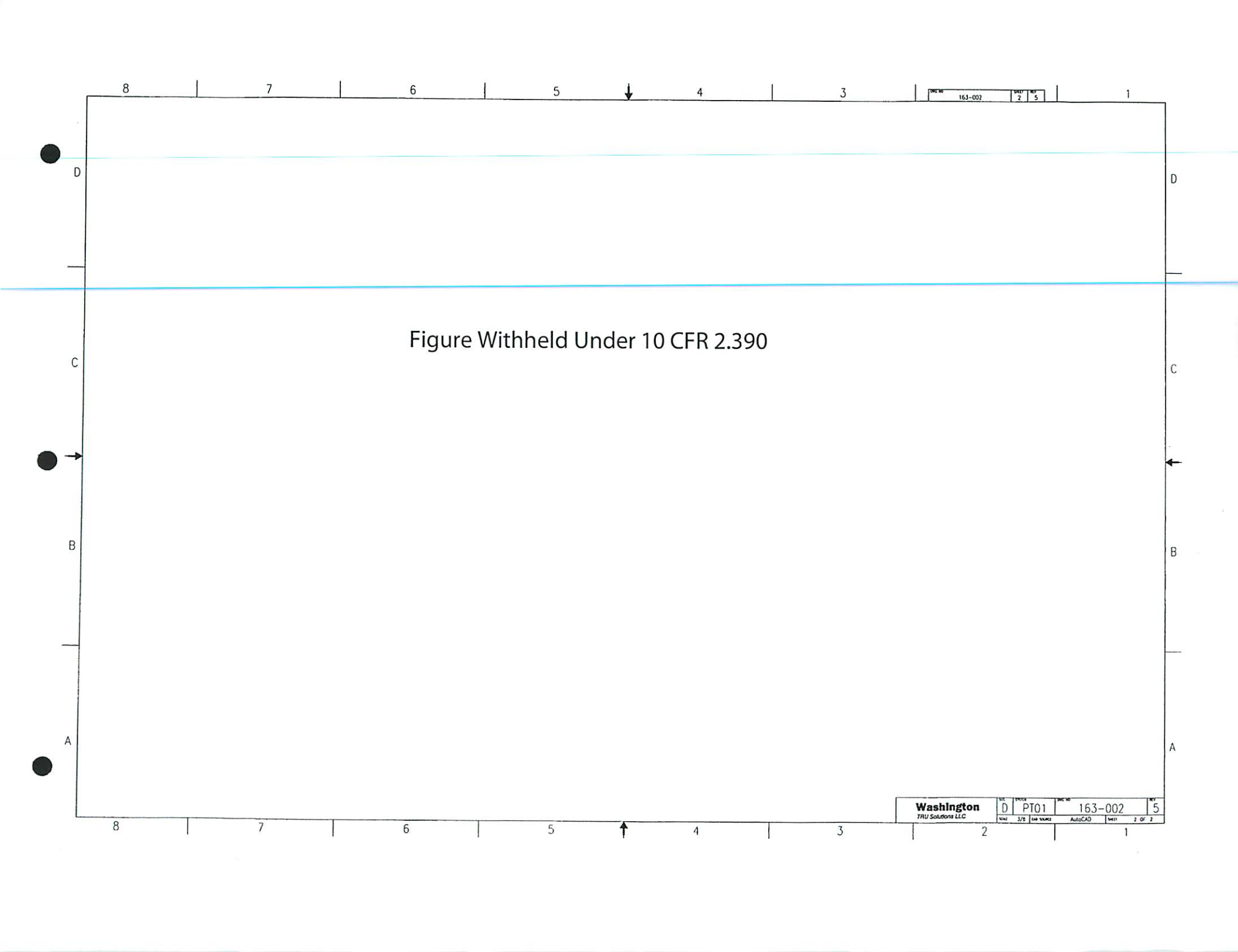
Figure Withheld Under 10 CFR 2.390

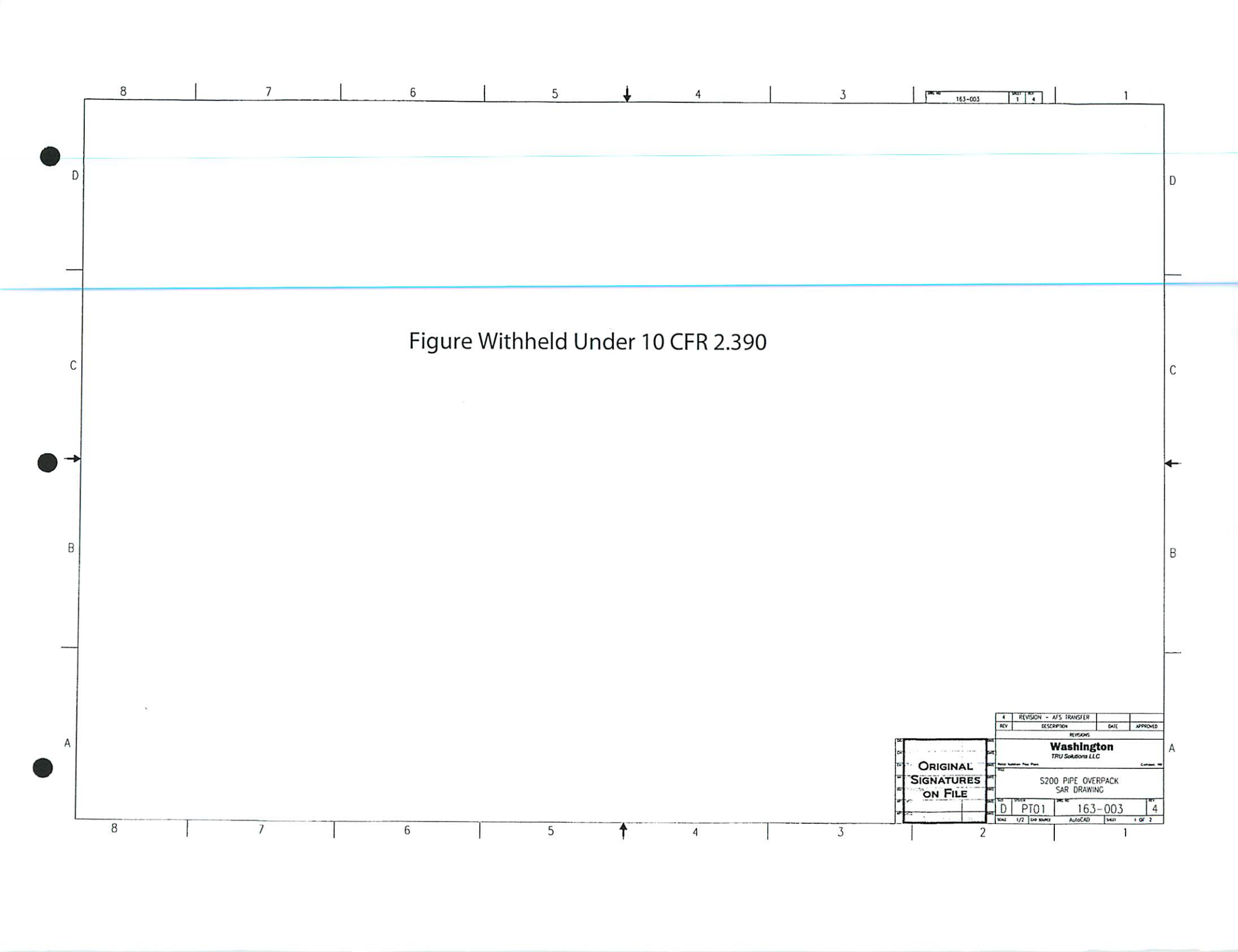
Figure Withheld Under 10 CFR 2.390
ORIGINAL SIGNATURES ON FILE
Washington
TRU Solutions LLC
S200 PIPE OVERPACK
SAR DRAWING
163-003
4
REVISION - AFS TRANSFER

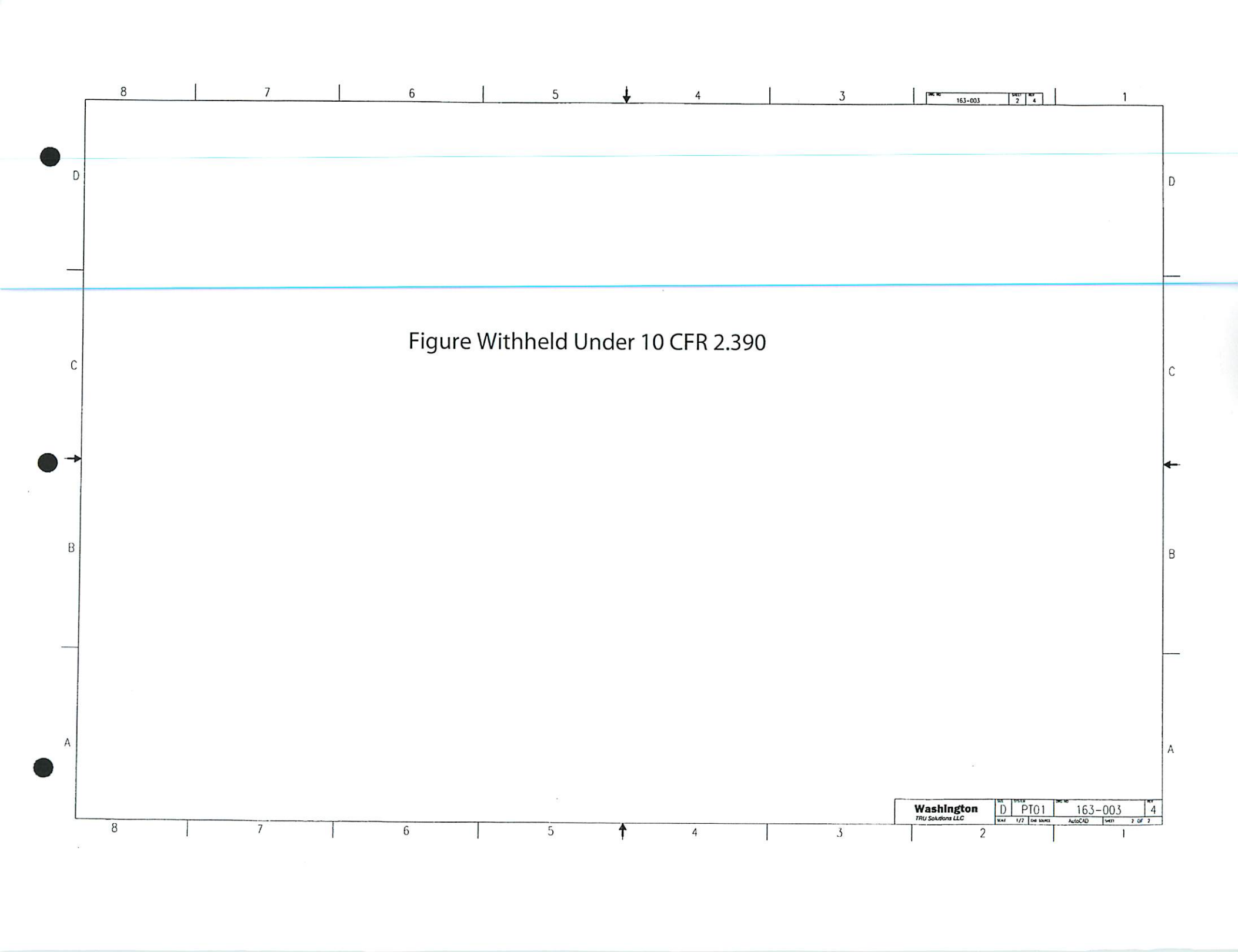
Figure Withheld Under 10 CFR 2.390

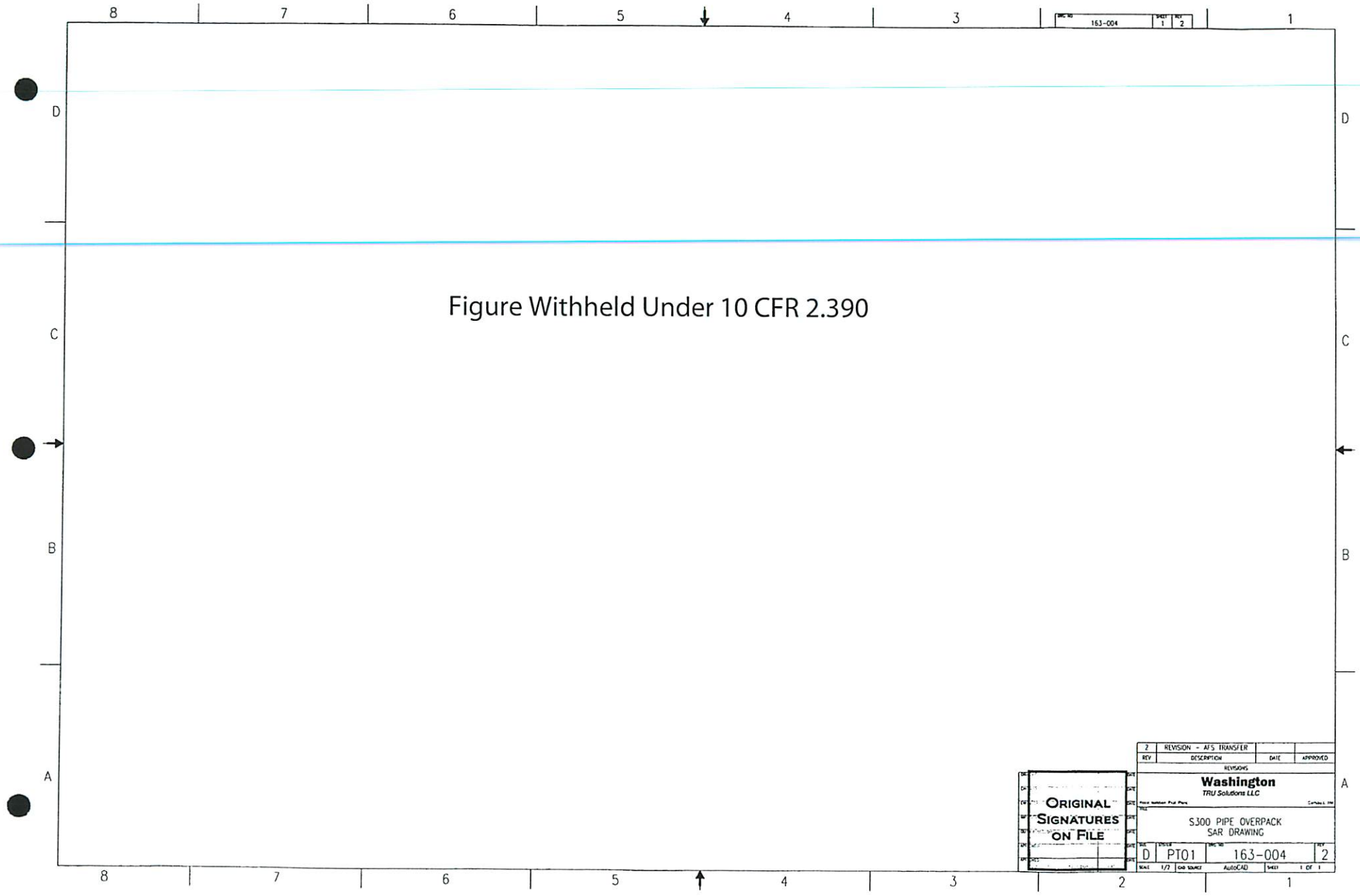
Figure Withheld Under 10 CFR 2.390
ORIGINAL SIGNATURES ON FILE
Washington
TRU Solutions LLC
S300 PIPE OVERPACK
SAR DRAWING
163-004
PT01

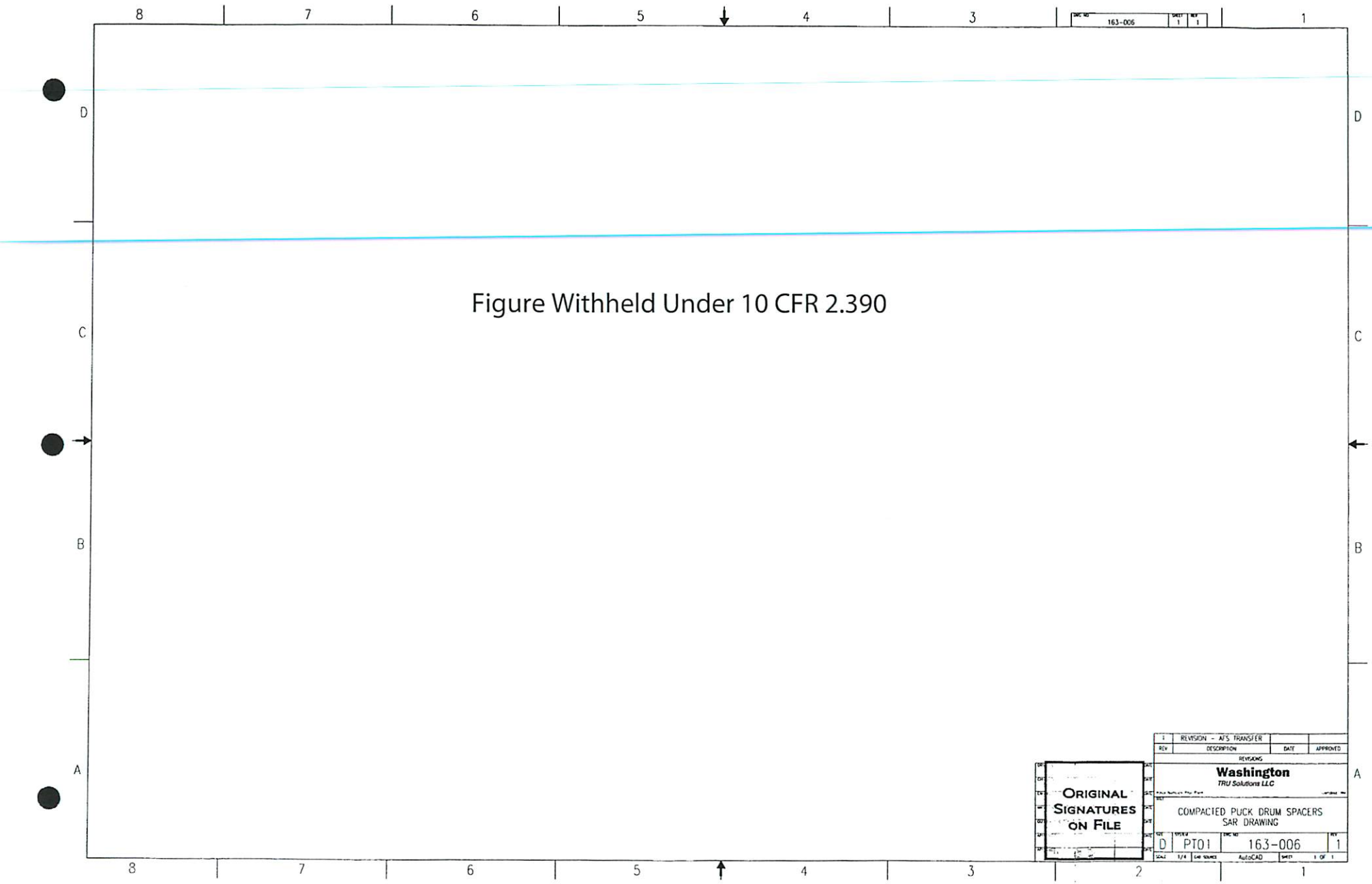
Figure Withheld Under 10 CFR 2.390
ORIGINAL SIGNATURES ON FILE
REVISION - AFS TRANSFER
REVISIONS
Washington
TRU Solutions LLC
COMPACTED PUCK DRUM SPACERS
SAR DRAWING
163-006

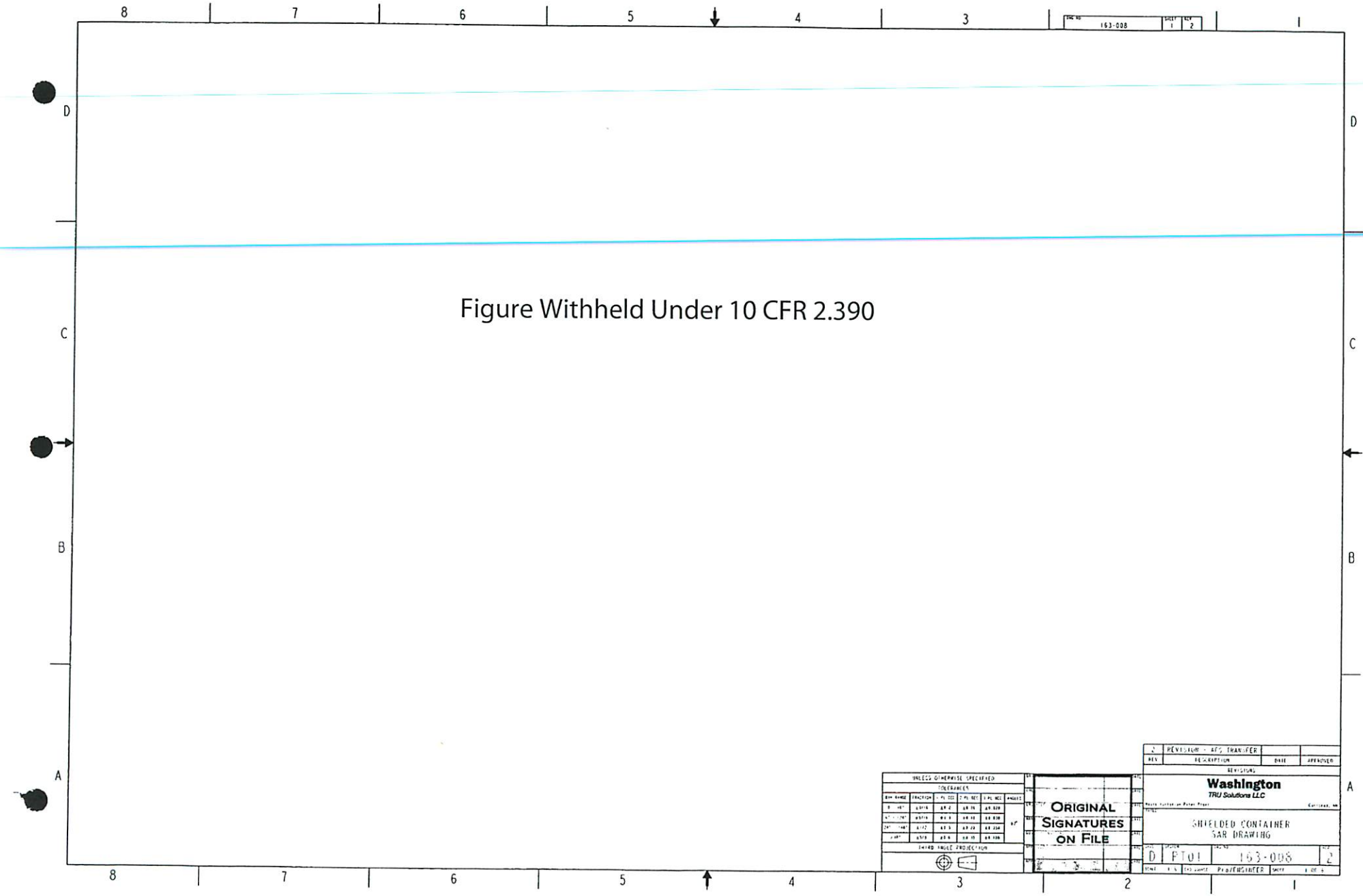
Figure Withheld Under 10 CFR 2.390
ORIGINAL SIGNATURES ON FILE
Washington
TRU Solutions LLC
SHIELDED CONTAINER
SAR DRAWING
163-008

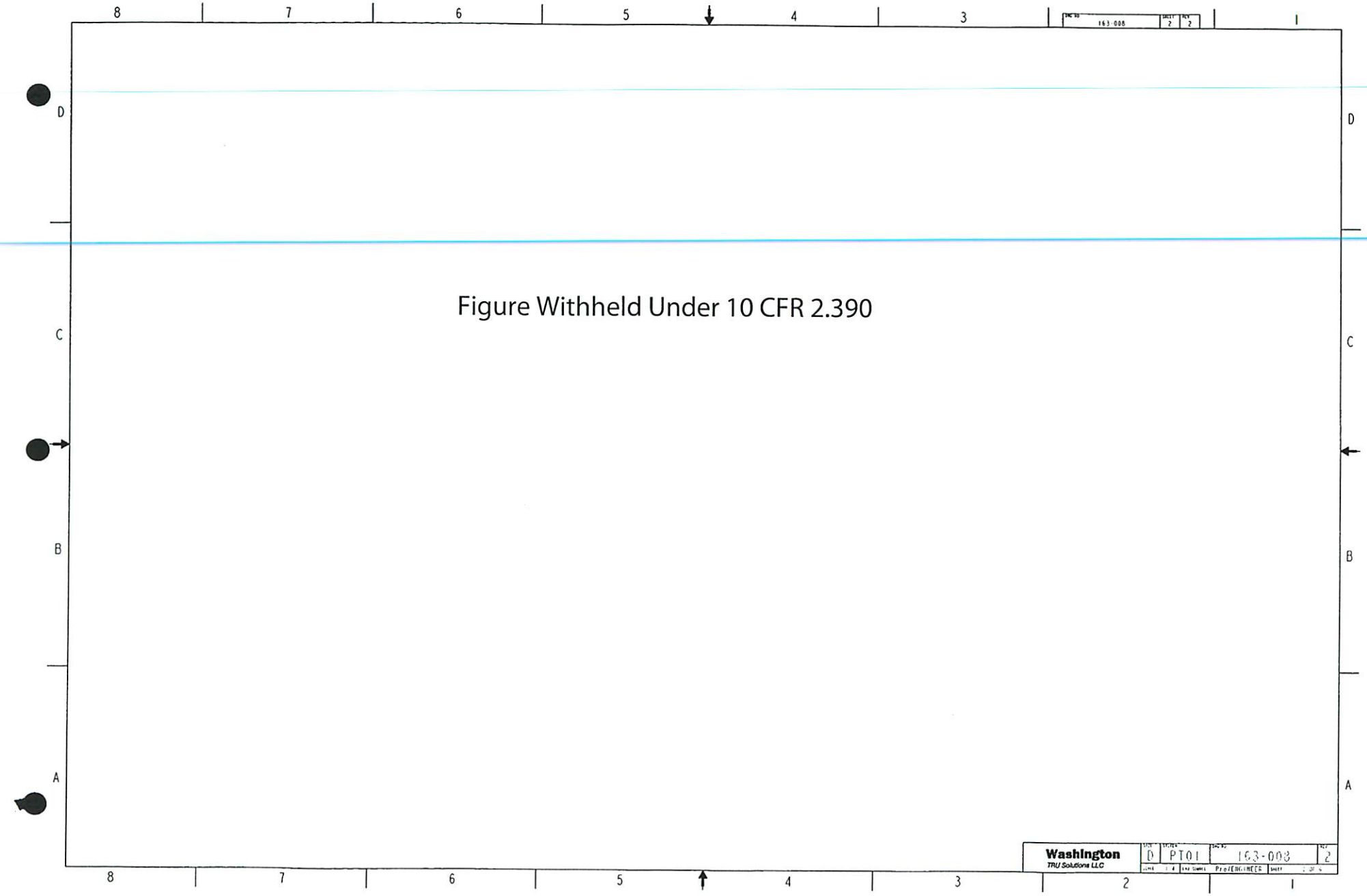
Figure Withheld Under 10 CFR 2.390
Washington
TRU Solutions LLC
PT01
163-003

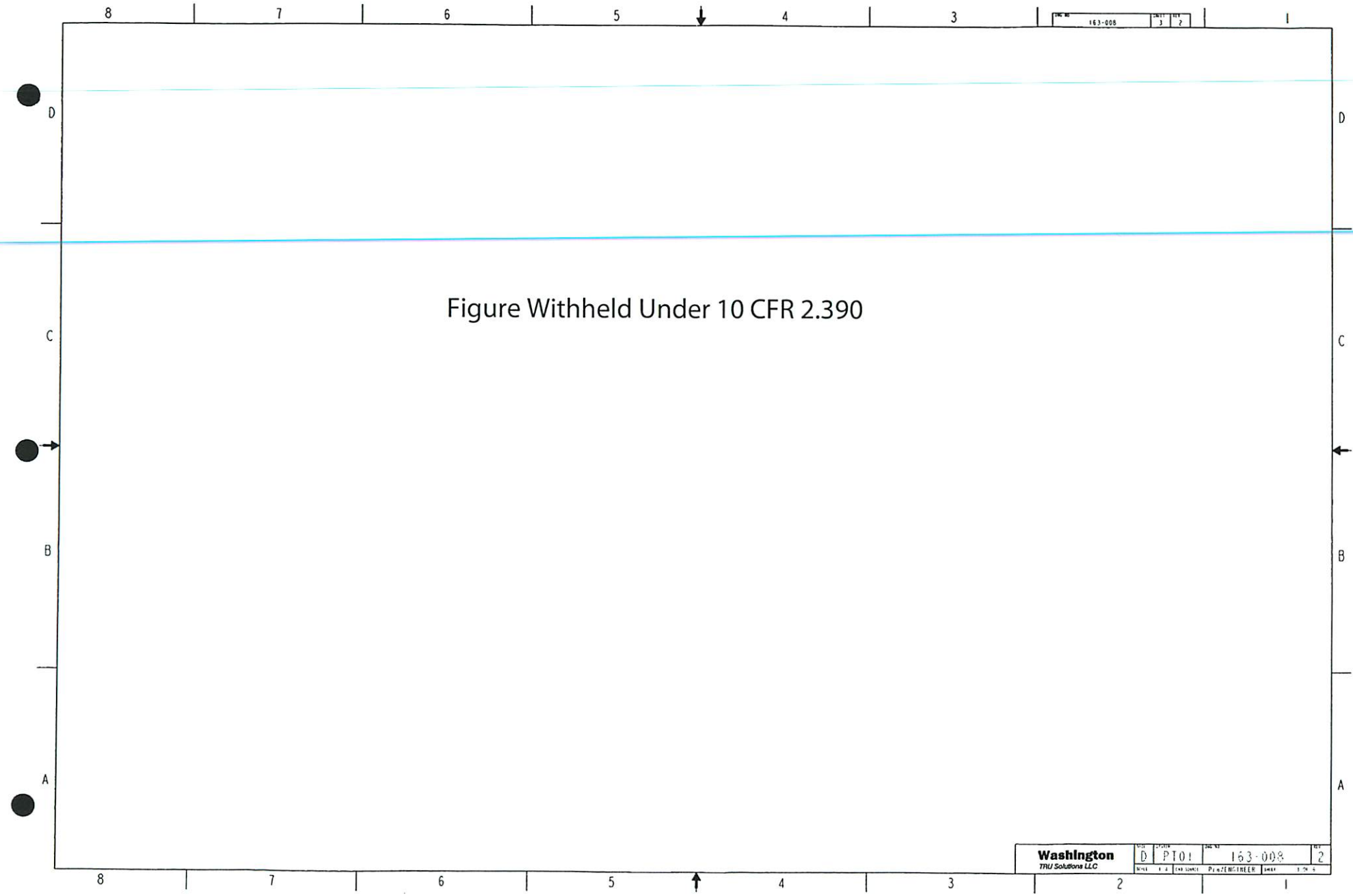
Figure Withheld Under 10 CFR 2.390
Washington
TRU Solutions LLC
D
PTOI
163-008
2

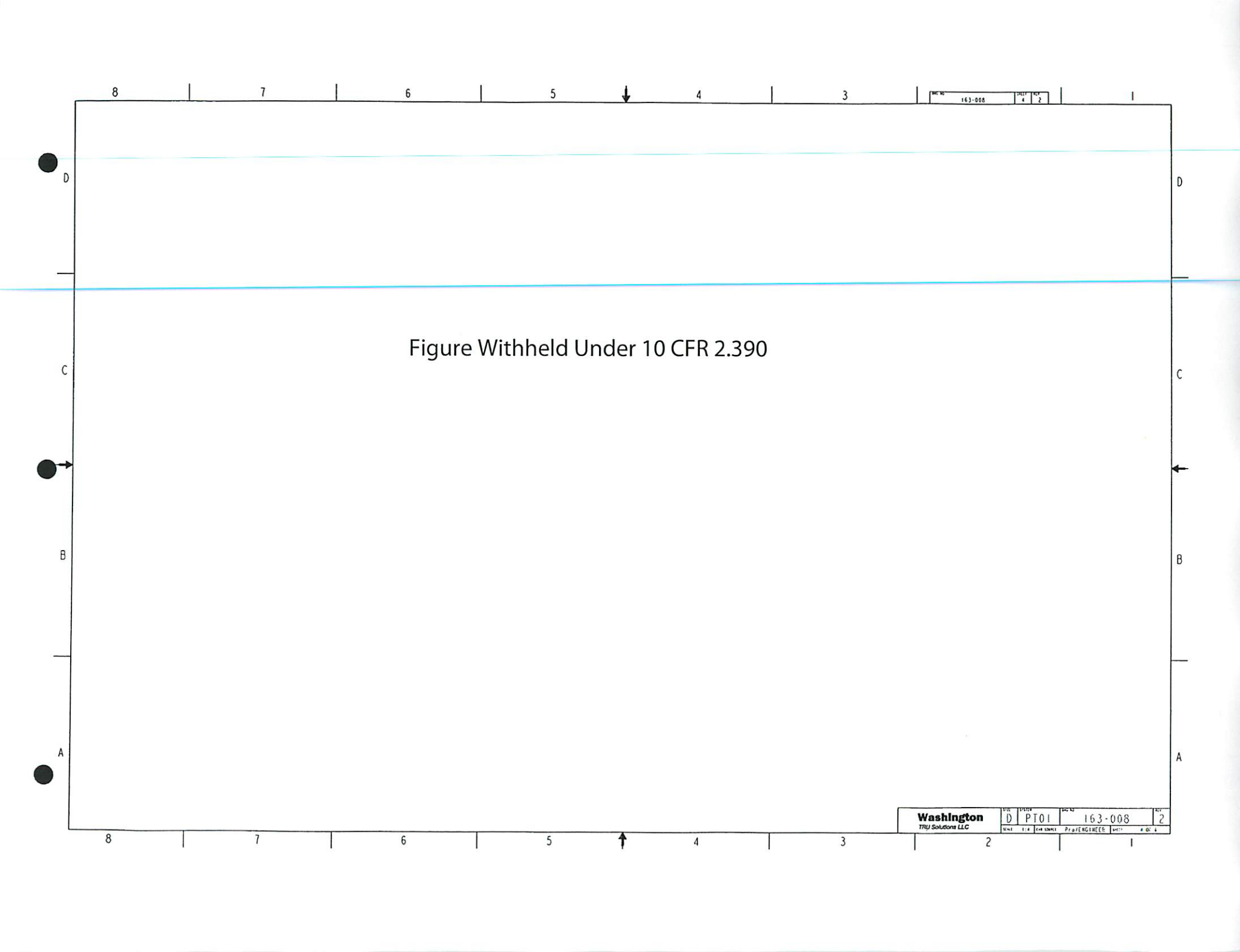
Figure Withheld Under 10 CFR 2.390

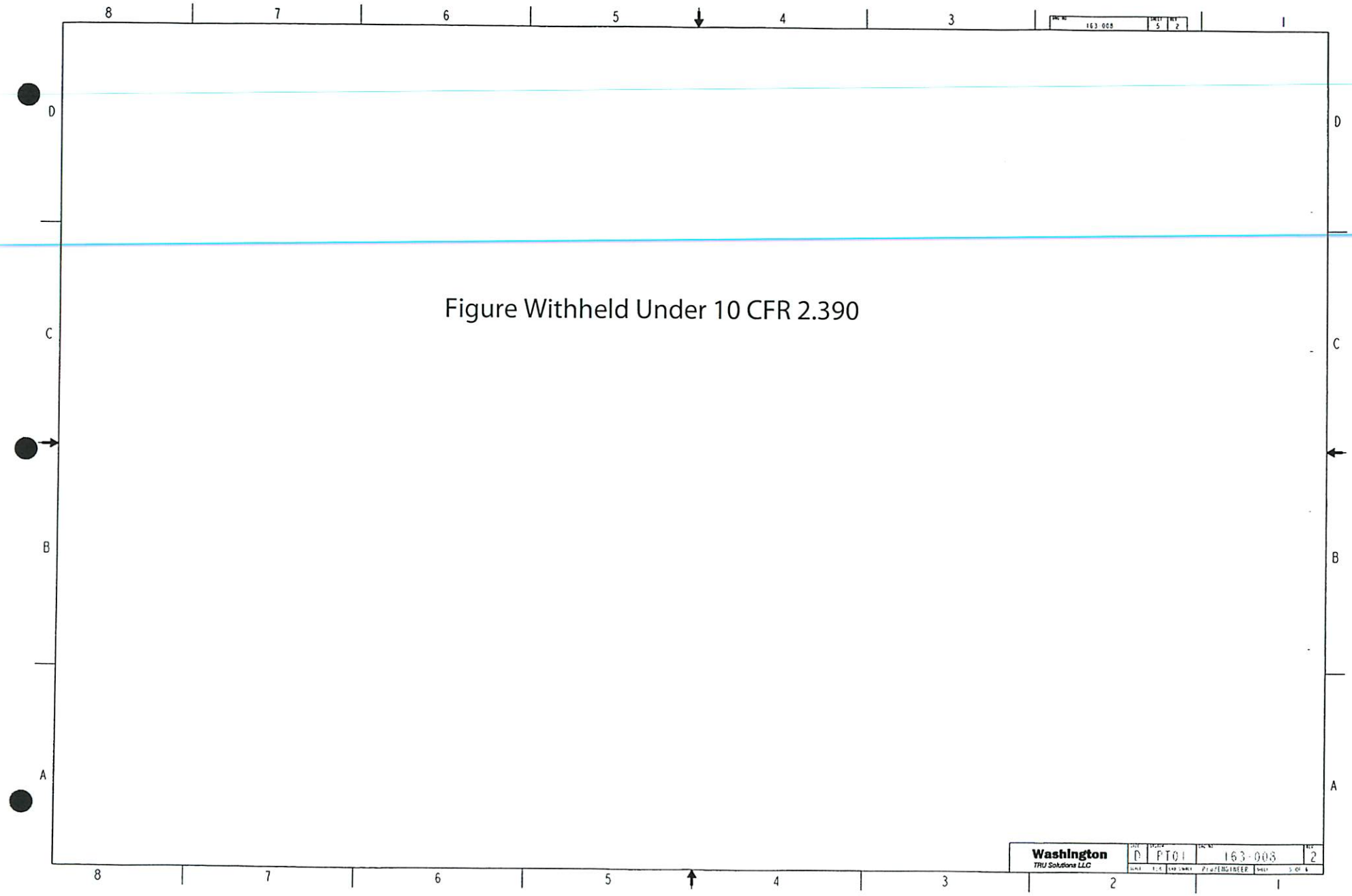
Figure Withheld Under 10 CFR 2.390
Washington
TRU Solutions LLC
163-003

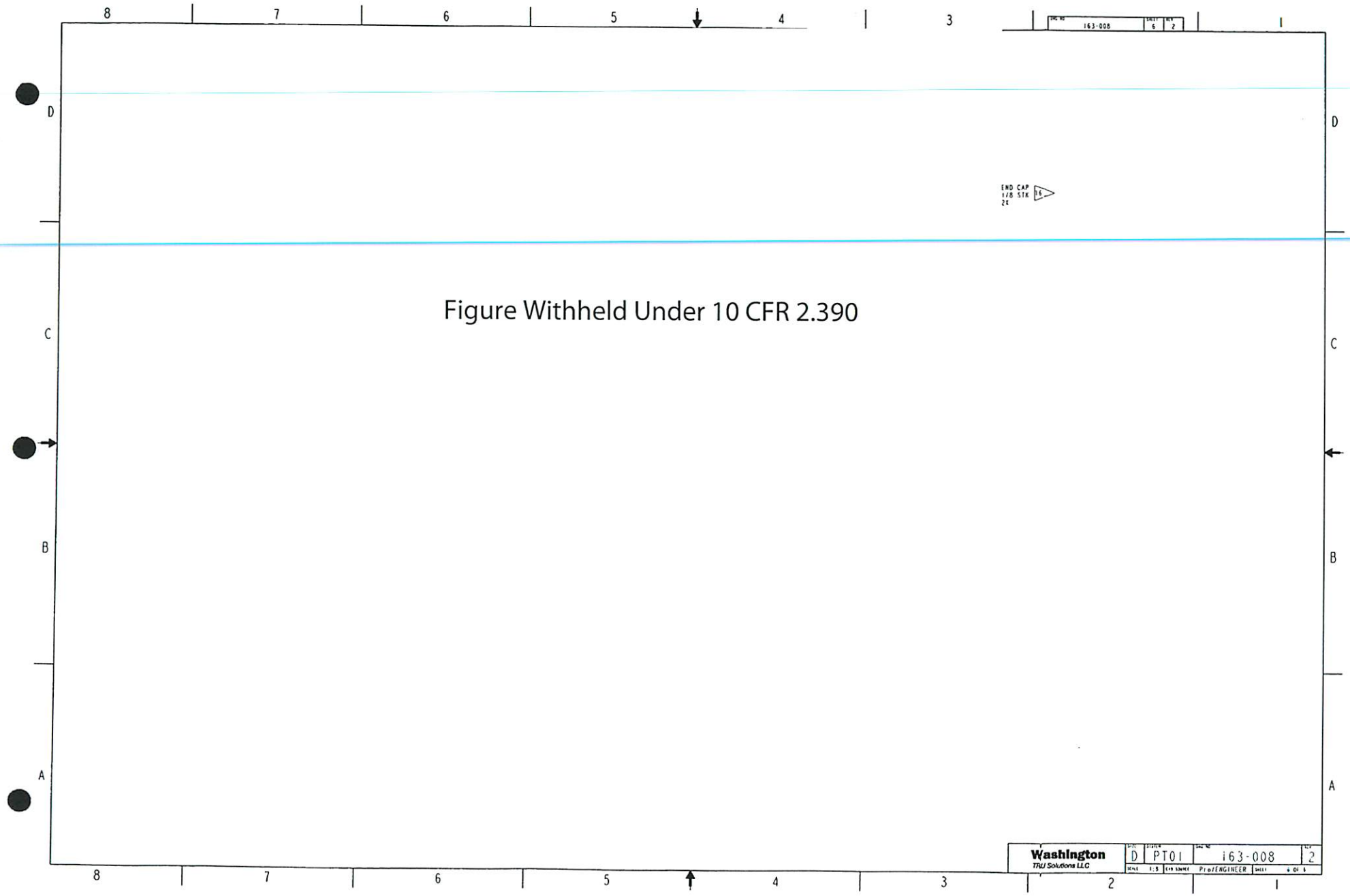
END CAP
1/8 STK
2x
Figure Withheld Under 10 CFR 2.390
Washington
TRU Solutions LLC
D
PT01
163-008
2

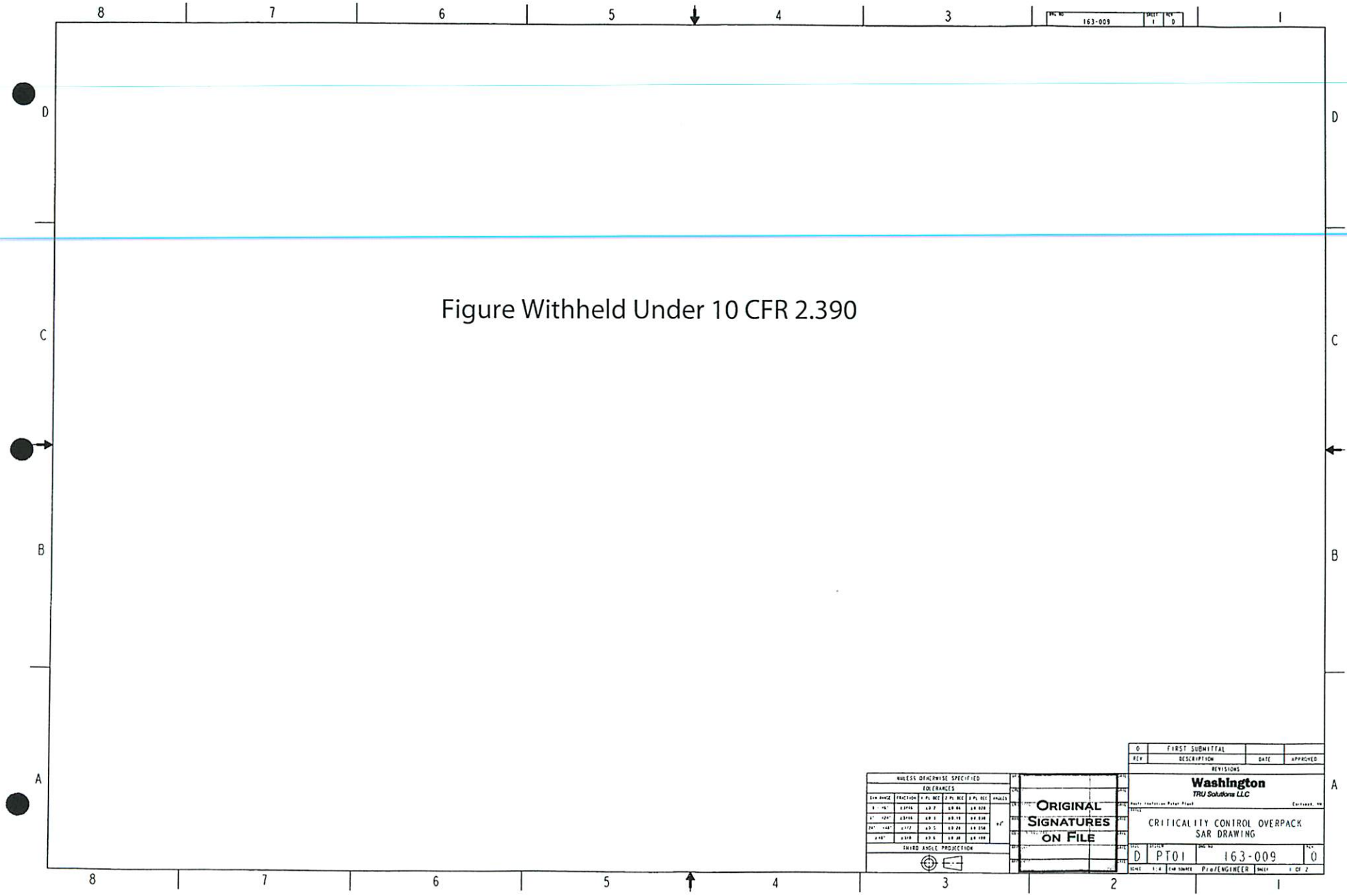
Figure Withheld Under 10 CFR 2.390
ORIGINAL SIGNATURES ON FILE
Washington
TRU Solutions LLC
CRITICALITY CONTROL OVERPACK
SAR DRAWING
163-009

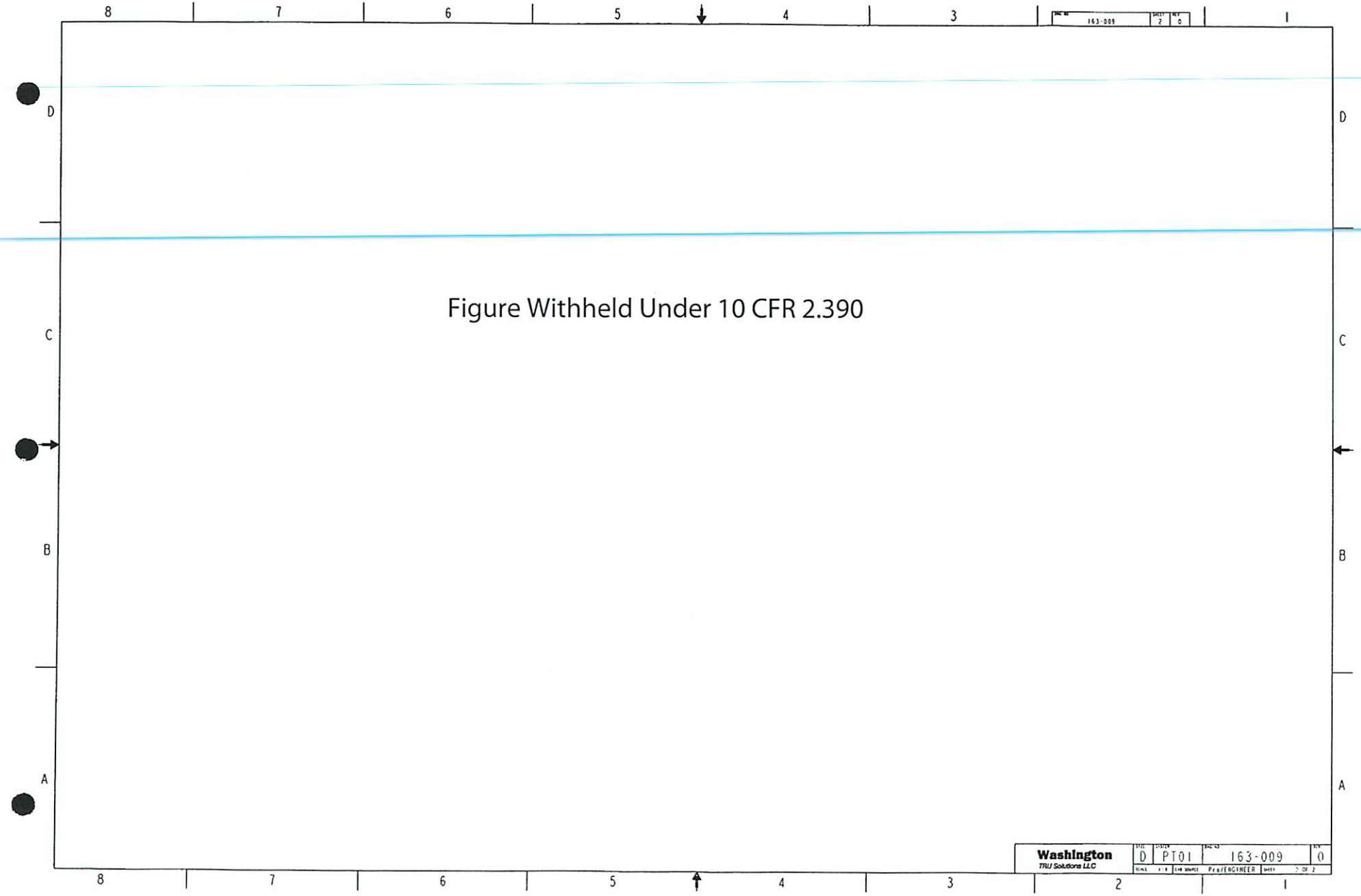
Figure Withheld Under 10 CFR 2.390
Washington
TRU Solutions LLC
D
PT01
163-009
0

1.3.2 Glossary of Terms and Acronyms

55-Gallon Drum – A payload container yielding 55 gallons.

85-Gallon Drum – A payload container with a range of dimensions yielding 75 to 88 gallons.

85-Gallon Drum Overpacks – A payload container consisting of a 55-gallon drum overpacked within an 85-gallon drum of the appropriate dimensions.

100-Gallon Drum – A payload container yielding 100 gallons.

Aluminum Honeycomb Spacer Assembly – An assembly that is located within each end of the ICV. The aluminum honeycomb spacer assembly supplements the ICV void volume to accommodate gas generated by the payload material, and acts as an energy-absorbing barrier between the payload and the ICV torispherical heads for axial loads.

ASME – American Society of Mechanical Engineers.

ASME B&PVC – ASME Boiler and Pressure Vessel Code.

CCO – Criticality Control Overpack

CCC – Criticality Control Container

CTU – Certification Test Unit

CH-TRAMPAC – Contact-Handled Transuranic Waste Authorized Methods for Payload Control.

CH-TRU Waste – Contact-Handled Transuranic Waste.

HalfPACT Package – The package consisting of a HalfPACT packaging and the Payload.

HalfPACT Packaging – The packaging consisting of an outer confinement assembly (OCA), an inner containment vessel (ICV), and two aluminum honeycomb spacer assemblies.

ETU – Engineering Test Unit.

ICV – Inner Containment Vessel.

ICV Body – The assembly consisting of the ICV lower seal flange, the cylindrical vessel, and the ICV lower torispherical head.

ICV Inner Vent Port Plug – The brass plug and accompanying O-ring seal that provides the pressure boundary in the ICV vent port penetration.

ICV Lid – The assembly consisting of the ICV upper seal flange, the ICV locking ring, a short section of cylindrical vessel, and the ICV upper torispherical head.

ICV Lock Bolts – The three, 1/2-inch, socket head cap screws used to secure the ICV locking ring in the locked position.

ICV Locking Ring – The component that connects and locks the ICV upper seal flange to the ICV lower seal flange; included as an ICV lid component.

ICV Lower Seal Flange – The ICV body's sealing interface containing two O-ring grooves, the ICV vent port access, and the ICV test port.

ICV Main O-ring Seal – The upper elastomeric O-ring seal in the ICV lower seal flange; forms the containment boundary.

ICV Outer Vent Port Plug – The brass plug and accompanying O-ring seal that provides the containment boundary in the ICV vent port penetration.

ICV Seal Test Port – The radial penetration between the ICV main O-ring seal and ICV main test O-ring seal to allow leakage rate testing of the ICV main O-ring seal.

ICV Seal Test Port Plug – The brass plug and accompanying O-ring seal for the ICV seal test port.

ICV Seal Test Port Insert – A welded-in, replaceable component within the ICV lower seal flange that interfaces with the ICV seal test port plug.

ICV Main Test O-ring Seal – The lower elastomeric O-ring seal in the ICV lower seal flange; forms the test boundary for leakage rate testing.

ICV Upper Seal Flange – The ICV lid's sealing interface containing a mating sealing surface for the ICV lower seal flange and location for a wiper O-ring seal.

ICV Vent Port – The radial penetration into the ICV cavity that is located in the ICV lower seal flange.

ICV Vent Port Cover – The outer brass cover that directly protects the ICV vent port plugs.

Inner Containment Vessel – The assembly (comprised of an ICV lid and ICV body) providing the primary level of containment for the payload. Within each end of the inner containment vessel (ICV) is an aluminum honeycomb spacer assembly.

Locking Z-Flange – The z-shaped shell situated between the upper and lower Z-flanges that connects to the OCV locking ring; allows external operation of the OCV locking ring.

Lower Z-Flange – The z-shaped shell in the OCA body, connecting the OCA outer shell to the OCV lower seal flange.

OCA – Outer Confinement Assembly.

OCA Body – The assembly consisting of the OCV lower seal flange, the OCV cylindrical and conical shells, the OCV lower torispherical head, the lower Z-flange, the OCA cylindrical shell, the OCA lower flat head, corner reinforcing angles, tie-down structures, ceramic fiber paper, and polyurethane foam.

OCA Inner Thermal Shield – The L-shaped, 16-gauge (0.060-inch thick), inner shield that holds fiberglass insulating material against the OCV locking ring thereby preventing hot gasses and flames from directly impinging on the OCV sealing region in the event of a HAC fire.

OCA Lid – The assembly consisting of the OCV upper seal flange, the OCV locking ring, a short section of cylindrical vessel, the OCV upper torispherical head, the upper and locking Z-flanges, the inner and outer thermal shields, a short section of cylindrical shell, the OCA upper torispherical head, corner reinforcing angles, ceramic fiber paper, and polyurethane foam.

OCA Lock Bolts – The six 1/2-inch, socket head cap screws used to secure the OCV locking ring in the locked position.

OCA Lower Head – The lower ASME flat head comprising the OCA outer shell.

OCA Outer Thermal Shield – The 14-gauge (0.075-inch thick) × 6⅛-inch wide outer shield surrounding the OCA lid-to-body joint that prevents hot gasses and flames from entering the joint in the event of a HAC fire.

OCA Upper Head – The upper ASME torispherical head comprising the OCA outer shell.

OCV – Outer Confinement Vessel.

OCV Locking Ring – The component that connects and locks the OCV upper seal flange to the OCV lower seal flange; included as an OCA lid component.

OCV Lower Seal Flange – The OCA body's sealing interface containing two O-ring grooves.

OCV Main O-ring Seal – The optional upper O-ring seal in the OCV lower seal flange; forms the confinement boundary.

OCV Main Test O-ring Seal – The optional lower O-ring seal in the OCV lower seal flange; forms the test boundary for optional leakage rate testing.

OCV Seal Test Port – The radial penetration between the OCV main O-ring seal and OCV main test O-ring seal to allow optional leakage rate testing of the OCV main O-ring seal.

OCV Seal Test Port Access Plug – The 1½-inch NPT plug located at the outside end of the OCV seal test port access tube (i.e., at the outside surface of the OCA lid outer shell).

OCV Seal Test Port Insert – A welded-in, replaceable component within the OCV lower seal flange that interfaces with the OCV seal test port plug.

OCV Seal Test Port Plug – The brass plug and accompanying optional O-ring seal for the OCV seal test port.

OCV Seal Test Port Thermal Plug – The foam or ceramic fiber plug located within the OCV seal test port access tube that thermally protects the OCV seal test port region.

OCV Upper Seal Flange – The OCA lid's sealing interface containing a mating sealing surface for the OCV lower seal flange.

OCV Vent Port – The radial penetration into the OCV cavity that is located in the OCV conical shell.

OCV Vent Port Access Plug – The 1½-inch NPT plug located at the outside end of the OCV vent port access tube (i.e., at the outside surface of the OCA body outer shell).

OCV Vent Port Access Tube – The fiberglass tube allowing external access to the OCV vent port.

OCV Vent Port Cover – The outer brass cover that directly protects the OCV vent port plug.

OCV Vent Port Plug – The brass plug and accompanying optional O-ring seal that provides the confinement boundary in the OCV vent port penetration.

OCV Vent Port Thermal Plug – The foam or ceramic fiber plug located within the OCV vent port access tube that thermally protects the OCV vent port region.

Outer Confinement Assembly – The assembly (comprised of an OCA lid and OCA body) providing a secondary level of confinement for the payload when its optional O-ring seals are utilized. The Outer Confinement Assembly (OCA) completely surrounds the Inner Containment

Vessel and consists of an exterior stainless steel shell, a relatively thick layer of polyurethane foam and an inner stainless steel boundary that forms the Outer Confinement Vessel (OCV).

Outer Confinement Vessel – The innermost boundary of the Outer Confinement Assembly.

Packaging – The assembly of components necessary to ensure compliance with packaging requirements as defined in 10 CFR §71.4. Within this SAR, the packaging is denoted as the HalfPACT packaging.

Package – The packaging with its radioactive contents, or payload, as presented for transportation as defined in 10 CFR §71.4. Within this SAR, the package is denoted as the HalfPACT contact-handled transuranic waste package, or equivalently, the HalfPACT package.

Payload – Contact-handled transuranic (CH-TRU) waste or other authorized contents such as tritium-contaminated materials contained within approved payload containers. In this SAR, the payload includes a payload pallet for handling when drums are used. Any additional dunnage used that is external to the payload containers is also considered to be part of the payload. Payload requirements are defined by the CH-TRAMPAC.

Payload Container – Payload containers may be 55-gallon drums, pipe overpacks, criticality control overpacks (CCOs), 85-gallon drums (including overpacks), 100-gallon drums, standard waste boxes (SWB), or shielded containers (SC).

Payload Pallet – A lightweight pallet used for handling drum-type payload containers.

Payload Spacer – A component of the same basic design as the payload pallet; used to control (reduce) vertical clearance within the ICV with 55-gallon drum, short 85-gallon drum, 100-gallon drum, and SWB payload containers.

Pipe Component – A stainless steel container used for packaging specific waste forms within a 55-gallon drum. The pipe component is exclusively used as part of the pipe overpack.

Pipe Overpack – A payload container consisting of a pipe component positioned by dunnage within a 55-gallon drum with a rigid, polyethylene liner and lid. Seven pipe overpack assemblies will fit within the HalfPACT packaging.

RTV – Room Temperature Vulcanizing.

SAR – Safety Analysis Report (this document).

Shielded Container – A specialized payload container for use within the HalfPACT packaging that provides gamma shielding. Three shielded containers are surrounded by radial and axial dunnage assemblies and loaded using a triangular payload pallet within the HalfPACT packaging.

Standard Waste Box – A specialized payload container for use within the HalfPACT packaging. One standard waste box can fit within the HalfPACT packaging.

SWB – Standard Waste Box.

Upper Z-Flange – The z-shaped shell in the OCA lid, connecting the OCA outer shell to the OCV upper seal flange.

2.0 STRUCTURAL EVALUATION

This section presents evaluations demonstrating that the HalfPACT package meets all applicable structural criteria. The HalfPACT packaging, consisting of an outer confinement assembly (OCA), with an integral outer confinement vessel (OCV), and an inner containment vessel (ICV), with aluminum honeycomb spacer assemblies, is evaluated and shown to provide adequate protection for the payload. Normal conditions of transport (NCT) and hypothetical accident condition (HAC) evaluations, using analytic and empirical techniques, are performed to address 10 CFR 71[1] performance requirements. Analytic demonstration techniques comply with the methodology presented in NRC Regulatory Guides 7.6[2] and 7.8[3].

The HalfPACT package possesses strong similarities with the licensed TRUPACT-II package (NRC Certificate of Compliance No. 9218). All features of the HalfPACT package are essentially identical to those of the TRUPACT-II package. The only major exception is the removal of 30 inches of cylindrical sidewall length from the OCA and ICV bodies.

Numerous component and scale tests were successfully performed on the TRUPACT-II package during its development phase. Subsequent TRUPACT-II certification testing involved three, full scale certification test units (CTUs). The TRUPACT-II CTUs were subjected to a series of free drop and puncture drop tests, and two of the three TRUPACT-II CTUs were subjected to fire testing. Despite the great degree of similarity between the HalfPACT and TRUPACT-II packages, a full scale HalfPACT engineering test unit (ETU) and CTU were also subjected to a series of free drop, puncture drop, and fire tests. Both the HalfPACT ETU and CTU remained leaktight[4] throughout certification testing. Details of the certification test program are provided in Appendix 2.10.3, *Certification Tests*.

2.1 Structural Design

2.1.1 Discussion

A comprehensive discussion on the HalfPACT package design and configuration is provided in Section 1.2, *Package Description*. Specific discussions relating to the aspects important to demonstrating the structural configuration and performance to design criteria for the HalfPACT package are provided in the following sections. Standard fabrication methods are utilized to fabricate the HalfPACT packaging.

---

[1] Title 10, Code of Federal Regulations, Part 71 (10 CFR 71), *Packaging and Transportation of Radioactive Material*, 01-01-12 Edition.

[2] U. S. Nuclear Regulatory Commission, Regulatory Guide 7.6, *Design Criteria for the Structural Analysis of Shipping Cask Containment Vessels*, Revision 1, March 1978.

[3] U. S. Nuclear Regulatory Commission, Regulatory Guide 7.8, *Load Combinations for the Structural Analysis of Shipping Casks for Radioactive Material*, Revision 1, March 1989.

[4] Leaktight is defined as leakage of 1×10^{-7} standard cubic centimeters per second (scc/s), air, or less per ANSI N14.5-1997, *American National Standard for Radioactive Materials – Leakage Tests on Packages for Shipment*, American National Standards Institute, Inc. (ANSI).

2.1.1.1 Containment Vessel Structure (ICV)

The containment vessel cylindrical shell structure is fabricated in accordance with the tolerance requirements of the ASME Boiler and Pressure Vessel Code, Section III[5], Division 1, Subsection NE, Article NE-4220, as delineated on the drawings in Appendix 1.3.1, *Packaging General Arrangement Drawings*. The containment vessel shell-to-shell joints are fabricated in accordance with the ASME Boiler and Pressure Vessel Code, Section III, Division 1, Subsection NB, Article NB-4230, as delineated on the drawings in Appendix 1.3.1, *Packaging General Arrangement Drawings*.

All containment vessel heads are flanged torispherical heads, fabricated in accordance with the ASME Boiler and Pressure Vessel Code, Section VIII, Division 1[6], as delineated on the drawings in Appendix 1.3.1, *Packaging General Arrangement Drawings*.

All seal flange material is ultrasonically or radiographically test inspected in accordance with the ASME Boiler and Pressure Vessel Code, Section III, Division 1, Subsection NB, Article NB-2500 and Section V[7], Article 5 (ultrasonic) or Article 2 (radiograph), as delineated on the drawings in Appendix 1.3.1, *Packaging General Arrangement Drawings*.

Circumferential and longitudinal welds for the containment vessel shells, seal flanges, and locking ring are full penetration welds, subjected to visual and liquid penetrant examinations, and radiographically test inspected, as delineated on the drawings in Appendix 1.3.1, *Packaging General Arrangement Drawings*. Visual weld examinations are performed in accordance with AWS D1.6[8]. Liquid penetrant examinations are performed on the final pass in accordance with the ASME Boiler and Pressure Vessel Code, Section III, Division 1, Subsection NB, Article NB-5000 and Section V, Article 6. Radiograph test inspections are performed in accordance with the ASME Boiler and Pressure Vessel Code, Section III, Division 1, Subsection NB, Article NB-2500 and Section V, Article 2.

For the ICV vent port penetration, and lifting sockets, liquid penetrant examinations are performed on the final pass for single pass welds and on the root and final passes for multipass welds in accordance with the ASME Boiler and Pressure Vessel Code, Section III, Division 1, Subsection NB, Article NB-5000 and Section V, Article 6, as delineated on the drawings in Appendix 1.3.1, *Packaging General Arrangement Drawings*.

The maximum weld reinforcement for containment vessel welds shall be 3/32-inch in accordance with the ASME Boiler and Pressure Vessel Code, Section III, Division 1, Subsection NB, Article NB-4426, Paragraph NB-4426.1, as delineated on the drawings in Appendix 1.3.1, *Packaging General Arrangement Drawings*.

---

[5] American Society of Mechanical Engineers (ASME) Boiler and Pressure Vessel Code, Section III, *Rules for Construction of Nuclear Power Plant Components*, 1995 Edition, 1997 Addenda.

[6] American Society of Mechanical Engineers (ASME) Boiler and Pressure Vessel Code, Section VIII, Division 1, *Rules for Construction of Pressure Vessels*, 1995 Edition, 1997 Addenda.

[7] American Society of Mechanical Engineers (ASME) Boiler and Pressure Vessel Code, Section V, *Nondestructive Examination*, 1995 Edition, 1997 Addenda.

[8] ANSI/AWS D1.6, *Structural Welding Code – Stainless Steel*, American Welding Society (AWS).

2.1.1.2 Non-Containment Vessel Structures (OCV and OCA)

All non-containment vessel shell-to-shell joints and transitions in thickness, such as from the 1/4-inch thick OCV lower head to the 3/16-inch thick OCV shell and the 3/8-to-1/4-inch thick OCA outer shell transition, are fabricated in accordance with the ASME Boiler and Pressure Vessel Code, Section III, Division 1, Subsection NF, Article NF-4230, as delineated on the drawings in Appendix 1.3.1, *Packaging General Arrangement Drawings.*

The OCV has a top and bottom, flanged torispherical head, and the OCA outer shell has a top, flanged torispherical head and bottom, flanged flat head that are fabricated in accordance with the ASME Boiler and Pressure Vessel Code, Section VIII, Division 1, as delineated on the drawings in Appendix 1.3.1, *Packaging General Arrangement Drawings.*

Circumferential and longitudinal welds for the non-containment vessel shells are full penetration welds, subjected to visual and liquid penetrant examinations, as delineated on the drawings in Appendix 1.3.1, *Packaging General Arrangement Drawings.* Visual weld examinations are performed in accordance with AWS D1.6. Liquid penetrant examinations are performed on the final pass in accordance with the ASME Boiler and Pressure Vessel Code, Section III, Division 1, Subsection NF, Article NF-5000.

The maximum weld reinforcement for non-containment vessel welds shall be 3/32 inch in accordance with the ASME Boiler and Pressure Vessel Code, Section III, Division 1, Subsection NF, Article NF-4400, as delineated on the drawings in Appendix 1.3.1, *Packaging General Arrangement Drawings.*

2.1.2 Design Criteria

Proof of performance for the HalfPACT package is achieved by a combination of analytic and empirical evaluations. The acceptance criteria for analytic assessments are in accordance with Regulatory Guide 7.6 and Section III of the ASME Boiler and Pressure Vessel Code. The acceptance criterion for empirical assessments is a demonstration that the containment boundary remains leaktight throughout NCT and HAC certification testing. Additionally, package deformations obtained from certification testing must be such that deformed geometry assumptions used in subsequent thermal, shielding, and criticality evaluations are validated.

The remainder of this section presents the detailed acceptance criteria used for all analytic structural assessments of the HalfPACT package.

2.1.2.1 Analytic Design Criteria (Allowable Stresses)

This section defines the stress allowables for primary membrane, primary bending, secondary, shear, peak, and buckling stresses for containment and non-containment structures. These stress allowables are used for all analytic assessments of HalfPACT package structural performance. Regulatory Guide 7.6 is used in conjunction with Regulatory Guide 7.8 to evaluate the package integrity. Material yield strengths used in the analytic acceptance criteria, S_y, ultimate strengths, S_u, and design stress intensity values, S_m, are presented in Table 2.3-1 of Section 2.3, *Mechanical Properties of Materials.*

2.1.2.1.1 Containment Structure (ICV)

A summary of allowable stresses used for containment structures is presented in Table 2.1-1. These data are consistent with Regulatory Guide 7.6, and the ASME Boiler and Pressure Vessel Code, Section III, Subsection NB-3000 and Appendix F.

2.1.2.1.2 Non-Containment Structures (OCV and OCA)

A summary of allowable stresses used for non-containment structures is presented in Table 2.1-2. For conservatism, the allowable stresses applicable to containment structures presented in Table 2.1-1 are utilized for OCV evaluations.

For evaluation of lifting devices, the allowable stresses are limited to one-third of the material yield strength, consistent with the requirements of 10 CFR §71.45(a). For evaluation of tie-down devices, the allowable stresses are limited to the material yield strength, consistent with the requirements of 10 CFR §71.45(b).

For evaluations involving polyurethane foam, primary, load controlled compressive stresses are limited to two-thirds of the parallel-to-rise or perpendicular-to-rise compressive strength (as applicable) at 10% strain. Use of a two-thirds factor on compressive strength ensures elastic behavior of the polyurethane foam.

2.1.2.2 Miscellaneous Structural Failure Modes

2.1.2.2.1 Brittle Fracture

By avoiding the use of ferritic steels in the HalfPACT packaging, brittle fracture concerns are precluded. Specifically, most primary structural components are fabricated of Type 304 austenitic stainless steel. Since this material does not undergo a ductile-to-brittle transition in the temperature range of interest (down to -40 °F), it is safe from brittle fracture.

The lock bolts used to secure the ICV and OCV locking rings in the locked position are stainless steel, socket head cap screws ensuring that brittle fracture is not of concern. Other fasteners used in the HalfPACT packaging assembly, such as the 36, 1/4-inch screws attaching the locking Z-flange to the OCV locking ring, provide redundancy and are made from stainless steel, again eliminating brittle fracture concerns.

2.1.2.2.2 Fatigue Assessment

2.1.2.2.2.1 Normal Operating Cycles

Normal operating cycles do not present a fatigue concern for the various HalfPACT packaging components. Most HalfPACT packaging components exhibit little-to-no stress concentrations, and by satisfying the allowable limit for range of primary-plus-secondary stress intensity for NCT ($3.0S_m$), the allowable fatigue stress limit for the expected number of operating cycles is satisfied. For HalfPACT packaging components that do exhibit stress concentrations, stresses are low enough that allowable fatigue stress limits are again satisfied.

The maximum number of operating cycles reasonably expected for the HalfPACT package is 3,640, and is based on two round trips per week for 35 years. Conservatively, 5,000 cycles (or in excess of 1 cycle every 3 days) is used in the following calculations. A cycle is defined as the process of the internal pressure within the ICV increasing gradually from zero psig at the time of

loading, to 50 psig (the maximum normal operating pressure, MNOP, per Section 3.4.4, *Maximum Internal Pressure*) during transport and then returning to 0 psig when the containment vessel is vented prior to unloading the payload. This scenario is conservative because most shipments will never generate pressure to the magnitude of the MNOP, and the system could never achieve MNOP in less than the assumed transportation cycle of three days.

From Figure I-9.2.1 and Table I-9.1 of the ASME Boiler and Pressure Vessel Code[9], the fatigue allowable alternating stress intensity amplitude, S_a, for 5,000 cycles is 76,000 psi. This value, when multiplied by the ratio of elastic hot NCT modulus at 160 °F (the package wall temperature from Section 2.6.1, *Heat*) to a modulus at 70 °F, $27.8(10)^6/28.3(10)^6$, results in a fatigue allowable alternating stress intensity amplitude at 160 °F of 74,657 psi. The non-fatigue allowable stress intensity range, from the ASME Boiler and Pressure Vessel Code, Section III, Division 1, Subsection NB-3222.2, is 60,000 psi ($3.0S_m$, where S_m is 20,000 psi from Table 2.3-1 in Section 2.3, *Mechanical Properties of Materials*, at 160 °F). The alternating stress intensity is one-half of this range, or 30,000 psi. Thus, in the absence of stress concentrations, the fatigue allowable alternating stress intensity will not govern the HalfPACT packaging design.

Regions of stress concentrations for the package occur in the ICV and OCV seal flanges and locking rings. The maximum range of primary-plus-secondary stress intensity occurs between the case of maximum internal pressure under NCT hot conditions (see Section 2.6.1.3, *Stress Calculations*) and the vacuum case. For the seal flanges or locking rings the maximum primary-plus-secondary stress intensity is 27,922 psi from Table 2.6-5 (ICV Load Case 1). The stress range is therefore 27,922 psi.

In accordance with Paragraph C.3 of Regulatory Guide 7.6, a stress concentration factor of four will conservatively be applied to the value of maximum stress intensity from above. The resultant range of peak stress intensity, correcting the modulus of elasticity for temperature, becomes:

$$S_{range} = (27{,}922)(4)\left(\frac{28.3(10)^6}{27.8(10)^6}\right) = 113{,}697 \text{ psi}$$

where the modulus of elasticity at 70 °F is $28.3(10)^6$ psi, and the modulus of elasticity at 160 °F is $27.8(10)^6$ psi, both from Table 2.3-1 in Section 2.3, *Mechanical Properties of Materials*. The alternating stress intensity is one-half of this range, or:

$$S_{alt} = \left(\frac{1}{2}\right)113{,}697 = 56{,}849 \text{ psi}$$

From Figure I-9.2.1 and Table I-9.1 of the ASME Boiler and Pressure Vessel Code, the allowable number of cycles for an alternating stress intensity amplitude of 56,849 psi is 16,627, or 233% more than the 5,000 cycles conservatively considered herein.

2.1.2.2.2.2 Normal Vibration Over the Road

Fatigue associated with normal vibration over the road is addressed in Section 2.6.5, *Vibration*.

[9] American Society of Mechanical Engineers (ASME) Boiler and Pressure Vessel Code, Section III, *Rules for Construction of Nuclear Power Plant Components*, Appendix I, *Design Stress Intensity Values, Allowable Stresses, Material Properties, and Design Fatigue Curves*, 1995 Edition, 1997 Addenda.

2.1.2.2.2.3 Extreme Total Stress Intensity Range

Per paragraph C.7 of Regulatory Guide 7.6:

> The extreme total stress intensity range (including stress concentrations) between the initial state, the fabrication state, the normal operating conditions, and the accident conditions should be less than twice the adjusted value (adjusted to account for modulus of elasticity at the highest temperature) of S_a at 10 cycles given by the appropriate design fatigue curves.

Since the response of the HalfPACT package to accident conditions is typically evaluated empirically rather than analytically, the extreme total stress intensity range has not been quantified. However, the full scale certification test unit (see Appendix 2.10.3, *Certification Tests*) was tested at relatively low ambient temperatures during free drop and puncture testing, as well as exposure to a fully engulfing pool fire event. The CTU was also fabricated in accordance with the drawings in Appendix 1.3.1, *Packaging General Arrangement Drawings*, thus incurring prototypic fabrication induced stresses, increased internal pressure equal to 150% of MNOP during fabrication pressure testing, and reduced internal pressure (i.e., a full vacuum during leak testing) conditions as part of initial acceptance. Exposure to these extreme conditions while demonstrating leaktight containment resulting from certification testing satisfies the intent of the previously defined extreme total stress intensity range requirement.

2.1.2.2.3 Buckling Assessment

Buckling, per Regulatory Guide 7.6, is an unacceptable failure mode for the ICV. The intent of this provision is to preclude large deformations that would compromise the validity of linear analysis assumptions and quasi-linear stress allowables, as given in Paragraph C.6 of Regulatory Guide 7.6.

Buckling prevention criteria is applicable to the ICV containment boundary within the HalfPACT packaging. For conservatism, the criteria is also applied to the OCV confinement boundary. Shells for both vessels incorporate cylindrical mid-sections with torispherical heads at each end. The different geometric regions are considered separately to demonstrate that buckling will not occur for the two vessels. The methodology of ASME Boiler and Pressure Vessel Code Case N-284-1[10] is applied for the cylindrical regions of the containment and confinement vessels (buckling analysis details are provided in Section 2.7.6, *Immersion – All Packages*). The methodology of the ASME Boiler and Pressure Vessel Code, Section III, Subsection NE, is applied for the torispherical heads.

Consistent with Regulatory Guide 7.6 philosophy, factors of safety corresponding to ASME Boiler and Pressure Vessel Code, Level A and Level D service conditions are employed for NCT and HAC loadings, respectively, with factors of safety of 2.00 and 1.34, respectively.

It is also noted that 30-foot drop tests performed on full scale models with the package in various orientations produced no evidence of buckling of any of the ICV and OCV shells (see Appendix 2.10.3, *Certification Tests*). Certification testing does not provide a specific determination of the margin of safety against buckling, but is considered as evidence that buckling will not occur.

---

[10] American Society of Mechanical Engineers (ASME) Boiler and Pressure Vessel Code, Section III, *Rules for Construction of Nuclear Power Plant Components*, Division 1, Class MC, Code Case N-284-1, *Metal Containment Shell Buckling Design Methods*, 1995 Edition, 1997 Addenda.

Table 2.1-1 – Containment Structure Allowable Stress Limits

Stress Category	NCT	HAC
General Primary Membrane Stress Intensity	S_m	Lesser of: $2.4S_m$, $0.7S_u$
Local Primary Membrane Stress Intensity	$1.5S_m$	Lesser of: $3.6S_m$, S_u
Primary Membrane + Bending Stress Intensity	$1.5S_m$	Lesser of: $3.6S_m$, S_u
Range of Primary + Secondary Stress Intensity	$3.0S_m$	Not Applicable
Pure Shear Stress	$0.6S_m$	$0.42S_u$
Peak	Per Section 2.1.2.2.2, *Fatigue Assessment*	
Buckling	Per Section 2.1.2.2.3, *Buckling Assessment*	

Table 2.1-2 – Non-Containment Structure Allowable Stress Limits

Stress Category	NCT	HAC
General Primary Membrane Stress Intensity	Greater of: S_m, S_y	$0.7S_u$
Local Primary Membrane Stress Intensity	Greater of: $1.5S_m$, S_y	S_u
Primary Membrane + Bending Stress Intensity	Greater of: $1.5S_m$, S_y	S_u
Range of Primary + Secondary Stress Intensity	Greater of: $3.0S_m$, S_y	Not Applicable
Pure Shear Stress	Greater of: $0.6S_m$, $0.6S_y$	$0.42S_u$
Peak	Per Section 2.1.2.2.2, *Fatigue Assessment*	
Buckling	Per Section 2.1.2.2.3, *Buckling Assessment*	

This page intentionally left blank.

2.2 Weights and Centers of Gravity

The maximum gross weight of the HalfPACT package, including a maximum payload weight of 7,600 pounds, is 18,100 pounds. The vertical center of gravity (CG) is situated 43.8 inches above the bottom surface of the package. These values are used in the lifting and tie-down calculations presented in Section 2.5, *Lifting and Tie-down Standards for All Packages*. These results are based on an assumption of a payload configuration consisting of seven, 1,000 pound, 55-gallon drums having their individual CGs located at the drum mid-height. All other payload configurations result in a lower, package gross weight and CG than the 55-gallon drum payload configuration. With reference to Figure 2.2-1, a detailed breakdown of the HalfPACT package component weights and CG is summarized in Table 2.2-1. The five-inch thick payload spacer is used with the 55-gallon drum, short 85-gallon drum, 100-gallon drum, and standard waste box (SWB) payload configurations. The shielded container payload configuration utilizes a triangular payload pallet, an upper and lower axial dunnage assembly, and a radial dunnage assembly in lieu of the payload pallet and payload spacer utilized for drums and the SWB.

2.2.1 Effect of a Radial Payload Imbalance

A radial offset of the CG could occur if the payload drums do not all have the same weight, or if the SWB is not uniformly loaded. The maximum offset of the radial CG is calculated in the following paragraphs.

Seven 55-Gallon Drum Payload Configuration:

Since the maximum weight of any one drum is 1,000 pounds, and since the arrangement of seven drums is symmetric, the maximum payload weight can be associated only with a payload CG located on the package centerline. Deviation from the package centerline can only occur with a less-than-maximum total payload weight. The worst case CG offset occurs for an arrangement of four minimum weight (empty) 55-gallon drums, each having a weight of 60 pounds, together with three maximum weight (fully loaded) 55-gallon drums, each having a weight of 1,000 pounds, located in adjacent outside positions, as illustrated in Figure 2.2-2. A 55-gallon drum has a nominal outer diameter of 24 inches. For this case, the worst case radial location of the payload CG is:

$$\bar{r} = \frac{(24.00)(1{,}000) + 2(12.00)(1{,}000) + (0)(60) - 2(12.00)(60) - (24.00)(60)}{3\,(1{,}000) + 4(60)} = 13.93 \; inches$$

The pipe overpack and criticality control overpack payload configurations, since they are enclosed and centered by dunnage within a 55-gallon drum, are enveloped by the foregoing considerations. For an empty package weight of 10,500 pounds, a payload pallet weight of 350 pounds, and a payload spacer weight of 250 pounds, (see Table 2.2-1), the worst case radial offset of the CG of the entire HalfPACT package is:

$$\bar{R} = \frac{(13.93)[3(1{,}000) + 4(60)]}{10{,}500 + 350 + 250 + 3(1{,}000) + 4(60)} = 3.15 \text{ inches}$$

This radial offset equates to only 3.3% of the HalfPACT package's outer diameter of 94⅜ inches. The effect of this relatively small radial offset may be neglected.

Standard Waste Box Payload Configuration:

The maximum weight of a loaded SWB is 4,000 pounds; the weight of an empty SWB is 640 pounds. The maximum contents therefore amount to 4,000 - 640 = 3,360 pounds. The CG of the contents is conservatively assumed to be located at a distance of 17.75 inches from the geometric center (i.e., one-quarter the SWB length), as shown in Figure 2.2-3. For this case, the worst case radial location of the payload CG is:

$$\bar{r} = \frac{(17.75)(3,360)}{4,000} = 14.9 \text{ inches}$$

For an empty package weight of 10,500 pounds and a payload spacer weight of 250 pounds, (see Table 2.2-1), the maximum radial offset of the CG of the entire HalfPACT is:

$$\bar{R} = \frac{(14.9)(4,000)}{10,500+250+4,000} = 4.04 \text{ inches}$$

This radial offset equates to only 4.3% of the HalfPACT package's outer diameter of 94⅜ inches. As before, the effect of this relatively small radial offset may be neglected.

Four 85-Gallon Drum Payload Configuration:

The term "85-gallon drum" refers to drums of 75 to 88 gallons, as discussed in Section 1.1, *Introduction*. As for the 55-gallon drum payload configuration, the maximum weight of a loaded 85-gallon drum is 1,000 pounds. The worst case CG offset occurs for an arrangement of two minimum weight (empty), tall 85-gallon drums, each having a weight of approximately 81 pounds, together with two maximum weight (fully loaded), tall 85-gallon drums, each having a weight of 1,000 pounds, located adjacent, as illustrated in Figure 2.2-4. A tall 85-gallon drum has a nominal outer diameter of 28⅝ inches. For this case, the worst case radial location of the payload CG is:

$$\bar{r} = \frac{2(14.31)(1,000) - 2(14.31)(81)}{2(1,000) + 2(81)} = 12.2 \text{ inches}$$

For an empty package weight of 10,500 pounds, a payload pallet weight of 350 pounds, and a payload spacer weight of 250 pounds, (see Table 2.2-1), the maximum radial offset of the CG of the entire HalfPACT is:

$$\bar{R} = \frac{(12.2)[2(1,000) + 2(81)]}{10,500+350+2(1,000)+2(81)} = 2.03 \text{ inches}$$

This radial offset equates to only 2.1% of the HalfPACT package's outer diameter of 94⅜ inches. As before, the effect of this relatively small radial offset may be neglected.

Three 100-Gallon Drum Payload Configuration:

As for the 55-gallon drum payload configuration, the maximum weight of a loaded 100-gallon drum is 1,000 pounds. The worst case CG offset occurs for an arrangement of two minimum weight (empty), 100-gallon drums, each having a weight of 95 pounds, together with one maximum weight (fully loaded), 100-gallon drum of 1,000 pounds, as illustrated in Figure 2.2-5.

A 100-gallon drum has a nominal outer diameter of 32 inches. For this case, the worst case radial location of the payload CG is:

$$\bar{r} = \frac{(18.48)(1{,}000) - 2(9.24)(95)}{1{,}000 + 2(95)} = 14.1 \text{ inches}$$

For an empty package weight of 10,500 pounds, a payload pallet weight of 350 pounds, and a payload spacer weight of 250 pounds, (see Table 2.2-1), the maximum radial offset of the CG of the entire HalfPACT is:

$$\bar{R} = \frac{(14.1)[1{,}000 + 2(95)]}{10{,}500 + 350 + 250 + 1{,}000 + 2(95)} = 1.37 \text{ inches}$$

This radial offset equates to only 1.5% of the HalfPACT package's outer diameter of 94⅜ inches. As before, the effect of this relatively small radial offset may be neglected.

Three Shielded Container Payload Configuration:

The maximum weight of a loaded shielded container is 2,260 pounds; the weight of an empty shielded container is 1,726 pounds. The worst case CG offset occurs for an arrangement of two minimum weight (empty), shielded containers, each having a weight of 1,726 pounds, together with one maximum weight (fully loaded), shielded container of 2,260 pounds, as illustrated in Figure 2.2-6. A shielded container has a nominal outer diameter of 23 inches. For this case, the worst case radial location of the payload CG is:

$$\bar{r} = \frac{(13.28)(2{,}260) - 2(6.64)(1{,}726)}{2{,}260 + 2(1{,}726)} = 1.24 \text{ inches}$$

For an empty package weight of 10,500 pounds, a triangular payload pallet weight of 112 pounds, an upper and lower axial dunnage weight of 132 pounds each, and a radial dunnage weight of 444 pounds, (see Table 2.2-1), the maximum radial offset of the CG of the entire HalfPACT is:

$$\bar{R} = \frac{(1.24)[2{,}260 + 2(1{,}726)]}{10{,}500 + 112 + 2(132) + 444 + 2{,}260 + 2(1{,}726)} = 0.42 \text{ inches}$$

This radial offset equates to only 0.4% of the HalfPACT package's outer diameter of 94⅜ inches. As before, the effect of this relatively small radial offset may be neglected.

2.2.2 Effect of an Axial Payload Imbalance

The maximum height of the package CG is associated with a uniformly loaded payload, where the CG of the payload containers is located at their mid-height. Due to a payload of non-uniform density or possible settling of the payload contents, the CG height of the payload containers may decrease somewhat. The seven 55-gallon drum payload configuration, since it is the heaviest payload, will result in greatest potential shift in axial CG. The greatest shift in location of the CG of an individual drum is bounded by one-quarter of the drum height, i.e., a shift from the drum mid-height to the quarter height. Thus, for a total 55-gallon drum height of 35 inches, the axial shift is 35/4 = 8.75 inches downward. Since the empty weight of a 55-gallon drum is 60 pounds, the maximum weight of contents of one drum is 1,000 - 60 = 940 pounds. The

greatest downward shift in CG location of the HalfPACT packaging, assuming the CG location of all seven drums is at one quarter of the drum height instead of at mid-height, therefore is:

$$\Delta\bar{h} = \frac{7(8.75)(940)}{18{,}100} = 3.2 \text{ inches}$$

The axial offset amounts to only 3.5% of the total HalfPACT package height of 91½ inches. The effect of this relatively small axial offset may be neglected. As an example, in the case of a hypothetical accident condition (HAC) puncture event where the puncture bar axis passes through the CG of the HalfPACT package, the variation in CG location of 3.2 inches slightly exceeds half the puncture bar diameter resulting in a variation of the puncture bar orientation of less than 4 degrees. In addition, vertical reduction of the CG would have no effect on lifting forces, and would serve to reduce tie-down forces. Therefore, the lifting and tie-down calculations, and the HAC free drop and puncture tests, are performed using a value that bounds the maximum CG height presented in Table 2.2-1, and the downward axial offset is conservatively neglected.

Table 2.2-1 – HalfPACT Weight and Center of Gravity

Item	Weight, pounds		Height to CG, inches①	
	Component	Assembly	Component	Assembly
Outer Confinement Assembly (OCA)		8,250		41.2
• Lid	3,600		67.1	
• Body	4,650		21.2	
Inner Containment Vessel (ICV)		2,250		47.3
• Lid	825		66.5	
• Body	1,225		34.9	
• Aluminum Honeycomb Spacers	200		43.5	
Total Empty Package		10,500		42.5
Payload and Payload Components		7,600		45.5
• Payload (Seven 55-Gallon Drums)	7,000		46.6	
• Payload Pallet	350		40.2	
• Payload Spacer	250		23.6	
Total Loaded Package (Maximum)		18,100		43.8
Payload and Payload Components		7,600		44.2
• Payload (Three Shielded Containers)	6,780		44.5	
• Triangular Payload Pallet	112		25.1	
• Axial Dunnage Assemblies	264		43.0	
• Radial Dunnage Assembly	444		44.5	
Total Load Package (Maximum)		18,100		43.2

Note:

① The reference datum is the bottom of the HalfPACT package.

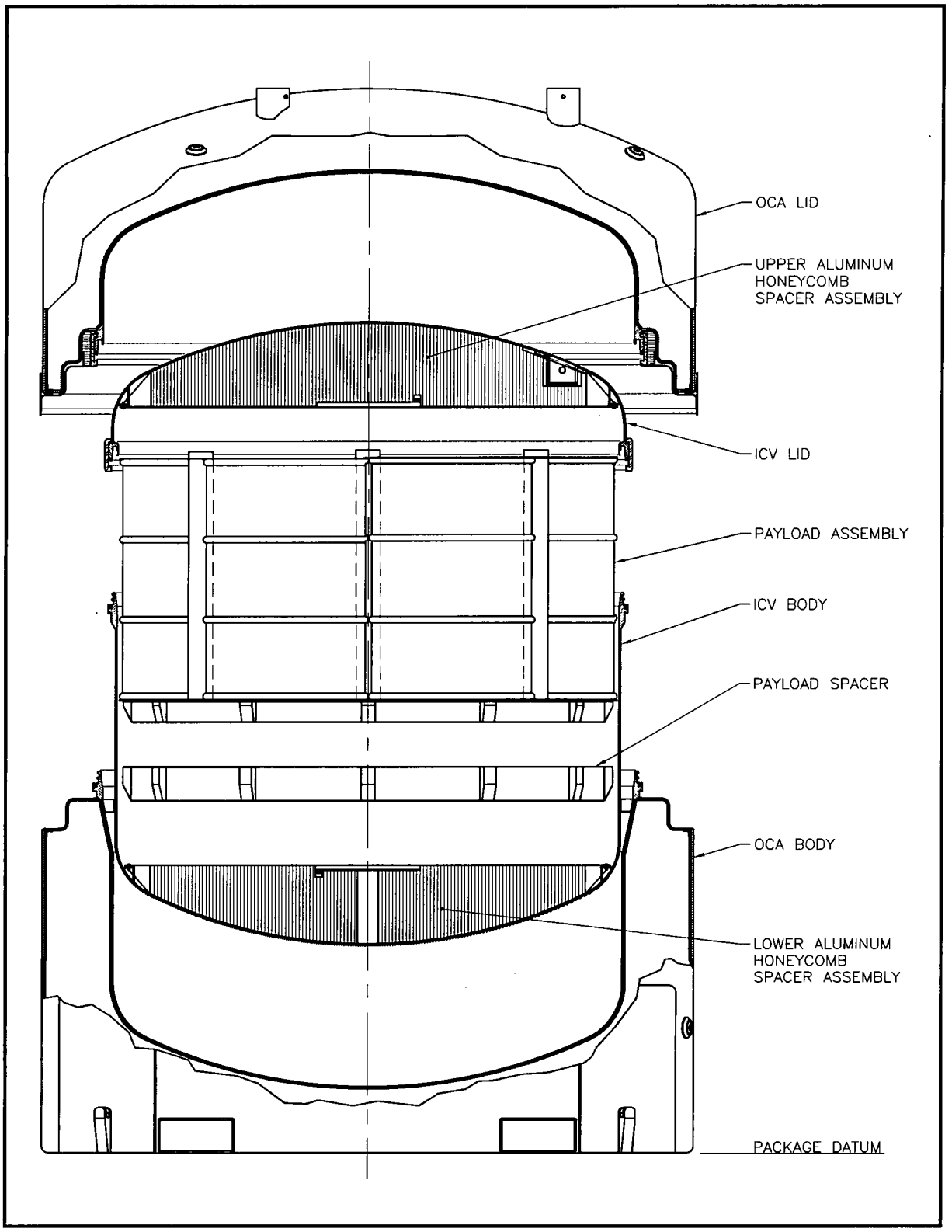

Figure 2.2-1 – HalfPACT Package Components

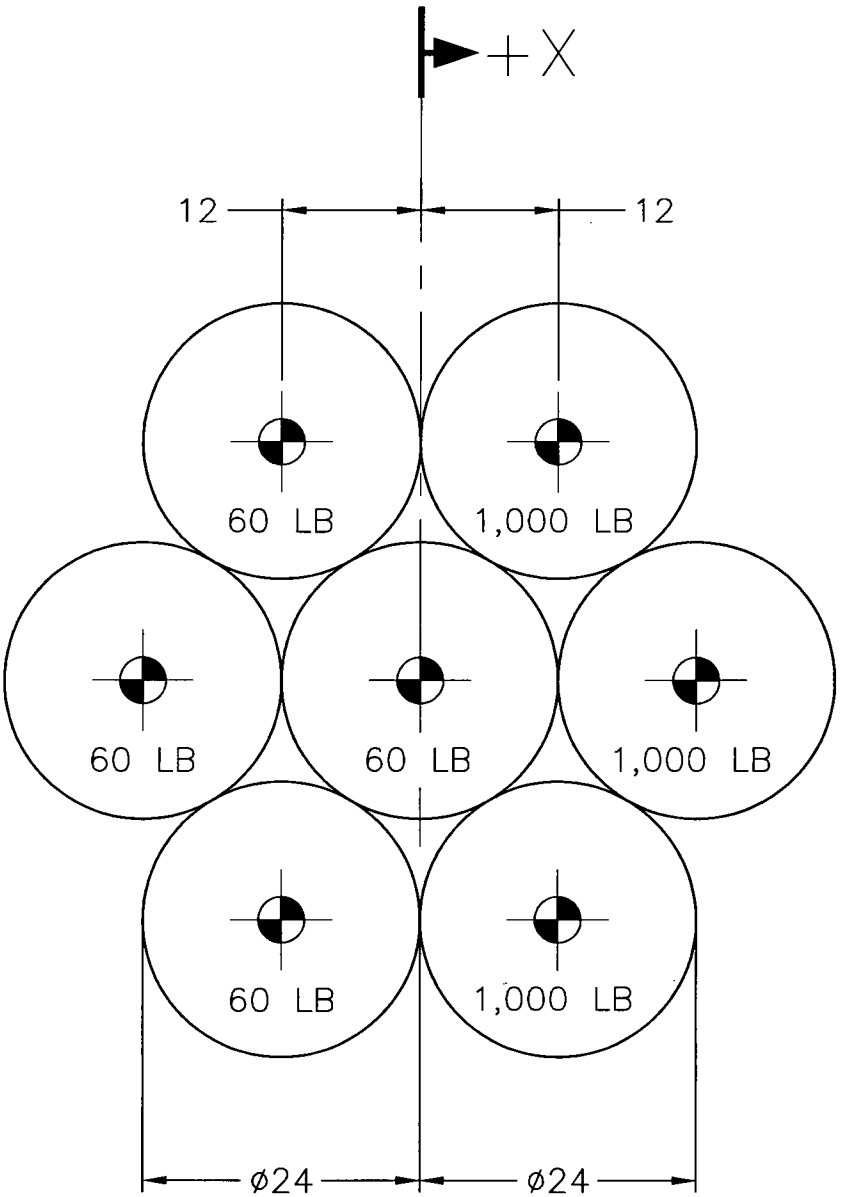

Figure 2.2-2 – Radial Shift of CG for Seven 55-Gallon Drum Payload

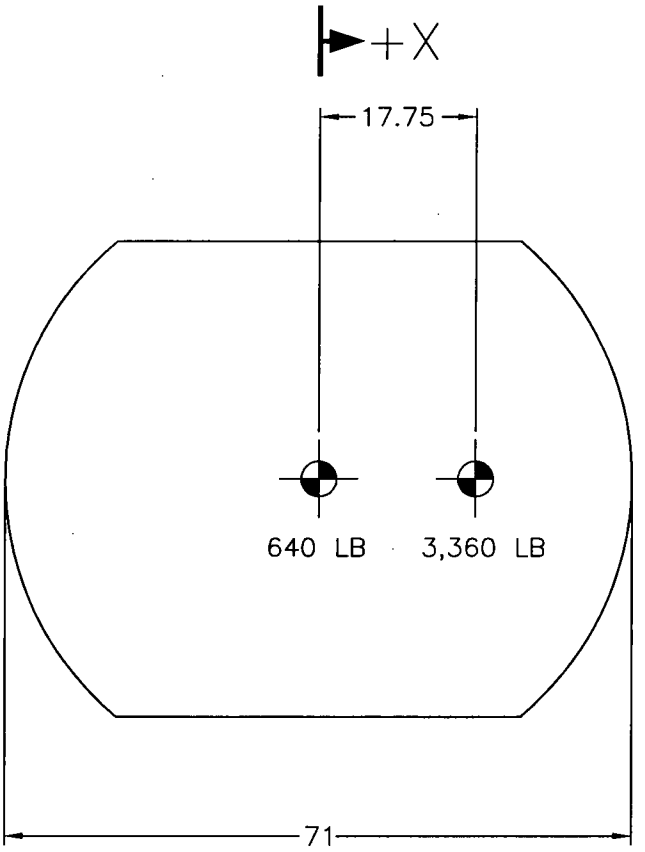

Figure 2.2-3 – Radial Shift of CG for SWB Payload

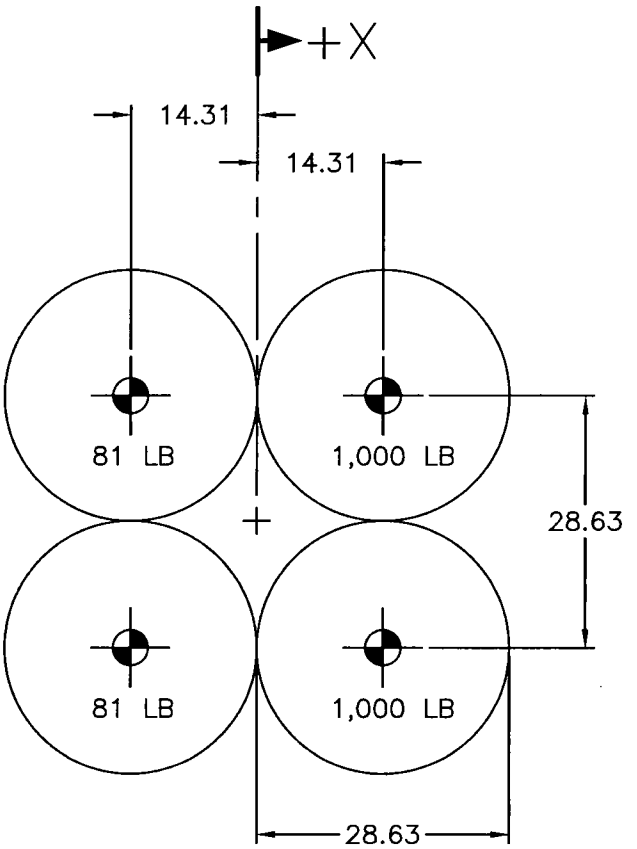

Figure 2.2-4 – Radial Shift of CG for Four 85-Gallon Drum Payload

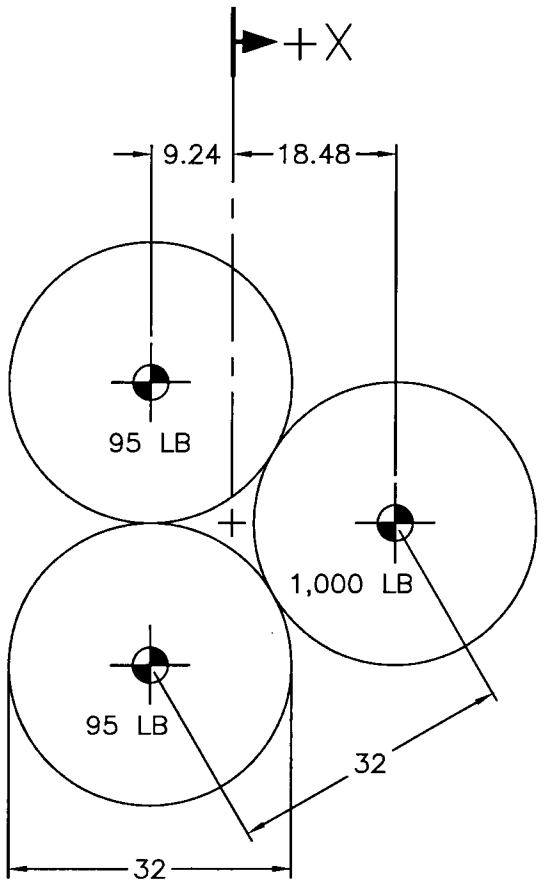

Figure 2.2-5 – Radial Shift of CG for Three 100-Gallon Drum Payload

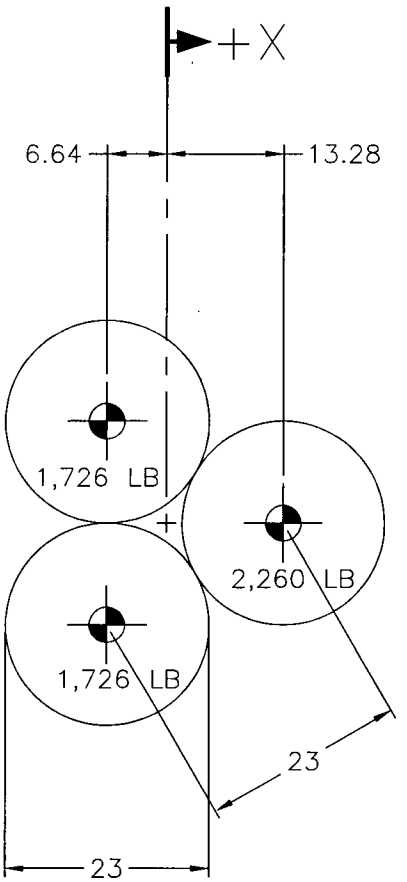

Figure 2.2-6 – Radial Shift of CG for Three Shielded Container Payload

This page intentionally left blank.

2.3 Mechanical Properties of Materials

The major structural components, i.e., the outer confinement assembly (OCA) outer shells, outer confinement vessel (OCV), and inner containment vessel (ICV), of the HalfPACT packaging are fabricated of Type 304, austenitic stainless steel and 8¼ lb/ft^3 (nominal density) polyurethane foam. Other materials performing a structural function are ASTM B16 brass (for the ICV and OCV vent port and seal test port plugs and covers), aluminum honeycomb (for the ICV aluminum honeycomb spacer assemblies), 300 series stainless steel (for the ICV and OCV locking ring lock bolts, and for attaching the locking Z-flange to the OCV locking ring), and ASTM A564, Type 630, stainless steel (joint pins for the OCV and ICV locking rings). Several varieties of non-structural materials are also utilized. Representative non-structural materials include butyl rubber and other elastomeric O-ring seals, a silicone wear pad, aluminum guide tubes for the OCA lid lift operation, ceramic fiber paper, fiberglass insulation, and plastic fire consumable foam cavity vent plugs. The drawings presented in Appendix 1.3.1, *Packaging General Arrangement Drawings*, delineate the specific material(s) used for each HalfPACT packaging component.

The remainder of this section presents and discusses pertinent mechanical properties for the materials that perform a structural function. Section 2.3.1, *Mechanical Properties Applied to Analytic Evaluations*, presents all properties used in analytic structural evaluations of the HalfPACT package. Most normal conditions of transport (NCT) tests are demonstrated analytically. Section 2.3.2, *Mechanical Properties Applied to Certification Testing*, presents the mechanical properties associated with components whose performance is demonstrated via certification testing. With the exception of immersion, all hypothetical accident condition (HAC) tests are demonstrated via certification testing.

2.3.1 Mechanical Properties Applied to Analytic Evaluations

Analytic evaluations are performed for the basic OCA, OCV, and ICV shells, seal flanges, and locking rings, comprised of Type 304 stainless steel. Table 2.3-1 presents the mechanical properties for the Type 304 stainless steel used in the HalfPACT packaging. Each of the mechanical properties of Type 304 stainless steel is taken from Section II, Parts A and D, of the ASME Boiler and Pressure Vessel Code.[1]

All analyses of the basic OCA, OCV, and ICV shells, seal flanges and locking rings utilize the properties presented for ASTM A240, Type 304, stainless steel. With the exception of elongation, which is not specifically used in the linear elastic analytic assessments, all materials presented in Table 2.3-1 exhibit equivalent or better properties than the ASTM A240 material. Minimum elongation values are important regarding testing and are therefore discussed in Section 2.3.2, *Mechanical Properties Applied to Certification Testing*. The density of stainless steel is taken as 0.29 lb/in^3, and Poisson's Ratio is 0.3.

Unlike the other ASTM materials specified in Table 2.3-1, ASTM A276 material does not have an identical ASME material specification. However, structural use of ASTM A276 is as an option for the OCA rolled angles used at the lid-to-body interface and the OCA lid lifting straps.

[1] American Society of Mechanical Engineers (ASME) Boiler and Pressure Vessel Code, Section II, *Materials, Part A – Ferrous Material Specifications*, and *Materials, Part D – Properties*, 1995 Edition, 1997 Addenda.

As these components are not part of the containment boundary, the use of ASTM A276, whose chemical and mechanical properties are identical to ASTM A479, is justified. Thus, material properties of ASTM A276 versus temperature are taken to be the same as for ASTM A479.

The analytic assessments of the polyurethane foam used in the HalfPACT packaging are limited to the NCT internal pressure, differential thermal expansion, and lifting load cases. The data summarized in Table 2.3-2 are established according to the procedures outlined in Section 8.1.4.1, *Polyurethane Foam*. Detailed stress-strain relationships for the polyurethane foam are not required for analysis since analytic assessments for the NCT or HAC free drop or puncture events are not performed. However, as discussed in Section 2.3.2, *Mechanical Properties Applied to Certification Testing*, since HalfPACT package performance is demonstrated by certification testing, and performance is a function of foam properties, compressive stress-strain characteristics and installation techniques are carefully controlled.

Material properties are linearly interpolated between, or, if necessary, extrapolated beyond the temperature values shown. For example, when a temperature outside a tabulated range is of interest (e.g., low temperature properties to -40 °F), data are extrapolated. When a particular analysis requires data extrapolation, it is identified within the applicable section of this chapter.

2.3.2 Mechanical Properties Applied to Certification Testing

The primary means of demonstrating the structural performance capabilities of the HalfPACT packaging under imposed NCT and HAC free drops, puncture, and thermal (fire) events is via certification testing. The overall response of the HalfPACT packaging to these events is dependent on the characteristics of several structural components. The characteristics of the polyurethane foam used in the OCA are of primary importance regarding HalfPACT package performance. For this reason, the method of installation of the foam material into the OCA, and the foam's compressive stress-strain characteristics are carefully controlled and monitored. Section 8.1.4.1, *Polyurethane Foam*, presents the details associated with foam installation and performance testing. Importantly, all HalfPACT packages will respond similarly to free drop, puncture, and thermal events. Thermal performance of the foam is discussed in Section 3.2, *Summary of Thermal Properties of Materials*.

At the time of polyurethane foam installation, test samples are retained from each foam pour, as discussed in Section 8.1.4.1, *Polyurethane Foam*. Using these samples, each foam pour is tested for compressive strength at strains of 10%, 40%, and 70%, both parallel and perpendicular to the direction of foam rise. To be acceptable, the average compressive strength of all tested samples from a single foamed component (i.e., the OCA lid or OCA body) for a particular rise direction is to fall within ±15% of the corresponding nominal compressive stress. Additionally, the stress value of any single test specimen from a single pour is to fall within ±20% of the corresponding nominal compressive stress.

In addition to controls on foam compressive stress, OCA foam thicknesses are controlled by the tolerances shown on the drawings provided in Appendix 1.3.1, *Packaging General Arrangement Drawings*. The foam thickness tolerance at the OCA top and sides is set at approximately ±5% of the nominal thickness. In regions where foam strains are very small (e.g., bottom end), a slightly greater thickness tolerance (approximately ±8%) is allowed. The thickness tolerance is set at approximately one-third the magnitude of the compressive stress tolerance to minimize the effect on package performance in the unlikely event that both tolerances are simultaneously at their

extreme values in a given HalfPACT packaging assembly. Importantly, in the unlikely event that compressive stress and thickness tolerances are simultaneously at their worst case extremes, the net effect of combining the two tolerances is nearly identical to the compressive stress tolerance acting alone. This is directly attributable to the fact that a long portion of the compressive stress-strain curve for foam (at strains of ~50% or less) exhibits a relatively shallow slope (i.e., "plateau"). Consequently, although small changes in foam thickness directly affect foam strains, small changes in strain while on the plateau portion of the stress-strain curve do not significantly affect stress. As demonstrated by testing (documented in Appendix 2.10.3, *Certification Tests*), the HalfPACT packaging deformations due to 30-foot free drops were relatively small, demonstrating that resultant foam strains remained within the "plateau" portion of the compressive stress-strain curve.

In addition to the polyurethane foam, the performance of other primary HalfPACT packaging structural components is addressed by certification testing rather than by analysis. These components include the ASTM B16, Alloy 360, half-hard temper, brass vent port plugs, the ICV upper and lower aluminum honeycomb spacer assemblies, the 300 series stainless steel socket head cap screws used to secure the locking rings in the locked position, the ASTM A564, Type 630, Condition 1150, stainless steel pins used in the locking ring joints, and the 1/4-inch, 300 series stainless steel pan head screws used to attach the locking Z-flange to the OCV locking ring. As indicated above, and on the drawings provided in Appendix 1.3.1, *Packaging General Arrangement Drawings*, each of these components has a specific material callout thereby providing a specific control on its mechanical properties. The structurally significant mechanical properties for these materials are presented in Table 2.3-3.

With the exception of the aluminum honeycomb spacer assemblies, the 1/4-inch stainless steel pan head screws, and the OCV lock bolts, all of the above components remained intact during certification testing, and showed essentially no evidence of distress. By design, the aluminum honeycomb spacer assemblies were partially crushed as a result of the certification test program, but still provided adequate protection for the ICV torispherical heads from the simulated payload of seven, rigid, concrete-filled, 55-gallon drums.

The optional use of Type 304 stainless steel forgings or castings instead of ASTM A240 plate material for the OCV and ICV seal flanges and locking rings is stated on the drawings provided in Appendix 1.3.1, *Packaging General Arrangement Drawings*. As shown in Table 2.3-1, the ASTM A182 forging option and ASTM A351 casting option provide equivalent or improved strength, but a somewhat reduced elongation than does the ASTM A240. The reduced elongation values (30% for ASTM A182 and 35% for ASTM A351 versus 40% for ASTM A240 material) are acceptable based on the results of the certification testing program. Relatively little permanent deformation was observed for the OCV or ICV seal flanges and locking rings as a result of certification testing, indicating that strains were well below the 30% minimum elongation provided by any of the specified materials. Any of the three material options are therefore acceptable for fabricating HalfPACT packagings.

This page intentionally left blank.

Table 2.3-1 – Mechanical Properties of Type 304 Stainless Steel Components (for Analysis)

Material Specification	① Minimum Elongation (%)	Temperature (°F)	② Yield Strength, S_y ($\times 10^3$ psi)	③ Ultimate Strength, S_u ($\times 10^3$ psi)	④ Allowable Strength, S_m ($\times 10^3$ psi)	⑤ Elastic Modulus, E ($\times 10^6$ psi)	⑥ Thermal Expansion Coefficient, α ($\times 10^{-6}$ in/in/°F)
ASTM A213	35	≤ -20	30.0	75.0	20.0	28.8⑦	8.21⑦
ASTM A240	40	70	30.0	75.0	20.0	28.3	-----
ASTM A312	30	100	30.0	75.0	20.0	-----	8.55
ASTM A376	25	200	25.0	71.0	20.0	27.6	8.79
ASTM A479	30	300	22.5	66.0	20.0	27.0	9.00
Type 304		400	20.7	64.4	18.7	26.5	9.19
ASTM A182 Type F304 (<5 inch thick)	30	-20	30.0	75.0	20.0	28.8⑦	8.21⑦
		70	30.0	75.0	20.0	28.3	-----
		100	30.0	75.0	20.0	-----	8.55
		200	25.0	71.0	20.0	27.6	8.79
		300	22.5	66.0	20.0	27.0	9.00
		400	20.7	64.4	18.7	26.5	9.19
ASTM A351 Grade CF8A	35	-20	35.0	77.0	23.3	28.8⑦	8.21⑦
		70	35.0	77.0	23.3	28.3	-----
		100	35.0	77.0	23.3	-----	8.55
		200	29.1	72.8	23.3	27.6	8.79
		300	26.3	67.8	22.6	27.0	9.00
		400	24.2	66.1	21.8	26.5	9.19

Notes: ① ASME Code, Section II, Part A.
② ASME Code, Section II, Part D, Table Y-1.
③ ASME Code, Section II, Part D, Table U.
④ ASME Code, Section II, Part D, Table 2A.
⑤ ASME Code, Section II, Part D, Table TM-1, Material Group G.
⑥ ASME Code, Section II, Part D, Table TE-1, 18Cr-8Ni, Coefficient B.
⑦ Interpolated/extrapolated

This page intentionally left blank.

Table 2.3-2 – Mechanical Properties of Polyurethane Foam (for Analysis)

Property	Direction	Nominal Room Temperature Value
Compressive Strength, S	Axial (Parallel-to-Rise)	235 psi
	Radial (Perpendicular-to-Rise)	195 psi
Compressive Modulus, E	Axial (Parallel-to-Rise)	6,810 psi
	Radial (Perpendicular-to-Rise)	4,773 psi
Thermal Expansion Coefficient, α	-----	3.5×10^{-5} in/in/°F
Poisson's Ratio, ν	-----	0.33
Density, ρ	-----	8.25 lb/ft^3

Table 2.3-3 – Mechanical Properties of Metallic Materials (for Testing)

Material	Minimum Mechanical Properties (unless otherwise specified)	Notes
ASTM B16, Alloy 360 Brass, Half-Hard Temper	σ_y = 25,000 psi σ_u = 55,000 psi	-----
Hexcel ACG-3/8-.003-3.6P Aluminum Honeycomb	σ_{bc} = 340 psi ±15% (Bare Compressive Strength) σ_c = 120 psi ±15% (Crush Strength)	①
300 Series Stainless Steel Socket Head Cap Screws	σ_y = 40,000 psi σ_u = 80,000 psi	②
ASTM A564, Type 630, Condition 1150, Stainless Steel	σ_y = 105,000 psi σ_u = 135,000 psi	③
1/4-inch, 300 Series Stainless Steel Pan Head Screws	σ_y = 30,000 psi σ_u = 75,000 psi	④

Notes:

① *Mechanical Properties of Hexcel Honeycomb Materials*, TSB-120 (Technical Service Bulletin 120), Hexcel, 1992. The term "Bare Compressive Strength" is defined as the maximum strength that is exhibited by the honeycomb material at the onset of crushing. The term "Crush Strength" is defined as the average compressive strength that is sustained as the honeycomb material undergoes crushing.

② UNBRAKO Socket Screw Products Catalog, Copyright 1988, SPS Technologies.

③ ASME Code, Section II, Part D, Table 2A, 1995 Edition, 1997 Addenda.

④ Industrial Fasteners Institute, *Fastener Standard*, Fifth Edition.

This page intentionally left blank.

2.4 General Standards for All Packages

This section defines the general standards for all packages. The HalfPACT package, with an outer confinement vessel (OCV) that is integral to an outer confinement assembly (OCA), and an inner containment vessel (ICV) for primary containment, meets all requirements delineated for this section.

2.4.1 Minimum Package Size

The minimum transverse dimension (i.e., the diameter) of the HalfPACT package is 94⅜ inches, and the minimum longitudinal dimension (i.e., the height) is 91½ inches. Thus, the requirement of 10 CFR §71.43(a)[1] is satisfied.

2.4.2 Tamper-indicating Feature

Tamper-indicating seals are installed at one OCA lock bolt location and at the OCV vent port access plug, as delineated on the drawings in Appendix 1.3.1, *Packaging General Arrangement Drawings*. A lock wire device is used between two tie-points. For the OCV lock bolt, the tie-points are the bolt head and the locking Z-flange. The two tie-points for the OCV vent port access plug are the plug itself and a bolt tapped and welded to the OCA body outer shell. Failure of either tamper-indicating device provides evidence of possible unauthorized access. Thus, the requirement of 10 CFR §71.43(b) is satisfied.

2.4.3 Positive Closure

The HalfPACT package cannot be opened unintentionally. Both the OCA and ICV lids are attached to their respective bodies with locking rings. The OCV locking ring is secured with six, 1/2-13UNC, OCA lock bolts through the attached locking Z-flange. Similarly, the ICV locking ring is secured in the locked position with three, 1/2-13UNC, ICV lock bolts. For either lid, the presence of a single, lock bolt will prevent lid removal.

The OCV vent port has three levels of protection against inadvertent opening: 1) the OCV vent port access plug, 2) the OCV vent port cover, and 3) the OCV vent port plug. Each of these components are secured via threaded fittings. The ICV vent port has two levels of protection against inadvertent opening: 1) the ICV vent port cover, and 2) the ICV vent port plug. Thus, the requirements of 10 CFR §71.43(c) are satisfied.

2.4.4 Chemical and Galvanic Reactions

The major materials of construction of the HalfPACT packaging (i.e., austenitic stainless steel, aluminum, brass, polyurethane foam, ceramic fiber paper, fiberglass insulation, butyl rubber O-ring seals and other elastomeric materials) will not have significant chemical, galvanic or other reactions in air, inert gas or water environments, thereby satisfying the requirements of 10 CFR §71.43(d). These materials have been previously used, without incident, in radioactive material (RAM) packages for transport of similar payload materials. Specifically, these

[1] Title 10, Code of Federal Regulations, Part 71 (10 CFR 71), *Packaging and Transportation of Radioactive Material*, 01-01-12 Edition.

materials of construction have been used in the TRUPACT-II package[2] for many years without incident, utilizing the same materials of construction and carrying identical payloads as will be carried in the HalfPACT package. A successful RAM packaging history combined with successful use of these fabrication materials in similar industrial environments ensures that the integrity of the HalfPACT package will not be compromised by any chemical, galvanic or other reactions. The materials of construction and the payload are further evaluated below for potential reactions.

2.4.4.1 Packaging Materials of Construction

The HalfPACT packaging is primarily constructed of Type 304 stainless steel. This material is highly corrosion resistant to most environments. The metallic structure of the HalfPACT packaging is composed entirely of this material and compatible 300 series weld material. The weld material and processes have been selected in accordance with the ASME Boiler and Pressure Vessel Code[3] to provide as good or better material properties, including corrosion resistance, as the base material. Since both the base and weld materials are 300 series materials, they have nearly identical electrochemical potential thereby minimizing any galvanic corrosion that could occur.

The stainless steel within the OCA foam cavity is lined with a ceramic fiber paper, composed of alumina silica. This material is nonreactive with either the polyurethane foam or the stainless steel, both dry or in water. The ceramic fiber paper and the silicone adhesive are very low in free chlorides to minimize the potential for stress corrosion of the OCA structure.

The polyurethane foam that is used in the OCA is essentially identical to previously licensed transportation packagings, such as the TRUPACT-II (Docket 71-9218), NuPac 125B (Docket 71-9200), and NuPac PAS-1 (Docket 71-9184). All of these packagings have had a long and successful record of performance demonstrating that the polyurethane foam does not cause any adverse conditions with the packaging. The polyurethane foam in the OCA is a rigid, closed-cell (non-water absorbent) foam that is very low in free halogens and chlorides, as discussed in Section 8.1.4.1, *Polyurethane Foam*. The polyurethane foam material cavity is sealed with plastic pipe plugs to preclude the entrance of moisture.

Aluminum honeycomb is used in the HalfPACT packaging for the two, ICV aluminum honeycomb spacer assemblies in the upper and lower ICV torispherical heads. Aluminum honeycomb material is used for dunnage only, and is not used as any part of the HalfPACT packaging's containment boundary. The aluminum honeycomb is maintained at relatively low temperatures ensuring that no adverse reaction could occur at aluminum/steel interfaces that would compromise the packaging's containment integrity. Of final note, aluminum material is slightly anodic which serves to protect the stainless steel of the ICV.

The various brass fittings and plugs used in the HalfPACT packaging are very corrosion resistant. Like aluminum, brass material is slightly anodic to the stainless steel. Any damage that could occur to the brass is easily detectable since the fittings are all handled each time the HalfPACT package is loaded and unloaded.

---

[2] U.S. Department of Energy (DOE), *Safety Analysis Report for the TRUPACT-II Shipping Package*, USNRC Certificate of Compliance 71-9218, U.S. Department of Energy, Carlsbad Field Office, Carlsbad, New Mexico.

[3] American Society of Mechanical Engineers (ASME) Boiler and Pressure Vessel Code, Section III, *Rules for Construction of Nuclear Power Plant Components*, 1995 Edition, 1997 Addenda.

The various elastomers (e.g., butyl rubber, polyester, silicone, etc.) that are used in the O-rings, annulus foam ring, debris shield, wear pad, etc., contain no corrosives that would react adversely affect the HalfPACT packaging. These materials are organic in nature and noncorrosive to the stainless steel containment boundary of the HalfPACT packaging.

2.4.4.2 Payload Interaction with Packaging Materials of Construction

The materials of construction of the HalfPACT packaging are checked for compatibility with the various payload chemistries when the payloads are evaluated for chemical compatibility. All payload materials are in approved payload containers delineated in the CH-TRAMPAC[4].

The payload is typically further confined within multiple layers of plastic for radiological health purposes. This configuration ensures that the payload material has an insignificant level of contact with the HalfPACT packaging materials of construction. However, the evaluation of compatibility is based on complete interaction of payload materials with the packaging.

The design of the HalfPACT package is for transport of CH-TRU materials and other authorized payloads that are limited in form to solid or solidified material. Corrosive materials, pressurized containers, explosives, non-radioactive pyrophorics, and liquid volumes greater than 1% are prohibited. These restrictions ensure that the waste in the payload is in a non-reactive form for safe transport in the HalfPACT package. For a comprehensive discussion defining acceptable payload properties, see the CH-TRAMPAC.

2.4.5 Valves

Neither the OCV nor the ICV have valves. However, beside their respective lids, the ICV and the OCV each have a vent port penetration into their containment and confinement cavities, respectively. These vent port penetrations are sealed using threaded vent port plugs comprised of brass material. Since the ICV is entirely contained within the OCV during transport, a tamper indicating device is not necessary. Access to the OCV vent port penetration is prevented by a lockwire that secures the OCV vent port access plug, as discussed in Section 2.4.2, *Tamper-indicating Feature*. Thus, the requirements of 10 CFR §71.43(e) are satisfied.

2.4.6 Package Design

As shown in Chapter 2.0, *Structural Evaluation*, Chapter 3.0, *Thermal Evaluation*, Chapter 5.0, *Shielding Evaluation*, and Chapter 6.0, *Criticality Evaluation*, the structural, thermal, shielding, and criticality requirements, respectively, of 10 CFR §71.43(f) are satisfied for the HalfPACT package.

2.4.7 External Temperatures

As shown in Table 3.5-1 from Section 3.5.3, *Package Temperatures*, the maximum accessible surface temperature with maximum internal decay heat load and no insolation is 102 °F. Since the maximum external temperature does not exceed 185 °F, the requirements of 10 CFR §71.43(g) are satisfied.

---

[4] U.S. Department of Energy (DOE), *Contact-Handled Transuranic Waste Authorized Methods for Payload Control* (CH-TRAMPAC), U.S. Department of Energy, Carlsbad Field Office, Carlsbad, New Mexico.

2.4.8 Venting

The HalfPACT package does not include any features intended to allow continuous venting during transport. Thus, the requirements of 10 CFR §71.43(h) are satisfied.

2.5 Lifting and Tie-down Standards for All Packages

For analysis of the lifting and tie-down components of the HalfPACT packaging, material properties from Section 2.3, *Mechanical Properties of Materials*, are taken at a bounding temperature of 160 °F per Section 2.6.1.1, *Summary of Pressures and Temperatures*. The primary structural materials are Type 304 stainless steel, and polyurethane foam that is used in the outer confinement assembly (OCA).

A loaded HalfPACT package is only lifted by fork lift pockets, located at the bottom of the OCA body. For this case, HalfPACT package lifting loads act parallel to the direction of foam rise. The nominal compressive strength of the polyurethane foam, as delineated in Table 2.3-2 of Section 2.3.1, *Mechanical Properties Applied to Analytic Evaluations*, is reduced by 15% to account for manufacturing tolerance; polyurethane foam manufacturing tolerances are discussed in Section 8.1.4.1.2.3.2, *Parallel-to-Rise Compressive Stress*. The nominal compressive strength of the polyurethane foam is further reduced by 25% to account for elevated temperature effects, as discussed in Section 2.6.1.1, *Summary of Pressures and Temperatures*.

Properties of Type 304 stainless steel and polyurethane foam, parallel to the direction of foam rise accounting for manufacturing tolerances and elevated temperature, are summarized below.

Material Property	Value	Reference
Type 304 Stainless Steel at 160 °F		
Elastic Modulus, E	27.8×10^6 psi	Table 2.3-1
Yield Strength, σ_y	27,000 psi	
Shear Stress, equal to $(0.6)\sigma_y$	16,200 psi	
Polyurethane Foam (parallel-to-rise) at 160 °F		
Minimum compressive strength, σ_c	150 psi	Table 2.3-2
Bearing stress, assumed equal to $(2/3)\sigma_c$	100 psi	

2.5.1 Lifting Devices

This section demonstrates that the fork lift pockets, the only attachments designed to lift the HalfPACT package, are designed with a minimum safety factor of three against yielding, per the requirements of 10 CFR §71.45(a). The lifting devices in the OCA lid are restricted to only lifting the OCA lid, and the lifting devices in the ICV lid are restricted to only lifting an ICV lid or empty ICV. Although these lifting devices are designed with a minimum safety factor of three against yielding, detailed analyses are not specifically included herein since these lifting devices are not intended for lifting a HalfPACT package.

When lifting the entire package, the applied lift force without yielding is simply three times the total package weight of 18,100 pounds, as given in Section 2.2, *Weights and Centers of Gravity*.

$$F_L = (3)(18{,}100) = 54{,}300 \text{ pounds}$$

The entire package is lifted via two fork lift pockets located at the bottom of the OCA. Loads are considered to be concentrated at the fork lift pocket interfaces and act parallel to the direction of foam rise. For the purposes of this analysis, the minimum assumed fork width is 8 inches, and the minimum assumed engagement length is 60 inches. The total bearing area for two forks is:

$$A = (2)(8)(60) = 960 \text{ in}^2$$

Assuming the entire lifted load is carried directly into the polyurethane foam, thereby ignoring any beneficial load carrying associated with the presence of the relatively stiff stainless steel fork lift pocket and OCA outer shell, the compressive stress is:

$$\sigma_c = \frac{F_1}{A} = \frac{54{,}300}{960} = 57 \text{ psi}$$

The allowable compressive stress for the polyurethane foam is 100 psi. Therefore, the margin of safety is:

$$MS = \frac{100}{57} - 1 = +0.75$$

2.5.2 Tie-down Devices

The HalfPACT package is secured to its dedicated semi-trailer at four points, two on each trailer main beam. For railcar shipments, the HalfPACT package is secured to an adapter that mimics the trailer's four attachment points. Subsequent use of the term "trailer" or "trailer main beam(s)" encompass the railcar adapter and railcar frame. The attachment is made using trailer tie-down devices that pass over the tie-down lugs located at the bottom of the OCA body. The semi-trailer is also fitted with kick plates at the four tie-down points to provide horizontal restraint (blocking). The tie-down scheme utilized for the HalfPACT package is illustrated in Figure 2.5-1 and Figure 2.5-2.

Inertial loads of 10*g* longitudinally, 5*g* laterally, and 2*g* vertically, per 10 CFR §71.45(b)(1), are applied through the HalfPACT package center of gravity, conservatively assumed to be 45 inches above the package's base. The horizontal loads of 10*g* longitudinally and 5*g* laterally are reacted in compression against the kick plates. The resultant overturning moment is reacted in compression on a trailer main beam and in tension by the four tie-down lugs. The vertical load applied to the center of gravity (2*g*) is evenly reacted at the four tie-down points, and is assumed to act in the direction (up or down) that maximizes the total tie-down load (i.e., down for the compressive reaction point and up for the tensile reaction points).

2.5.2.1 Tie-down Forces

Tensile tie-down points are on a 48.4-inch radius circle (to the center of the tie-down lugs, in line with the tie-down fixture). The compressive reaction point is at the trailer main beam, occurring at the edge of the tie-down lug's doubler plate, a radius of 47.56 inches. A plan view of the tie-down geometry is depicted in Figure 2.5-3, including a corresponding free-body force diagram. If the HalfPACT package is treated as a rigid body, the reaction forces may be determined from the following set of equations:

$$F_1L_1 + F_2L_2 + F_3L_3 + F_4L_4 = HF_g$$

$$\frac{F_1}{L_1} = \frac{F_2}{L_2} = \frac{F_3}{L_3} = \frac{F_4}{L_4} = k$$

$$F_1 + F_2 + F_3 + F_4 = F_c$$

where, the height of the package center of gravity above its base, H = 45 inches, the horizontal inertia force, $F_g = 18{,}100 \times (10^2 + 5^2)^{1/2} = 202{,}364$ pounds, and the tie-down lug reaction lengths, $L_1 = 47.56 - 47.52 = 0.04$ inches, $L_2 = 47.56 - 21.16 = 26.40$ inches, $L_3 = 47.56 + 21.16 = 68.72$ inches, and $L_4 = 47.56 + 47.52 = 95.08$ inches. Solving for k:

$$k = \frac{HF_g}{L_1^2 + L_2^2 + L_3^2 + L_4^2} = \frac{(45)(202{,}364)}{(0.04)^2 + (26.40)^2 + (68.72)^2 + (95.08)^2} = 630 \text{ lb/in}$$

Therefore, $F_1 = k \times L_1 = 25$ pounds, $F_2 = k \times L_2 = 16{,}632$ pounds, $F_3 = k \times L_3 = 43{,}294$ pounds, $F_4 = k \times L_4 = 59{,}900$ pounds, and $F_c = 119{,}851$ pounds. The maximum vertical tensile force on any single tie-down lug, including the contribution of the vertical load of 2*g*, is then found as:

$$F_{t\,max} = 59{,}900 + \frac{(2g)(18{,}100)}{4 \text{ lugs}} = 68{,}950 \text{ pounds}$$

Similarly, the maximum compressive force is found as:

$$F_{c\,max} = 119{,}851 + \frac{(2g)(18{,}100)}{4 \text{ lugs}} = 128{,}901 \text{ pounds}$$

Since the line of action of the combined 10*g* longitudinal and the 5*g* lateral accelerations pass almost exactly over the centerline of the kickplate (27.6° for the kickplate centerline versus 26.6° for the line of action of the force), the total horizontal reaction force is conservatively assumed to be reacted against a single kickplate. This force is given by:

$$F_h = F_g = 202{,}364 \text{ pounds}$$

2.5.2.2 Tie-down Stress Due to a Vertical Tensile Load

Several failure modes are considered for the vertical tensile force on the tie-down lug. Shear failure of the tie-down lug itself is not an issue because the shear area of the lug is much greater than the lug attachment welds. The remaining failure modes, as illustrated in Figure 2.5-4, are:

(a) Shear and bending failure of the tie-down lug welds (shear + bending loads),

(b) Tearout of the tie-down lug doubler plate at the lug weld outline,

(c) Shear failure of the welds attaching the lug doubler plate to the OCA outer shell, and

(d) Tearout of the OCA outer shell at the doubler outline.

2.5.2.2.1 Failure of the Tie-down Lug Welds Due to Shear and Bending Loads

Figure 2.5-5 presents dimensional details of the tie-down, including an appropriate free-body diagram. The length of the tie-down lug weld along the two sides is 5.49 inches. The arc length of the weld across the top of the lug is 3.38 inches. The groove weld at the bottom is 2.38 inches long. On three sides, the weld is a 3/8-inch fillet over a 3/8-inch groove. The minimum throat

length for this weld is 0.375/(sin 45°) = 0.53 inches. For the 3/8-inch groove weld at the bottom, the minimum throat length is 0.375 inches. Thus, the total shear area for the weld is:

$$A_s = [(2)(5.49) + 3.38](0.53) + (2.38)(0.375) = 8.50 \text{ in}^2$$

The maximum shearing force, V, is the maximum tensile force, F_{tmax} = 68,950 pounds from Section 2.5.2.1, *Tie-down Forces*, resulting in a corresponding shear stress of:

$$\tau_V = \frac{V}{A_s} = \frac{68{,}950}{8.50} = 8{,}112 \text{ psi}$$

The maximum weld shear stress due to bending is found using the standard beam bending formula, but by treating the weld as a line[1], or:

$$\tau_B = \frac{Mc}{I}$$

where, M is the moment on weld group, c is the maximum weld distance from the weld group centroid, and I is the moment of inertia of weld group. The weld group centroid, relative to the bottom edge of the tie-down lug, is:

$$\bar{y} = \frac{(0.53)(3.38)(6.00) + 2(0.53)(5.49)(5.49/2)}{(0.53)(3.38) + 2(0.53)(5.49) + (0.375)(2.38)} = 3.143 \text{ inches}$$

where the centroid of the arc formed by the weld at the top of the tie-down lug is located 6.00 inches above the base of the lug. For the sides, the contribution to the moment of inertia is:

$$I_s = 2\left[\frac{tL^3}{12} + Ad^2\right] = 2\left[\frac{(0.53)(5.49)^3}{12} + (0.53)(5.49)\left(3.143 - \frac{5.49}{2}\right)^2\right] = 15.54 \text{ in}^4$$

For the top (arc-shaped) weld, conservatively ignoring the moment of inertia about its own centroid, the contribution to the moment of inertia is:

$$I_t = Ad^2 = (0.53)(3.38)(6.00 - 3.143)^2 = 14.62 \text{ in}^4$$

For the bottom weld, the contribution to the moment of inertia is:

$$I_b = Ad^2 = (0.375)(2.38)(3.143)^2 = 8.82 \text{ in}^4$$

Summing the contributions from each part of the weld group, the total moment of inertia of the weld group, treated as a line, is:

$$I = I_s + I_t + I_b = 15.54 + 14.62 + 8.82 = 38.98 \text{ in}^4$$

The distance from the centroid of the weld group to the extreme fiber is c = 3.143 inches. The line of action for the vertical force is 0.7 inches from the side of the tie-down doubler plate, as illustrated in Figure 2.5-5. Therefore, the shear stress on the weld group due to bending is:

[1] Shigley, *Mechanical Engineering Design*, Third Edition, McGraw-Hill, Inc., 1977, Section 7-4, *Bending in Welded Joints*.

$$\tau_B = \frac{Mc}{I} = \frac{(68{,}950)(0.7)(3.143)}{38.98} = 3{,}892 \text{ psi}$$

The maximum shear stress in the tie-down lug weld due to the shear and bending loads is:

$$\tau = \sqrt{\tau_V^2 + \tau_B^2} = \sqrt{(8{,}112)^2 + (3{,}892)^2} = 8{,}997 \text{ psi}$$

The allowable shear stress for the tie-down lug welds is 16,200 psi. Therefore, the margin of safety is:

$$MS = \frac{16{,}200}{8{,}997} - 1 = +0.80$$

2.5.2.2.2 Tearout of the Tie-down Doubler Plate at the Tie-Down Lug Weld Outline

Assume that a rectangular region equal to $2.88 + 2 \times 0.375 = 3.63$ inches wide by $(6.25 + 0.375) = 6.63$ inches high, tears out from the 3/8-inch thick doubler plate. Under the direct shear load of 68,520 pounds, the top edge will be in direct tension while the sides and bottom will be in direct shear. Conservatively assuming the top and sides are all in direct shear, the shear area in the 3/8-inch thick, tie-down doubler plate is:

$$A_p = [3.63 + 2(6.63)](0.375) = 6.33 \text{ in}^2$$

The shear area of the 1.0-inch groove weld attaching the bottom of the doubler plate to the OCA body flat head is:

$$A_w = (3.63)(1.0) = 3.63 \text{ in}^2$$

Thus, the total shear area is:

$$A_s = A_p + A_w = 6.33 + 3.63 = 9.96 \text{ in}^2$$

The maximum shearing force, V, is the maximum tensile force, $F_{tmax} = 68{,}950$ pounds from Section 2.5.2.1, *Tie-down Forces*, resulting in a corresponding shear stress of:

$$\tau_V = \frac{V}{A_s} = \frac{68{,}950}{9.96} = 6{,}923 \text{ psi}$$

The maximum weld shear stress due to bending is found using the standard beam bending formula, but by treating the weld as a line, or:

$$\tau_B = \frac{Mc}{I}$$

where, M is the moment on weld group, c is the maximum weld distance from the weld group centroid, and I is the moment of inertia of weld group. The weld group centroid, relative to the bottom edge of the tie-down lug, is:

$$\bar{y} = \frac{(0.375)(3.63)(6.63) + 2(0.375)(6.63)(6.63/2) + (1.0)(3.63)(1.0/2)}{(0.375)(3.63) + 2(0.375)(6.63) + (1.0)(3.63)} = 2.742 \text{ inches}$$

For the sides of the rectangular region, the contribution to the moment of inertia is:

$$I_s = 2\left[\frac{tL^3}{12} + Ad^2\right] = 2\left[\frac{(0.375)(6.63)^3}{12} + (0.375)(6.63)\left(2.742 - \frac{6.63}{2}\right)^2\right] = 19.85\,\text{in}^4$$

For the top of the rectangular region, the contribution to the moment of inertia is:

$$I_t = \frac{Lt^3}{12} + Ad^2 = \frac{(3.63)(0.375)^3}{12} + (0.375)(3.63)(6.63 - 2.742)^2 = 20.59\,\text{in}^4$$

For the bottom groove weld, the contribution to the moment of inertia is:

$$I_b = \frac{Lt^3}{12} + Ad^2 = \frac{(3.63)(1.0)^3}{12} + (1.0)(3.63)\left(2.742 - \frac{1.0}{2}\right)^2 = 18.55\,\text{in}^4$$

Summing the contributions from each part of the rectangular region, the total moment of inertia of the weld group, treated as a line, is:

$$I = I_s + I_t + I_b = 19.85 + 20.59 + 18.55 = 58.99\ \text{in}^4$$

The distance from the centroid of the rectangular region to the extreme fiber is c = 6.63 – 2.742 = 3.888 inches. The line of action for the vertical force is 0.7 + 0.375/2 = 0.89 inches from the center of the tie-down doubler plate. Therefore, the shear stress due to bending is:

$$\tau_B = \frac{Mc}{I} = \frac{(68{,}950)(0.89)(3.888)}{58.99} = 4{,}103\,\text{psi}$$

The maximum shear stress in the tie-down doubler plate due to the shear and bending loads is:

$$\tau = \sqrt{\tau_V^2 + \tau_B^2} = \sqrt{(6{,}923)^2 + (4{,}103)^2} = 8{,}048\,\text{psi}$$

The allowable shear stress for the tie-down doubler plate is 16,200 psi. Therefore, the margin of safety is:

$$MS = \frac{16{,}200}{8{,}048} - 1 = +1.01$$

2.5.2.2.3 Shear Failure of the Tie-down Lug Doubler Plate to OCA Outer Shell Welds

The tie-down lug doubler plate is 24 inches square, and welded to the OCA outer shell on its top and sides with 1/4-inch fillet welds. Although the bottom weld is a groove weld, conservatively assume it acts as a 1/4-inch fillet weld, resulting in a total weld length of 96 inches. In addition, 30, 1½-inch diameter, 1/4-inch fillet welds supplement the peripheral fillet welds, providing an additional 30 × π(1.5) = 141 inches of weld. Thus, the total weld length is 237 inches, resulting in a weld shear area of:

$$A_s = (0.25)(\sin 45°)(237) = 41.9\ \text{in}^2$$

The weld shear area is much greater than determined in both previous cases (i.e., $A_s = 8.50\ \text{in}^2$ for Section 2.5.2.2.1, *Failure of the Tie-down Lug Welds Due to Shear and Bending Loads*, and $A_s = 9.96\ \text{in}^2$ for Section 2.5.2.2.2, *Tearout of the Tie-down Doubler Plate at the Tie-Down Lug*

Weld Outline). Thus, the weld shear stress for the same vertical load will be correspondingly less. Similarly, a much larger moment of inertia will be determined for a nearly identical bending moment, thereby resulting in a substantially reduced bending stress. In conclusion, by inspection the resulting margin of safety will correspondingly be much greater and does not need to be explicitly determined.

2.5.2.2.4 Tearout of the OCA Outer Shell at the Tie-Down Lug Doubler Plate Outline

A potential failure mode for the tie-down hardware is tearout of the 1/4-inch thick OCA outer shell just outboard of the 24.0-inch square doubler plate. The downward acting force puts the OCA shell adjacent to the top edge of the doubler plate in direct tension. The OCA outer shell immediately adjacent to the sides and bottom edge of the doubler plate is in direct shear.

Assume that the 24- × 24-inch tie-down lug doubler plate tears out from 1/4-inch thick OCA outer shell. Under the direct shear load of 68,520 pounds, the top edge will be in direct tension while the sides and bottom will be in direct shear. Conservatively assuming that all sides are all in direct shear, the shear area in the 1/4-inch thick OCA outer shell is:

$$A_s = 4(24)(0.25) = 24.0 \text{ in}^2$$

Once again, the shell shear area is much greater than determined in both previous cases (i.e., $A_s = 8.50$ in^2 for Section 2.5.2.2.1, *Failure of the Tie-down Lug Welds Due to Shear and Bending Loads*, and $A_s = 9.96$ in^2 for Section 2.5.2.2.2, *Tearout of the Tie-down Doubler Plate at the Tie-Down Lug Weld Outline*). Thus, the weld shear stress for the same vertical load will be correspondingly less. As before, a much larger moment of inertia will be determined for a nearly identical bending moment, thereby resulting in a substantially reduced bending stress. In conclusion, by inspection the resulting margin of safety will correspondingly be much greater and does not need to be explicitly determined.

2.5.2.3 Tie-down Stress Due to a Vertical Compressive Load

The stresses in the HalfPACT package due to a vertical compressive load may be analyzed by two bounding cases. First, the combination of overturning and vertical, 2*g* inertial compressive loads carried through the OCA outer shell and tie-down lug doubler plate, and second, the 2*g* inertial compressive load carried entirely by the polyurethane foam.

2.5.2.3.1 Bearing Stress in the OCA Outer Shell and Tie-down Lug Doubler Plate

The vertical compressive tie-down load is carried in bearing against the semi-trailer main beams. Conservatively assume that this load is carried only by the cylindrical portion of the OCA outer shell and doubler that is directly over the trailer main beams and tie-down support structure. With reference to Figure 2.5-3, the arc length, s, of the OCA that spans the trailer main beams is:

$$s = R\left(\frac{\pi}{180}\right)(\phi_1 - \phi_2) = (47.56)\left(\frac{\pi}{180}\right)\left[\sin^{-1}\left(\frac{32}{47.56}\right) - \sin^{-1}\left(\frac{18}{47.56}\right)\right] = 16.64 \text{ inches}$$

For an OCA outer shell thickness of 1/4 inches, and a tie-down lug doubler plate thickness of 3/8 inches, the area is:

$$A = (16.64)(0.25 + 0.375) = 10.40 \text{ in}^2$$

Thus, from Section 2.5.2.1, *Tie-down Forces*, the maximum compressive force is F_{cmax} = 128,901 pounds, and the corresponding compressive stress is:

$$\sigma_c = \frac{F_{cmax}}{A} = \frac{128{,}901}{10.40} = 12{,}394 \text{ psi}$$

The allowable stress for the OCA outer shell and tie-down lug doubler plate is 27,000 psi. Therefore, the margin of safety is:

$$MS = \frac{27{,}000}{12{,}394} - 1 = +1.18$$

2.5.2.3.2 Compressive Stress in the Polyurethane Foam

The HalfPACT package is supported on the two main trailer beams during transport. With reference to Figure 2.5-3, the length, L, under the OCA that spans the trailer main beams is:

$$L = 2\sqrt{(47.56)^2 - (22)^2} = 84.3 \text{ inches}$$

For two, 8-inch wide trailer main beams, the total compressive area is:

$$A = 2(8)(84.3) = 1{,}349 \text{ in}^2$$

Conservatively ignoring the load carrying capacity of the OCA outer shell and fork lift pockets, the compressive stress in the polyurethane foam due to a 2*g* vertical (downward) inertial force is:

$$\sigma_c = \frac{2(18{,}100)}{A} = \frac{36{,}200}{1{,}349} = 27 \text{ psi}$$

The allowable stress for the polyurethane foam is 100 psi. Therefore, the margin of safety is:

$$MS = \frac{100}{27} - 1 = +2.70$$

2.5.2.4 Tie-down Stresses Due to a Horizontal Compressive Load

The horizontal load, F_h = 202,364 pounds, determined in Section 2.5.2.1, *Tie-down Forces*, is reacted by a single tie-down weldment. The following sections consider the bearing stress in the tie-down weldment, and the shear stresses in the welds holding the horizontal tripler plate to the doubler plate, and the doubler plate to the lower OCA flat head. Based on their relative thicknesses, assume that one-quarter the horizontal load is carried through the 1/4-inch thick OCA flat head, one-quarter is carried through the 1/4-inch thick doubler plate, and one-half is carried through the 1/2-inch thick tripler plate.

2.5.2.4.1 Bearing Stress in the Tie-down Weldment

The horizontal load, F_h = 202,364 pounds, is carried from the 8.0 inch wide trailer kickplate through the horizontal doubler and tripler plates welded inside the lower OCA flat head, as illustrated in Figure 2.5-3. For a kickplate length, L = 8 inches, a bottom shell thickness, t_s = 1/4 inch, a doubler plate thickness, t_d = 1/4 inch, and a tripler plate thickness, t_t = 1/2 inch, the area available to carry the horizontal compressive load at the kickplate interface is:

$$A = L(t_s + t_d + t_t) = (8.0)(0.25 + 0.25 + 0.5) = 8.0 \text{ in}^2$$

The corresponding compressive (bearing) stress is:

$$\sigma_c = \frac{F_h}{A} = \frac{202{,}364}{8.0} = 25{,}296 \text{ psi}$$

The allowable bearing stress for the OCA outer shell, including the horizontal doubler and tripler plates, is 27,000 psi. Therefore, the margin of safety is:

$$MS = \frac{27{,}000}{25{,}296} - 1 = +0.07$$

2.5.2.4.2 Shear Stress in the Tripler Plate Welds

Based on the assumed load distribution in Section 2.5.2.4, *Tie-down Stresses Due to a Horizontal Compressive Load*, the force on the welds attaching the tripler plate to the doubler plate is then one-half of 202,364 pounds, or 101,182 pounds. The tripler plate is welded with 3/8-inch fillet welds along three of its edges, and a 1/2-inch groove weld along the outer edge. The two side welds are approximately 8 inches long, and the back weld is 7 inches long, for a total, 3/8-inch fillet weld length of 23 inches. Four, 1½-inch diameter, 3/8-inch fillet welds supplement the peripheral 3/8-inch fillet welds, providing an additional $4 \times \pi(1.5) = 18.85$ inches of 3/8-inch fillet weld. Thus, the total 3/8-inch fillet weld length is 41.85 inches. In addition, the 10-inch long outer edge is welded with a 1/2-inch groove weld. The resulting weld shear area is:

$$A_s = (0.375)(\sin 45°)(41.85) + (0.5)(10) = 16.1 \text{ in}^2$$

Thus, the shear stress in the tripler plate fillet welds is:

$$\tau = \frac{101{,}182}{16.1} = 6{,}285 \text{ psi}$$

The allowable shear stress for the tripler plate welds is 16,200 psi. Therefore, the margin of safety is:

$$MS = \frac{16{,}200}{6{,}285} - 1 = +1.58$$

As an option, the tripler plate may be one inch thick and welded into a cutout through the 1/4-inch thick lower OCA flat head and 1/4-inch thick doubler plate in the same orientation and location as shown in Figure 2.5-6. Full penetration groove welds are used around the periphery of the tripler plate (i.e., a one-inch groove weld along the outside, 10-inch long edge, and 1/2-inch groove welds along the remaining three edges). The two side welds are approximately 8 inches long, and the back weld is 7 inches long, for a total weld length of 23 inches. The resulting weld shear area is:

$$A = (0.5)(23) + (1.0)(10) = 21.5 \text{ in}^2$$

Thus, the shear stress in the tripler plate groove welds is:

$$\tau = \frac{101{,}182}{21.5} = 4{,}706 \text{ psi}$$

The allowable shear stress for the tripler plate welds is 16,200 psi. Therefore, the margin of safety is:

$$MS = \frac{16{,}200}{4{,}706} - 1 = +2.44$$

2.5.2.4.3 Shear Stress in the Doubler Plate Welds

Based on the assumed load distribution in Section 2.5.2.4, *Tie-down Stresses Due to a Horizontal Compressive Load*, the force on the welds attaching the doubler plate to the OCA flat head is then one-half plus one-quarter of 202,364 pounds, or 151,773 pounds. The doubler plate is welded with 1/4-inch fillet welds along its four inner edges, for a total 1/4-inch fillet weld length of approximately 35 inches. Eighteen, 1-inch diameter, 1/4-inch fillet welds supplement the peripheral 1/4-inch fillet welds, providing an additional $18 \times \pi(1.0) = 56$ inches of 1/4-inch fillet weld. Thus, the total 1/4-inch fillet weld length is 91 inches. In addition, the 20 inch long outer edge is welded with a 1/4-inch groove weld. The resulting weld shear area is:

$$A_s = (0.25)(\sin 45°)(91) + (0.25)(20) = 21.1 \text{ in}^2$$

Thus, the shear stress in the doubler plate fillet welds is:

$$\tau = \frac{151{,}773}{21.1} = 7{,}193 \text{ psi}$$

The allowable shear stress for the doubler plate welds is 16,200 psi. Therefore, the margin of safety is:

$$MS = \frac{16{,}200}{7{,}193} - 1 = +1.25$$

2.5.2.5 Response of the Package if Treated as a Fixed Cantilever Beam

The preceding sections considered stresses in a localized region in and around the tie-down components. This section demonstrates that a more global response of the HalfPACT package to tie-down loads is also acceptable. For this assessment, the HalfPACT package is treated as a cantilever beam, fixed at its base. The 1/4-inch thick, OCA outer shell is conservatively assumed to be the only structural member resisting the applied 10*g*, 5*g* and 2*g* inertia loads. Stress intensity, SI, in the OCA outer shell is determined as follows:

$$SI = 2\sqrt{\left(\frac{\sigma}{2}\right)^2 + \tau^2} = \sqrt{\left(\frac{P}{A} + \frac{Mc}{I}\right)^2 + \left(\frac{2V}{A}\right)^2}$$

where, for 2*g* vertically, the axial force, $P = (2)(18{,}100) = 36{,}200$ pounds, the bending moment from Section 2.5.2.1, *Tie-down Forces*, $M = HF_g = (45)(202{,}364) = 9{,}106{,}380$ in-lbs, the extreme fiber distance, $c = \frac{1}{2}(94\frac{3}{8}) = 47.2$ inches, the horizontal shear force, $V = F_g = 202{,}364$ inches, the OCA outer shell cross-sectional area, $A = (\pi/4)[(94.375)^2 - (93.875)^2] = 74$ in^2, and the OCA outer shell moment of inertia, $I = (\pi/64)[(94.375)^4 - (93.875)^4] = 81{,}869$ in^4. The resulting stress intensity is:

$$SI = \sqrt{\left(\frac{36{,}200}{74} + \frac{(9{,}106{,}380)(47.2)}{81{,}869}\right)^2 + \left(\frac{2(202{,}364)}{74}\right)^2} = 7{,}928 \text{ psi}$$

The allowable stress intensity for the OCA outer shell is 27,000 psi. Therefore, the margin of safety is:

$$MS = \frac{27{,}000}{7{,}928} - 1 = +2.41$$

2.5.2.6 Summary

All margins of safety for tie-down loads, per 10 CFR §71.45(b)(1), are positive. The smallest tensile or shear margin of safety, MS = +0.80, is for failure of the welds attaching the tie-down lug to the doubler plate, indicating that this will be the mode of failure for the tie-downs under an excessive load condition. Note that compressive modes of failure are not considered relevant in the excessive load evaluation. In accordance with 10 CFR §71.45(b)(3), this failure mode does not compromise the performance capabilities of the HalfPACT package since no main shell is breached. Finally, it is noted that the fork lift pockets and OCA lifting sockets are not intended to be used as tie-down devices, and are appropriately disabled to prevent inadvertent use. The fork lift pockets and OCA lifting sockets are disabled by affixing a plate over each pocket and a cover over the each socket respectively (see the drawings in Appendix 1.3.1, *Packaging General Arrangement Drawings*).

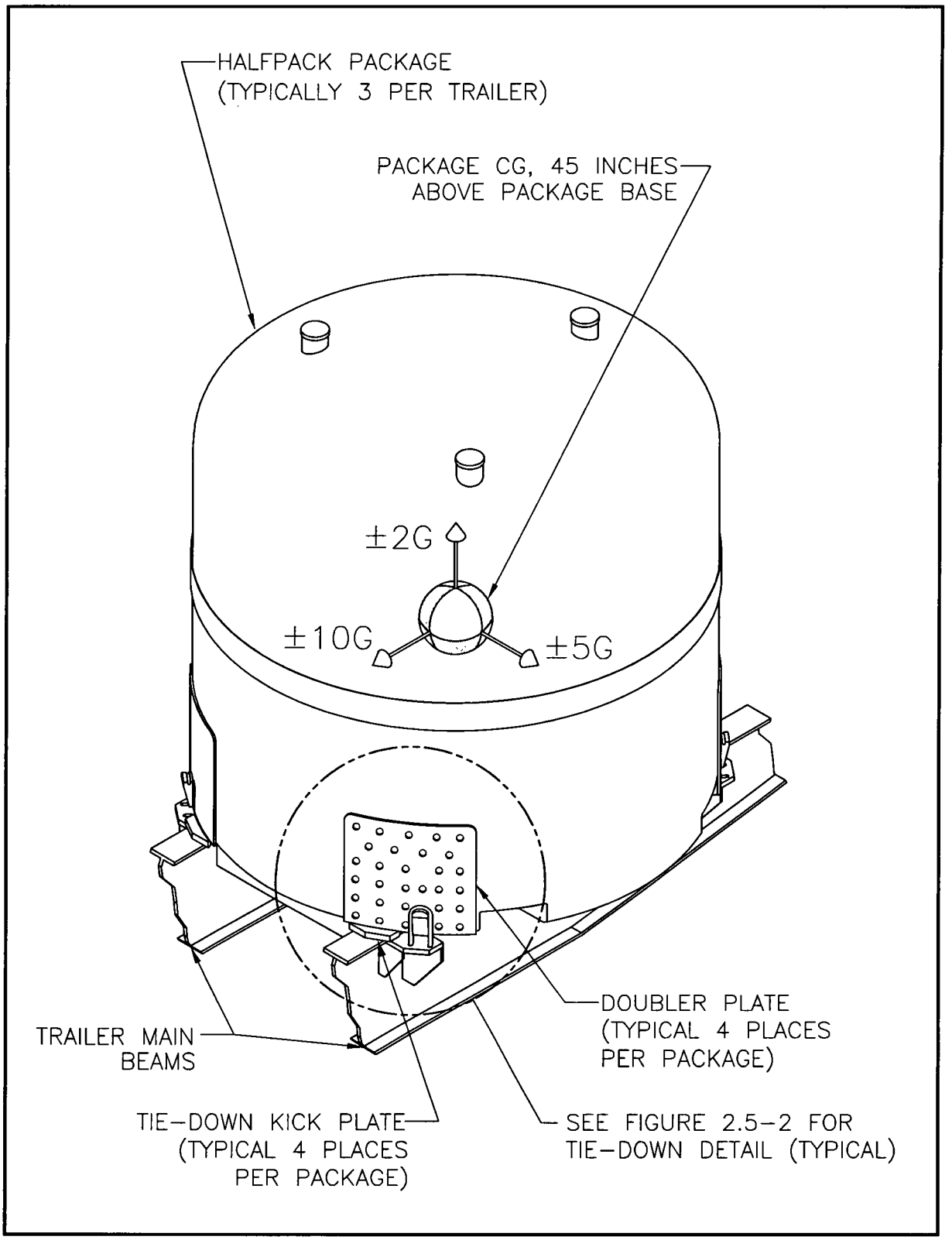

Figure 2.5-1 – Tie-down Device Layout

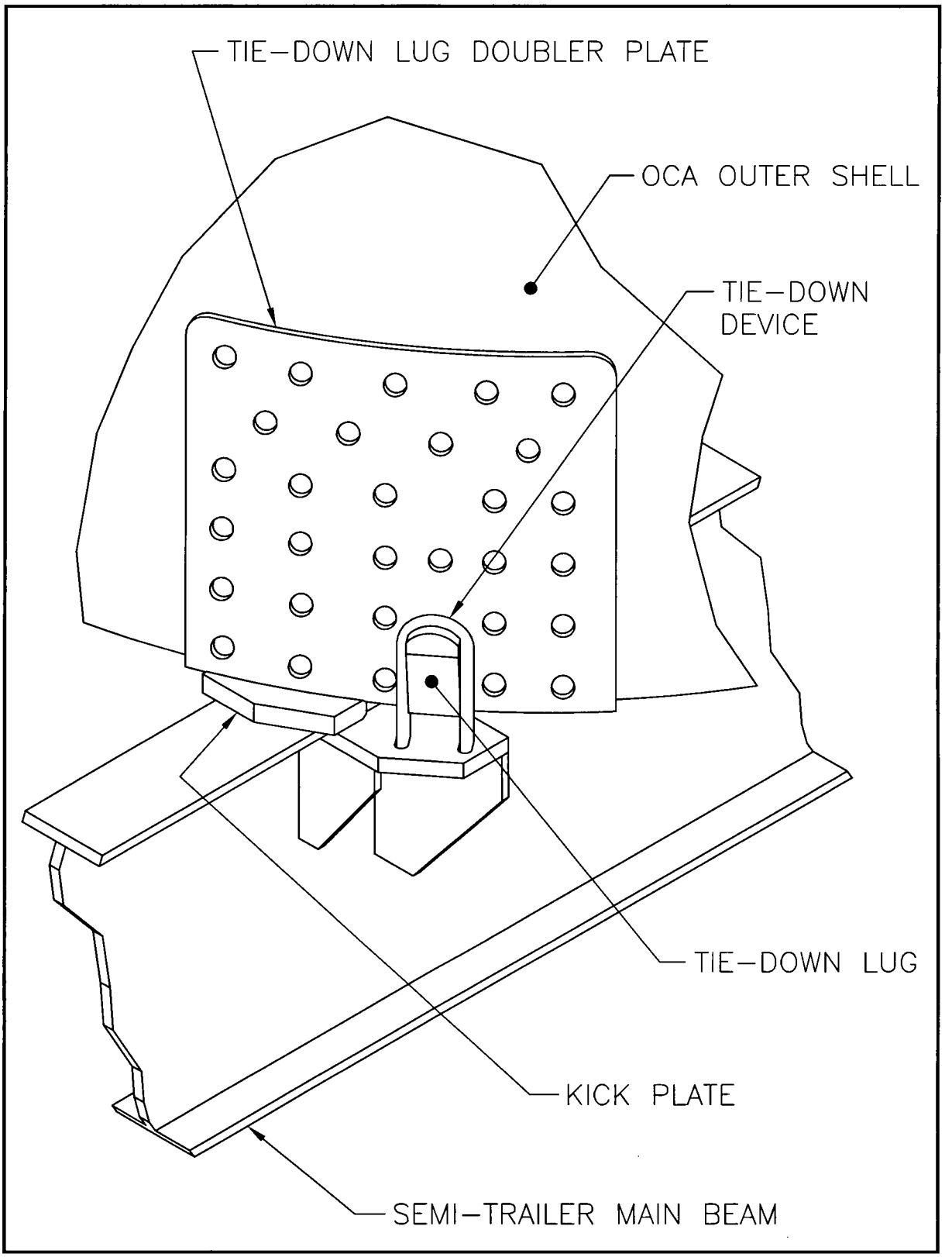

Figure 2.5-2 – Tie-down Device Detail

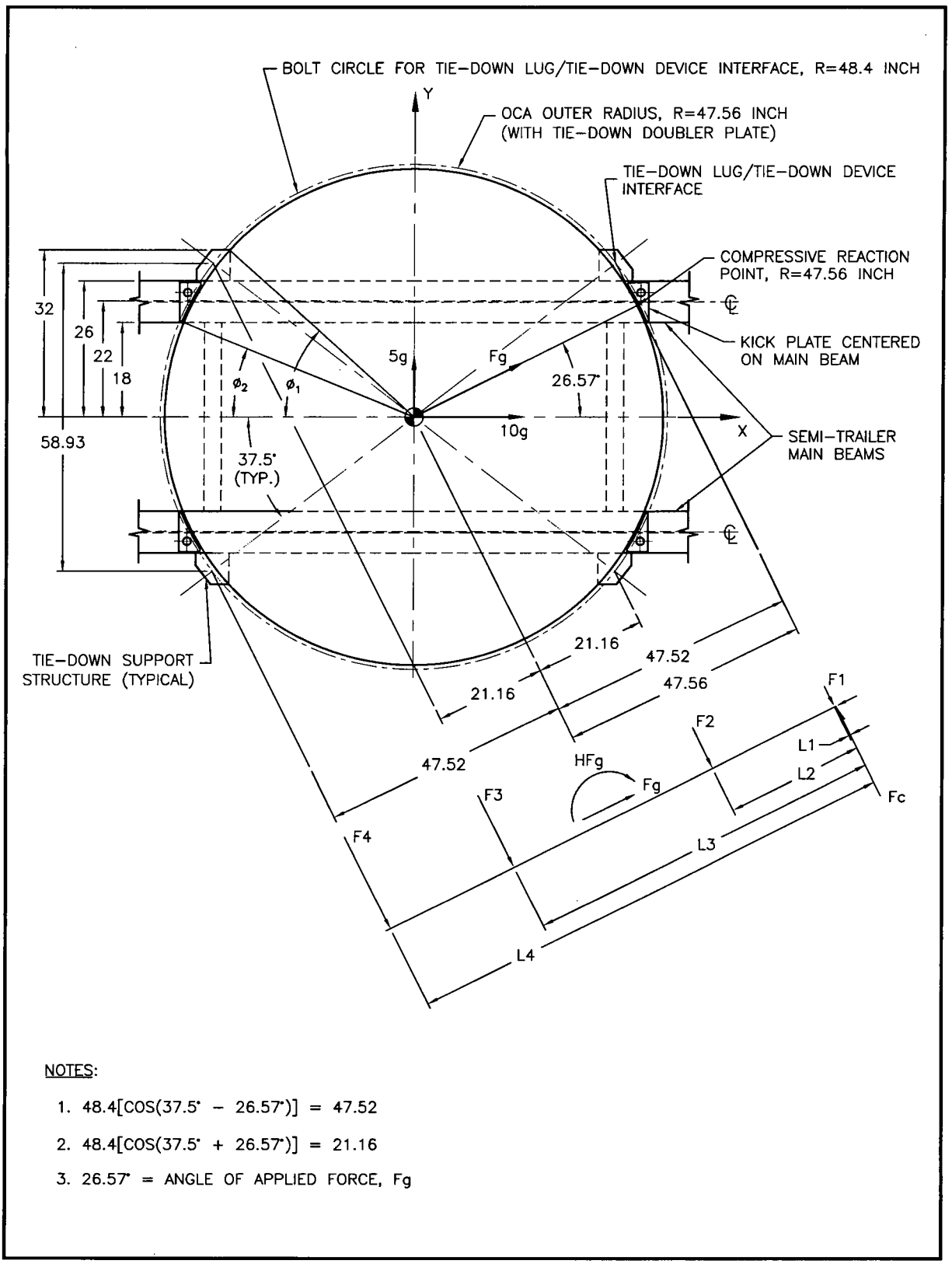

NOTES:

1. 48.4[COS(37.5° − 26.57°)] = 47.52
2. 48.4[COS(37.5° + 26.57°)] = 21.16
3. 26.57° = ANGLE OF APPLIED FORCE, Fg

Figure 2.5-3 – Tie-down Plan View and Reaction Force Diagram

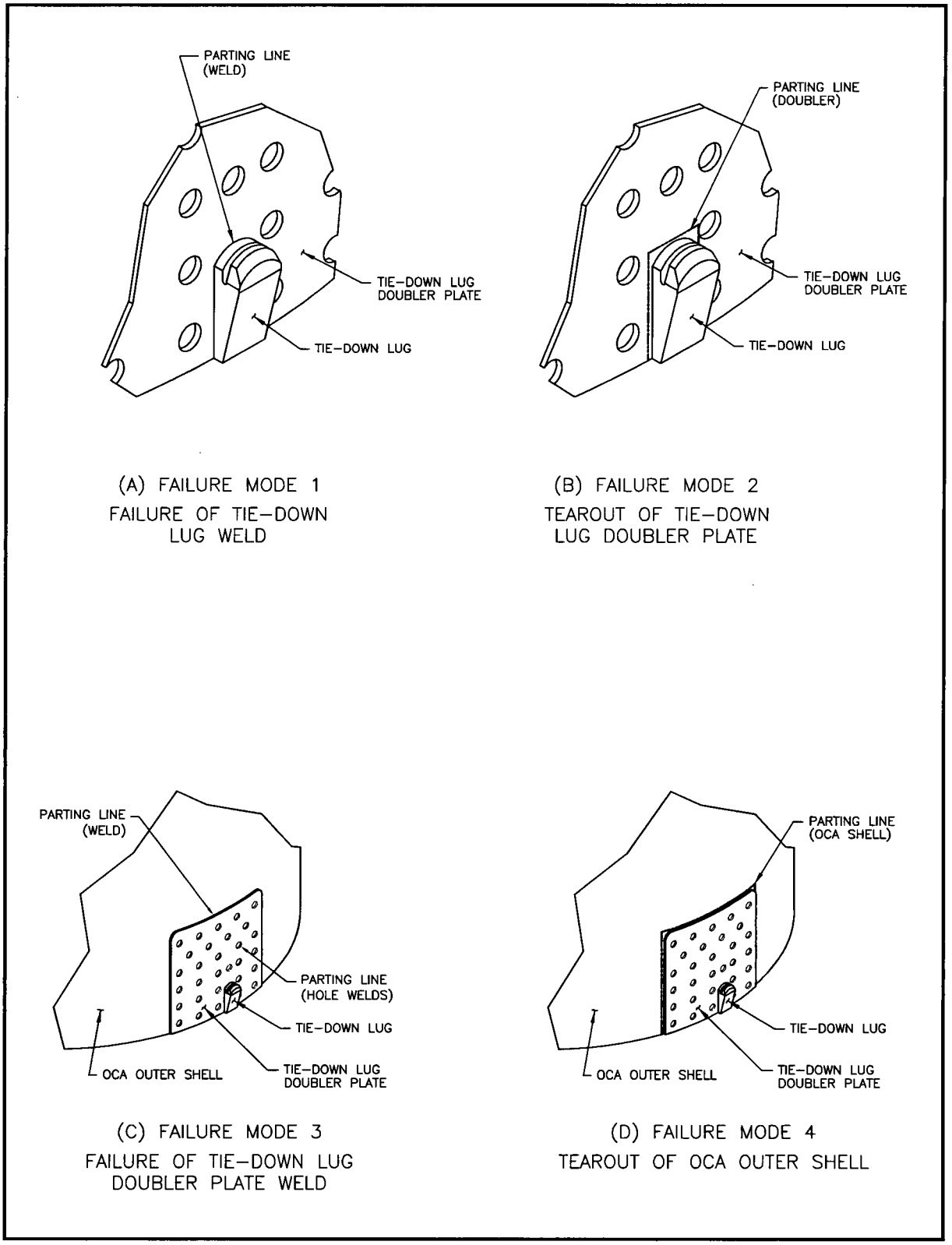

Figure 2.5-4 – Tie-down Tensile/Shear Failure Modes

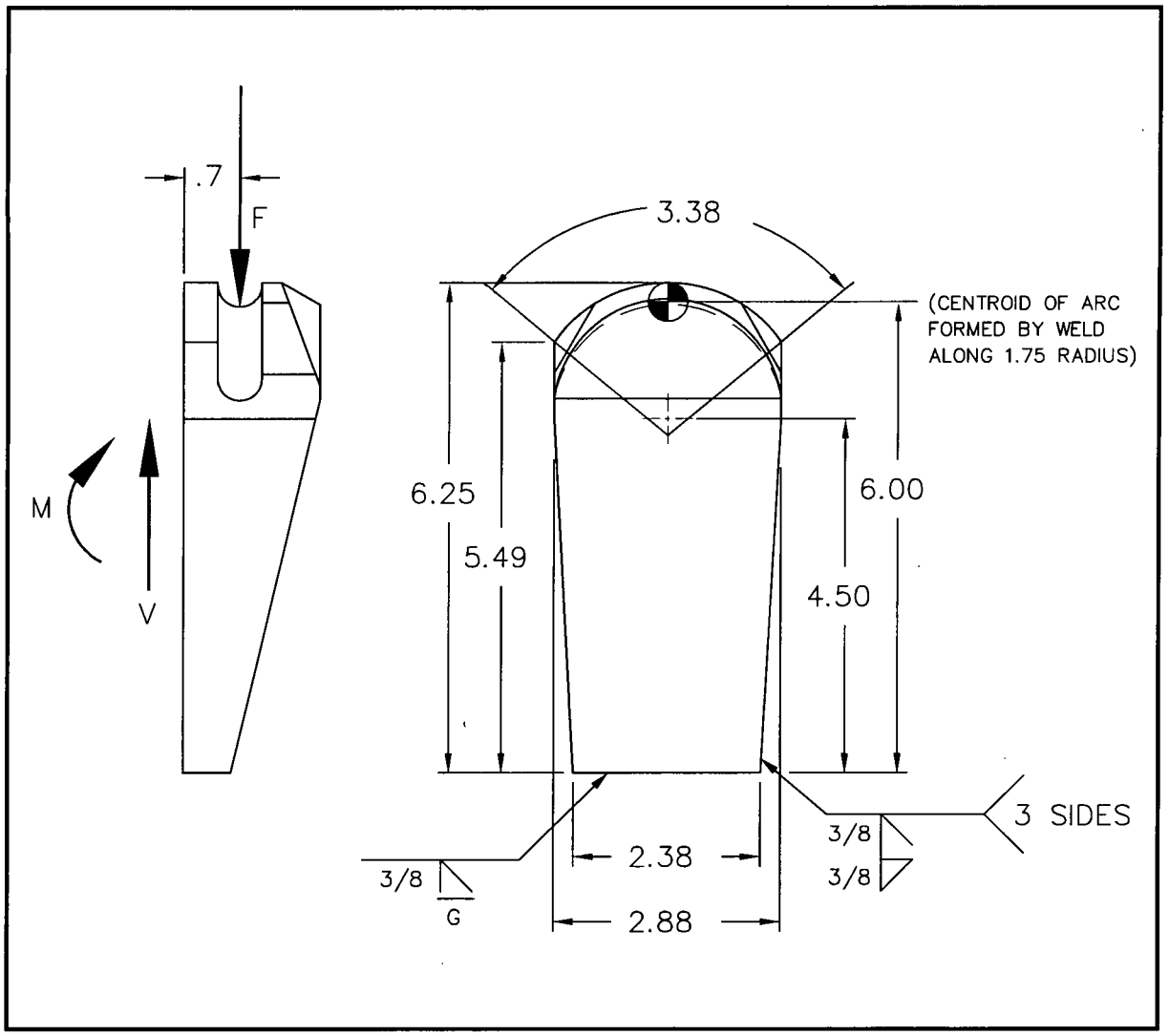

Figure 2.5-5 – Tie-down Lug Dimensions and Load Diagram

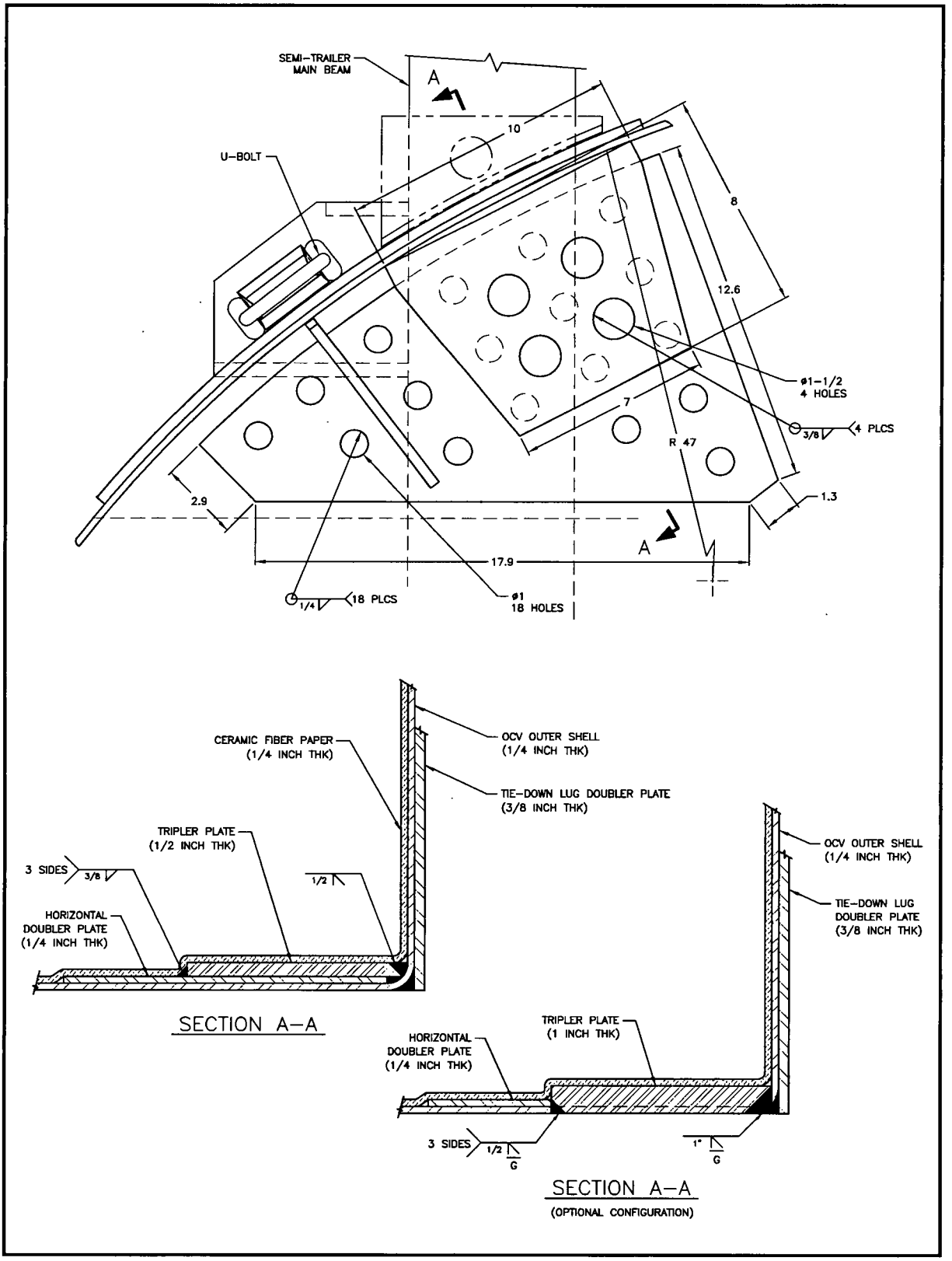

Figure 2.5-6 – Horizontal Doubler and Tripler Plate Details

This page intentionally left blank.

2.6 Normal Conditions of Transport

The HalfPACT package, when subjected to the normal conditions of transport (NCT) specified in 10 CFR §71.71[1], is shown to meet the performance requirements specified in Subpart E of 10 CFR 71. As discussed in the introduction to this chapter, with the exception of the NCT free drop, the primary proof of NCT performance is via analytic methods. Regulatory Guide 7.6[2] criteria are demonstrated as acceptable for all NCT analytic evaluations presented in this section. Specific discussions regarding brittle fracture and fatigue are presented in Section 2.1.2.2, *Miscellaneous Structural Failure Modes*, and are shown not to be limiting cases for the HalfPACT package design. The ability of the butyl O-ring containment seals to remain leaktight is documented in Appendix 2.10.2, *Elastomer O-ring Seal Performance Tests*.

With the exception of the NCT free drop evaluation, analyses for heat, cold, reduced external pressure, increased external pressure, and vibration are performed in this section. Allowable stress limits are consistent with Table 2.1-1 and Table 2.1-2 in Section 2.1.2.1, *Analytic Design Criteria (Allowable Stresses)*, using temperature-adjusted material properties taken from Table 2.3-1 in Section 2.3.1, *Mechanical Properties Applied to Analytic Evaluations*.

For the analytic assessments performed within this section, properties for Type 304 stainless steel are based on data from Table 2.3-1 from Section 2.3.1, *Mechanical Properties Applied to Analytic Evaluations*). Similarly, the bounding values for polyurethane foam compressive strength are based on data from Table 2.3-2 in Section 2.3.1, *Mechanical Properties Applied to Analytic Evaluations*. Polyurethane foam compressive strength is further adjusted ±15% to account for manufacturing tolerance. At elevated NCT temperatures (i.e., 160 °F), the nominal compressive strength is reduced 25% for elevated temperature effects and reduced 15% for manufacturing tolerance. At reduced NCT temperatures (i.e., -40 °F), the nominal compressive strength is increased 50% for reduced temperature effects and increased 15% for manufacturing tolerance.

Properties of Type 304 stainless steel and polyurethane foam are summarized below.

Material Property	Material Property Value (psi)			Reference
	-40 °F	70 °F	160 °F	
Type 304 Stainless Steel				
Elastic Modulus, E	28.8×10^6	28.3×10^6	27.8×10^6	Table 2.3-1
Design Stress Intensity, S_m	20,000	20,000	20,000	
Yield Strength, S_m	30,000	30,000	27,000	
Polyurethane Foam Compressive Strength				
Parallel-to-Rise Direction, σ_c	405	235	150	Table 2.3-2
Perpendicular-to-Rise Direction, σ_c	336	195	124	

[1] Title 10, Code of Federal Regulations, Part 71 (10 CFR 71), *Packaging and Transportation of Radioactive Material*, 01-01-12 Edition.

[2] U. S. Nuclear Regulatory Commission, Regulatory Guide 7.6, *Design Criteria for the Structural Analysis of Shipping Cask Containment Vessels*, Revision 1, March 1978.

Finite element analysis methods are utilized to determine stresses in the HalfPACT packaging structure at various temperature extremes, including the effects of differential thermal expansion, when appropriate, and internal (I) and external (E) pressure combinations, as summarized below.

Load Case Number	Reference Section	Differential Expansion?	Pressure Differential	Temperature		Table Number	Figure Numbers
				Uniform	Reference		
OCA Case 1	§2.6.1	No	61.2 psig (I)	160 °F	160 °F	2.6-1	2.6-1/-2
OCA Case 2	§2.6.1	Yes	61.2 psig (I)	160 °F	70 °F	2.6-2	2.6-3/-4
OCA Case 3	§2.6.2	Yes	0 psig	-40 °F	70 °F	2.6-3	2.6-5/-6
OCA Case 4	§2.6.4	No	14.7 psig (E)	70 °F	70 °F	2.6-4	2.6-7/-8
ICV Case 1	§2.6.1	No	61.2 psig (I)	160 °F	160 °F	2.6-5	2.6-9/-10
ICV Case 2	§2.6.4	No	14.7 psig (E)	70 °F	70 °F	2.6-6	2.6-11/-12

For the NCT free drop evaluation, a certification test program was undertaken using a HalfPACT engineering and certification test unit (ETU and CTU, respectively). Results from certification testing demonstrated that under NCT free drop conditions, two leaktight levels of containment were maintained. NCT certification testing also demonstrated the HalfPACT package's ability to survive subsequent HAC 30-foot free drop, puncture, and fire tests was not compromised. Analyses are performed, when appropriate, to supplement or expand on the available test results. This combination of analytic and test, structural evaluations provides an initial configuration for NCT thermal, shielding and criticality performance. In accordance with 10 CFR §71.43(f), the evaluations performed herein successfully demonstrate that under NCT tests the HalfPACT package experiences "no substantial reduction in the effectiveness of the packaging". Summaries of the more significant aspects of the full scale free drop testing are included in Section 2.6.7, *Free Drop*, with details presented in Appendix 2.10.3, *Certification Tests*.

2.6.1 Heat

The NCT thermal analyses presented in Section 3.4, *Thermal Evaluation for Normal Conditions of Transport*, consists of exposing the HalfPACT package to direct sunlight and 100 °F still air per the requirements of 10 CFR §71.71(b). Although the actual internal heat load is a function of the particular payload configuration being transported, this section utilizes the maximum internal heat allowed within a HalfPACT package, or 30 thermal watts. The 30 thermal watt case results in maximum temperature gradients throughout the HalfPACT package.

2.6.1.1 Summary of Pressures and Temperatures

The maximum normal operating pressure (MNOP) is 50 psig, as determined in Section 3.4.4, *Maximum Internal Pressure*. The pressure stress analyses within this section combine the internal pressure of 50 psig due to MNOP with a reduced external pressure, per 10 CFR §71.71(c)(3), of 3.5 psia (11.2 psig). The net resulting internal pressure utilized in all NCT structural analyses considering internal pressure is therefore 61.2 psig.

The NCT heat input results in modest temperatures and temperature gradients throughout the HalfPACT package. Maximum temperatures for the major packaging components are summarized

in Table 3.4-1 from Section 3.4.2, *Maximum Temperatures*. As shown in Table 3.4-1, all packaging temperatures remain at or below 155 °F. For conservatism, structural analyses of the OCA and ICV utilize a uniform bounding temperature of 160 °F. Use of a uniform bounding temperature is also conservative since material strengths are lowest at the highest temperatures. In addition, in the case of the OCA, the main contributor to thermal stress is the result of differential expansion of the polyurethane foam and the surrounding stainless steel. Also shown by the temperatures presented in Table 3.4-1, temperature gradients are modest for the NCT heat condition. Thus, temperature gradients are reasonably ignored in the analyses herein.

2.6.1.2 Differential Thermal Expansion

With NCT temperatures throughout the packaging being relatively uniform, (i.e., no significant temperature gradients), the concern with differential expansions is limited to regions of the HalfPACT packaging that employ adjacent materials with sufficiently different coefficients of thermal expansion. The OCA is a double-wall, composite construction of polyurethane foam between inner and outer shells of stainless steel. The polyurethane foam expands and contracts to a much greater degree than the surrounding stainless steel shells resulting in stresses due to differential thermal expansion. Finite element analyses presented in the following sections quantify these differential thermal expansion stresses. Differential thermal expansion stresses are negligible in the ICV for three reasons: 1) the temperature distribution throughout the entire ICV is relatively uniform, 2) the ICV is fabricated from only one type of structural material, and 3) the ICV is not radially or axially constrained within a tight-fitting structure (i.e., the OCV).

2.6.1.3 Stress Calculations

A finite element model of the OCA is used to determine the stresses due to the combined effects of pressure loads, and temperature loads due to differential thermal expansion. The details of this model are presented in Appendix 2.10.1.1, *Outer Confinement Assembly (OCA) Structural Analysis*. The ICV is also analyzed for the combined effects of pressure and temperature using a finite element model that is described in Appendix 2.10.1.2, *Inner Containment Vessel (ICV) Structural Analysis*. For the NCT heat condition, evaluations include two load cases for the OCA and one load case for the ICV.

Maximum stress intensities are determined for each component, and classified according to primary or secondary, membrane or bending. Classification of stress intensities is per Table NB-3217-1 of the ASME Boiler and Pressure Vessel Code[3]. Maximum stress intensities are presented for the maximum general primary membrane stress intensity, P_m, the maximum local primary membrane stress intensity, P_L, the maximum primary membrane (general or local) plus primary bending stress intensity, $P_m + P_b$ or $P_L + P_b$, and the maximum primary plus secondary stress intensity, $P_m + P_b + Q$ or $P_L + P_b + Q$.

OCA Load Case 1 (see Table 2.6-1 and Figure 2.6-1 and Figure 2.6-2): This analysis is performed at a uniform temperature of 160 °F, but with the reference temperature also set to 160 °F thereby eliminating any differential thermal expansion stresses. The internal pressure considers the effects of a maximum normal operating pressure (MNOP) of 50 psig, internal,

[3] American Society of Mechanical Engineers (ASME) Boiler and Pressure Vessel Code, Section III, *Rules for Construction of Nuclear Power Plant Components*, 1995 Edition, 1997 Addenda.

coupled with a reduced external pressure of 3.5 psia (i.e., 11.2 psig, internal). The net result is an internal pressure of 50.0 + 11.2 = 61.2 psig.

P_m = 19,061 psi, located in the OCV shell at the cylindrical/conical transition,

P_L = 28,084 psi, located in the knuckle region of the upper OCV torispherical head,

$P_L + P_b$ = 20,256 psi, located in the OCV shell at the cylindrical/conical transition, and

$P_L + P_b + Q$ = 39,884 psi, located in the knuckle region of the lower OCV torispherical head.

OCA Load Case 2 (see Table 2.6-2 and Figure 2.6-3 and Figure 2.6-4): This analysis is performed at a uniform temperature of 160 °F, but with the reference temperature set to 70 °F thereby including any differential thermal expansion stresses. As with OCA Load Case 1, the MNOP is coupled with the reduced external pressure for a net internal pressure of 61.2 psig. The use of these two cases allows primary stress intensities (from pressure loads) to be considered independently of secondary stress intensities (from differential thermal expansion loads).

$P_L + P_b + Q$ = 40,200 psi, located in the knuckle region of the lower OCV torispherical head.

ICV Load Case 1 (see Table 2.6-5 and Figure 2.6-9 and Figure 2.6-10): This analysis is performed at a uniform temperature of 160 °F, but with the reference temperature also set to 160 °F thereby eliminating any differential thermal expansion stresses. As with OCA Load Cases 1 and 2, the MNOP is coupled with the reduced external pressure for a net internal pressure of 61.2 psig.

P_m = 15,251 psi, located in the upper ICV seal flange/shell transition,

P_L = 26,968 psi, located in the knuckle region of the upper ICV torispherical head,

$P_L + P_b$ = 22,336 psi, located in the upper ICV seal flange/shell transition, and

$P_L + P_b + Q$ = 38,304 psi, located in the knuckle region of the upper ICV torispherical head.

Polyurethane foam stress intensities are insignificant for OCA Load Case 1 (maximum stress intensity is 3 psi) and achieve a maximum value of 26 psi for OCA Load Case 2. Based on the perpendicular-to-rise direction at 160 °F, the minimum, polyurethane foam margin of safety is:

$$MS = \frac{124}{26} - 1 = +3.77$$

2.6.1.4 Comparison with Allowable Stresses

Section 2.1.2, *Design Criteria*, presents the design criteria for structural evaluation of the HalfPACT packaging. The containment vessel design criteria for NCT analyses are in accordance with Regulatory Guide 7.6, which uses as a basis the criteria defined for Level A service limits in Section III of the ASME Boiler and Pressure Vessel Code[4]. Load combinations follow the guidelines of Regulatory Guide 7.8[5].

From Table 2.3-1 in Section 2.3.1, *Mechanical Properties Applied to Analytic Evaluations*, the design stress intensity for Type 304 stainless steel used in the ICV and OCV is S_m = 20,000 psi at 160 °F. From Table 2.1-1 in Section 2.1.2.1.1, *Containment Structure (ICV)*, the allowable

[4] American Society of Mechanical Engineers (ASME) Boiler and Pressure Vessel Code, Section III, *Rules for Construction of Nuclear Power Plant Components*, 1995 Edition, 1997 Addenda.

[5] U. S. Nuclear Regulatory Commission, Regulatory Guide 7.8, *Load Combinations for the Structural Analysis of Shipping Casks for Radioactive Material*, Revision 1, March 1989.

stress intensities for the NCT hot condition is S_m for general primary membrane stress intensity (P_m), $1.5S_m$ for local primary membrane stress intensity (P_L), $1.5S_m$ for primary membrane (general or local) plus primary bending stress intensity ($P_m + P_b$ or $P_L + P_b$), and $3.0S_m$ for the range of primary plus secondary stress intensity ($P_m + P_b + Q$ or $P_L + P_b + Q$).

Maximum stress intensity, allowable stress intensity, and minimum margins of safety for each stress category and each load case are presented in Table 2.6-1, Table 2.6-2, and Table 2.6-5 for each of the cases discussed above. Since all margins of safety are positive, the design criteria are satisfied.

2.6.1.5 Range of Primary Plus Secondary Stress Intensities

Per Paragraph C.4 of Regulatory Guide 7.6, the maximum range of primary plus secondary stress intensity for NCT must be less than $3.0S_m$. This limitation on stress intensity range applies to the entire history of NCT loadings and not only to the stresses from each individual load transient.

2.6.1.5.1 Range of Primary Plus Secondary Stress Intensities for the OCA

The extreme ends of the stress range are determined from OCA Load Case 2 (from Section 2.6.1, *Heat*) and OCA Load Case 4 (from Section 2.6.4, *Increased External Pressure*). One extreme, OCA Load Case 2 represents the case of maximum internal pressure coupled with reduced external pressure, plus the effect of differential thermal expansion associated with heat-up from 70 °F to 160 °F. The other extreme, OCA Load Case 4, considers the effect of a minimum internal pressure at 70 °F. Note that combinations of other OCA load cases such as increased external pressure (20 psia, 5.3 psig) plus cool-down from 70 °F to -20 °F were also considered and found not to be bounding for the stress intensity range calculation.

The maximum range of primary plus secondary stress intensity occurs in the knuckle region of the lower OCV torispherical head (element 320). The extreme values of stress intensity are 40,200 psi and 9,641 psi from Table 2.6-2 and Table 2.6-4 for OCA Load Cases 2 and 4, respectively. Since OCA Load Cases 2 and 4 have opposite loads, the maximum range of primary plus secondary stress intensity is simply 40,200 + 9,641 = 49,841 psi. The allowable stress intensity is $3.0S_m$, where S_m = 20,000 psi for Type 304 stainless steel at 160 °F. The margin of safety is:

$$MS = \frac{3(20{,}000)}{49{,}841} - 1 = +0.20$$

The positive margin of safety indicates that the design criterion is satisfied.

2.6.1.5.2 Range of Primary Plus Secondary Stress Intensities for the ICV

The extreme ends of the stress range are determined from ICV Load Case 1 (from Section 2.6.1, *Heat*) and ICV Load Case 2 (from Section 2.6.4, *Increased External Pressure*). One extreme, ICV Load Case 1 represents the case of maximum internal pressure coupled with reduced external pressure, plus the effect of differential thermal expansion associated with heat-up from 70 °F to 160 °F. The other extreme, ICV Load Case 2, considers the effect of a minimum internal pressure at 70 °F.

The extreme values of stress intensity are 38,304 psi and 9,104 psi from Table 2.6-5 and Table 2.6-6 for ICV Load Cases 1 and 2, respectively, conservatively ignoring the fact that the extreme values occur at locations remote from each other. Since ICV Load Cases 1 and 2 have opposite loads, the maximum range of primary plus secondary stress intensity is simply 38,304 + 9,104

= 47,408 psi. The allowable stress intensity is $3.0S_m$, where S_m = 20,000 psi for Type 304 stainless steel at 160 °F. The margin of safety is:

$$MS = \frac{3(20{,}000)}{47{,}408} - 1 = +0.27$$

The positive margin of safety indicates that the design criterion is satisfied.

2.6.2 Cold

The NCT cold condition consists of exposing the HalfPACT packaging to a steady-state ambient temperature of -40 °F. Insolation and payload internal decay heat are assumed to be zero. These conditions will result in a uniform temperature throughout the package of -40 °F. With no internal heat load (i.e., no contents to produce heat and, therefore, pressure), the net pressure differential is assumed to be zero (14.7 psia internal, 14.7 psia external).

For the OCA, the principal structural concern due to the NCT cold condition is the effect of the differential expansion of the polyurethane foam relative to the surrounding stainless steel shells. During the cool-down from 70 °F to -40 °F, the foam material shrinks onto the OCV because thermal expansion coefficient for foam is greater than stainless steel. The resulting stresses are discussed in Section 2.6.2.1, *Stress Calculations*.

Differential thermal expansion stresses are negligible in the ICV for three reasons: 1) the temperature distribution throughout the entire ICV is relatively uniform, 2) the ICV is fabricated from only one type of structural material, and 3) the ICV is not radially or axially constrained within a tight-fitting structure (i.e., the OCV).

Brittle fracture at -40 °F is addressed in Section 2.1.2.2.1, *Brittle Fracture*. Performance of the O-ring seals at -40 °F is discussed in Appendix 2.10.2, *Elastomer O-ring Seal Performance Tests*.

2.6.2.1 Stress Calculations

A finite element model of the OCA is used to determine the stresses due to the combined effects of pressure loads, and temperature loads due to differential thermal expansion. The details of this model are presented in Appendix 2.10.1.1, *Outer Confinement Assembly (OCA) Structural Analysis*. For the NCT cold condition, evaluations include one load case for the OCA.

Maximum stress intensities are determined for each component, and classified according to primary or secondary, membrane or bending. Classification of stress intensities is per Table NB-3217-1 of the ASME Boiler and Pressure Vessel Code. Membrane and membrane plus bending stresses due to differential thermal expansion are classified as secondary stresses (Q). Since there are no pressure loads, primary stresses (P_m, P_L, and $P_m + P_b$ or $P_L + P_b$) are equal to zero.

OCA Load Case 3 (see Table 2.6-3 and Figure 2.6-5 and Figure 2.6-6): This analysis is performed at a uniform temperature of -40 °F, but with the reference temperature set to 70 °F thereby including differential thermal expansion stresses. For a uniform temperature cold case at -40 °F, both payload decay heat and solar heat are assumed to be zero. These conditions result in an internal pressure of 14.7 psia balanced with an external pressure of 14.7 psia, for a net pressure differential of zero.

$P_L + P_b + Q$ = 5,772 psi, located in the lower OCV seal flange/Z-flange junction.

Polyurethane foam stress intensities are relatively small for OCA Load Case 3 (maximum stress intensity is 15 psi). Conservatively based on the perpendicular-to-rise direction at 160 °F, the minimum, polyurethane foam margin of safety is:

$$MS = \frac{124}{15} - 1 = +7.27$$

2.6.2.2 Comparison with Allowable Stresses

Section 2.1.2, *Design Criteria*, presents the design criteria for structural evaluation of the HalfPACT packaging. The containment vessel design criteria for NCT analyses are in accordance with Regulatory Guide 7.6, which uses as a basis the criteria defined for Level A service limits in Section III of the ASME Boiler and Pressure Vessel Code. Load combinations follow the guidelines of Regulatory Guide 7.8.

From Table 2.3-1 in Section 2.3.1, *Mechanical Properties Applied to Analytic Evaluations*, the design stress intensity for Type 304 stainless steel used in the ICV and OCV is $S_m = 20{,}000$ psi at -40 °F. From Table 2.1-1 in Section 2.1.2.1.1, *Containment Structure (ICV)*, the allowable stress intensity for the NCT cold condition is $3.0S_m$ for the range of primary plus secondary stress intensity ($P_m + P_b + Q$ or $P_L + P_b + Q$).

Maximum stress intensity, allowable stress intensity, and minimum margins of safety for each stress category and each load case are presented in Table 2.6-3 for OCA Load Case 3. Since all margins of safety are positive, the design criteria are satisfied.

Since the NCT cold condition results in shrinking of the polyurethane foam onto the OCV shell, compressive stresses develop in the OCV shell. The buckling evaluation within Section 2.6.4, *Increased External Pressure*, demonstrates that the compressive stresses due to increased external pressure do not exceed the NCT allowable stresses. The compressive stresses generated during the NCT cold condition are bounded by the NCT increased external pressure condition, therefore no explicit buckling evaluation is required for the NCT cold condition.

2.6.3 Reduced External Pressure

The effect of a reduced external pressure of 3.5 psia (11.2 psig internal pressure), per 10 CFR §71.71(c)(3), is negligible for the HalfPACT packaging. This conclusion is based on the analyses presented in Section 2.6.1, *Heat*, addressing the ability of both the ICV and OCV to independently withstand a maximum normal operating pressure (MNOP) of 50 psig, combined with a reduced external pressure of 3.5 psia, for a net effective internal pressure of 61.2 psig.

2.6.4 Increased External Pressure

The effect of an increased external pressure of 20 psia (5.3 psig external pressure), per 10 CFR §71.71(c)(4), is negligible for the HalfPACT packaging. Both the ICV and OCV are designed to withstand a full vacuum equivalent to 14.7 psi external pressure during acceptance leakage rate testing of the HalfPACT package, as described in Section 8.1.3, *Fabrication Leakage Rate Tests*. Therefore, the worst case NCT external pressure loading is 14.7 psig.

The external pressure induces small compressive stresses in the ICV and OCV that are limited by stability (buckling) requirements. Buckling assessments are performed for the OCV and ICV in

Section 2.6.4.3, *Buckling Assessment of the Torispherical Heads*, and Section 2.6.4.4, *Buckling Assessment of the Cylindrical Shells.*

2.6.4.1 Stress Calculations

A finite element model of the OCA is used to determine the stresses due to the effect of a pressure load. The details of this model are presented in Appendix 2.10.1.1, *Outer Confinement Assembly (OCA) Structural Analysis.* The ICV is also analyzed for the effects of a pressure using a finite element model that is described in Appendix 2.10.1.2, *Inner Containment Vessel (ICV) Structural Analysis.* For the NCT increased external pressure condition, evaluations include one load case for the OCA and one load case for the ICV.

Maximum stress intensities are determined for each component, and classified according to primary or secondary, membrane or bending. Classification of stress intensities is per Table NB-3217-1 of the ASME Boiler and Pressure Vessel Code. Maximum stress intensities are presented for the maximum general primary membrane stress intensity, P_m, the maximum local primary membrane stress intensity, P_L, the maximum primary membrane (general or local) plus primary bending stress intensity, $P_m + P_b$ or $P_L + P_b$, and the maximum primary plus secondary stress intensity, $P_m + P_b + Q$ or $P_L + P_b + Q$.

OCA Load Case 4 (see Table 2.6-4 and Figure 2.6-7 and Figure 2.6-8): This analysis is performed at a uniform temperature of 70 °F, and the reference temperature also set to 70 °F thereby eliminating any differential thermal expansion stresses. The external pressure is 14.7 psig.

P_m = 4,748 psi, located in the OCV shell at the cylindrical/conical transition,

P_L = 6,852 psi, located in the knuckle region of the upper OCV torispherical head,

$P_L + P_b$ = 5,087 psi, located in the OCV shell at the cylindrical/conical transition, and

$P_L + P_b + Q$ = 9,641 psi, located in the knuckle region of the lower OCV torispherical head.

ICV Load Case 2 (see Table 2.6-6 and Figure 2.6-11 and Figure 2.6-12): This analysis is performed at a uniform temperature of 70 °F, but with the reference temperature also set to 70 °F thereby eliminating any differential thermal expansion stresses. As with OCA Load Case 4, the external pressure is 14.7 psig.

P_m = 3,635 psi, located in the crown region of the upper ICV torispherical head,

P_L = 6,384 psi, located in the knuckle region of the upper ICV torispherical head,

$P_L + P_b$ = 4,656 psi, located in the crown region of the upper ICV torispherical head, and

$P_L + P_b + Q$ = 9,104 psi, located in the knuckle region of the upper ICV torispherical head.

Polyurethane foam stress intensities are insignificant for OCA Load Case 4.

2.6.4.2 Comparison with Allowable Stresses

Section 2.1.2, *Design Criteria*, presents the design criteria for structural evaluation of the HalfPACT packaging. The containment vessel design criteria for NCT analyses are in accordance with Regulatory Guide 7.6, which uses as a basis the criteria defined for Level A service limits in Section III of the ASME Boiler and Pressure Vessel Code. Load combinations follow the guidelines of Regulatory Guide 7.8.

From Table 2.3-1 in Section 2.3.1, *Mechanical Properties Applied to Analytic Evaluations*, the design stress intensity for Type 304 stainless steel used in the ICV and OCV is S_m = 20,000 psi at 160 °F. From Table 2.1-1 in Section 2.1.2.1.1, *Containment Structure (ICV)*, the allowable

stress intensities for the NCT increased external pressure condition is S_m for general primary membrane stress intensity (P_m), $1.5S_m$ for local primary membrane stress intensity (P_L), $1.5S_m$ for primary membrane (general or local) plus primary bending stress intensity ($P_m + P_b$ or $P_L + P_b$), and $3.0S_m$ for the range of primary plus secondary stress intensity ($P_m + P_b + Q$ or $P_L + P_b + Q$).

Maximum stress intensity, allowable stress intensity, and minimum margins of safety for each stress category and each load case are presented in Table 2.6-4 and Table 2.6-6 for each of the cases discussed above. Since all margins of safety are positive, the design criteria are satisfied.

2.6.4.3 Buckling Assessment of the Torispherical Heads

The buckling analysis of the torispherical heads is based on the methodology outlined in Paragraph NE-3133.4(e), *Torispherical Heads*, of the ASME Boiler and Pressure Vessel Code, Section III, Subsection NE. The results from following this methodology are summarized below.

Parameter	OCV Torispherical Head		ICV Torispherical Head	
	Upper	Lower	Upper	Lower
R	77.3125	74.1250	74.3750	73.1250
T	0.25	0.25	0.25	0.25
$A = \frac{0.125}{(R/T)}$	0.00040	0.00042	0.00042	0.00043
B[6]	5,000	5,000	5,000	5,000
$P_a = \frac{B}{(R/T)}$	16.2	16.9	16.8	17.1

The smallest allowable pressure, P_a, is 16.2 psig for the OCV upper head. For an applied external pressure of 14.7 psig, the corresponding buckling margin of safety is:

$$MS = \frac{16.2}{14.7} - 1 = +0.10$$

Since the margin of safety in the worst case is positive, it is concluded that none of the OCV or ICV torispherical heads will buckle for an external pressure of 14.7 psig.

2.6.4.4 Buckling Assessment of the Cylindrical Shells

The cylindrical portions of the OCV and ICV are evaluated using ASME Boiler and Pressure Vessel Code Case N-284-1[7]. Consistent with Regulatory Guide 7.6 philosophy, a factor of

[6] Factor B is found from American Society of Mechanical Engineers (ASME) Boiler and Pressure Vessel Code, Section II, *Materials*, Part D, *Properties*, Subpart 3, *Charts and Tables for Determining the Shell Thickness of Components Under External Pressure*, Figure HA-1, *Chart for Determining Shell Thickness of Components Under External Pressure When Constructed of Austenitic Steel (18Cr–8Ni, Type 304)*, 1995 Edition, 1997 Addenda. Conservatively, the 400 °F temperature curve is used for each case.

safety of 2.0 is applied for NCT buckling evaluations per ASME Code Case N-284-1, corresponding to ASME Code, Service Level A conditions.

Buckling analysis geometry parameters are summarized in Table 2.6-7, and loading parameters are summarized in Table 2.6-8. The cylindrical shell buckling analysis conservatively utilizes an OCV and ICV temperature of 160 °F, consistent with Section 2.6.1, *Heat*. The stresses are determined using an external pressure of 14.7 psig. The hoop stress, σ_θ, axial stress, σ_ϕ, and in-plane shear stress, $\sigma_{\phi\theta}$, are found from:

$$\sigma_\theta = \frac{Pr}{t} \qquad \sigma_\phi = \frac{Pr}{2t} \qquad \sigma_{\phi\theta} = \frac{Pr}{4t}$$

where P is the applied external pressure of 14.7 psi, r is the mean radius, and t is the cylindrical shell thickness. As shown in Table 2.6-9, since all interaction check parameters are less than 1.0, as required, the design criteria are satisfied.

2.6.5 Vibration

By comparing the alternating stresses arising during NCT with the established endurance limits of the HalfPACT packaging materials of construction, the effects of vibration normally incident to transport are shown to be acceptable. These comparisons apply the methodology and limits of NRC Regulatory Guide 7.6. By conservatively comparing NCT stresses with endurance stress limits for an infinite service life, the development of accurate vibratory loading cycles is not required. The vibration evaluation is comprehensively addressed in the following sections.

2.6.5.1 Vibratory Loads Determination

ANSI N14.23[8] provides a basis for estimating peak truck trailer vibration inputs. A summary of peak vibratory accelerations for a truck semi-trailer bed with light loads (less than 15 tons) is provided in Table 2 of ANSI N14.23. The component accelerations are given in Table 2 as 1.3*g* longitudinally, 0.5*g* laterally, and 2.0*g* vertically. Three fully loaded HalfPACT packages on a single trailer will exceed the light load limit, but acceleration magnitudes associated with light loads are conservative for heavy loads per Table 2 of ANSI N14.23. The commentary provided within Section 4.2, *Package Response*, of ANSI N14.23 states that recent "tests conducted by Sandia National Laboratories have shown that the *truck bed* accelerations provide an upper bound on *cask* (response) accelerations." Based upon these data, conservatively assume the peak acceleration values from Table 2 are applied to the HalfPACT package in a continuously cycling fashion.

The compressive stress in the polyurethane foam for a 2g vertical acceleration is determined by conservatively ignoring the contributory effect of the OCA outer shell and dividing a maximum weight HalfPACT package (18,100 pounds) by the projected area of the package's bottom. The projected area of a HalfPACT package is simply $(\pi/4)(94.375)^2 = 6{,}995$ in^2. Therefore, the compressive stress is (2)(18,100)/6,995 = 5 psi. This stress is negligible compared to the parallel-to-rise compressive strength of 150 psi for polyurethane foam at 160 °F, as discussed in

[7] American Society of Mechanical Engineers (ASME) Boiler and Pressure Vessel Code, Section III, *Rules for Construction of Nuclear Power Plant Components*, Division 1, Class MC, Code Case N-284-1, *Metal Containment Shell Buckling Design Methods*, 1995 Edition, 1997 Addenda.

[8] ANSI N14.23, *Design Basis for Resistance to Shock and Vibration of Radioactive Material Packages Greater than One Ton in Truck Transport* (Draft), 1980, American National Standards Institute, Inc, (ANSI).

Section 2.6.1, *Heat*. Therefore, the remainder of the NCT vibration evaluation addresses only the structural steel portions of the HalfPACT packaging.

2.6.5.2 Calculation of Alternating Stresses

The HalfPACT package is a compact right circular cylinder. As such, the stresses developed as a result of transportation vibration become significant only where concentrated in the vicinity of the tie-downs and package interfaces with the transport vehicle. This fact allows the stress analyses of Section 2.5.2, *Tie-down Devices*, to serve as the basis for derivation of alternating stress estimates.

The analyses of Section 2.5.2, *Tie-down Devices*, identify three maximum stress locations of importance in the immediate vicinity of the tie-down lugs:

1. **Tiedown lug weld shear stresses due to tensile tie-down forces.** Under a combined set of tie-down forces (i.e., 10*g* longitudinally, 5*g* laterally, and 2*g* vertically), the tie-down lug vertical tensile force is F_{tmax} = 68,950 pounds. The corresponding tie-down lug weld shear stress is τ = 8,997 psi, from Section 2.5.2.2.1, *Failure of the Tie-down Lug Welds Due to Shear and Bending Loads*. Weld shear stresses associated with unit accelerations (i.e., 1*g*) are derived from these values, as presented in Table 2.6-10. Under unit horizontal and vertical accelerations, the maximum weld shear stresses are 699 psi and 590 psi, respectively, as shown in Table 2.6-10.
2. **OCA outer shell compressive membrane stresses due to vertical compressive loads.** Under a combined set of tie-down forces (i.e., 10*g* longitudinally, 5*g* laterally, and 2*g* vertically), the OCA outer shell and tie-down lug doubler plate vertical compressive load is F_{cmax} = 128,901 pounds. The corresponding compressive membrane stress is σ_c = 12,394 psi, from Section 2.5.2.3.1, *Bearing Stress in the OCA Outer Shell and Tie-down Lug Doubler Plate*. Compressive membrane stresses associated with unit accelerations (i.e., 1*g*) are derived from these values, as presented in Table 2.6-11. Under unit horizontal and vertical accelerations, the maximum membrane compression stresses are 1,031 psi and 435 psi, respectively, as shown in Table 2.6-11.
3. **OCA tie-down weldment compressive membrane stresses due to horizontal compressive loads.** Under a combined set of tie-down forces (i.e., 10*g* longitudinally, 5*g* laterally, and 2*g* vertically), the OCA tie-down weldment horizontal compressive load is F_h = 202,364 pounds. The corresponding compressive membrane stress is σ_c = 25, 296 psi, from Section 2.5.2.4.1, *Bearing Stress in the Tie-down Weldment*. Compressive membrane stresses associated with unit accelerations (i.e., 1*g*) are derived from these values, as presented in Table 2.6-12. Under unit horizontal accelerations, the maximum membrane compression stress is 2,263 psi, as shown in Table 2.6-12.

Alternating stress intensities, S_{alt}, due to 1*g* unit accelerations are calculated directly from the above values since there are no other measurable stresses acting on the package at the locations considered. Unit alternating stress intensities at the three evaluated locations are found as shown in Table 2.6-13, making use of the definition of alternating stress intensity as one-half of the range of stress intensity at the location of interest, and the definition of stress intensity as twice the shear stress.

These maximum alternating stress intensity unit values correspond to stresses in the bevel-plus-fillet welds used to attach the tie-down lugs to the tie-down lug doubler plates. A stress concentration factor of four is conservatively applied in accordance with Paragraph C.3.d of

Regulatory Guide 7.6. Normalizing the unit values to the peak acceleration estimates given in Section 2.6.5.1, *Vibratory Loads Determination*, and including the stress concentration factor of four and assuming these worst cases occur at the same location, results in the following conservative estimates of alternating stress intensity associated with the vibratory environments.

For the maximum horizontal alternating stress intensity of 1,132 psi from Table 2.6-13:

$$S_{alt} = 4(1{,}132)\sqrt{(1.3)^2 + (0.5)^2} = 6{,}307 \text{ psi}$$

and, for the maximum vertical alternating stress intensity of 590 psi from Table 2.6-13:

$$S_{alt} = 4(590)(2.0) = 4{,}720 \text{ psi}$$

Assuming a simultaneous application of the above alternating stress intensities associated with horizontal and vertical loads yields a maximum alternating stress of 6,307 + 4,720 = 11,027 psi.

2.6.5.3 Stress Limits and Results

The permissible alternating stress intensity, S_a, is given by conservatively using the minimum asymptotic value from the design fatigue curves in Table I-9.2.2 of the ASME Boiler and Pressure Vessel Code[9]. For design fatigue curve C at 10^{11} cycles, S_a = 13,600 psi, based on an elastic modulus of $28.3(10)^6$ psi. This value, when multiplied by the ratio of the elastic modulus at 160 °F of $27.8(10)^6$ psi to an elastic modulus at 70 °F of $28.3(10)^6$ psi results in an allowable alternating stress intensity amplitude at 160 °F of:

$$S_a = 13{,}600\left(\frac{27.8}{28.3}\right) = 13{,}360 \text{ psi}$$

Finally, a conservative estimate of the margin of safety for vibratory effects becomes:

$$MS = \frac{S_a}{S_{alt}} - 1 = \frac{13{,}360}{11{,}027} - 1 = +0.21$$

2.6.6 Water Spray

The materials of construction utilized for the HalfPACT package are such that the water spray test identified in 10 CFR §71.71(c)(6) will have a negligible effect on the package.

2.6.7 Free Drop

Since the maximum gross weight of the HalfPACT package is 18,100 pounds, a 3-foot free drop is required per 10 CFR §71.71(c)(7). As discussed in Appendix 2.10.3, *Certification Tests*, a NCT, 3-foot side drop, aligned over the OCV vent port, was performed on a HalfPACT package certification test unit (CTU) as an initial condition for subsequent hypothetical accident condition (HAC) tests. Leakage rate testing following certification testing demonstrated the ability of the

[9] American Society of Mechanical Engineers (ASME) Boiler and Pressure Vessel Code, Section III, *Rules for Construction of Nuclear Power Plant Components*, Appendix I, *Design Stress Intensity Values, Allowable Stresses, Material Properties, and Design Fatigue Curves*, 1995 Edition, 1997 Addenda.

HalfPACT package to maintain leaktight (i.e., 1.0×10^{-7} standard cubic centimeters per second (scc/sec), air) sealing integrity. Therefore, the requirements of 10 CFR §71.71(c)(7) are met.

2.6.8 Corner Drop

This test does not apply, since the package weight is in excess of 100 kg (220 pounds), and the materials do not include wood or fiberboard, as delineated in 10 CFR §71.71(c)(8).

2.6.9 Compression

This test does not apply, since the package weight is in excess of 5,000 kg (11,000 pounds), as delineated in 10 CFR §71.71(c)(9).

2.6.10 Penetration

The one-meter (40-inch) drop of a 13-pound, hemispherically-headed, 1¼-inch diameter, steel cylinder, as delineated in 10 CFR §71.71(c)(10), is of negligible consequence to the HalfPACT package. This is due to the fact that the HalfPACT package is designed to minimize the consequences associated with the much more limiting case of a 40 inch drop of the entire package onto a puncture bar as discussed in Section 2.7.3, *Puncture*. The 1/4-inch minimum thickness, OCA outer shell, the tie-down lugs and doubler plates, and the vent port and seal test port penetrations are not damaged by the penetration event.

Table 2.6-1 – Summary of Stress Results for OCA Load Case 1

Component	Location	Stress Intensity (psi)			
		General Primary Membrane (P_m)	Local Primary Membrane (P_L)	Primary Membrane + Bending ($P_{mL}+P_b$)	Primary plus Secondary ($P_{mL}+P_b+Q$)
OCV Shells	Cylindrical and Conical Shells	19,061 (Element 329)	-----	20,256 (Element 329)	-----
OCV Upper and Lower Torispherical Heads	Crown	13,366 (Element 339)	-----	18,739 (Element 340)	-----
	Knuckle	-----	28,084 (Element 337)	-----	39,884 (Element 320)
OCV Upper and Lower Seal Flanges	Shell side of the thickness transition	-----	-----	-----	32,358 (Node 2010)
	Flange side of the thickness transition	-----	-----	-----	20,129 (Node 2016)
OCV Locking Ring	Any location	-----	-----	-----	24,493 (Node 3050)
OCA Outer Shell and Z-flanges	Any location	9,114 (Element 414)	-----	14,215 (Element 414)	-----
Maximum Stress Intensity		19,061	28,084	20,256	39,884
Allowable Stress Intensity		20,000 (S_m)	30,000 ($1.5S_m$)	30,000 ($1.5S_m$)	60,000 ($3.0S_m$)
Minimum Margin of Safety		+0.05	+0.07	+0.48	+0.50

Table 2.6-2 – Summary of Stress Results for OCA Load Case 2

Component	Location	Stress Intensity (psi)			
		General Primary Membrane (P_m)	Local Primary Membrane (P_L)	Primary Membrane + Bending ($P_{mL}+P_b$)	Primary plus Secondary ($P_{mL}+P_b+Q$)
OCV Shells	Cylindrical and Conical Shells	-----	-----	-----	20,144 (Element 329)
OCV Upper and Lower Torispherical Heads	Crown	-----	-----	-----	18,831 (Element 340)
	Knuckle	-----	-----	-----	40,200 (Element 320)
OCV Upper and Lower Seal Flanges	Shell side of the thickness transition	-----	-----	-----	32,569 (Node 2010)
	Flange side of the thickness transition	-----	-----	-----	20,271 (Node 2016)
OCV Locking Ring	Any location	-----	-----	-----	24,503 (Node 3050)
OCA Outer Shell and Z-flanges	Any location	-----	-----	-----	12,385 (Element 399)
Maximum Stress Intensity		-----	-----	-----	40,200
Allowable Stress Intensity		20,000 (S_m)	30,000 ($1.5S_m$)	30,000 ($1.5S_m$)	60,000 ($3.0S_m$)
Minimum Margin of Safety		-----	-----	-----	+0.49

Table 2.6-3 – Summary of Stress Results for OCA Load Case 3

Component	Location	Stress Intensity (psi)			
		General Primary Membrane (P_m)	Local Primary Membrane (P_L)	Primary Membrane + Bending ($P_{mL} + P_b$)	Primary plus Secondary ($P_{mL} + P_b + Q$)
OCV Shells	Cylindrical and Conical Shells	-----	-----	-----	854 (Element 327)
OCV Upper and Lower Torispherical Heads	Crown	-----	-----	-----	538 (Element 309)
	Knuckle	-----	-----	-----	1,040 (Element 323)
OCV Upper and Lower Seal Flanges	Shell side of the thickness transition	-----	-----	-----	450 (Node 2001)
	Flange side of the thickness transition	-----	-----	-----	911 (Node 1040)
OCV Locking Ring	Any location	-----	-----	-----	0
OCA Outer Shell and Z-flanges	Any location	-----	-----	-----	5,772 (Element 393)
Maximum Stress Intensity		-----	-----	-----	5,772
Allowable Stress Intensity		20,000 (S_m)	30,000 ($1.5S_m$)	30,000 ($1.5S_m$)	60,000 ($3.0S_m$)
Minimum Margin of Safety		-----	-----	-----	+9.40

Table 2.6-4 – Summary of Stress Results for OCA Load Case 4

Component	Location	Stress Intensity (psi)			
		General Primary Membrane (P_m)	Local Primary Membrane (P_L)	Primary Membrane + Bending ($P_{mL} + P_b$)	Primary plus Secondary ($P_{mL} + P_b + Q$)
OCV Shells	Cylindrical and Conical Shells	4,748 (Element 329)	-----	5,087 (Element 329)	-----
OCV Upper and Lower Torispherical Heads	Crown	3,323 (Element 339)	-----	4,569 (Element 340)	-----
	Knuckle	-----	6,852 (Element 337)	-----	9,641 (Element 320)
OCV Upper and Lower Seal Flanges	Shell side of the thickness transition	-----	-----	-----	3,507 (Node 1016)
	Flange side of the thickness transition	-----	-----	-----	3,741 (Node 1164)
OCV Locking Ring	Any location	-----	-----	-----	4 (Node 3181)
OCA Outer Shell and Z-flanges	Any location	858 (Element 399)	-----	1,135 (Element 399)	-----
Maximum Stress Intensity		4,748	6,852	5,087	9,641
Allowable Stress Intensity		20,000 (S_m)	30,000 ($1.5S_m$)	30,000 ($1.5S_m$)	60,000 ($3.0S_m$)
Minimum Margin of Safety		+3.21	+3.38	+4.90	+5.22

Table 2.6-5 – Summary of Stress Results for ICV Load Case 1

Component	Location	Stress Intensity (psi)			
		General Primary Membrane (P_m)	Local Primary Membrane (P_L)	Primary Membrane + Bending ($P_{mL} + P_b$)	Primary plus Secondary ($P_{mL} + P_b + Q$)
ICV Shells	Cylindrical and Conical Shells	15,251 (Element 364)	-----	22,336 (Element 365)	-----
ICV Upper and Lower Torispherical Heads	Crown	15,242 (Element 376)	-----	19,519 (Element 377)	-----
	Knuckle	-----	26,968 (Element 373)	-----	38,304 (Element 374)
ICV Upper and Lower Seal Flanges	Shell side of the thickness transition	-----	-----	-----	34,042 (Node 2058)
	Flange side of the thickness transition	-----	-----	-----	27,922 (Node 2053)
ICV Locking Ring	Any location	-----	-----	-----	22,190 (Node 3046)
Maximum Stress Intensity		15,251	26,968	22,336	38,304
Allowable Stress Intensity		20,000 (S_m)	30,000 ($1.5S_m$)	30,000 ($1.5S_m$)	60,000 ($3.0S_m$)
Minimum Margin of Safety		+0.31	+0.11	+0.34	+0.57

Table 2.6-6 – Summary of Stress Results for ICV Load Case 2

Component	Location	Stress Intensity (psi)			
		General Primary Membrane (P_m)	Local Primary Membrane (P_L)	Primary Membrane + Bending ($P_{mL}+P_b$)	Primary plus Secondary ($P_{mL}+P_b+Q$)
ICV Shells	Cylindrical and Conical Shells	2,363 (Element 361)	-----	2,551 (Element 363)	-----
ICV Upper and Lower Torispherical Heads	Crown	3,635 (Element 376)	-----	4,656 (Element 377)	-----
	Knuckle	-----	6,382 (Element 373)	-----	9,104 (Element 374)
ICV Upper and Lower Seal Flanges	Shell side of the thickness transition	-----	-----	-----	2,706 (Node 2054)
	Flange side of the thickness transition	-----	-----	-----	3,640 (Node 1129)
ICV Locking Ring	Any location	-----	-----	-----	56 (Node 3046)
Maximum Stress Intensity		3,635	6,382	4,656	9,104
Allowable Stress Intensity		20,000 (S_m)	30,000 ($1.5S_m$)	30,000 ($1.5S_m$)	60,000 ($3.0S_m$)
Minimum Margin of Safety		+4.50	+3.70	+5.44	+5.59

Table 2.6-7 – Buckling Geometry Parameters per Code Case N-284-1

Geometry and Material Input		
	ICV	**OCV**
Mean Radius, inch	36.44	36.91
Shell Thickness, inch	0.25	0.188
Length, inch	36.0①	32.0②
Geometry Output (nomenclature consistent with ASME Code Case N-284-1)		
R =	36.44	36.91
t =	0.25	0.188
R/t =	145.76	196.85
ℓ_ϕ =	36.0	32.0
ℓ_θ =	228.94	231.89
M_ϕ =	11.93	12.16
M_θ =	75.85	88.15
M =	11.93	12.16

Notes:

① The ICV length is conservatively measured from five inches below the top of the lower ICV seal flange (at the beginning of the 1/4-inch wall thickness) to an assumed support point located one-third of the depth of the lower ICV torispherical head below the head-to-shell interface.

② The OCV length is conservatively measured from the top of the tapered wall portion (just below the lower OCV seal flange) to an assumed support point located one-third of the depth of the lower OCV torispherical head below the head-to-shell interface.

Table 2.6-8 – Stress Results for 14.7 psig External Pressure

ICV		OCV	
Axial Stress, σ_ϕ	1,071	Axial Stress, σ_ϕ	1,443
Hoop Stress, σ_θ	2,143	Hoop Stress, σ_θ	2,886
Shear Stress, $\sigma_{\phi\theta}$	536	Shear Stress, $\sigma_{\phi\theta}$	722

Table 2.6-9 – Buckling Summary for 14.7 psig External Pressure

Condition	ICV	OCV	Remarks
Capacity Reduction Factors (-1511)			
$\alpha_{\phi L}$ =	0.2575	0.2575	
$\alpha_{\theta L}$ =	0.8000	0.8000	
$\alpha_{\phi\theta L}$ =	0.8000	0.8000	
Plasticity Reduction Factors (-1611)			
η_{ϕ} =	0.5877	0.7307	
η_{θ} =	1.0000	1.0000	
$\eta_{\phi\theta}$ =	0.4474	0.5740	
Theoretical Buckling Values (-1712.1.1)			
C_{ϕ} =	0.6050	0.6050	
$\sigma_{\phi eL}$ =	115,720 psi	85,697 psi	
$C_{\theta r}$ =	0.0855	0.0837	
$\sigma_{\theta eL} = \sigma_{reL}$ =	16,354 psi	11,854 psi	
$C_{\theta h}$ =	0.0815	0.0798	
$\sigma_{\theta eL} = \sigma_{heL}$ =	15,581 psi	11,302 psi	
$C_{\phi\theta}$ =	0.2184	0.2162	
$\sigma_{\phi\theta eL}$ =	41,770 psi	30,615 psi	
Elastic Interaction Equations (-1713.1.1)			
σ_{xa} =	22,237 psi	16,466 psi	
σ_{ha} =	9,302 psi	6,748 psi	
σ_{ra} =	9,764 psi	7,077 psi	
$\sigma_{\tau a}$ =	24,937 psi	18,278 psi	
Axial + Hoop ⇨ Check (a):	*N/A*	*N/A*	
Axial + Hoop ⇨ Check (b):	*N/A*	*N/A*	
Axial + Shear ⇨ Check (c):	*0.0697*	*0.1287*	<1 ∴ OK
Hoop + Shear ⇨ Check (d):	*0.3144*	*0.5873*	<1 ∴ OK
Axial + Hoop + Shear ⇨ Check (e,a):	*N/A*	*N/A*	
Axial + Hoop + Shear ⇨ Check (e,b):	*N/A*	*N/A*	
Inelastic Interaction Equations (-1713.2.1)			
σ_{xc} =	13,069 psi	12,032 psi	
σ_{rc} =	9,764 psi	7,077 psi	
$\sigma_{\tau c}$ =	11,157 psi	10,492 psi	
Axial + Hoop ⇨ Check (a):	*0.3135*	*0.5841*	<1 ∴ OK
Axial + Shear ⇨ Check (b):	*0.1218*	*0.1750*	<1 ∴ OK
Hoop + Shear ⇨ Check (c):	*0.3182*	*0.5873*	<1 ∴ OK

Table 2.6-10 – Tie-down Lug Weld Shear Stresses

Case and Orientation	Load Factors (*gs*)	Load (pounds)	Shear Stress (psi)
Combined	10(x), 5(y), 2(z)	68,950	8,997
Horizontal	$[10^2 + 5^2]^{½} = 11.18$ (unit horizontal of 1*g*)	59,900 (5,358)	7,816 (699)
Vertical	2.00 (unit vertical of 1*g*)	9,050 (4,025)	1,181 (590)

Table 2.6-11 – OCA Outer Shell Compressive Membrane Stresses

Case and Orientation	Load Factors (*gs*)	Load (pounds)	Membrane Stress (psi)
Combined	10(x), 5(y), 2(z)	128,901	12,394
Horizontal	$[10^2 + 5^2]^{½} = 11.18$ (unit horizontal of 1*g*)	119,851 (10,720)	11,524 (1,031)
Vertical	2.00 (unit vertical of 1*g*)	9,050 (4,025)	870 (435)

Table 2.6-12 – OCA Tie-down Weldment Compressive Membrane Stresses

Case and Orientation	Load Factors (*gs*)	Load (pounds)	Membrane Stress (psi)
Horizontal	$[10^2 + 5^2]^{½} = 11.18$ (unit horizontal of 1*g*)	202,364 (18,100)	25,296 (2,263)

Table 2.6-13 – Maximum Unit Alternating Stress Intensities

Case and Orientation	Alternating Stress Intensity
Lug Weld Shear	$S_{alt} = \frac{2\tau_{max}}{2}$ = 699 psi, Horizontal = 590 psi, Vertical
OCA Shell Compression	$S_{alt} = \frac{\sigma_{max}}{2}$ = 516 psi, Horizontal = 218 psi, Vertical
OCA Base Compression	$S_{alt} = \frac{\sigma_{max}}{2}$ = 1,132 psi, Horizontal
Maximum Unit Values	= 1,132 psi, Horizontal = 590 psi, Vertical

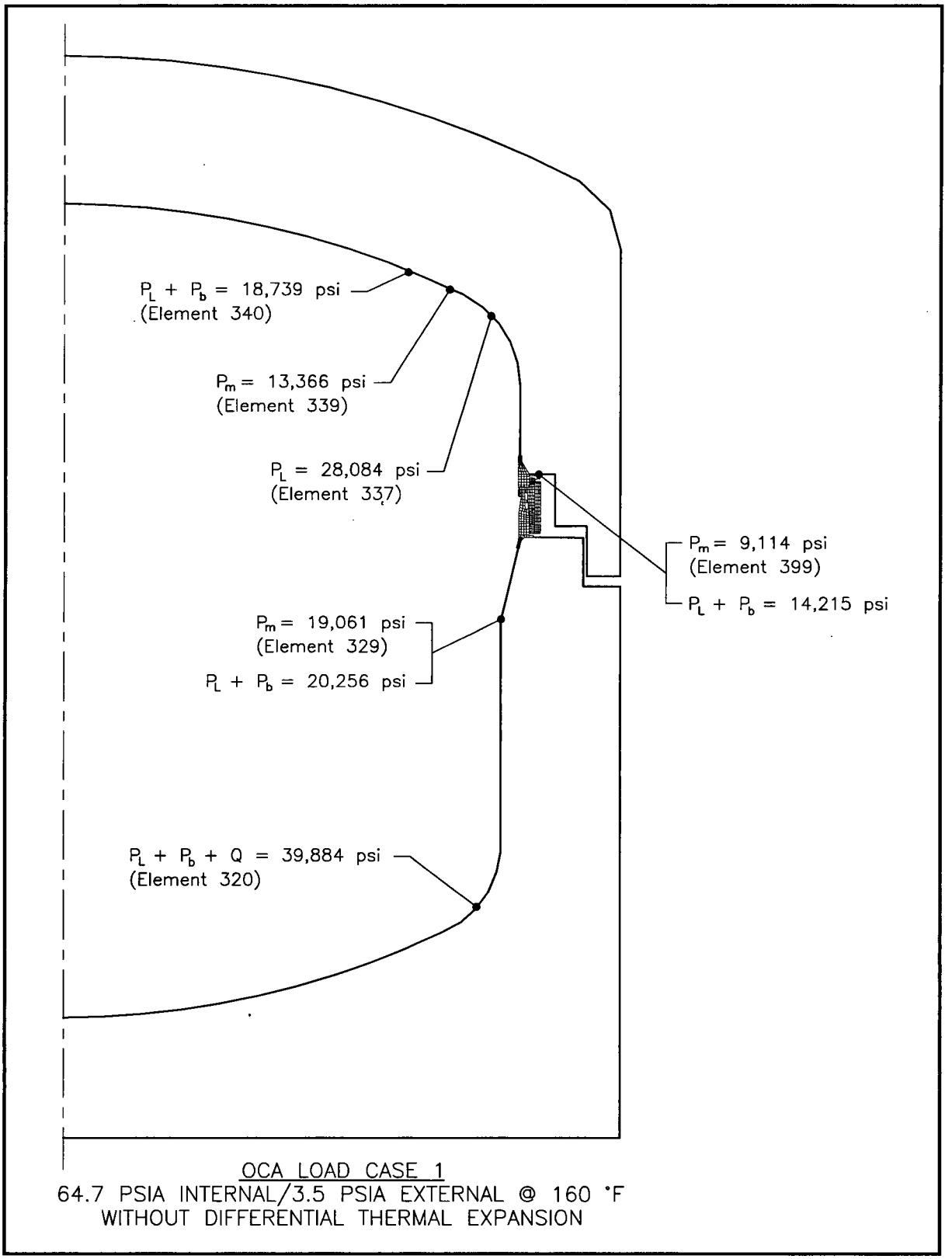

Figure 2.6-1 – OCA Load Case 1, Overall Model

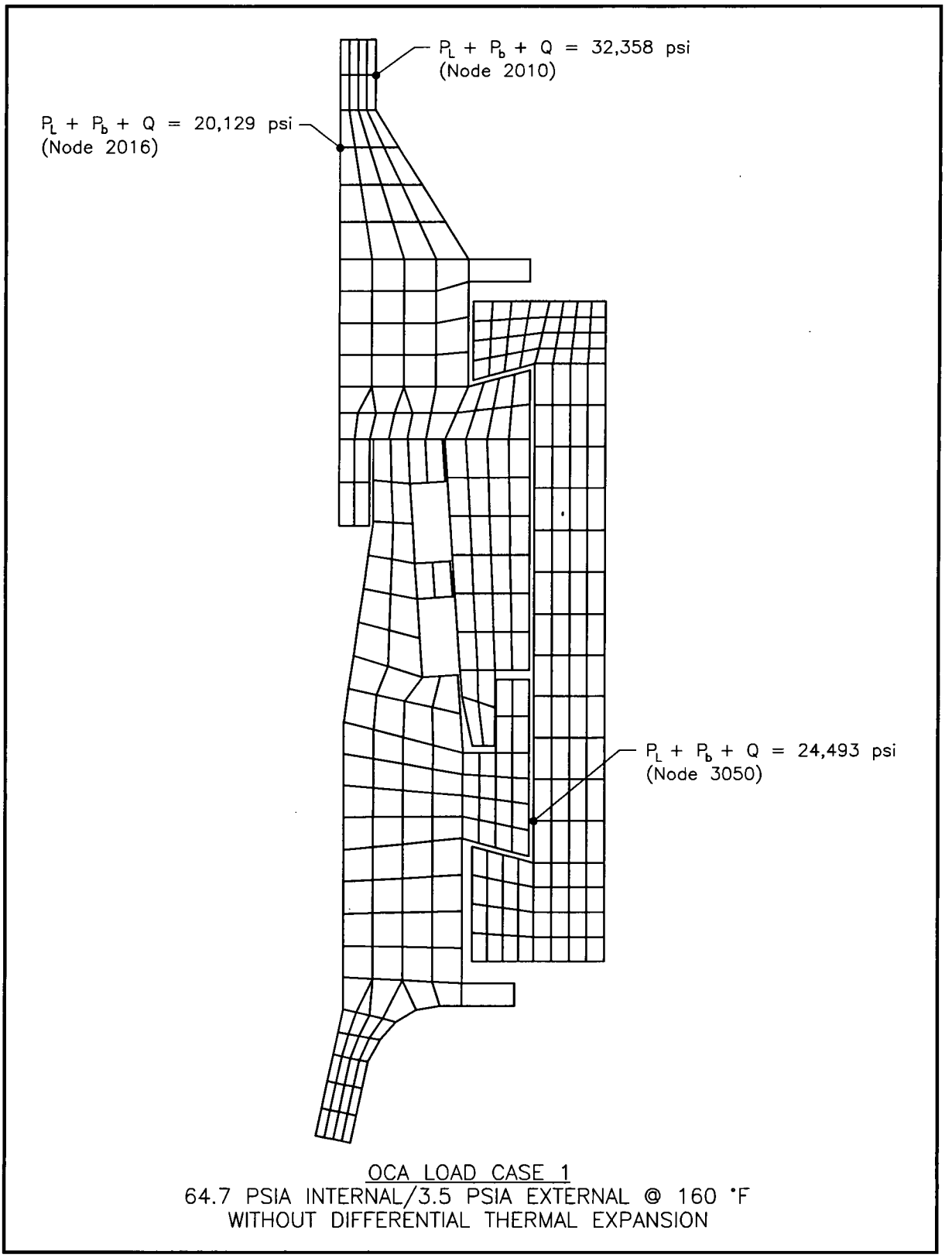

Figure 2.6-2 – OCA Load Case 1, Seal Region Detail

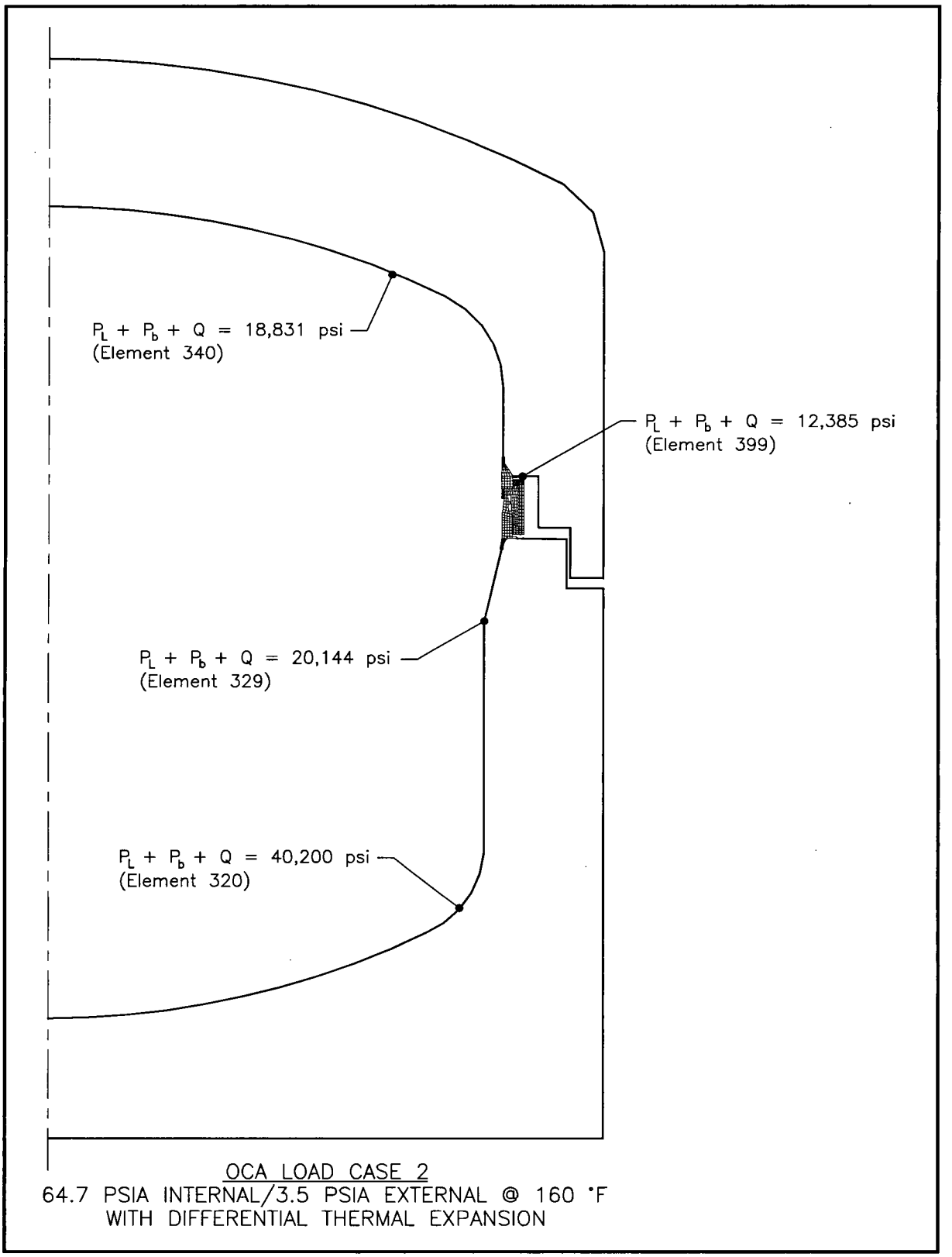

Figure 2.6-3 – OCA Load Case 2, Overall Model

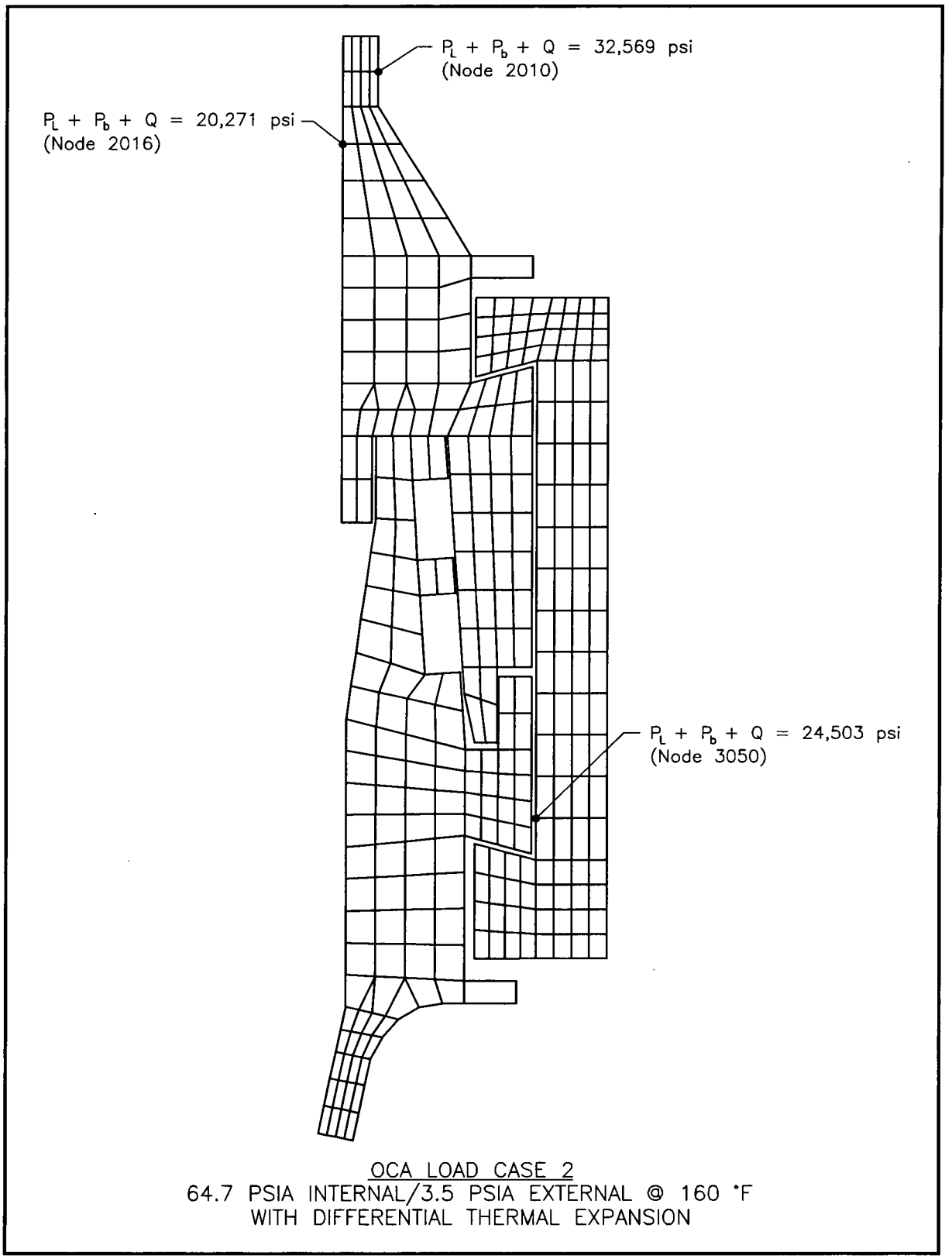

Figure 2.6-4 – OCA Load Case 2, Seal Region Detail

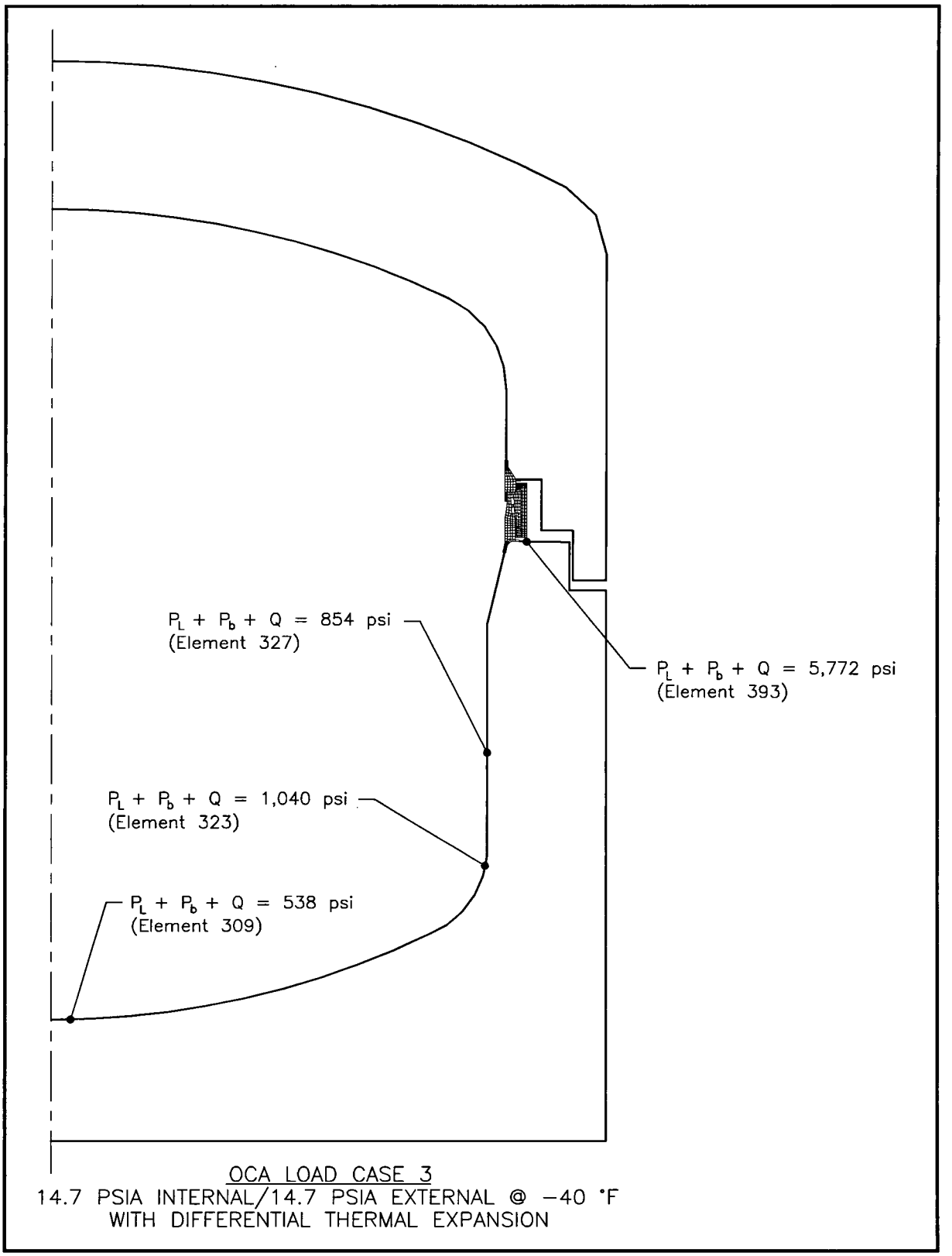

Figure 2.6-5 – OCA Load Case 3, Overall Model

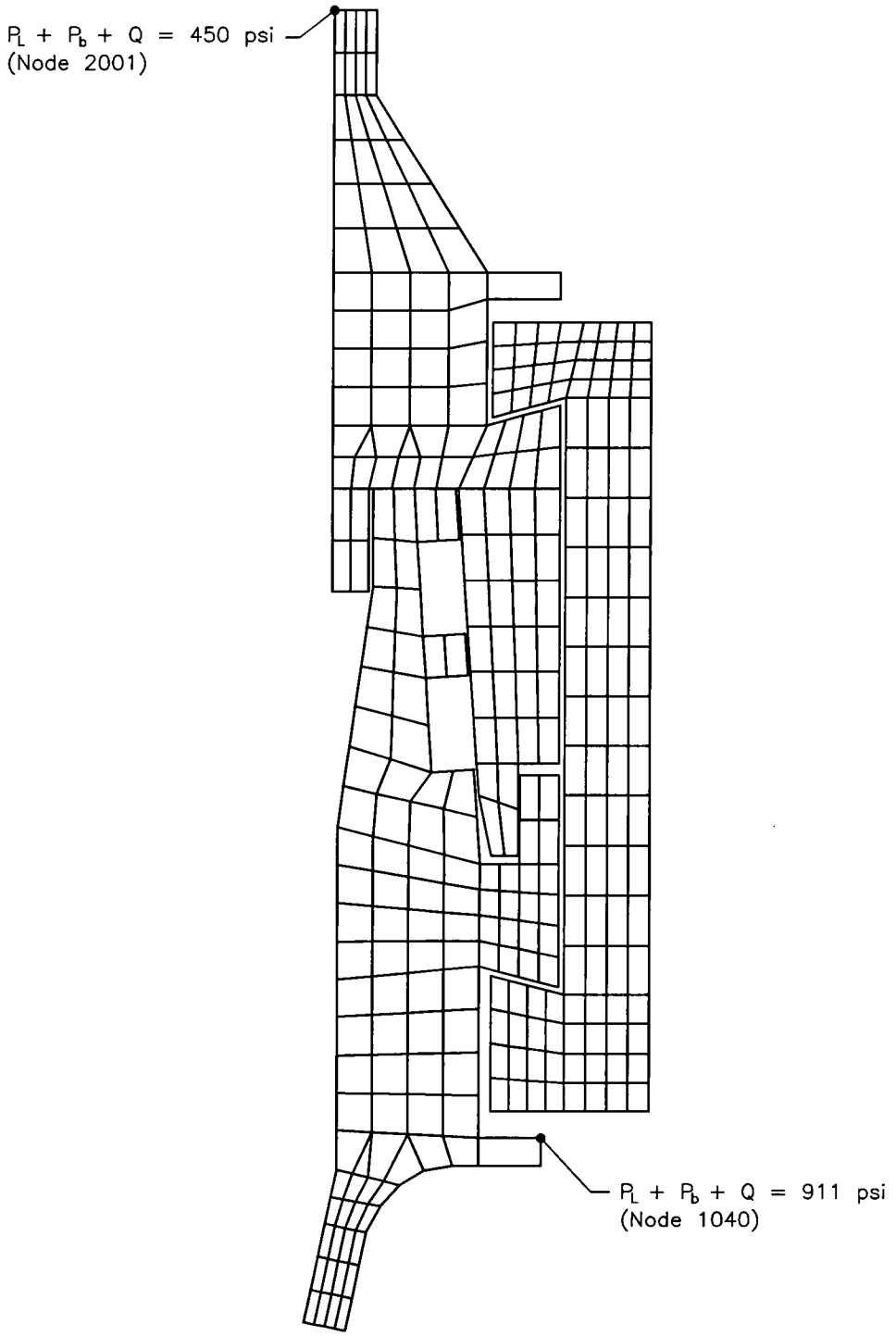

Figure 2.6-6 – OCA Load Case 3, Seal Region Detail

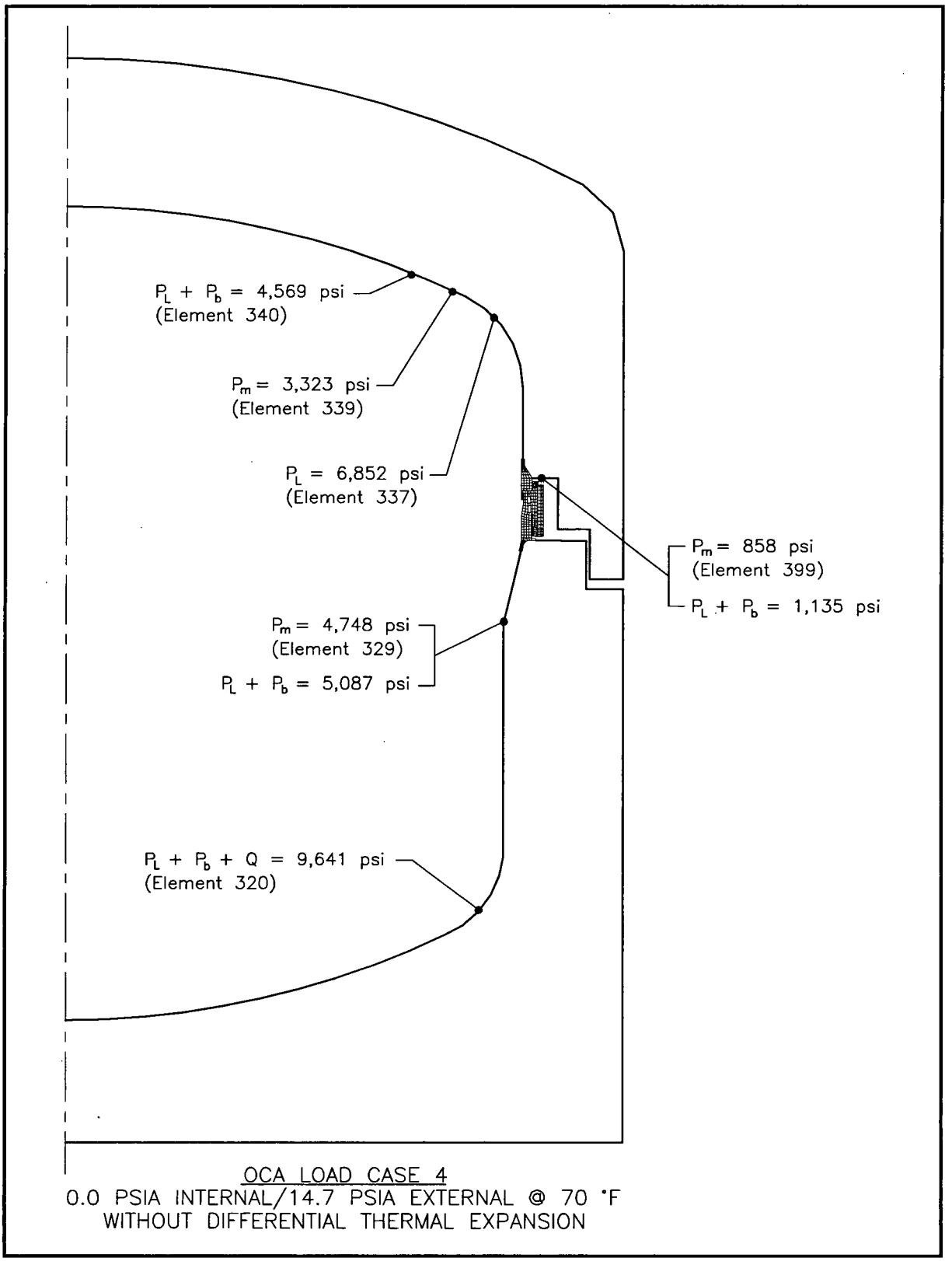

Figure 2.6-7 – OCA Load Case 4, Overall Model

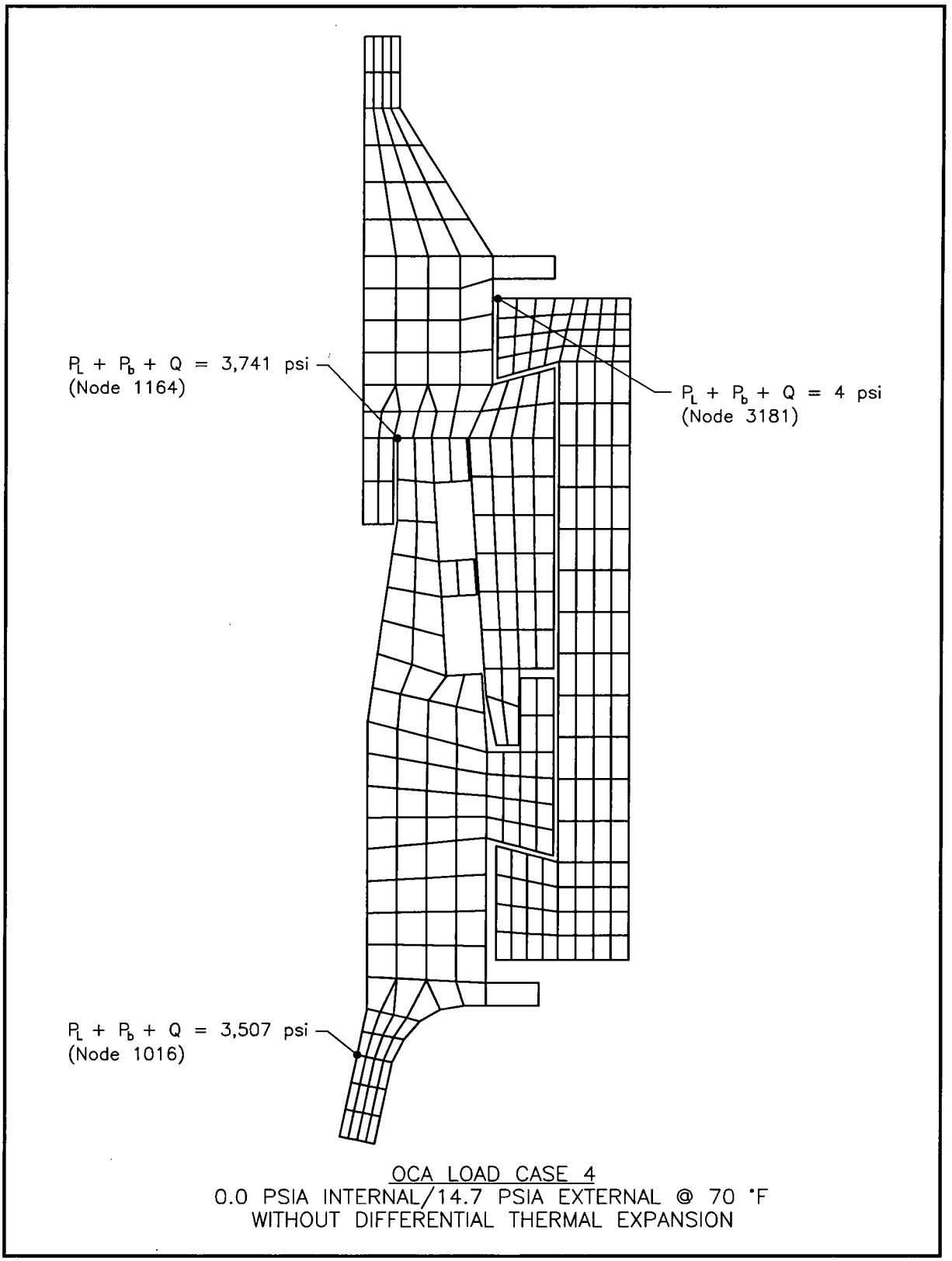

Figure 2.6-8 – OCA Load Case 4, Seal Region Detail

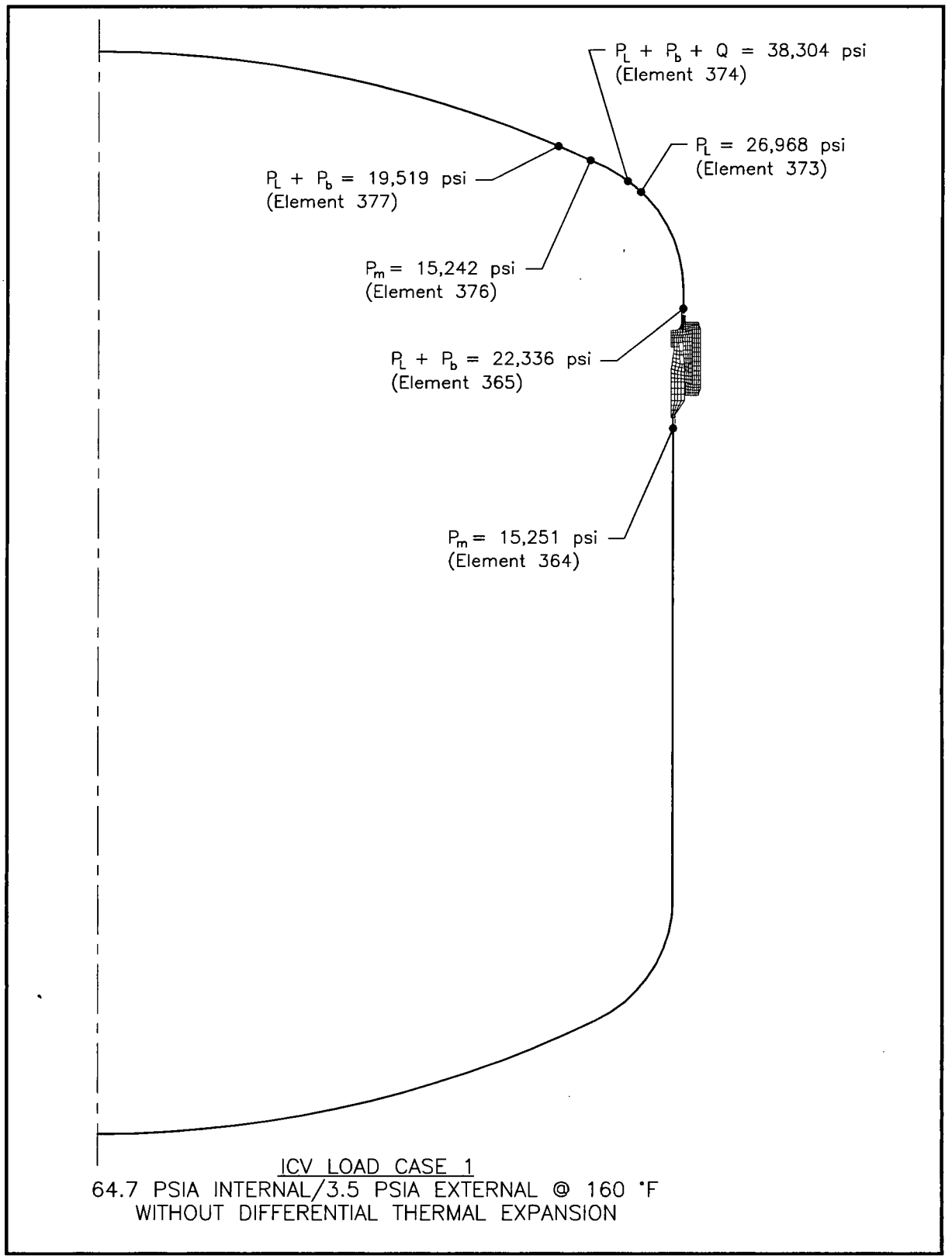

Figure 2.6-9 – ICV Load Case 1, Overall Model

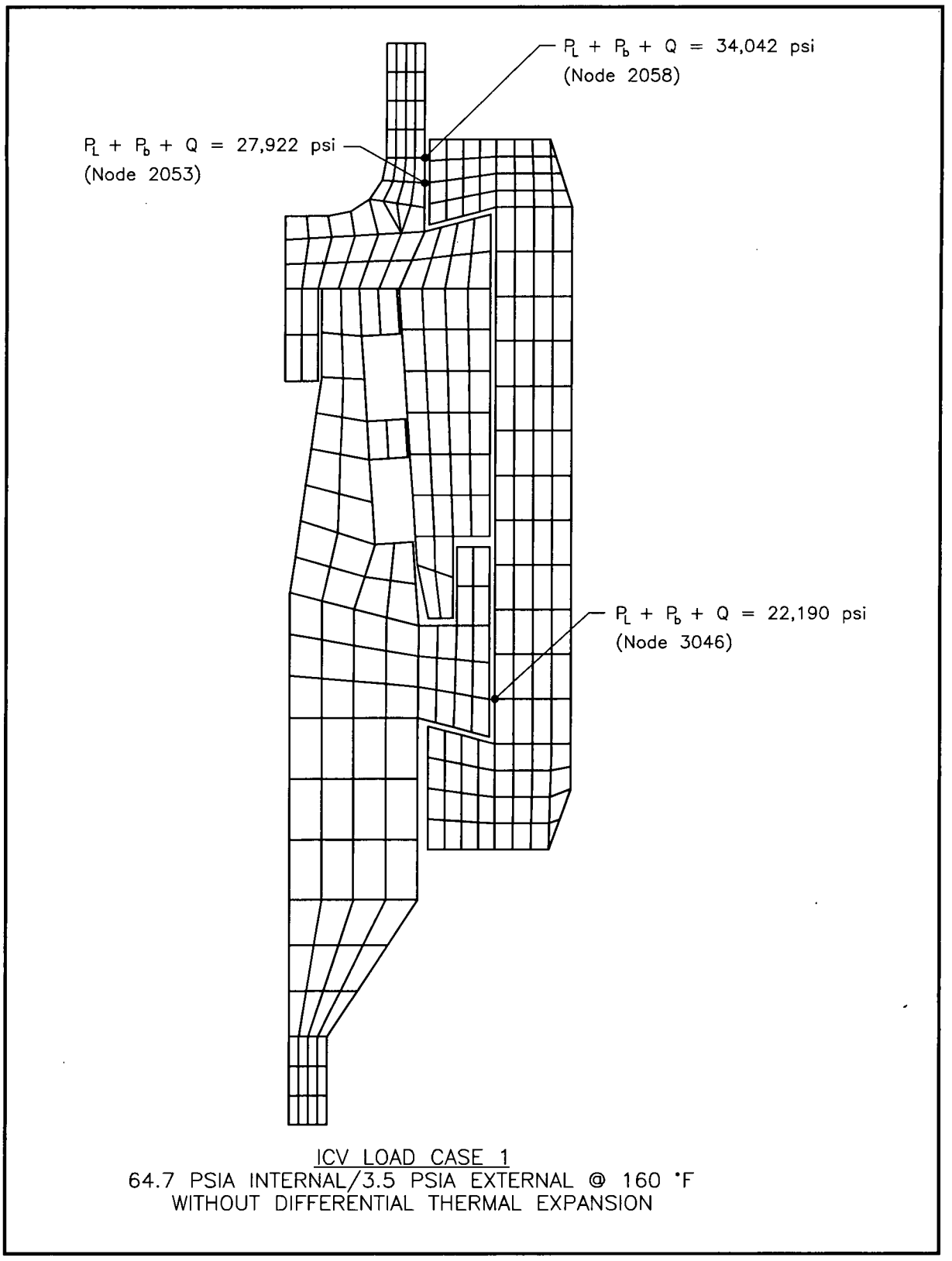

Figure 2.6-10 – ICV Load Case 1, Seal Region Detail

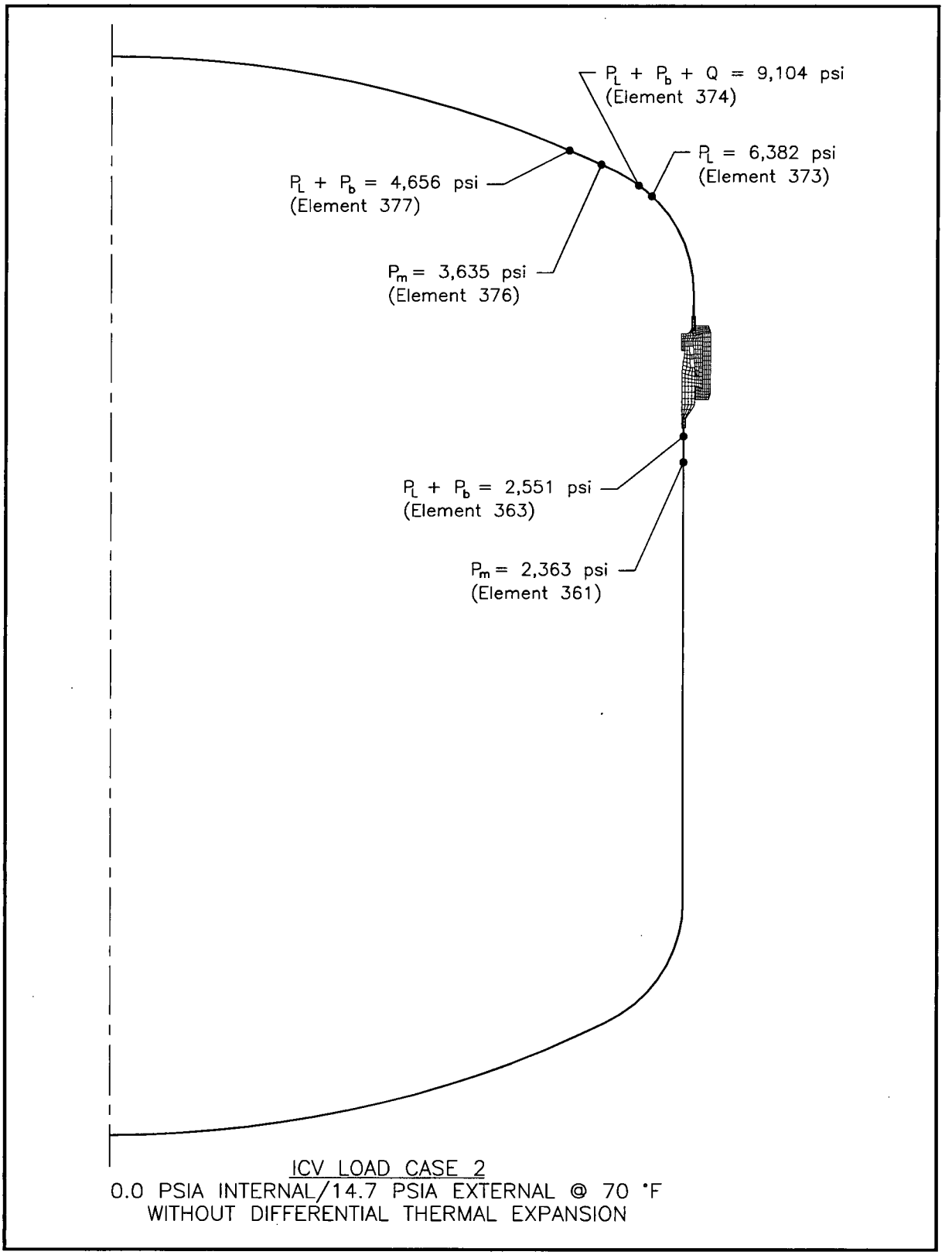

Figure 2.6-11 – ICV Load Case 2, Overall Model

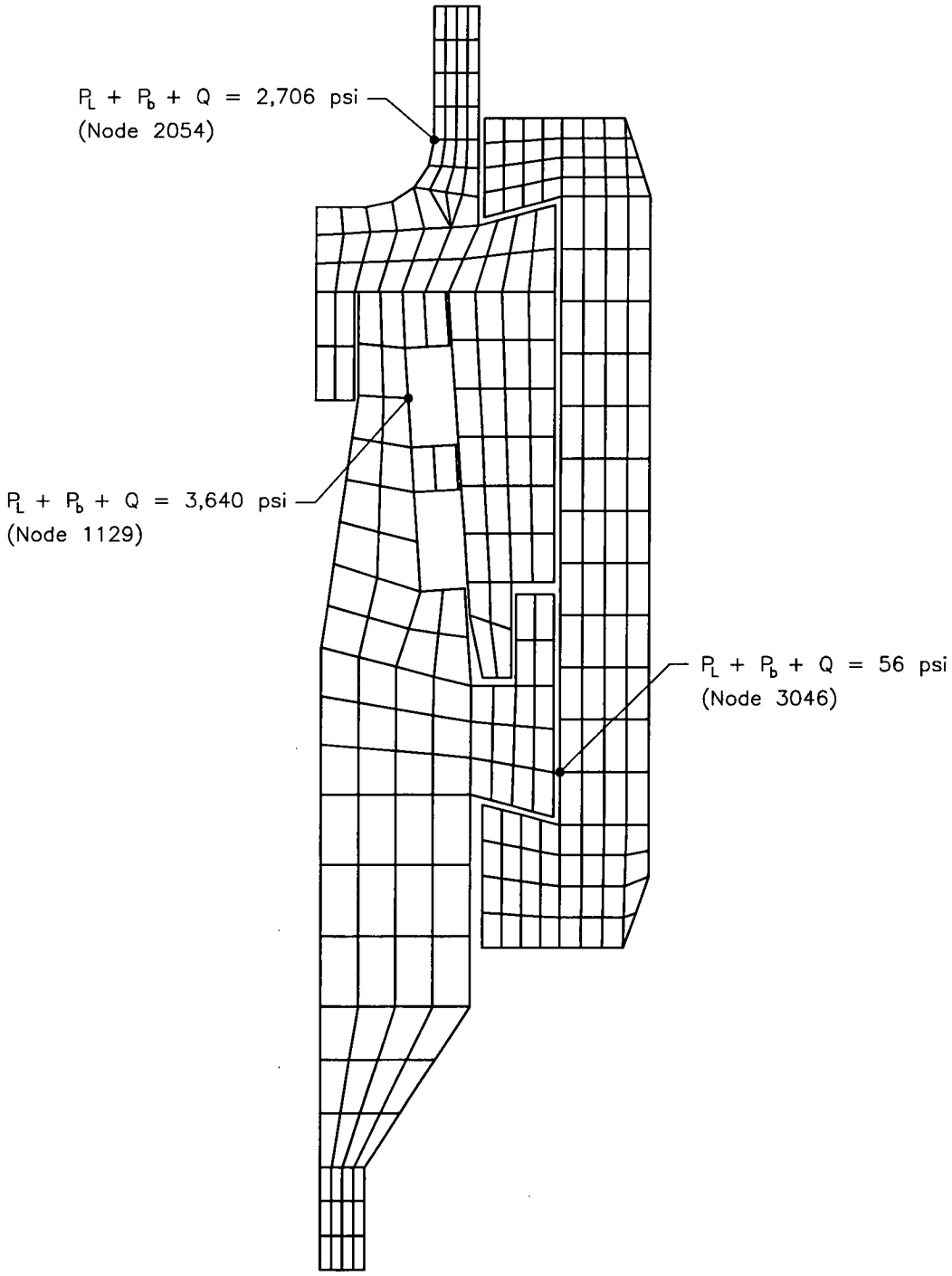

Figure 2.6-12 – ICV Load Case 2, Seal Region Detail

2.7 Hypothetical Accident Conditions

The HalfPACT package, when subjected to the sequence of hypothetical accident condition (HAC) tests specified in 10 CFR §71.73[1], subsequent to the sequence of normal conditions of transport (NCT) tests specified in 10 CFR §71.71, is shown to meet the performance requirements specified in Subpart E of 10 CFR 71. As indicated in the introduction to Chapter 2.0, *Structural Evaluation*, with the exception of the immersion test, the primary proof of performance for the HAC tests is via the use of full scale testing. In particular, free drop, puncture, and fire testing of both a HalfPACT engineering test unit (ETU), and a HalfPACT certification test unit (CTU) confirms that both the inner containment vessel (ICV) and outer containment (now confinement) vessel (OCV) boundaries remained leaktight after a worst case HAC sequence. Observations from testing of the ETU and CTU also confirm the conservative nature of deformed geometry assumptions used in the criticality assessment provided Chapter 6.0, *Criticality Evaluation*, respectively.

Test results are summarized in Section 2.7.8, *Summary of Damage*, with details provided in Appendix 2.10.3, *Certification Tests*. Immersion is addressed by analysis, employing acceptance criteria consistent with NRC Regulatory Guide 7.6[2].

For the analytic assessments performed within this section, properties for Type 304 stainless steel are based on data from Table 2.3-1 from Section 2.3.1, *Mechanical Properties Applied to Analytic Evaluations*). Similarly, the bounding values for the compressive strength of polyurethane foam are based on data from Table 2.3-2 from Section 2.3.1, *Mechanical Properties Applied to Analytic Evaluations*. Polyurethane foam compressive strength is further adjusted ±15% to account for manufacturing tolerance. At elevated HAC temperatures (i.e., 160 °F), the nominal compressive strength is reduced 25% for elevated temperature effects and reduced 15% for manufacturing tolerance. At reduced HAC temperatures (i.e., -20 °F), the nominal compressive strength is increased 40% for reduced temperature effects and increased 15% for manufacturing tolerance.

Properties of Type 304 stainless steel and polyurethane foam, as applied to analytic assessments within this section, are summarized below.

Material Property	Material Property Value (psi)			Reference
	-20 °F	70 °F	160 °F	
Type 304 Stainless Steel				
Elastic Modulus, E	28.8×10^6	28.3×10^6	27.8×10^6	Table 2.3-1
Design Stress Intensity, S_m	20,000	20,000	20,000	
Yield Strength, S_m	30,000	30,000	27,000	
Polyurethane Foam Compressive Strength				
Parallel-to-Rise Direction, σ_c	378	235	150	Table 2.3-2
Perpendicular-to-Rise Direction, σ_c	314	195	124	

[1] Title 10, Code of Federal Regulations, Part 71 (10 CFR 71), *Packaging and Transportation of Radioactive Material*, 01-01-12 Edition.

[2] U. S. Nuclear Regulatory Commission, Regulatory Guide 7.6, *Design Criteria for the Structural Analysis of Shipping Cask Containment Vessels*, Revision 1, March 1978.

2.7.1 Free Drop

Subpart F of 10 CFR 71 requires performing a free drop test in accordance with the requirements of 10 CFR §71.73(c)(1). The free drop test involves performing a 30-foot, HAC free drop onto a flat, essentially unyielding, horizontal surface, with the package striking the surface in a position (orientation) for which maximum damage is expected. The ability of the HalfPACT package to adequately withstand this specified free drop condition is demonstrated via testing of two full scale, HalfPACT test packages.

2.7.1.1 Technical Basis for the Free Drop Tests

To properly select a worst case package orientation for the 30-foot free drop event, items that could potentially compromise containment integrity, shielding integrity, and/or criticality safety of the HalfPACT package must be clearly identified. For the HalfPACT package design, the foremost item to be addressed is the ability of the containment seals to remain leaktight. Shielding integrity is not a controlling case for the reasons described in Chapter 5.0, *Shielding Evaluation*. Criticality safety is conservatively evaluated based on measured physical damage to the outer containment (now confinement) assembly (OCA) shells and polyurethane foam from certification testing, as described in Chapter 6.0, *Criticality Evaluation*.

The leaktight capability of the containment seals may be compromised by two methods: 1) as a result of excessive sealing surface deformation leading to reduced seal compression, and/or 2) as a result of thermal degradation of the seal material itself in a subsequent fire event. Importantly, these methods require significant impact damage to the surrounding polyurethane foam. In other words, a significant reduction in polyurethane foam thickness or a gross exposure of the foam through splits or punctures in the OCA outer shell would have to occur near the main O-ring seal or vent port seal region.

Additional items for consideration include the possibility of separating the OCA lid from the OCA body (or significantly opening up the nominal 1/2-inch gap which exists between the upper and lower Z-flanges at the lid to body interface), and buckling of the OCV or ICV from a bottom end drop.

For the above reasons, testing must include impact orientations that affect the upper end of the HalfPACT package, with particularly emphasis in the closure region. Loads and resultant deformations occurring over the lower half of the package does not present a worst case regarding the leaktight capability of the seals or the separation of the OCA lid from the OCA body. However, as discussed above, a bottom end drop is of interest regarding the possibility of shell buckling because of the high axial acceleration forces imparted to the package.

In addition to package orientation, initial test conditions such as temperatures and pressures must be selected to complete the definition of the conditions existing at the time of a HAC free drop. In general, higher temperatures at the time of a drop test result in greater deformations and lesser acceleration loads than do lower temperatures. This is due primarily to the modest temperature sensitivity of the energy absorbing polyurethane foam used within the HalfPACT OCA.

Appendix 2.10.3, *Certification Tests*, provides a comprehensive report of the certification test process and results. Discussions specific to the configuration of the test units are provided in Appendix 2.10.3.4, *Test Unit Description*. Discussions specific to orientations of the test units for free drop, puncture, and fire tests, including initial test conditions, are provided in Appendix

2.10.3.5, *Technical Basis for Tests*. Discussions specific to test sequences for selected tests for the test units is provided in Appendix 2.10.3.6, *Test Sequence for Selected Free Drop, Puncture Drop, and Fire Tests*.

2.7.1.2 Test Sequence for the Selected Tests

Based on the above general discussions, the ETU was tested for three specific, HAC 30-foot free drop conditions for inclusion in the engineering test program. Similarly, based on results from ETU testing, the CTU was tested for two specific, HAC 30-foot free drop conditions for inclusion in the certification test program. Although only a single "worst case" 30-foot drop is required by 10 CFR §71.73(c)(1), multiple tests were performed to ensure that the most vulnerable package features were subjected to "worst case" loads and deformations. The specific conditions selected for ETU and CTU free drop testing are summarized in Table 2.7-1 and Table 2.7-2, respectively.

2.7.1.3 Summary of Results from the Free Drop Tests

Successful HAC free drop testing of the ETU and CTU indicates that the various HalfPACT packaging design features are adequately designed to withstand the HAC 30-foot free drop event. The most important result of the testing program was the demonstrated ability of the OCV and ICV to remain leaktight[3]. Significant results of free drop testing common to both test units are as follows:

- There was no evidence of buckling of either the ICV or OCV shells. Modest damage to the containment vessel shells did occur, an amount somewhat in excess of what was reported in the *TRUPACT-II package SAR*[4]. However, it is clear that the damage noted for the HalfPACT package corresponds to the much heavier payload drum's interaction with the packaging wall.
- No excessive distortion of the seal flange regions occurred for either the ICV or OCV, although some permanent deformation was noted.
- There was no rupture of the 3/8-inch thick, OCA outer shell.
- Observed permanent deformations of the HalfPACT packaging were less than those assumed for the criticality evaluation.

A comprehensive summary of free drop test results is provided in Appendix 2.10.3.7, *Test Results*.

2.7.2 Crush

Subpart F of 10 CFR 71 requires performing a dynamic crush test in accordance with the requirements of 10 CFR §71.73(c)(2). Since the HalfPACT package weight exceeds 1,100 pounds, the dynamic crush test is not required.

2.7.3 Puncture

Subpart F of 10 CFR 71 requires performing a puncture test in accordance with the requirements of 10 CFR §71.73(c)(3). The puncture test involves a 40-inch free drop of a package onto the

---

[3] "Leaktight" is a leakage rate not exceeding 1×10^{-7} standard cubic centimeters per second (scc/sec), air, as defined in ANSI N14.5-1997, *American National Standard for Radioactive Materials – Leakage Tests on Packages for Shipment*, American National Standards Institute, Inc. (ANSI).

[4] U.S. Department of Energy (DOE), *Safety Analysis Report for the TRUPACT-II Shipping Package*, USNRC Certificate of Compliance 71-9218, U.S. Department of Energy, Carlsbad Area Office, Carlsbad, New Mexico.

upper end of a solid, vertical, cylindrical, mild steel bar mounted on an essentially unyielding, horizontal surface. The bar must be six inches in diameter, with the top surface horizontal and its edge rounded to a radius of not more than 1/4 inch. The package is to be oriented in a position for which maximum damage will occur. The minimum length of the bar is to be eight inches. The ability of the HalfPACT package to adequately withstand this specified puncture drop condition is demonstrated via testing of two full scale, HalfPACT test packages.

2.7.3.1 Technical Basis for the Puncture Drop Tests

To properly select a worst case package orientation for the puncture drop event, items that could potentially compromise containment integrity, shielding integrity, and/or criticality safety of the HalfPACT package must be clearly identified. For the HalfPACT package design, the foremost item to be addressed is the ability of the containment seals to remain leaktight. Shielding integrity is not a controlling case for the reasons described in Chapter 5.0, *Shielding Evaluation.* Criticality safety is conservatively evaluated based on measured physical damage to the OCA shells and polyurethane foam from certification testing, as described in Chapter 6.0, *Criticality Evaluation.*

For the HalfPACT design, the primary item to be addressed for the puncture drop is the ability of the containment seals to remain leaktight. The leaktight capability of the O-ring seals would be most easily compromised by imposing gross deformations in the sealing region. These types of deformations are of concern from a mechanical viewpoint (i.e., leakage caused by excessive relative movement of the sealing surfaces). In addition, such deformations are of concern from a thermal viewpoint (i.e., leakage caused by thermal degradation of the butyl O-ring seals in a subsequent fire). Importantly, for mechanical damage to occur in the seal regions, the puncture event would have to result in a gross rupturing of the OCA outer shell near the O-ring seals. This could allow the puncture bar to reach and directly impact the OCA seal flanges or locking ring. Similarly, for thermal degradation of the butyl O-ring seals to occur in a subsequent fire, damage to the OCA outer shell near the O-ring seals would again have to occur as a result of the puncture event. Another item associated with the puncture event is the possibility of the puncture bar penetrating the OCA outer shell and rupturing the OCV. Puncture is most likely to occur if the center of gravity of the package is directly in-line with the puncture bar, and the surface of the package is oriented at an angle to the bar axis. If the center of gravity of the package is not in-line with the puncture bar, puncture is less likely since package potential energy is transformed into rotational kinetic energy. Puncture is also more likely if the puncture bar impacts the package surface adjacent to a package shell weld seam. Observations from prior testing indicate that impacts with the package surface, normal to the axis of the puncture bar, will not lead to penetration of the OCA exterior shell. This is the primary reason for utilizing a torispherical head for the OCA lid. The torispherical head results in the puncture bar being oriented normal to the package surface when the center of gravity of the package is directly over the puncture bar. Further, a 3/8-inch thick OCA outer shell is used near the closure region to ensure that no puncture will occur in this region, regardless of impact angle.

In addition to package orientation, initial test conditions such as temperatures and pressures must be selected to complete the definition of the conditions existing at the time of a HAC puncture drop. In general, higher temperatures at the time of a puncture test result in greater deformations and lesser acceleration loads than do lower temperatures. This is due primarily to the modest temperature sensitivity of the polyurethane foam used within the HalfPACT OCA.

Appendix 2.10.3, *Certification Tests*, provides a comprehensive report of the certification test process and results. Discussions specific to the configuration of the test units are provided in Appendix 2.10.3.4, *Test Unit Description*. Discussions specific to orientations of the test units for free drop, puncture, and fire tests, including initial test conditions, are provided in Appendix 2.10.3.5, *Technical Basis for Tests*. Discussions specific to test sequences for selected tests for the test units is provided in Appendix 2.10.3.6, *Test Sequence for Selected Free Drop, Puncture Drop, and Fire Tests*.

2.7.3.2 Test Sequence for the Selected Tests

Based on the above general discussions, the ETU was specifically tested for four HAC puncture drop conditions as part of the engineering test program. Similarly, based on results from ETU testing, the CTU was specifically tested for three HAC puncture drop conditions as part of the certification test program. Although only a single "worst case" puncture drop is required by 10 CFR §71.73(c)(3), multiple tests were performed to ensure that the most vulnerable package features were subjected to "worst case" loads and deformations. The specific conditions selected for ETU and CTU puncture drop testing are summarized in Table 2.7-1 and Table 2.7-2, respectively.

2.7.3.3 Summary of Results from the Puncture Drop Tests

Successful HAC puncture drop testing of the ETU and CTU indicates that the various HalfPACT packaging design features are adequately designed to withstand the HAC puncture drop event. As with the free drop test, the most important result of the testing program was the demonstrated ability of the OCV and ICV to remain leaktight. Significant results of puncture drop testing common to both test units are as follows:

- Besides the obvious permanent damage to the OCA outer shell at the location of the various puncture bar impacts, there was evidence of some permanent deformation of the OCV shell. The most significant damage occurred at the OCV vent port fitting during testing of the CTU. The cumulative effects of the NCT and HAC free drops, and the subsequent puncture drop caused successively greater permanent deformation to the region adjacent to the vent port fitting. A crack was noted in the inner weld of the CTU's OCV vent port fitting, but not in the outer weld of the OCV vent port fitting. Subsequent helium leak testing determined that OCV containment integrity was maintained. Although essentially identical in configuration, the ETU did not have a similarly cracked weld. See Appendix 2.10.3.7.2.8, *CTU Post-Test Disassembly*, for additional discussion regarding this result.
- Penetration of the OCA outer shell occurred below the 3/8-to-1/4-inch thick, OCA outer shell weld during testing of the ETU. The same test, repeated for certification testing, did not reproduce the hole. This result was due to lengthening the 3/8-inch thick, OCA outer shell from 12 to 18 inches, correspondingly changing the impact angle sufficiently to prevent penetration through the adjacent 1/4-inch thick shell.
- There was no rupture of the 3/8-inch thick, OCA outer shell. However, for both test units (ETU and CTU) a linear tear occurred along the weld at the 3/8-to-1/4-inch shell transition in the OCA body outer shell.

A comprehensive summary of test results is provided in Appendix 2.10.3.7, *Test Results*.

2.7.4 Thermal

Subpart F of 10 CFR 71 requires performing a thermal test in accordance with the requirements of 10 CFR §71.73(c)(4). To demonstrate the performance capabilities of the HalfPACT package when subjected to the HAC thermal test specified in 10 CFR §71.73(c)(4), two full scale prototype test units were burned in two, separate, fully engulfing pool fires. Each test unit was subjected to a variety of HAC, 30-foot free drop and puncture tests prior to being burned, as discussed in Section 2.7.1, *Free Drop*, and Section 2.7.3, *Puncture*. Testing of the engineering test unit (ETU) preceded testing of the certification test unit (CTU), and was used for the purpose of accessing the effect of the various HAC tests. Planning to determine a worst case certification test scenario for the CTU was based ETU responses to a comprehensive set of HAC tests. Further, while the CTU had passive, temperature indicating labels to report post-test temperatures, the ETU did not. Thus, information reported herein considers only test results of the CTU.

As discussed further in Appendix 2.10.3, *Certification Tests*, the CTU was oriented horizontally in a stand a distance one meter above the fuel per the requirements of 10 CFR §71.73(c)(4). The CTU was oriented circumferentially at an angle of 305° to position the damage from Drops 1, 2, and 4 (0°; aligned with the vent ports) and the damage from Drop 5 (250°) a distance 1/2 meter above the lowest part of the package while on the stand (i.e., 1½ meters above the fuel[5]). This particular arrangement put the maximum drop damage in the hottest part of the fire.

During the HAC fire test, the average wind speed was determined to be approximately 4 miles per hour. As discussed in Appendix 2.10.3, *Certification Tests*, the duration of the fully engulfing, HAC fire test was approximately 33 minutes, and the ambient air temperature was 51 °F.

2.7.4.1 Summary of Pressures and Temperatures

Package pressures and temperatures due to the HAC fire test are presented in Appendix 2.10.3, *Certification Tests*. Detailed discussions regarding measured temperatures are provided in Section 3.5.3, *Package Temperatures*. Detailed discussions regarding calculated pressures are provided in Section 3.5.4, *Maximum Internal Pressure*.

2.7.4.1.1 Summary of Temperatures

No active temperature measuring devices were employed prior to, during, or following the HAC fire test. Further, measurement of the OCA outer shell temperature does not represent the OCV or ICV temperatures due to the large internal mass and thick, thermally insulating foam used within the OCA. As discussed in Section 3.1.1, *Packaging*, the temperatures of the OCV, ICV, and payload are effectively decoupled from the OCA outer shell and polyurethane foam for short term thermal transients. Instead, the initial temperature of CTU No. 1 may be estimated based on the ambient temperature of the Sandia National Laboratory testing facilities in the six weeks prior to

[5] M. E. Schneider and L. A. Kent, *Measurements of Gas Velocities and Temperatures in a Large Open Pool Fire*, Sandia National Laboratories (reprinted from *Heat and Mass Transfer in Fire*, A. K. Kulkarni and Y. Jaluria, Editors, HTD-Vol. 73 (Book No. H00392), American Society of Mechanical Engineers). Figure 3 shows that maximum temperatures occur at an elevation approximately 2.3 meters above the pool floor. The pool was initially filled with water and fuel to a level of 0.814 meters. The maximum temperatures therefore occur approximately 1½ meters above the level of the fuel, i.e., 1/2 meter above the lowest part of the package when set one meter above the fuel source per the requirements of 10 CFR §71.73(c)(4).

the HAC fire test[6]. Climatological data for Albuquerque, New Mexico, during the month of March and first two weeks of April 1998 shows an average temperature of 48 °F for those six weeks. Thus, when adjusting for the elevation difference between the testing facilities and Albuquerque, the initial temperature for HAC fire testing is taken as 43 °F.

Following completion of fire testing, the maximum measured OCV seal region temperature was 200 °F. Upwardly adjusting for the lower, pre-fire starting temperature by 90 °F results in a projected maximum OCV seal region temperature of 290 °F. The maximum measured ICV seal region temperature was 110 °F. Also, upwardly adjusting for the lower, pre-fire starting temperature by 90 °F results in a projected maximum ICV seal region temperature of 200 °F.

2.7.4.1.2 Summary of Pressures

The maximum internal pressure for the ICV is conservatively determined by assuming the air temperature within the ICV is at the maximum seal temperature of 200 °F. The ICV pressure increase, ΔP_{ICV}, using an initial maximum ICV wall temperature of 154 °F (from Table 3.4-1) at an initial pressure equal to the MNOP of 50 psig (64.7 psia), is determined using ideal gas relationships:

$$\frac{P_1}{T_1}=\frac{P_2}{T_2} \Rightarrow \frac{P_{154\,°F}}{T_{154\,°F}}=\frac{P_{200\,°F}}{T_{200\,°F}} \Rightarrow P_{200\,°F}=P_{154\,°F}\left(\frac{T_{200\,°F}}{T_{154\,°F}}\right)$$

$$P_{200\,°F}=64.7\left(\frac{200+460}{154+460}\right)=69.5\text{ psia (54.8 psig)}$$

$$\Delta P_{ICV}=54.8-50.0=4.8\text{ psig}$$

Thus, the maximum internal pressure for the ICV for HAC is 54.8 psig, resulting in a net pressure increase of 4.8 psig.

The maximum internal pressure for the OCV is conservatively determined by assuming the air temperature within the OCV, 245 °F, is the average of the maximum ICV and OCV seal temperatures of 200 °F and 290 °F, respectively. The initial air temperature within the OCV, 152 °F, is the average of the maximum OCV and ICV wall temperatures of 150 °F and 154 °F, respectively (from Table 3.4-1). The OCV pressure increase, ΔP_{OCV}, using at an initial pressure equal to the MNOP of 50 psig (64.7 psia), is determined using ideal gas relationships:

$$\frac{P_1}{T_1}=\frac{P_2}{T_2} \Rightarrow \frac{P_{152\,°F}}{T_{152\,°F}}=\frac{P_{245\,°F}}{T_{245\,°F}} \Rightarrow P_{245\,°F}=P_{152\,°F}\left(\frac{T_{245\,°F}}{T_{152\,°F}}\right)$$

$$P_{245\,°F}=64.7\left(\frac{245+460}{152+460}\right)=74.5\text{ psia (59.8 psig)}$$

$$\Delta P=59.8-50.0=9.8\text{ psig}$$

[6] CTU No. 1 was located at Sandia National Laboratories' Coyote Canyon drop test facility for the month of March, 1998, and the Lurance Canyon burn facility for the first two weeks of April, 1998. CTU No. 1 was burned on April 14, 1998. The elevation difference between the two test facilities and the city of Albuquerque results in an average ambient temperature approximately 5 °F cooler than Albuquerque.

Thus, the maximum internal pressure for the OCV for HAC is 59.8 psig, resulting in a net pressure increase of 9.8 psig.

2.7.4.2 Differential Thermal Expansion

Fire testing of two, full scale HalfPACT prototypes indicate that the effects associated with differential thermal expansion of the various packaging components are negligible. Subsequent to all NCT and HAC free drop, puncture drop, and fire tests, comprehensive helium leak testing of both the ICV and OCV demonstrated that differential thermal expansion does not affect the capability to remain leaktight.

2.7.4.3 Stress Calculations

As shown in Section 2.7.4.1.2, *Summary of Pressures*, the internal pressure within the ICV increases 4.8 psig (+10%), and within the OCV increases 9.8 psig (+20%) due to the HAC fire test. Pressure stresses due to the HAC fire test corresponding increase a maximum of 20%. With reference to Table 2.1-1 in Section 2.1.2.1.1, *Containment Structure (ICV)*, the HAC allowable stress intensity for general primary membrane stresses (applicable to pressure loads) is 240% of the NCT allowable stress intensity. Therefore, a HAC pressure stress increase of 20% will not exceed the HAC allowable stresses. Further, the pressure stresses in conjunction with stresses associated with differential thermal expansion are limited to an acceptable level since both the ICV and OCV were shown to be leaktight after all NCT and HAC free drop, puncture drop, and fire tests (see Appendix 2.10.3.7, *Test Results*).

2.7.4.4 Comparison with Allowable Stresses

As discussed in Section 2.7.4.3, *Stress Calculations*, further quantification of stresses in the various HalfPACT package components is not required.

2.7.5 Immersion – Fissile Material

Subpart F of 10 CFR 71 requires performing an immersion test for fissile material packages in accordance with the requirements of 10 CFR §71.73(c)(5). The criticality evaluation presented in Chapter 6.0, *Criticality Evaluation*, assumes optimum hydrogeneous moderation of the contents, thereby conservatively addressing the effects and consequences of water in-leakage.

2.7.6 Immersion – All Packages

Subpart F of 10 CFR 71 requires performing an immersion test for all packages in accordance with the requirements of 10 CFR §71.73(c)(6). For the HalfPACT package design, the effect of a 21 psig external pressure due to immersion in 50 feet of water is applied to the ICV and OCV.

The external pressure induces small compressive stresses in the ICV and OCV that are limited by stability (buckling) requirements. Buckling assessments are performed for the OCV and ICV in Section 2.7.6.1, *Buckling Assessment of the Torispherical Heads*, and Section 2.7.6.2, *Buckling Assessment of the Cylindrical Shells.*

2.7.6.1 Buckling Assessment of the Torispherical Heads

The buckling analysis of the torispherical heads is based on the methodology outlined in Paragraph NE-3133.4(e), *Torispherical Heads*, of the ASME Boiler and Pressure Vessel Code, Section III[7], Subsection NE. Since the external pressure loading due to immersion may be classified as Level D, the allowable buckling stress and, therefore, the allowable pressure, can be increased by 150% per paragraph NE-3222.2. The results from following this methodology are summarized below.

Parameter	OCV Torispherical Head		ICV Torispherical Head	
	Upper	Lower	Upper	Lower
R	77.3125	74.1250	74.3750	73.1250
T	0.25	0.25	0.25	0.25
$A = \frac{0.125}{(R/T)}$	0.00040	0.00042	0.00042	0.00043
B[8]	5,000	5,000	5,000	5,000
$P_a = \frac{(1.5)B}{(R/T)}$	24.3	25.3	25.2	25.6

The smallest allowable pressure, P_a, is 24.3 psig for the OCV upper head. For an applied external pressure of 21 psig, the corresponding buckling margin of safety is:

$$MS = \frac{24.3}{21} - 1 = +0.16$$

Since the margin of safety in the worst case is positive, it is concluded that none of the OCV or ICV torispherical heads will buckle for an external pressure of 21 psig.

2.7.6.2 Buckling Assessment of the Cylindrical Shells

The cylindrical portions of the OCV and ICV are evaluated using ASME Boiler and Pressure Vessel Code Case N-284-1[9]. Consistent with Regulatory Guide 7.6 philosophy, a factor of safety of 1.34 is applied for HAC buckling evaluations per ASME Code Case N-284-1, corresponding to ASME Code, Service Level D conditions.

---

[7] American Society of Mechanical Engineers (ASME) Boiler and Pressure Vessel Code, Section III, *Rules for Construction of Nuclear Power Plant Components*, 1995 Edition, 1997 Addenda.

[8] Factor B is found from American Society of Mechanical Engineers (ASME) Boiler and Pressure Vessel Code, Section II, *Materials*, Part D, *Properties*, Subpart 3, *Charts and Tables for Determining the Shell Thickness of Components Under External Pressure*, Figure HA-1, *Chart for Determining Shell Thickness of Components Under External Pressure When Constructed of Austenitic Steel (18Cr–8Ni, Type 304)*, 1995 Edition, 1997 Addenda. Conservatively, the 400 °F temperature curve is used for each case.

[9] American Society of Mechanical Engineers (ASME) Boiler and Pressure Vessel Code, Section III, *Rules for Construction of Nuclear Power Plant Components*, Division 1, Class MC, Code Case N-284-1, *Metal Containment Shell Buckling Design Methods*, 1995 Edition, 1997 Addenda.

Buckling analysis geometry parameters are summarized in Table 2.7-3, and loading parameters are summarized in Table 2.7-4. The cylindrical shell buckling analysis conservatively utilizes an OCV and ICV temperature of 160 °F, consistent with Section 2.6.1, *Heat*. The stresses are determined using an external pressure of 21 psig. The hoop stress, σ_θ, axial stress, σ_ϕ, and in-plane shear stress, $\sigma_{\phi\theta}$, are found from:

$$\sigma_\theta = \frac{Pr}{t} \qquad \sigma_\phi = \frac{Pr}{2t} \qquad \sigma_{\phi\theta} = \frac{Pr}{4t}$$

where P is the applied external pressure of 21 psi, r is the mean radius, and t is the cylindrical shell thickness. As shown in Table 2.7-5, since all interaction check parameters are less than 1.0, as required, the design criteria are satisfied.

2.7.7 Deep Water Immersion Test

Subpart E of 10 CFR 71 requires performing a deep water immersion test in accordance with 10 CFR §71.61. Since the HalfPACT does not transport payloads with an activity of greater than 10^5 A_2, this requirement does not apply.

2.7.8 Summary of Damage

As discussed in the previous sections, the cumulative damaging effects of free drop, puncture drop, and fire tests were satisfactorily withstood by the HalfPACT packaging during both engineering and certification testing. Subsequent helium leak testing confirmed that containment integrity was maintained throughout the test series. Therefore, the requirements of 10 CFR §71.73 have been adequately met.

Table 2.7-1 – Summary of HalfPACT Engineering Test Unit (ETU) Tests and Results

Test No.	Test Description	Test Unit Angular Orientation		Remarks
		Axial (0° = horizontal)	Circumferential (0° = vent ports)	
1	NCT, 3-foot side drop opposite the OCV vent and seal test ports	0°	200°	NCT impact in region expected to produce worst case cumulative damage to package.
2	HAC, 30-foot side drop opposite the OCV vent and seal test ports	0°	200°	HAC impact in region expected to produce worst case cumulative damage to package.
3	NCT, 3-foot side drop on the OCV vent port	0°	0°	NCT impact in OCV vent port region.
4	HAC, 30-foot side drop on the OCV vent port	0°	0°	HAC impact in OCV vent port region.
5	NCT, 3-foot center-of-gravity-over-corner drop between tie-down doubler plates	43°	110°	NCT impact at location not tested during previous TRUPACT-II certification tests.
6	HAC, 30-foot center-of-gravity-over-corner drop between tie-down doubler plates	43°	110°	HAC impact at location not tested during previous TRUPACT-II certification tests.
7	HAC, puncture drop at the 1/4-to-3/8, OCA body shell weld (below weld)	20°	200°	Attempt to cause hole in shell below 1/4-to-3/8, OCA body shell weld.
8	HAC, puncture drop on OCV vent port	1°	0°	Puncture in region expected to produce worst case cumulative damage to package.
9	HAC, puncture drop at Test 6 damage	43°	110°	Attempt to cause hole in existing damage.
10	HAC, puncture drop at the 1/4-to-3/8, OCA body shell weld (above weld)	9°	290°	Attempt to cause linear tear in 1/4-to-3/8, OCA body shell weld.
11	HAC, fire test	0°	145°	Circumferential orientation places damage from Tests 4 and 8 in hottest part of fire.

Table 2.7-2 – Summary of Selected Certification Test Unit (CTU) Tests

Test No.	Test Description	Test Unit Angular Orientation		Remarks
		Axial (0° = horizontal)	Circumferential (0° = vent ports)	
1	NCT, 3-foot side drop on the OCV vent port	0°	0°	NCT impact in region expected to produce worst case cumulative damage to package.
2	HAC, 30-foot side drop on the OCV vent port	0°	0°	HAC impact in region expected to produce worst case cumulative damage to package.
3	HAC, 30-foot, 5° corner drop on the OCA top knuckle, slapdown on the tiedown lug	5°	147½°	Drop orientation producing maximum load on closure region.
4	HAC, puncture drop on the OCV vent port	1½°	0°	Puncture in region expected to produce worst case cumulative damage to package.
5	HAC, puncture drop at the 1/4-to-3/8, OCA body shell weld (below weld)	16°	110°	Attempt to cause hole in shell below 1/4-to-3/8, OCA body shell weld.
6	HAC, puncture drop at the 1/4-to-3/8, OCA body shell weld (above weld)	23°	250°	Attempt to cause linear tear in 1/4-to-3/8, OCA body shell weld.
7	HAC, fire test	0°	55° or 305° ① (max damage)	Circumferential orientation based on results of Tests 5 and 6.

Notes:

① The 55° or 305° circumferential orientation is downward; package bottom is one meter above the fuel surface.

Table 2.7-3 – Buckling Geometry Parameters per Code Case N-284-1

Geometry and Material Input		
	ICV	**OCV**
Mean Radius, inch	36.44	36.91
Shell Thickness, inch	0.25	0.188
Length, inch	36.0①	32.0②
Geometry Output (nomenclature consistent with ASME Code Case N-284-1)		
R =	36.44	36.91
t =	0.25	0.188
R/t =	145.76	196.85
ℓ_ϕ =	36.0	32.0
ℓ_θ =	228.94	231.89
M_ϕ =	11.93	12.16
M_θ =	75.85	88.15
M =	11.93	12.16

Notes:

① The ICV length is conservatively measured from five inches below the top of the lower ICV seal flange (at the beginning of the 1/4-inch wall thickness) to an assumed support point located one-third of the depth of the lower ICV torispherical head below the head-to-shell interface.

② The OCV length is conservatively measured from the top of the tapered wall portion (just below the lower OCV seal flange) to an assumed support point located one-third of the depth of the lower OCV torispherical head below the head-to-shell interface.

Table 2.7-4 – Stress Results for 21 psig External Pressure

ICV		OCV	
Axial Stress, σ_ϕ	1,530	Axial Stress, σ_ϕ	2,067
Hoop Stress, σ_θ	3,061	Hoop Stress, σ_θ	4,133
Shear Stress, $\sigma_{\phi\theta}$	765	Shear Stress, $\sigma_{\phi\theta}$	1,031

Table 2.7-5 – Buckling Summary for 21 psig External Pressure

Condition	ICV	OCV	Remarks
Capacity Reduction Factors (-1511)			
$\alpha_{\phi L}$ =	0.2575	0.2575	
$\alpha_{\theta L}$ =	0.8000	0.8000	
$\alpha_{\phi\theta L}$ =	0.8000	0.8000	
Plasticity Reduction Factors (-1611)			
η_{ϕ} =	0.5877	0.7307	
η_{θ} =	1.0000	1.0000	
$\eta_{\phi\theta}$ =	0.4474	0.5740	
Theoretical Buckling Values (-1712.1.1)			
C_{ϕ} =	0.6050	0.6050	
$\sigma_{\phi eL}$ =	115,720 psi	85,687 psi	
$C_{\theta r}$ =	0.0855	0.0837	
$\sigma_{\theta eL} = \sigma_{reL}$ =	16,354 psi	11,854 psi	
$C_{\theta h}$ =	0.0815	0.0798	
$\sigma_{\theta eL} = \sigma_{heL}$ =	15,581 psi	11,302 psi	
$C_{\phi\theta}$ =	0.2184	0.2162	
$\sigma_{\phi\theta eL}$ =	41,770 psi	30,611 psi	
Elastic Interaction Equations (-1713.1.1)			
σ_{xa} =	14,899 psi	11,032 psi	
σ_{ha} =	6,232 psi	4,521 psi	
σ_{ra} =	6,542 psi	4,742 psi	
$\sigma_{\tau a}$ =	16,708 psi	12,246 psi	
Axial + Hoop ⇨ Check (a):	*N/A*	*N/A*	
Axial + Hoop ⇨ Check (b):	*N/A*	*N/A*	
Axial + Shear ⇨ Check (c):	*0.0730*	*0.1343*	<1 ∴ OK
Hoop + Shear ⇨ Check (d):	*0.3290*	*0.6121*	<1 ∴ OK
Axial + Hoop + Shear ⇨ Check (e,a):	*N/A*	*N/A*	
Axial + Hoop + Shear ⇨ Check (e,b):	*N/A*	*N/A*	
Inelastic Interaction Equations (-1713.2.1)			
σ_{xc} =	8,756 psi	8,061 psi	
σ_{rc} =	6,542 psi	4,742 psi	
$\sigma_{\tau c}$ =	7,475 psi	7,029 psi	
Axial + Hoop ⇨ Check (a):	*0.3276*	*0.6086*	<1 ∴ OK
Axial + Shear ⇨ Check (b):	*0.1282*	*0.1896*	<1 ∴ OK
Hoop + Shear ⇨ Check (c):	*0.3322*	*0.6192*	<1 ∴ OK

2.8 Special Form

This section does not apply for the HalfPACT package, since special form is not claimed.

This page intentionally left blank.

2.9 Fuel Rods

This section does not apply for the HalfPACT package, since fuel rods are not included as an approved payload configuration.

This page intentionally left blank.

2.10 Appendices

2.10.1 *Finite Element Analysis (FEA) Models*

2.10.2 *Elastomer O-ring Seal Performance Tests*

2.10.3 *Certification Tests*

This page intentionally left blank.

2.10.1 Finite Element Analysis (FEA) Models

2.10.1.1 Outer Confinement Assembly (OCA) Structural Analysis

Finite element analyses (FEA) are performed on the OCA structure to determine the stress states of the various components under normal conditions of transport (NCT) loads. The FEA analyses are performed using ANSYS® 5.3[1]. The OCA FEA model is comprised of six separate major structural components, modeled as shown in Figure 2.10.1-1:

- upper OCV seal flange
- lower OCV seal flange
- OCV locking ring
- OCV shells
- OCA shells and Z-flanges
- polyurethane foam

The lower and upper seal flanges, locking ring and polyurethane foam are modeled using 2-D, isoparametric solid elements (PLANE42). The quadrilateral elements are defined by four nodal points (a triangular element may be formed by defining duplicate the 3rd and 4th node numbers), each having two degrees of freedom: translations in the nodal x-direction (radial) and y-direction (axial).

The upper and lower OCA shells (OCA lid and body shells, respectively) are modeled using 2-D, axisymmetric conical shell elements (SHELL51). The lineal elements are defined by two nodal points, each having three degrees of freedom: translations in the nodal x-direction (radial) and y-direction (axial), and rotation about the nodal z-axis (hoop). In addition, the axisymmetric conical shell element is biaxial, with membrane and bending capabilities. The OCA inner shell defines the outer confinement vessel (OCV).

Relatively stiff, 2-D elastic beams (BEAM3) are utilized to maintain bending continuity between the three degree of freedom conical shell elements and two degree of freedom, isoparametric solid elements. Specifically, for both the lower and upper OCV seal flanges, four stiff beams are placed at each junction between the shell elements and the solid elements of the seal flanges. These elements are included to transmit the moment (i.e., to maintain slope continuity) between the shell and flange portions of the model, and have a negligible effect on the stress results.

Three sets of 2-D interface elements (CONTAC12) are utilized to connect the lower and upper OCV seal flanges to each other and to the OCV locking ring. The interface element is capable of supporting a load only in the direction normal to the surfaces, and is frictionless in the tangential direction. The interface element has two degrees of freedom at each node: translations in the nodal x-direction (radial) and y-direction (axial). A contact stiffness of 1×10^9 lb/in is chosen to reflect the relatively high interface stiffness when closed. Three sets of interface elements are used in these analyses: 1) between the lower OCV seal flange and the OCV locking ring, 2) between the upper OCV seal flange and the OCV locking ring, and 3) between the lower OCV seal flange and the upper OCV seal flange. Relatively flexible spring elements (COMBIN14) having a spring stiffness of 1×10^2 lb/in are also used at these same locations to improve model stability and to reduce interface element convergence time. The resulting forces in these springs are small, having a negligible effect on the stress results.

[1] ANSYS®, Inc., *ANSYS Engineering Analysis System User's Manual for ANSYS® Revision 5.3*, Houston, PA.

Interface elements are also located along the entire shell-to-foam periphery to allow relative motion between the steel shells and the polyurethane foam. This approach effectively models the ceramic fiber paper by allowing compression-only forces, and assumes no shear continuity or tension effects. A contact stiffness of 1×10^5 lb/in is chosen to reflect the interface stiffness between the shells, ceramic fiber paper, and polyurethane foam. Stress results in the package shells and OCV seal flanges exhibit a negligible dependence on the actual magnitude of the gap contact stiffness.

To account for the tangential (hoop) direction slotting for the lower OCV seal flange and OCV locking ring in the axisymmetric model, the material properties in the directly affected regions are modified. Specifically, material properties for the shaded elements in the lower OCV seal flange and OCV locking ring, illustrated on Figure 2.10.1-1, are modified to reflect only one-half the stainless steel being present for strength purposes. Specifically, the elastic modulus in the x- and y-directions is reduced to one-half their normal value (since only approximately one-half the material remains in the slotted regions), and the elastic modulus in the z-direction is set to set to a very low value to eliminate virtually all tangential (hoop) stiffness in the slotted regions. In addition, Poisson's ratio is set at the normal value of 0.3 for the x-y plane, but is set to zero in the y-z and x-z planes. In these ways, the analyses accurately depict the stress levels in all regions.

The global origin of the nodal coordinate system is located at the bottom center of the OCA body, as shown in Figure 2.10.1-1. As such, the nodal x-axis corresponds to the radial direction, the nodal y-axis corresponds to the axial direction, and the nodal z-axis corresponds to the tangential (or hoop) direction. The model is constrained from translating in the radial direction and rotating about the hoop axis at the y-z symmetry plane at x equal zero. The model is also constrained from translating in the axial direction at a single node on the OCV locking ring.

2.10.1.1.1 OCA Structural Analysis – Load Case 1

For OCA Load Case 1, the OCA structural analysis uses a 50 psig (64.7 psia) internal pressure, corresponding to the maximum normal operating pressure (MNOP) from Section 3.4.4, *Maximum Internal Pressure*, coupled with a reduced external pressure of 3.5 psia (equivalently an 11.2 psig internal pressure), per Section 2.6.3, *Reduced External Pressure*, and 10 CFR §71.51(c)(3)[2]. The net internal pressure for this case is 61.2 psig, applied throughout the inner periphery of the model. Relative to the upper and lower OCV seal flanges, the internal pressure does not extend beyond (below) the top of the upper main O-ring seal groove.

A uniform temperature of 160 °F, per Section 2.6.1.1, *Summary of Pressures and Temperatures*, is utilized to determine the temperature-dependent, material property values. The only material properties affected by a temperature of 160 °F are the elastic modulus and the thermal expansion coefficient for the stainless steel. Consistent with Table 2.3-1 in Section 2.3.1, *Mechanical Properties Applied to Analytic Evaluations*, the elastic modulus and thermal expansion coefficient for Type 304 stainless steel are $27.8(10)^6$ psi and $8.694(10)^{-6}$ inches/inch/°F, respectively, at a temperature of 160 °F.

The material properties for the polyurethane foam are consistent with those specified in Section 2.3.1, *Mechanical Properties Applied to Analytic Evaluations*. The elastic modulus in the x-

[2] Title 10, Code of Federal Regulations, Part 71 (10 CFR 71), *Packaging and Transportation of Radioactive Material*, 01-01-12 Edition.

(radial) and z- (hoop) directions is based on the perpendicular-to-rise value of 4,773 psi. Young's modulus in the y- (axial) direction is based on the parallel-to-rise value of 6,810 psi. In addition, Poisson's ratio is 0.33, and the thermal expansion coefficient is $3.5(10)^{-5}$ inches/inch/°F for the polyurethane foam. Due to the relatively low stiffness of the polyurethane foam compared with the surrounding stainless steel structures, temperature adjusting the foam's elastic modulus and thermal expansion coefficient will have a negligible effect on component stresses.

Both the reference and uniform temperature are set to 160 °F, thereby excluding the effects of differential thermal expansion for this case. The effects of differential thermal expansion are considered in Section 2.10.1.1.2, *OCA Structural Analysis – Load Case 2.*

For analysis model review, the ANSYS® input file is listed in Table 2.10.1-1.

2.10.1.1.2 OCA Structural Analysis – Load Case 2

For OCA Load Case 2, the OCA structural analysis uses a 50 psig (64.7 psia) internal pressure, corresponding to the maximum normal operating pressure (MNOP) from Section 3.4.4, *Maximum Internal Pressure*, coupled with a reduced external pressure of 3.5 psia (equivalently an 11.2 psig internal pressure), per Section 2.6.3, *Reduced External Pressure*, and 10 CFR §71.51(c)(3). The net internal pressure for this case is 61.2 psig, applied throughout the inner periphery of the model. Relative to the upper and lower OCV seal flanges, the internal pressure does not extend beyond (below) the top of the upper main O-ring seal groove.

A uniform temperature of 160 °F, per Section 2.6.1.1, *Summary of Pressures and Temperatures*, is utilized to determine the temperature-dependent, material property values. The only material properties affected by a temperature of 160 °F are the elastic modulus and the thermal expansion coefficient for the stainless steel. Consistent with Table 2.3-1 in Section 2.3.1, *Mechanical Properties Applied to Analytic Evaluations*, the elastic modulus and thermal expansion coefficient for Type 304 stainless steel are $27.8(10)^{6}$ psi and $8.694(10)^{-6}$ inches/inch/°F, respectively, at a temperature of 160 °F.

The material properties for the polyurethane foam are consistent with those specified in Section 2.3.1, *Mechanical Properties Applied to Analytic Evaluations*. The elastic modulus in the x- (radial) and z- (hoop) directions is based on the perpendicular-to-rise value of 4,773 psi. Young's modulus in the y- (axial) direction is based on the parallel-to-rise value of 6,810 psi. In addition, Poisson's ratio is 0.33, and the thermal expansion coefficient is $3.5(10)^{-5}$ inches/inch/°F for the polyurethane foam. Due to the relatively low stiffness of the polyurethane foam compared with the surrounding stainless steel structures, temperature adjusting the foam's elastic modulus and thermal expansion coefficient will have a negligible effect on component stresses.

The reference temperature is set to 70 °F, and the uniform temperature is set to 160 °F, thereby including the effects of differential thermal expansion for this case.

For analysis model review, the ANSYS® input file is listed in Table 2.10.1-2.

2.10.1.1.3 OCA Structural Analysis – Load Case 3

For OCA Load Case 3, the OCA structural analysis uses a 0.0 psig (14.7 psia) internal pressure coupled with an external pressure of 0.0 psig (14.7 psia) for a net pressure differential of 0.0 psig.

A uniform temperature of -40 °F, per Section 2.6.2, *Cold*, is utilized to determine the temperature-dependent, material property values. The only material properties affected by a temperature of

-40 °F are the elastic modulus and the thermal expansion coefficient for the stainless steel. Consistent with Table 2.3-1 in Section 2.3.1, *Mechanical Properties Applied to Analytic Evaluations*, the elastic modulus and thermal expansion coefficient for Type 304 stainless steel are $28.8(10)^6$ psi and $8.21(10)^{-6}$ inches/inch/°F, respectively, at a temperature of -40 °F.

The material properties for the polyurethane foam are consistent with those specified in Section 2.3.1, *Mechanical Properties Applied to Analytic Evaluations*. The elastic modulus in the x- (radial) and z- (hoop) directions is based on the perpendicular-to-rise value of 4,773 psi. Young's modulus in the y- (axial) direction is based on the parallel-to-rise value of 6,810 psi. In addition, Poisson's ratio is 0.33, and the thermal expansion coefficient is $3.5(10)^{-5}$ inches/inch/°F for the polyurethane foam. Due to the relatively low stiffness of the polyurethane foam compared with the surrounding stainless steel structures, temperature adjusting the foam's elastic modulus and thermal expansion coefficient will have a negligible effect on component stresses.

The reference temperature is set to 70 °F, and the uniform temperature is set to -40 °F, thereby including the effects of differential thermal expansion for this case.

For analysis model review, the ANSYS® input file is listed in Table 2.10.1-3.

2.10.1.1.4 OCA Structural Analysis – Load Case 4

For OCA Load Case 4, the OCA structural analysis uses a -14.7 psig (0.0 psia) internal pressure (i.e., full vacuum) coupled with a increased external pressure of 0.0 psig (14.7 psia), per Section 2.6.4, *Increased External Pressure*. The net external pressure for this case is 14.7 psig, applied throughout the inner periphery of the model. Relative to the upper and lower OCV seal flanges, the internal pressure does not extend beyond (below) the top of the upper main O-ring seal groove.

A uniform temperature of 70 °F is utilized to determine the temperature-dependent, material property values. The only material properties affected by a temperature of 70 °F are the elastic modulus and the thermal expansion coefficient for the stainless steel. Consistent with Table 2.3-1 in Section 2.3.1, *Mechanical Properties Applied to Analytic Evaluations*, the elastic modulus and thermal expansion coefficient for Type 304 stainless steel are $28.3(10)^6$ psi and $8.46(10)^{-6}$ inches/inch/°F, respectively, at a temperature of 70 °F.

The material properties for the polyurethane foam are consistent with those specified in Section 2.3.1, *Mechanical Properties Applied to Analytic Evaluations*. The elastic modulus in the x- (radial) and z- (hoop) directions is based on the perpendicular-to-rise value of 4,773 psi. Young's modulus in the y- (axial) direction is based on the parallel-to-rise value of 6,810 psi. In addition, Poisson's ratio is 0.33, and the thermal expansion coefficient is $3.5(10)^{-5}$ inches/inch/°F for the polyurethane foam. Due to the relatively low stiffness of the polyurethane foam compared with the surrounding stainless steel structures, temperature adjusting the foam's elastic modulus and thermal expansion coefficient will have a negligible effect on component stresses.

Both the reference and uniform temperature are set to 70 °F, thereby excluding the effects of differential thermal expansion for this case.

For analysis model review, the ANSYS® input file is listed in Table 2.10.1-4.

2.10.1.2 Inner Containment Vessel (ICV) Structural Analysis

Finite element analyses (FEA) are performed on the ICV structure to determine the stress states of the various components under normal conditions of transport (NCT) loads. The FEA analyses

are performed using ANSYS® 5.3. The ICV FEA model is comprised of four separate major structural components, modeled as shown in Figure 2.10.1-2:

- upper ICV seal flange
- lower ICV seal flange
- ICV locking ring
- ICV shells

The lower and upper seal flanges, and locking ring are modeled using 2-D, isoparametric solid elements (PLANE42). The quadrilateral elements are defined by four nodal points (a triangular element may be formed by defining duplicate the 3rd and 4th node numbers), each having two degrees of freedom: translations in the nodal x-direction (radial) and y-direction (axial).

The upper and lower ICV shells (ICV lid and body shells, respectively) are modeled using 2-D, axisymmetric conical shell elements (SHELL51). The lineal elements are defined by two nodal points, each having three degrees of freedom: translations in the nodal x-direction (radial) and y-direction (axial), and rotation about the nodal z-axis (hoop). In addition, the axisymmetric conical shell element is biaxial, with membrane and bending capabilities.

Relatively stiff, 2-D elastic beams (BEAM3) are utilized to maintain bending continuity between the three degree of freedom conical shell elements and two degree of freedom, isoparametric solid elements. Specifically, for both the lower and upper ICV seal flanges, four stiff beams are placed at each junction between the shell elements and the solid elements of the seal flanges. These elements are included to transmit the moment (i.e., to maintain slope continuity) between the shell and flange portions of the model, and have a negligible effect on the stress results.

Three sets of 2-D interface elements (CONTAC12) are utilized to connect the lower and upper ICV seal flanges to each other and to the ICV locking ring. The interface element is capable of supporting a load only in the direction normal to the surfaces, and is frictionless in the tangential direction. The interface element has two degrees of freedom at each node: translations in the nodal x-direction (radial) and y-direction (axial). A contact stiffness of 1×10^9 lb/in is chosen to reflect the relatively high interface stiffness when closed. Three sets of interface elements are used in these analyses: 1) between the lower ICV seal flange and the ICV locking ring, 2) between the upper ICV seal flange and the ICV locking ring, and 3) between the lower ICV seal flange and the upper ICV seal flange.

To account for the tangential (hoop) direction slotting for the lower ICV seal flange and ICV locking ring in the axisymmetric model, the material properties in the directly affected regions are modified. Specifically, material properties for the shaded elements in the lower ICV seal flange and ICV locking ring, illustrated on Figure 2.10.1-2, are modified to reflect only one-half the stainless steel being present for strength purposes. Specifically, the elastic modulus in the x- and y-directions is reduced to one-half their normal value (since only approximately one-half the material remains in the slotted regions), and the elastic modulus in the z-direction is set to set to a very low value to eliminate virtually all tangential (hoop) stiffness in the slotted regions. In addition, Poisson's ratio is set at the normal value of 0.3 for the x-y plane, but is set to zero in the y-z and x-z planes. In these ways, the analyses accurately depict the stress levels in all regions.

The global origin of the nodal coordinate system is located at the bottom center of the ICV body, as shown in Figure 2.10.1-2. As such, the nodal x-axis corresponds to the radial direction, the nodal y-axis corresponds to the axial direction, and the nodal z-axis corresponds to the tangential (or hoop) direction. The model is constrained from translating in the radial direction and rotating

about the hoop axis at the y-z symmetry plane at x equal zero. The model is also constrained from translating in the axial direction at a single node on the ICV locking ring.

2.10.1.2.1 ICV Structural Analysis – Load Case 1

For ICV Load Case 1, the ICV structural analysis uses a 50 psig (64.7 psia) internal pressure, corresponding to the maximum normal operating pressure (MNOP) from Section 3.4.4, *Maximum Internal Pressure*, coupled with a reduced external pressure of 3.5 psia (equivalently an 11.2 psig internal pressure), per Section 2.6.3, *Reduced External Pressure*, and 10 CFR §71.51(c)(3). The net internal pressure for this case is 61.2 psig, applied throughout the inner periphery of the model. Relative to the upper and lower ICV seal flanges, the internal pressure does not extend beyond (below) the top of the upper main O-ring seal groove.

A uniform temperature of 160 °F, per Section 2.6.1.1, *Summary of Pressures and Temperatures*, is utilized to determine the temperature-dependent, material property values. The only material properties affected by a temperature of 160 °F are the elastic modulus and the thermal expansion coefficient for the stainless steel. Consistent with Table 2.3-1 in Section 2.3.1, *Mechanical Properties Applied to Analytic Evaluations*, the elastic modulus and thermal expansion coefficient for Type 304 stainless steel are $27.8(10)^6$ psi and $8.694(10)^{-6}$ inches/inch/°F, respectively, at a temperature of 160 °F.

Both the reference and uniform temperature are set to 160 °F, thereby excluding the effects of differential thermal expansion for this case.

For analysis model review, the ANSYS® input file is listed in Table 2.10.1-5.

2.10.1.2.2 ICV Structural Analysis – Load Case 2

For ICV Load Case 4, the OCA structural analysis uses a -14.7 psig (0.0 psia) internal pressure (i.e., full vacuum) coupled with a increased external pressure of 0.0 psig (14.7 psia), per Section 2.6.4, *Increased External Pressure*. The net external pressure for this case is 14.7 psig, applied throughout the inner periphery of the model. Relative to the upper and lower ICV seal flanges, the internal pressure does not extend beyond (below) the top of the upper main O-ring seal groove.

A uniform temperature of 70 °F is utilized to determine the temperature-dependent, material property values. The only material properties affected by a temperature of 70 °F are the elastic modulus and the thermal expansion coefficient for the stainless steel. Consistent with Table 2.3-1 in Section 2.3.1, *Mechanical Properties Applied to Analytic Evaluations*, the elastic modulus and thermal expansion coefficient for Type 304 stainless steel are $28.3(10)^6$ psi and $8.46(10)^{-6}$ inches/inch/°F, respectively, at a temperature of 70 °F.

Both the reference and uniform temperature are set to 70 °F, thereby excluding the effects of differential thermal expansion for this case.

For analysis model review, the ANSYS® input file is listed in Table 2.10.1-6.

Table 2.10.1-1 – ANSYS® Input Listing for OCA Load Case 1

```
! initialize ANSYS
fini
/cle
/filename,oca_lc1,inp
/out,,txt

! start preprocessing the model
/prep7
/title, OCA Load Case 1: P=64.7/3.5 psia, T=160/160 F

! element types
et,1,42,,,1
et,2,51
et,3,42,,,1
et,4,12,,,,,,1
et,5,12,,,,,,1
et,6,3
et,7,14,,,2

! reference and uniform temperatures
tref,160
tunif,160

! material properties for non-slotted steel regions
ex,1,27.8e06
nuxy,1,.3
alpx,1,8.694e-06

! material properties for slotted steel regions
ex,2,13.9e06
ey,2,13.9e06
ez,2,1
nuxy,2,.3
nuxz,2,0
nuyz,2,0
alpx,2,8.694e-06
alpy,2,8.694e-06
alpz,2,8.694e-06

! material properties for the polyurethane foam
ex,3,4773
ey,3,6810
ez,3,4773
nuxy,3,.33
nuxz,3,.33
nuyz,3,.33
alpx,3,3.5e-5

! material properties for the rigid coupling elements
ex,4,27.8e06
nuxy,4,.3
alpx,4,8.694E-06

! element real constants
r,1,.25
r,2,.1875
r,3,.375
r,4,.075
r,5,,1e9,,1
r,6,-15,1e9,-.036
r,7,15,1e9,-.036
r,8,0,1e9,,1
r,9,1,1,1
r,10,1e2
r,101,-180.000,1e5,,1
r,102,-177.444,1e5,,1
r,103,-174.888,1e5,,1
r,104,-172.333,1e5,,1
r,105,-169.777,1e5,,1
r,106,-167.221,1e5,,1
r,107,-164.665,1e5,,1
r,108,-162.109,1e5,,1
r,109,-159.553,1e5,,1
r,110,-156.998,1e5,,1
r,111,-154.442,1e5,,1
r,112,-141.553,1e5,,1
r,113,-128.665,1e5,,1
r,114,-115.777,1e5,,1
r,115,-102.888,1e5,,1
r,116,-90.0000,1e5,,1
r,130,-102.000,1e5,,1
r,136,-77.1520,1e5,,1
r,137,-64.3041,1e5,,1
r,138,-51.4561,1e5,,1
r,139,-38.6081,1e5,,1
r,140,-25.7602,1e5,,1
r,141,-23.1841,1e5,,1
r,142,-20.6081,1e5,,1
r,143,-18.0321,1e5,,1
r,144,-15.4561,1e5,,1
r,145,-12.8801,1e5,,1
r,146,-10.3041,1e5,,1
r,147,-7.72805,1e5,,1
r,148,-5.15203,1e5,,1
r,149,-2.57602,1e5,,1
r,150,,1e5,,1
r,639,-58.7238,1e5,,1
r,640,-27.4476,1e5,,1
r,641,-24.7029,1e5,,1
r,642,-21.9581,1e5,,1
r,643,-19.2133,1e5,,1
r,644,-16.4686,1e5,,1
r,645,-13.7238,1e5,,1
r,646,-10.9790,1e5,,1
r,647,-8.23429,1e5,,1
r,648,-5.48952,1e5,,1
r,649,-2.74476,1e5,,1

! nodes for the lower seal flange
local,11,,38.24941495,50.051977923,,-12
n,1001
n,1005,.25
fill
n,1016,,.58677836
n,1020,.25,.58677836
fill
fill,1001,1016,2,1006,5,5,1
n,1026,,.896632635
local,12,,38.505,50
move,1026,11,0,999,0,12,-.065,999,0
fill,1016,1026,1,1021
local,11,1,39.12699808,50.47
n,1025,.5,148.5
n,1030,.5,129
n,1031,.5,109.5
n,1032,.5,90
csys,12
fill,1021,1025,3,1022,1,2,5
n,1033,.775,.97
n,1034,1.145,.97
n,1076,-.065,2.98
fill,1026,1076,8,1035,5
fill,1035,1076,7,1041,5
n,1060,.775,2.15593612
ngen,2,6,1033,1034,1,,.16
fill,1039,1060,3,1045,5
fill,1035,1039
fill,1041,1045,3,1042,1,4,5
n,1064,1.245,2.03
fill,1060,1064
n,1092,-.065,2.98
n,1096,.77960172,2.76
fill
n,1100,1.245,2.76
fill,1096,1100
fill,1056,1092,3,1065,9,9,1
ngen,3,9,1098,1100,1,,.26
n,1146,.14020351,4.4
fill,1092,1146,5,1101,9
n,1164,.14020351,4.98
fill,1146,1164,1,1155
local,11,,39.13520351,54.98,,-86.15
n,1168
n,1159,.3
ngen,3,-1,1159,1159,,,-.125
n,1148,.58,-.25
ngen,2,-18,1157,1159,1,.56
ngen,2,-9,1139,1141,1,.25
ngen,2,-27,1148,1148,,.81
ngen,2,-18,1130,1132,1,.56
fill,1096,1114,1,1105
csys,12
fill,1101,1105
fill,1110,1112,1,1111,,6,9
```

```
fill,1164,1168

! nodes for the upper seal flange
local,11,,38.405,52.81
n,2001,,5
n,2005,.25,5
fill
ngen,3,5,2001,2005,1,,-.25
n,2031,,3.45
n,2035,.91,3.45
fill
fill,2011,2031,3,2016,5,5,1
n,2051,,2.543442101
n,2055,.91,2.543442101
fill
fill,2031,2051,3,2036,5,4,1
n,2040,.91,3.29
fill,2040,2055,2,2045,5
n,2059,1.345,2.66
fill,2055,2059
n,2071,,2.17
n,2073,.21504507,2.17
fill
n,2077,.74504507,2.17
fill,2073,2077
fill,2051,2071,1,2060
fill,2054,2076,1,2065
fill,2060,2065
n,2081,1.345,2.17
fill,2077,2081
fill,2055,2077,1,2066,,5,1
n,2107,.85759646,.54
n,2109,1.10488343,.54
fill
n,2111,1.345,.54
fill,2109,2111
fill,2077,2107,5,2082,5,5,1
n,2117,.94488343
n,2119,1.10488343
fill
fill,2109,2119,1,2114
n,2112,.870715847,.35
fill,2112,2114
n,2120,1.345,3.45
n,2121,1.345,3.29
ngen,2,51,2071,2073,1,,-.305
ngen,2,3,2122,2124,1,,-.305

! nodes for the locking ring
local,11,,39.35,51.29
n,3001
n,3005,.435
fill
n,3009,.935
fill,3005,3009
n,3037,,.81
n,3041,.435,.693442101
fill
n,3045,.935,.693442101
fill,3041,3045
fill,3001,3037,3,3010,9,9,1
n,3145,,4.11
n,3149,.435,4.226557899
fill
n,3153,.935,4.226557899
fill,3149,3153
fill,3041,3149,11,3050,9,5,1
n,3181,,4.67
n,3185,.535,4.67
fill
n,3189,.935,4.67
fill,3185,3189
fill,3145,3181,3,3154,9,9,1

! nodes for the OCA inner shell (OCV)
local,11,1,,84.5
n,101,74.25,-90
n,111,74.25,-64.44174492
fill
local,12,1,28.3125,24.29659664
n,116,8.625
fill,111,116
csys
!n,117,36.9375,25.79659664
n,122,36.9375,43.95292590
fill,116,122
ngen,2,-879,1003,1003
fill,122,124
ngen,2,-1870,2003,2003
n,135,38.53,63.78649751
fill,133,135
local,12,1,29.905,63.78649751
n,140,8.625,64.23984399
fill,135,140
local,14,1,,1.8125
n,150,77.4375,90
fill,140,150

! nodes for the OCA outer shell
csys
n,601
n,613,47.0625
fill
n,622,47.0625,46.7775
fill,613,622
n,630,47.0625,47.6325
n,638,47.0625,75.3440689
fill,630,638
local,15,1,40.5625,75.3440689
n,640,6.5,62.55238078
fill,638,640
local,16,1,,-2.75
n,650,94.5,90
fill,640,650

! nodes for the polyurethane foam inner surface
csys
ngen,2,100,101,150,1
n,125,38.58338729,50.9
n,232,38.53,56.26

! nodes for the polyurethane foam outer surface
ngen,2,-100,601,650,1

! intermediate polyurethane foam nodes
fill,201,501,2,301,100,22,1
n,300,43.9375,50.9
n,331,41.5375,51.8825
n,332,41.5375,56.26
n,422,43.9375,46.7775
n,430,44.2375,47.6375
n,431,44.2375,51.8825
fill,222,422,1,322
fill,223,300,1,323
fill,332,532,1,432
fill,233,533,2,333,100,18,1

! nodes for the z-flanges
ngen,2,279,422,422,0
ngen,2,402,300,300,0
ngen,2,273,430,430,0
rp2,,,1,1
ngen,2,374,331,331,0
rp2,,,1,1

! elements for the lower seal flange
type,1
mat,1
real,1
e,1001,1002,1007,1006
rp4,1,1,1,1
egen,5,5,1,4,1
e,1026,1027,1036,1035
e,1027,1028,1036
e,1028,1029,1037,1036
e,1029,1030,1031,1037
e,1031,1032,1038,1037
rp3,1,1,1,1
e,1035,1036,1042,1041
rp4,1,1,1,1
e,1041,1042,1047,1046
rp4,1,1,1,1
egen,3,5,32,35,1
e,1056,1057,1066,1065
rp4,1,1,1,1
egen,4,9,44,47,1
mat,2
e,1060,1061,1070,1069
rp4,1,1,1,1
egen,4,9,60,63,1
egen,3,9,74,75,1
egen,3,9,56,59,1
```

```
egen,7,9,84,85,1
egen,3,1,99,99
egen,3,1,93,93

! elements for the upper seal flange
type,1
mat,1
real,1
e,2006,2007,2002,2001
rp4,1,1,1,1
egen,10,5,104,107,1
e,2040,2121,2120,2035
e,2060,2061,2052,2051
e,2061,2062,2052
e,2062,2063,2053,2052
e,2063,2064,2053
e,2064,2065,2054,2053
rp6,1,1,1,1
e,2071,2072,2061,2060
rp10,1,1,1,1
e,2122,2123,2072,2071
rp2,1,1,1,1
e,2125,2126,2123,2122
rp2,1,1,1,1
e,2082,2083,2078,2077
rp4,1,1,1,1
egen,6,5,169,172,1
egen,3,5,189,190,1

! elements for the locking ring
type,1
mat,2
real,1
e,3001,3002,3011,3010
rp4,1,1,1,1
egen,4,9,197,200,1
mat,1
e,3005,3006,3015,3014
rp4,1,1,1,1
egen,20,9,213,216,1
e,3145,3146,3155,3154
rp4,1,1,1,1
egen,4,9,293,296,1

! elements for the OCA inner shell (OCV)
type,2
mat,1
real,1
e,101,102
rp16,1,1
real,2
e,117,118
rp5,1,1
real,1
e,122,123
e,123,1003
e,2003,134
e,134,135
rp16,1,1

! elements for the OCA outer shell
real,1
e,601,602
rp18,1,1
real,3
e,619,620
rp3,1,1
e,630,631
rp8,1,1
real,1
e,638,639
rp12,1,1

! elements for the Z-flanges
real,4
e,622,701
e,701,702
e,702,1034
e,1034,1033
e,630,703
e,703,704
rp3,1,1
e,706,2120
e,2120,2035

! polyurethane foam elements
type,3
mat,3
real,1
e,201,301,302,202
rp22,1,1,1,1
e,224,223,323
e,301,401,402,302
rp21,1,1,1,1
e,322,422,300,323
e,300,125,224,323
e,401,501,502,402
rp21,1,1,1,1
e,333,233,232,332
e,233,333,334,234
rp17,1,1,1,1
e,331,431,432,332
rp19,1,1,1,1
e,430,530,531,431
rp20,1,1,1,1

! interface elements between the steel shells
!   and the polyurethane foam
type,5
mat,1
real,101
e,101,201
real,102
e,102,202
real,103
e,103,203
real,104
e,104,204
real,105
e,105,205
real,106
e,106,206
real,107
e,107,207
real,108
e,108,208
real,109
e,109,209
real,110
e,110,210
real,111
e,111,211
real,112
e,112,212
real,113
e,113,213
real,114
e,114,214
real,115
e,115,215
real,116
e,116,216
rp5,1,1
real,130
e,122,222
rp2,1,1
e,1003,224
real,101
e,702,300
e,701,422
e,622,522
real,150
e,706,332
e,705,331
e,704,431
e,703,430
e,630,530
real,116
e,300,702
e,422,701
e,706,332
e,705,331
e,704,431
e,703,430
e,2003,233
e,134,234
rp2,1,1
real,136
e,136,236
real,137
e,137,237
real,138
```

```
e,138,238
real,139
e,139,239
real,140
e,140,240
real,141
e,141,241
real,142
e,142,242
real,143
e,143,243
real,144
e,144,244
real,145
e,145,245
real,146
e,146,246
real,147
e,147,247
real,148
e,148,248
real,149
e,149,249
real,150
e,150,250
real,101
e,501,601
rp13,1,1
real,116
e,513,613
rp10,1,1
e,530,630
rp9,1,1
real,639
e,539,639
real,640
e,540,640
real,641
e,541,641
real,642
e,542,642
real,643
e,543,643
real,644
e,544,644
real,645
e,545,645
real,646
e,546,646
real,647
e,547,647
real,648
e,548,648
real,649
e,549,649
real,150
e,550,650

! interface elements between the lower seal flange
!   and the locking ring
type,4
mat,1
real,6
e,3038,1061
rp3,1,1

! interface elements between the upper seal flange
!   and the locking ring
type,4
mat,1
real,7
e,2056,3146
rp3,1,1

! interface elements between the lower seal flange
!   and the upper seal flange
type,5
mat,1
real,8
e,1164,2073
rp5,1,1

! couple the lower shell to the lower seal flange
type,6
mat,4
real,9
e,1001,1002
rp4,1,1

! couple the upper shell to the upper seal flange
type,6
mat,4
real,9
e,2001,2002
rp4,1,1

! springs between the lower seal flange
!   and the locking ring
type,7
mat,1
real,10
e,3038,1061
rp3,1,1

! springs between the upper seal flange
!   and the locking ring
type,7
mat,1
real,10
e,2056,3146
rp3,1,1

! springs between the lower seal flange
!   and the upper seal flange
type,7
mat,1
real,10
e,1164,2073
rp5,1,1

! displacement constraints
d,101,UX,0,,601,500,rotz
d,201,UX,0,,501,100
d,150,UX,0,,650,500,rotz
d,250,UX,0,,550,100
d,3099,UY,0
d,all,uz,0

! pressure loads
alls
pload=+(64.7-3.5)
p,101,102,pload,,122,1
p,123,1003,pload
p,1001,1006,pload,,1021,5
p,1026,1035,pload
p,1035,1041,pload
p,1041,1046,pload,,1051,5
p,1056,1065,pload,,1155,9
p,1164,1165,pload,,1167,1
p,1168,1159,pload
p,2077,2082,pload
p,2073,2074,pload,,2076,1
p,2127,2124,pload
p,2124,2073,pload
p,2125,2126,pload,,2126,1
p,2122,2125,pload
p,2071,2122,pload
p,2001,2006,pload,,2046,5
p,2051,2060,pload
p,2060,2071,pload
p,2003,134,pload
p,134,135,pload,,149,1

! delete unused nodes at seal flange interfaces
ndele,124
ndele,133

! solve the problem
fini
/solu
neqit,1000
alls
solv
fini
save

! post-process the problem
/post1
set
rsys,solu
ernorm,0
```

```
! table stress definitions for shell elements
nall
alls
esel,s,type,,2
etab,sit,nmisc,4
etab,sim,nmisc,9
etab,sib,nmisc,14

/com,
/com,
/com,
/com,++++++++++++++++++++
/com,+ lower seal flange +
/com,++++++++++++++++++++
/com,
/com,
nall
eall
nsel,s,node,,1000,1999,1
prns,prin

/com,
/com,
/com,
/com,++++++++++++++++++++
/com,+ upper seal flange +
/com,++++++++++++++++++++
/com,
/com,
nall
eall
nsel,s,node,,2000,2999,1
prns,prin

/com,
/com,
/com,
/com,+++++++++++++++++
/com,+ locking ring +
/com,+++++++++++++++++
/com,
/com,
nall
eall
nsel,s,node,,3000,3999,1
prns,prin

/com,
/com,
/com,
/com,++++++++++++++++++++++++++++++++++++++
/com,+ OCV cylindrical and conical shells +
/com,++++++++++++++++++++++++++++++++++++++
/com,
/com,
nall
eall
esel,s,elem,,324,331,1
pret

/com,
/com,
/com,
/com,++++++++++++++++++++++++++++++++++++++
/com,+ OCV torispherical head crown shells +
/com,++++++++++++++++++++++++++++++++++++++
/com,
/com,
nall
eall
esel,s,elem,,339,348,1    ! upper head
esel,a,elem,,309,318,1    ! lower head
pret

/com,
/com,
/com,
/com,++++++++++++++++++++++++++++++++++++++++++++
/com,+ OCV torispherical head knuckle shells +
/com,++++++++++++++++++++++++++++++++++++++++++++
/com,
/com,
nall
eall
esel,s,elem,,334,338,1    ! upper head
esel,a,elem,,319,323,1    ! lower head
pret

/com,
/com,
/com,
/com,++++++++++++++++++++++++++++++++++
/com,+ OCA outer shells and z-flanges +
/com,++++++++++++++++++++++++++++++++++
/com,
/com,
nall
eall
esel,s,elem,,349,399,1
pret

/com,
/com,
/com,
/com,++++++++++++++++++++++++++++++
/com,+ polyurethane foam elements +
/com,++++++++++++++++++++++++++++++
/com,
/com,
nall
eall
esel,s,elem,,415,559,1
prns,prin

! finalize ANSYS
nall
eall
save
/out,term
/eof
```

Table 2.10.1-2 – ANSYS® Input Listing for OCA Load Case 2

```
! initialize ANSYS
fini
/cle
/filename,oca_lc2,inp
/out,,txt

! start preprocessing the model
/prep7
/title, OCA Load Case 2: P=64.7/3.5 psia, T=160/70 F

! element types
et,1,42,,,1
et,2,51
et,3,42,,,1
et,4,12,,,,,,,1
et,5,12,,,,,,,1
et,6,3
et,7,14,,,2

! reference and uniform temperatures
tref,70
tunif,160

! material properties for non-slotted steel regions
ex,1,27.8e06
nuxy,1,.3
alpx,1,8.694e-06

! material properties for slotted steel regions
ex,2,13.9e06
ey,2,13.9e06
ez,2,1
nuxy,2,.3
nuxz,2,0
nuyz,2,0
alpx,2,8.694e-06
alpy,2,8.694e-06
alpz,2,8.694e-06

! material properties for the polyurethane foam
ex,3,4773
ey,3,6810
ez,3,4773
nuxy,3,.33
nuxz,3,.33
nuyz,3,.33
alpx,3,3.5e-5

! material properties for the rigid coupling elements
ex,4,27.8e06
nuxy,4,.3
alpx,4,8.694E-06

! element real constants
r,1,.25
r,2,.1875
r,3,.375
r,4,.075
r,5,,1e9,,1
r,6,-15,1e9,-.036
r,7,15,1e9,-.036
r,8,0,1e9,,1
r,9,1,1,1
r,10,1e2
r,101,-180.000,1e5,,1
r,102,-177.444,1e5,,1
r,103,-174.888,1e5,,1
r,104,-172.333,1e5,,1
r,105,-169.777,1e5,,1
r,106,-167.221,1e5,,1
r,107,-164.665,1e5,,1
r,108,-162.109,1e5,,1
r,109,-159.553,1e5,,1
r,110,-156.998,1e5,,1
r,111,-154.442,1e5,,1
r,112,-141.553,1e5,,1
r,113,-128.665,1e5,,1
r,114,-115.777,1e5,,1
r,115,-102.888,1e5,,1
r,116,-90.0000,1e5,,1
r,130,-102.000,1e5,,1
r,136,-77.1520,1e5,,1
r,137,-64.3041,1e5,,1
r,138,-51.4561,1e5,,1
r,139,-38.6081,1e5,,1
r,140,-25.7602,1e5,,1
r,141,-23.1841,1e5,,1
r,142,-20.6081,1e5,,1
r,143,-18.0321,1e5,,1
r,144,-15.4561,1e5,,1
r,145,-12.8801,1e5,,1
r,146,-10.3041,1e5,,1
r,147,-7.72805,1e5,,1
r,148,-5.15203,1e5,,1
r,149,-2.57602,1e5,,1
r,150,,1e5,,1
r,639,-58.7238,1e5,,1
r,640,-27.4476,1e5,,1
r,641,-24.7029,1e5,,1
r,642,-21.9581,1e5,,1
r,643,-19.2133,1e5,,1
r,644,-16.4686,1e5,,1
r,645,-13.7238,1e5,,1
r,646,-10.9790,1e5,,1
r,647,-8.23429,1e5,,1
r,648,-5.48952,1e5,,1
r,649,-2.74476,1e5,,1

! nodes for the lower seal flange
local,11,,38.24941495,50.051977923,,-12
n,1001
n,1005,.25
fill
n,1016,,.58677836
n,1020,.25,.58677836
fill
fill,1001,1016,2,1006,5,5,1
n,1026,,.896632635
local,12,,38.505,50
move,1026,11,0,999,0,12,-.065,999,0
fill,1016,1026,1,1021
local,11,1,39.12699808,50.47
n,1025,.5,148.5
n,1030,.5,129
n,1031,.5,109.5
n,1032,.5,90
csys,12
fill,1021,1025,3,1022,1,2,5
n,1033,.775,.97
n,1034,1.145,.97
n,1076,-.065,2.98
fill,1026,1076,8,1035,5
fill,1035,1076,7,1041,5
n,1060,.775,2.15593612
ngen,2,6,1033,1034,1,,.16
fill,1039,1060,3,1045,5
fill,1035,1039
fill,1041,1045,3,1042,1,4,5
n,1064,1.245,2.03
fill,1060,1064
n,1092,-.065,2.98
n,1096,.77960172,2.76
fill
n,1100,1.245,2.76
fill,1096,1100
fill,1056,1092,3,1065,9,9,1
ngen,3,9,1098,1100,1,,.26
n,1146,.14020351,4.4
fill,1092,1146,5,1101,9
n,1164,.14020351,4.98
fill,1146,1164,1,1155
local,11,,39.13520351,54.98,,-86.15
n,1168
n,1159,.3
ngen,3,-1,1159,1159,,,-.125
n,1148,.58,-.25
ngen,2,-18,1157,1159,1,.56
ngen,2,-9,1139,1141,1,.25
ngen,2,-27,1148,1148,,.81
ngen,2,-18,1130,1132,1,.56
fill,1096,1114,1,1105
csys,12
fill,1101,1105
fill,1110,1112,1,1111,,6,9
```

```
fill,1164,1168

! nodes for the upper seal flange
local,11,,38.405,52.81
n,2001,,5
n,2005,.25,5
fill
ngen,3,5,2001,2005,1,,-.25
n,2031,,3.45
n,2035,.91,3.45
fill
fill,2011,2031,3,2016,5,5,1
n,2051,,2.543442101
n,2055,.91,2.543442101
fill
fill,2031,2051,3,2036,5,4,1
n,2040,.91,3.29
fill,2040,2055,2,2045,5
n,2059,1.345,2.66
fill,2055,2059
n,2071,,2.17
n,2073,.21504507,2.17
fill
n,2077,.74504507,2.17
fill,2073,2077
fill,2051,2071,1,2060
fill,2054,2076,1,2065
fill,2060,2065
n,2081,1.345,2.17
fill,2077,2081
fill,2055,2077,1,2066,,5,1
n,2107,.85759646,.54
n,2109,1.10488343,.54
fill
n,2111,1.345,.54
fill,2109,2111
fill,2077,2107,5,2082,5,5,1
n,2117,.94488343
n,2119,1.10488343
fill
fill,2109,2119,1,2114
n,2112,.870715847,.35
fill,2112,2114
n,2120,1.345,3.45
n,2121,1.345,3.29
ngen,2,51,2071,2073,1,,-.305
ngen,2,3,2122,2124,1,,-.305

! nodes for the locking ring
local,11,,39.35,51.29
n,3001
n,3005,.435
fill
n,3009,.935
fill,3005,3009
n,3037,,.81
n,3041,.435,.693442101
fill
n,3045,.935,.693442101
fill,3041,3045
fill,3001,3037,3,3010,9,9,1
n,3145,,4.11
n,3149,.435,4.226557899
fill
n,3153,.935,4.226557899
fill,3149,3153
fill,3041,3149,11,3050,9,5,1
n,3181,,4.67
n,3185,.535,4.67
fill
n,3189,.935,4.67
fill,3185,3189
fill,3145,3181,3,3154,9,9,1

! nodes for the OCA inner shell (OCV)
local,11,1,,84.5
n,101,74.25,-90
n,111,74.25,-64.44174492
fill
local,12,1,28.3125,24.29659664
n,116,8.625
fill,111,116
csys
!n,117,36.9375,25.79659664
n,122,36.9375,43.95292590
fill,116,122

ngen,2,-879,1003,1003
fill,122,124
ngen,2,-1870,2003,2003
n,135,38.53,63.78649751
fill,133,135
local,12,1,29.905,63.78649751
n,140,8.625,64.23984399
fill,135,140
local,14,1,,1.8125
n,150,77.4375,90
fill,140,150

! nodes for the OCA outer shell
csys
n,601
n,613,47.0625
fill
n,622,47.0625,46.7775
fill,613,622
n,630,47.0625,47.6325
n,638,47.0625,75.3440689
fill,630,638
local,15,1,40.5625,75.3440689
n,640,6.5,62.55238078
fill,638,640
local,16,1,,-2.75
n,650,94.5,90
fill,640,650

! nodes for the polyurethane foam inner surface
csys
ngen,2,100,101,150,1
n,125,38.58338729,50.9
n,232,38.53,56.26

! nodes for the polyurethane foam outer surface
ngen,2,-100,601,650,1

! intermediate polyurethane foam nodes
fill,201,501,2,301,100,22,1
n,300,43.9375,50.9
n,331,41.5375,51.8825
n,332,41.5375,56.26
n,422,43.9375,46.7775
n,430,44.2375,47.6375
n,431,44.2375,51.8825
fill,222,422,1,322
fill,223,300,1,323
fill,332,532,1,432
fill,233,533,2,333,100,18,1

! nodes for the z-flanges
ngen,2,279,422,422,0
ngen,2,402,300,300,0
ngen,2,273,430,430,0
rp2,,,1,1
ngen,2,374,331,331,0
rp2,,,1,1

! elements for the lower seal flange
type,1
mat,1
real,1
e,1001,1002,1007,1006
rp4,1,1,1,1
egen,5,5,1,4,1
e,1026,1027,1036,1035
e,1027,1028,1036
e,1028,1029,1037,1036
e,1029,1030,1031,1037
e,1031,1032,1038,1037
rp3,1,1,1,1
e,1035,1036,1042,1041
rp4,1,1,1,1
e,1041,1042,1047,1046
rp4,1,1,1,1
egen,3,5,32,35,1
e,1056,1057,1066,1065
rp4,1,1,1,1
egen,4,9,44,47,1
mat,2
e,1060,1061,1070,1069
rp4,1,1,1,1
egen,4,9,60,63,1
egen,3,9,74,75,1
egen,3,9,56,59,1
```

```
egen,7,9,84,85,1
egen,3,1,99,99
egen,3,1,93,93

! elements for the upper seal flange
type,1
mat,1
real,1
e,2006,2007,2002,2001
rp4,1,1,1,1
egen,10,5,104,107,1
e,2040,2121,2120,2035
e,2060,2061,2052,2051
e,2061,2062,2052
e,2062,2063,2053,2052
e,2063,2064,2053
e,2064,2065,2054,2053
rp6,1,1,1,1
e,2071,2072,2061,2060
rp10,1,1,1,1
e,2122,2123,2072,2071
rp2,1,1,1,1
e,2125,2126,2123,2122
rp2,1,1,1,1
e,2082,2083,2078,2077
rp4,1,1,1,1
egen,6,5,169,172,1
egen,3,5,189,190,1

! elements for the locking ring
type,1
mat,2
real,1
e,3001,3002,3011,3010
rp4,1,1,1,1
egen,4,9,197,200,1
mat,1
e,3005,3006,3015,3014
rp4,1,1,1,1
egen,20,9,213,216,1
e,3145,3146,3155,3154
rp4,1,1,1,1
egen,4,9,293,296,1

! elements for the OCA inner shell (OCV)
type,2
mat,1
real,1
e,101,102
rp16,1,1
real,2
e,117,118
rp5,1,1
real,1
e,122,123
e,123,1003
e,2003,134
e,134,135
rp16,1,1

! elements for the OCA outer shell
real,1
e,601,602
rp18,1,1
real,3
e,619,620
rp3,1,1
e,630,631
rp8,1,1
real,1
e,638,639
rp12,1,1

! elements for the Z-flanges
real,4
e,622,701
e,701,702
e,702,1034
e,1034,1033
e,630,703
e,703,704
rp3,1,1
e,706,2120
e,2120,2035

! polyurethane foam elements
type,3
mat,3
real,1
e,201,301,302,202
rp22,1,1,1,1
e,224,223,323
e,301,401,402,302
rp21,1,1,1,1
e,322,422,300,323
e,300,125,224,323
e,401,501,502,402
rp21,1,1,1,1
e,333,233,232,332
e,233,333,334,234
rp17,1,1,1,1
e,331,431,432,332
rp19,1,1,1,1
e,430,530,531,431
rp20,1,1,1,1

! interface elements between the steel shells
!   and the polyurethane foam
type,5
mat,1
real,101
e,101,201
real,102
e,102,202
real,103
e,103,203
real,104
e,104,204
real,105
e,105,205
real,106
e,106,206
real,107
e,107,207
real,108
e,108,208
real,109
e,109,209
real,110
e,110,210
real,111
e,111,211
real,112
e,112,212
real,113
e,113,213
real,114
e,114,214
real,115
e,115,215
real,116
e,116,216
rp5,1,1
real,130
e,122,222
rp2,1,1
e,1003,224
real,101
e,702,300
e,701,422
e,622,522
real,150
e,706,332
e,705,331
e,704,431
e,703,430
e,630,530
real,116
e,300,702
e,422,701
e,706,332
e,705,331
e,704,431
e,703,430
e,2003,233
e,134,234
rp2,1,1
real,136
e,136,236
real,137
e,137,237
real,138
```

```
e,138,238
real,139
e,139,239
real,140
e,140,240
real,141
e,141,241
real,142
e,142,242
real,143
e,143,243
real,144
e,144,244
real,145
e,145,245
real,146
e,146,246
real,147
e,147,247
real,148
e,148,248
real,149
e,149,249
real,150
e,150,250
real,101
e,501,601
rp13,1,1
real,116
e,513,613
rp10,1,1
e,530,630
rp9,1,1
real,639
e,539,639
real,640
e,540,640
real,641
e,541,641
real,642
e,542,642
real,643
e,543,643
real,644
e,544,644
real,645
e,545,645
real,646
e,546,646
real,647
e,547,647
real,648
e,548,648
real,649
e,549,649
real,150
e,550,650

! interface elements between the lower seal flange
!   and the locking ring
type,4
mat,1
real,6
e,3038,1061
rp3,1,1

! interface elements between the upper seal flange
!   and the locking ring
type,4
mat,1
real,7
e,2056,3146
rp3,1,1

! interface elements between the lower seal flange
!   and the upper seal flange
type,5
mat,1
real,8
e,1164,2073
rp5,1,1

! couple the lower shell to the lower seal flange
type,6
mat,4
real,9
e,1001,1002
rp4,1,1

! couple the upper shell to the upper seal flange
type,6
mat,4
real,9
e,2001,2002
rp4,1,1

! springs between the lower seal flange
!   and the locking ring
type,7
mat,1
real,10
e,3038,1061
rp3,1,1

! springs between the upper seal flange
!   and the locking ring
type,7
mat,1
real,10
e,2056,3146
rp3,1,1

! springs between the lower seal flange
!   and the upper seal flange
type,7
mat,1
real,10
e,1164,2073
rp5,1,1

! displacement constraints
d,101,UX,0,,601,500,rotz
d,201,UX,0,,501,100
d,150,UX,0,,650,500,rotz
d,250,UX,0,,550,100
d,3099,UY,0
d,all,uz,0

! pressure loads
alls
pload=+(64.7-3.5)
p,101,102,pload,,122,1
p,123,1003,pload
p,1001,1006,pload,,1021,5
p,1026,1035,pload
p,1035,1041,pload
p,1041,1046,pload,,1051,5
p,1056,1065,pload,,1155,9
p,1164,1165,pload,,1167,1
p,1168,1159,pload
p,2077,2082,pload
p,2073,2074,pload,,2076,1
p,2127,2124,pload
p,2124,2073,pload
p,2125,2126,pload,,2126,1
p,2122,2125,pload
p,2071,2122,pload
p,2001,2006,pload,,2046,5
p,2051,2060,pload
p,2060,2071,pload
p,2003,134,pload
p,134,135,pload,,149,1

! delete unused nodes at seal flange interfaces
ndele,124
ndele,133

! solve the problem
fini
/solu
neqit,1000
alls
solv
fini
save

! post-process the problem
/post1
set
rsys,solu
ernorm,0
```

```
! table stress definitions for shell elements
nall
alls
esel,s,type,,2
etab,sit,nmisc,4
etab,sim,nmisc,9
etab,sib,nmisc,14

/com,
/com,
/com,
/com,++++++++++++++++++++
/com,+ lower seal flange +
/com,++++++++++++++++++++
/com,
/com,
nall
eall
nsel,s,node,,1000,1999,1
prns,prin

/com,
/com,
/com,
/com,++++++++++++++++++++
/com,+ upper seal flange +
/com,++++++++++++++++++++
/com,
/com,
nall
eall
nsel,s,node,,2000,2999,1
prns,prin

/com,
/com,
/com,
/com,+++++++++++++++++
/com,+ locking ring +
/com,+++++++++++++++++
/com,
/com,
nall
eall
nsel,s,node,,3000,3999,1
prns,prin

/com,
/com,
/com,
/com,++++++++++++++++++++++++++++++++++++
/com,+ OCV cylindrical and conical shells +
/com,++++++++++++++++++++++++++++++++++++
/com,
/com,
nall
eall
esel,s,elem,,324,331,1
pret

/com,
/com,
/com,
/com,++++++++++++++++++++++++++++++++++++
/com,+ OCV torispherical head crown shells +
/com,++++++++++++++++++++++++++++++++++++
/com,
/com,
nall
eall
esel,s,elem,,339,348,1    ! upper head
esel,a,elem,,309,318,1    ! lower head
pret

/com,
/com,
/com,
/com,++++++++++++++++++++++++++++++++++++++++++
/com,+ OCV torispherical head knuckle shells +
/com,++++++++++++++++++++++++++++++++++++++++++
/com,
/com,
nall
eall
esel,s,elem,,334,338,1    ! upper head
esel,a,elem,,319,323,1    ! lower head
pret

/com,
/com,
/com,
/com,++++++++++++++++++++++++++++++++++
/com,+ OCA outer shells and z-flanges +
/com,++++++++++++++++++++++++++++++++++
/com,
/com,
nall
eall
esel,s,elem,,349,399,1
pret

/com,
/com,
/com,
/com,++++++++++++++++++++++++++++++++
/com,+ polyurethane foam elements +
/com,++++++++++++++++++++++++++++++++
/com,
/com,
nall
eall
esel,s,elem,,415,559,1
prns,prin

! finalize ANSYS
nall
eall
save
/out,term
/eof
```

Table 2.10.1-3 – ANSYS® Input Listing for OCA Load Case 3

```
! initialize ANSYS
fini
/cle
/filename,oca_lc3,inp
/out,,txt

! start preprocessing the model
/prep7
/title, OCA Load Case 3: P=14.7/14.7 psia, T=-40/70 F

! element types
et,1,42,,,1
et,2,51
et,3,42,,,1
et,4,12,,,,,,1
et,5,12,,,,,,1
et,6,3
et,7,14,,,2

! reference and uniform temperatures
tref,70
tunif,-40

! material properties for non-slotted steel regions
ex,1,28.8e06
nuxy,1,.3
alpx,1,8.21e-06

! material properties for slotted steel regions
ex,2,14.4e06
ey,2,14.4e06
ez,2,1
nuxy,2,.3
nuxz,2,0
nuyz,2,0
alpx,2,8.21e-06
alpy,2,8.21e-06
alpz,2,8.21e-06

! material properties for the polyurethane foam
ex,3,4773
ey,3,6810
ez,3,4773
nuxy,3,.33
nuxz,3,.33
nuyz,3,.33
alpx,3,3.5e-5

! material properties for the rigid coupling elements
ex,4,28.8e06
nuxy,4,.3
alpx,4,8.21E-06

! element real constants
r,1,.25
r,2,.1875
r,3,.375
r,4,.075
r,5,,1e9,,1
r,6,-15,1e9,-.036
r,7,15,1e9,-.036
r,8,0,1e9,,1
r,9,1,1,1
r,10,1e2
r,101,-180.000,1e5,,1
r,102,-177.444,1e5,,1
r,103,-174.888,1e5,,1
r,104,-172.333,1e5,,1
r,105,-169.777,1e5,,1
r,106,-167.221,1e5,,1
r,107,-164.665,1e5,,1
r,108,-162.109,1e5,,1
r,109,-159.553,1e5,,1
r,110,-156.998,1e5,,1
r,111,-154.442,1e5,,1
r,112,-141.553,1e5,,1
r,113,-128.665,1e5,,1
r,114,-115.777,1e5,,1
r,115,-102.888,1e5,,1
r,116,-90.0000,1e5,,1
r,130,-102.000,1e5,,1
r,136,-77.1520,1e5,,1
r,137,-64.3041,1e5,,1
r,138,-51.4561,1e5,,1
r,139,-38.6081,1e5,,1
r,140,-25.7602,1e5,,1
r,141,-23.1841,1e5,,1
r,142,-20.6081,1e5,,1
r,143,-18.0321,1e5,,1
r,144,-15.4561,1e5,,1
r,145,-12.8801,1e5,,1
r,146,-10.3041,1e5,,1
r,147,-7.72805,1e5,,1
r,148,-5.15203,1e5,,1
r,149,-2.57602,1e5,,1
r,150,,1e5,,1
r,639,-58.7238,1e5,,1
r,640,-27.4476,1e5,,1
r,641,-24.7029,1e5,,1
r,642,-21.9581,1e5,,1
r,643,-19.2133,1e5,,1
r,644,-16.4686,1e5,,1
r,645,-13.7238,1e5,,1
r,646,-10.9790,1e5,,1
r,647,-8.23429,1e5,,1
r,648,-5.48952,1e5,,1
r,649,-2.74476,1e5,,1

! nodes for the lower seal flange
local,11,,38.24941495,50.051977923,,-12
n,1001
n,1005,.25
fill
n,1016,,.58677836
n,1020,.25,.58677836
fill
fill,1001,1016,2,1006,5,5,1
n,1026,,.896632635
local,12,,38.505,50
move,1026,11,0,999,0,12,-.065,999,0
fill,1016,1026,1,1021
local,11,1,39.12699808,50.47
n,1025,.5,148.5
n,1030,.5,129
n,1031,.5,109.5
n,1032,.5,90
csys,12
fill,1021,1025,3,1022,1,2,5
n,1033,.775,.97
n,1034,1.145,.97
n,1076,-.065,2.98
fill,1026,1076,8,1035,5
fill,1035,1076,7,1041,5
n,1060,.775,2.15593612
ngen,2,6,1033,1034,1,,.16
fill,1039,1060,3,1045,5
fill,1035,1039
fill,1041,1045,3,1042,1,4,5
n,1064,1.245,2.03
fill,1060,1064
n,1092,-.065,2.98
n,1096,.77960172,2.76
fill
n,1100,1.245,2.76
fill,1096,1100
fill,1056,1092,3,1065,9,9,1
ngen,3,9,1098,1100,1,,.26
n,1146,.14020351,4.4
fill,1092,1146,5,1101,9
n,1164,.14020351,4.98
fill,1146,1164,1,1155
local,11,,39.13520351,54.98,,-86.15
n,1168
n,1159,.3
ngen,3,-1,1159,1159,,,-.125
n,1148,.58,-.25
ngen,2,-18,1157,1159,1,.56
ngen,2,-9,1139,1141,1,.25
ngen,2,-27,1148,1148,,.81
ngen,2,-18,1130,1132,1,.56
fill,1096,1114,1,1105
csys,12
fill,1101,1105
fill,1110,1112,1,1111,,6,9
```

```
fill,1164,1168

! nodes for the upper seal flange
local,11,,38.405,52.81
n,2001,,5
n,2005,.25,5
fill
ngen,3,5,2001,2005,1,,-.25
n,2031,,3.45
n,2035,.91,3.45
fill
fill,2011,2031,3,2016,5,5,1
n,2051,,2.543442101
n,2055,.91,2.543442101
fill
fill,2031,2051,3,2036,5,4,1
n,2040,.91,3.29
fill,2040,2055,2,2045,5
n,2059,1.345,2.66
fill,2055,2059
n,2071,,2.17
n,2073,.21504507,2.17
fill
n,2077,.74504507,2.17
fill,2073,2077
fill,2051,2071,1,2060
fill,2054,2076,1,2065
fill,2060,2065
n,2081,1.345,2.17
fill,2077,2081
fill,2055,2077,1,2066,,5,1
n,2107,.85759646,.54
n,2109,1.10488343,.54
fill
n,2111,1.345,.54
fill,2109,2111
fill,2077,2107,5,2082,5,5,1
n,2117,.94488343
n,2119,1.10488343
fill
fill,2109,2119,1,2114
n,2112,.870715847,.35
fill,2112,2114
n,2120,1.345,3.45
n,2121,1.345,3.29
ngen,2,51,2071,2073,1,,-.305
ngen,2,3,2122,2124,1,,-.305

! nodes for the locking ring
local,11,,39.35,51.29
n,3001
n,3005,.435
fill
n,3009,.935
fill,3005,3009
n,3037,,.81
n,3041,.435,.693442101
fill
n,3045,.935,.693442101
fill,3041,3045
fill,3001,3037,3,3010,9,9,1
n,3145,,4.11
n,3149,.435,4.226557899
fill
n,3153,.935,4.226557899
fill,3149,3153
fill,3041,3149,11,3050,9,5,1
n,3181,,4.67
n,3185,.535,4.67
fill
n,3189,.935,4.67
fill,3185,3189
fill,3145,3181,3,3154,9,9,1

! nodes for the OCA inner shell (OCV)
local,11,1,,84.5
n,101,74.25,-90
n,111,74.25,-64.44174492
fill
local,12,1,28.3125,24.29659664
n,116,8.625
fill,111,116
csys
!n,117,36.9375,25.79659664
n,122,36.9375,43.95292590
fill,116,122
ngen,2,-879,1003,1003
fill,122,124
ngen,2,-1870,2003,2003
n,135,38.53,63.78649751
fill,133,135
local,12,1,29.905,63.78649751
n,140,8.625,64.23984399
fill,135,140
local,14,1,,1.8125
n,150,77.4375,90
fill,140,150

! nodes for the OCA outer shell
csys
n,601
n,613,47.0625
fill
n,622,47.0625,46.7775
fill,613,622
n,630,47.0625,47.6325
n,638,47.0625,75.3440689
fill,630,638
local,15,1,40.5625,75.3440689
n,640,6.5,62.55238078
fill,638,640
local,16,1,,-2.75
n,650,94.5,90
fill,640,650

! nodes for the polyurethane foam inner surface
csys
ngen,2,100,101,150,1
n,125,38.58338729,50.9
n,232,38.53,56.26

! nodes for the polyurethane foam outer surface
ngen,2,-100,601,650,1

! intermediate polyurethane foam nodes
fill,201,501,2,301,100,22,1
n,300,43.9375,50.9
n,331,41.5375,51.8825
n,332,41.5375,56.26
n,422,43.9375,46.7775
n,430,44.2375,47.6375
n,431,44.2375,51.8825
fill,222,422,1,322
fill,223,300,1,323
fill,332,532,1,432
fill,233,533,2,333,100,18,1

! nodes for the z-flanges
ngen,2,279,422,422,0
ngen,2,402,300,300,0
ngen,2,273,430,430,0
rp2,,,1,1
ngen,2,374,331,331,0
rp2,,,1,1

! elements for the lower seal flange
type,1
mat,1
real,1
e,1001,1002,1007,1006
rp4,1,1,1,1
egen,5,5,1,4,1
e,1026,1027,1036,1035
e,1027,1028,1036
e,1028,1029,1037,1036
e,1029,1030,1031,1037
e,1031,1032,1038,1037
rp3,1,1,1,1
e,1035,1036,1042,1041
rp4,1,1,1,1
e,1041,1042,1047,1046
rp4,1,1,1,1
egen,3,5,32,35,1
e,1056,1057,1066,1065
rp4,1,1,1,1
egen,4,9,44,47,1
mat,2
e,1060,1061,1070,1069
rp4,1,1,1,1
egen,4,9,60,63,1
egen,3,9,74,75,1
egen,3,9,56,59,1
```

```
egen,7,9,84,85,1
egen,3,1,99,99
egen,3,1,93,93

! elements for the upper seal flange
type,1
mat,1
real,1
e,2006,2007,2002,2001
rp4,1,1,1,1
egen,10,5,104,107,1
e,2040,2121,2120,2035
e,2060,2061,2052,2051
e,2061,2062,2052
e,2062,2063,2053,2052
e,2063,2064,2053
e,2064,2065,2054,2053
rp6,1,1,1,1
e,2071,2072,2061,2060
rp10,1,1,1,1
e,2122,2123,2072,2071
rp2,1,1,1,1
e,2125,2126,2123,2122
rp2,1,1,1,1
e,2082,2083,2078,2077
rp4,1,1,1,1
egen,6,5,169,172,1
egen,3,5,189,190,1

! elements for the locking ring
type,1
mat,2
real,1
e,3001,3002,3011,3010
rp4,1,1,1,1
egen,4,9,197,200,1
mat,1
e,3005,3006,3015,3014
rp4,1,1,1,1
egen,20,9,213,216,1
e,3145,3146,3155,3154
rp4,1,1,1,1
egen,4,9,293,296,1

! elements for the OCA inner shell (OCV)
type,2
mat,1
real,1
e,101,102
rp16,1,1
real,2
e,117,118
rp5,1,1
real,1
e,122,123
e,123,1003
e,2003,134
e,134,135
rp16,1,1

! elements for the OCA outer shell
real,1
e,601,602
rp18,1,1
real,3
e,619,620
rp3,1,1
e,630,631
rp8,1,1
real,1
e,638,639
rp12,1,1

! elements for the Z-flanges
real,4
e,622,701
e,701,702
e,702,1034
e,1034,1033
e,630,703
e,703,704
rp3,1,1
e,706,2120
e,2120,2035

! polyurethane foam elements
type,3
mat,3
real,1
e,201,301,302,202
rp22,1,1,1,1
e,224,223,323
e,301,401,402,302
rp21,1,1,1,1
e,322,422,300,323
e,300,125,224,323
e,401,501,502,402
rp21,1,1,1,1
e,333,233,232,332
e,233,333,334,234
rp17,1,1,1,1
e,331,431,432,332
rp19,1,1,1,1
e,430,530,531,431
rp20,1,1,1,1

! interface elements between the steel shells
!   and the polyurethane foam
type,5
mat,1
real,101
e,101,201
real,102
e,102,202
real,103
e,103,203
real,104
e,104,204
real,105
e,105,205
real,106
e,106,206
real,107
e,107,207
real,108
e,108,208
real,109
e,109,209
real,110
e,110,210
real,111
e,111,211
real,112
e,112,212
real,113
e,113,213
real,114
e,114,214
real,115
e,115,215
real,116
e,116,216
rp5,1,1
real,130
e,122,222
rp2,1,1
e,1003,224
real,101
e,702,300
e,701,422
e,622,522
real,150
e,706,332
e,705,331
e,704,431
e,703,430
e,630,530
real,116
e,300,702
e,422,701
e,706,332
e,705,331
e,704,431
e,703,430
e,2003,233
e,134,234
rp2,1,1
real,136
e,136,236
real,137
e,137,237
real,138
```

```
e,138,238
real,139
e,139,239
real,140
e,140,240
real,141
e,141,241
real,142
e,142,242
real,143
e,143,243
real,144
e,144,244
real,145
e,145,245
real,146
e,146,246
real,147
e,147,247
real,148
e,148,248
real,149
e,149,249
real,150
e,150,250
real,101
e,501,601
rp13,1,1
real,116
e,513,613
rp10,1,1
e,530,630
rp9,1,1
real,639
e,539,639
real,640
e,540,640
real,641
e,541,641
real,642
e,542,642
real,643
e,543,643
real,644
e,544,644
real,645
e,545,645
real,646
e,546,646
real,647
e,547,647
real,648
e,548,648
real,649
e,549,649
real,150
e,550,650

! interface elements between the lower seal flange
!   and the locking ring
type,4
mat,1
real,6
e,3038,1061
rp3,1,1

! interface elements between the upper seal flange
!   and the locking ring
type,4
mat,1
real,7
e,2056,3146
rp3,1,1

! interface elements between the lower seal flange
!   and the upper seal flange
type,5
mat,1
real,8
e,1164,2073
rp5,1,1

! couple the lower shell to the lower seal flange
type,6
mat,4
real,9
e,1001,1002
rp4,1,1

! couple the upper shell to the upper seal flange
type,6
mat,4
real,9
e,2001,2002
rp4,1,1

! springs between the lower seal flange
!   and the locking ring
type,7
mat,1
real,10
e,3038,1061
rp3,1,1

! springs between the upper seal flange
!   and the locking ring
type,7
mat,1
real,10
e,2056,3146
rp3,1,1

! springs between the lower seal flange
!   and the upper seal flange
type,7
mat,1
real,10
e,1164,2073
rp5,1,1

! displacement constraints
d,101,UX,0,,601,500,rotz
d,201,UX,0,,501,100
d,150,UX,0,,650,500,rotz
d,250,UX,0,,550,100
d,3099,UY,0
d,all,uz,0

! pressure loads
alls
pload=+(14.7-14.7)
p,101,102,pload,,122,1
p,123,1003,pload
p,1001,1006,pload,,1021,5
p,1026,1035,pload
p,1035,1041,pload
p,1041,1046,pload,,1051,5
p,1056,1065,pload,,1155,9
p,1164,1165,pload,,1167,1
p,1168,1159,pload
p,2077,2082,pload
p,2073,2074,pload,,2076,1
p,2127,2124,pload
p,2124,2073,pload
p,2125,2126,pload,,2126,1
p,2122,2125,pload
p,2071,2122,pload
p,2001,2006,pload,,2046,5
p,2051,2060,pload
p,2060,2071,pload
p,2003,134,pload
p,134,135,pload,,149,1

! delete unused nodes at seal flange interfaces
ndele,124
ndele,133

! solve the problem
fini
/solu
neqit,1000
alls
solv
fini
save

! post-process the problem
/post1
set
rsys,solu
ernorm,0
```

```
! table stress definitions for shell elements
nall
alls
esel,s,type,,2
etab,sit,nmisc,4
etab,sim,nmisc,9
etab,sib,nmisc,14

/com,
/com,
/com,
/com,++++++++++++++++++++
/com,+ lower seal flange +
/com,++++++++++++++++++++
/com,
/com,
nall
eall
nsel,s,node,,1000,1999,1
prns,prin

/com,
/com,
/com,
/com,++++++++++++++++++++
/com,+ upper seal flange +
/com,++++++++++++++++++++
/com,
/com,
nall
eall
nsel,s,node,,2000,2999,1
prns,prin

/com,
/com,
/com,
/com,+++++++++++++++++
/com,+ locking ring +
/com,+++++++++++++++++
/com,
/com,
nall
eall
nsel,s,node,,3000,3999,1
prns,prin

/com,
/com,
/com,
/com,++++++++++++++++++++++++++++++++++++++
/com,+ OCV cylindrical and conical shells +
/com,++++++++++++++++++++++++++++++++++++++
/com,
/com,
nall
eall
esel,s,elem,,324,331,1
pret

/com,
/com,
/com,
/com,++++++++++++++++++++++++++++++++++++++
/com,+ OCV torispherical head crown shells +
/com,++++++++++++++++++++++++++++++++++++++
/com,
/com,
nall
eall
esel,s,elem,,339,348,1    ! upper head
esel,a,elem,,309,318,1    ! lower head
pret

/com,
/com,
/com,
/com,++++++++++++++++++++++++++++++++++++++++++++
/com,+ OCV torispherical head knuckle shells +
/com,++++++++++++++++++++++++++++++++++++++++++++
/com,
/com,
nall
eall
esel,s,elem,,334,338,1    ! upper head
esel,a,elem,,319,323,1    ! lower head
pret

/com,
/com,
/com,
/com,++++++++++++++++++++++++++++++++++
/com,+ OCA outer shells and z-flanges +
/com,++++++++++++++++++++++++++++++++++
/com,
/com,
nall
eall
esel,s,elem,,349,399,1
pret

/com,
/com,
/com,
/com,++++++++++++++++++++++++++++++
/com,+ polyurethane foam elements +
/com,++++++++++++++++++++++++++++++
/com,
/com,
nall
eall
esel,s,elem,,415,559,1
prns,prin

! finalize ANSYS
nall
eall
save
/out,term
/eof
```

Table 2.10.1-4 – ANSYS® Input Listing for OCA Load Case 4

```
! initialize ANSYS
fini
/cle
/filename,oca_lc4,inp
/out,,txt

! start preprocessing the model
/prep7
/title, OCA Load Case 4: P=0.0/14.7 psia, T=70/70 F

! element types
et,1,42,,,1
et,2,51
et,3,42,,,1
et,4,12,,,,,,1
et,5,12,,,,,,1
et,6,3
et,7,14,,,2

! reference and uniform temperatures
tref,70
tunif,70

! material properties for non-slotted steel regions
ex,1,28.3e06
nuxy,1,.3
alpx,1,8.46e-06

! material properties for slotted steel regions
ex,2,14.15e06
ey,2,14.15e06
ez,2,1
nuxy,2,.3
nuxz,2,0
nuyz,2,0
alpx,2,8.46e-06
alpy,2,8.46e-06
alpz,2,8.46e-06

! material properties for the polyurethane foam
ex,3,4773
ey,3,6810
ez,3,4773
nuxy,3,.33
nuxz,3,.33
nuyz,3,.33
alpx,3,3.5e-5

! material properties for the rigid coupling elements
ex,4,28.3e06
nuxy,4,.3
alpx,4,8.46E-06

! element real constants
r,1,.25
r,2,.1875
r,3,.375
r,4,.075
r,5,,1e9,,1
r,6,-15,1e9,-.036
r,7,15,1e9,-.036
r,8,0,1e9,,1
r,9,1,1,1
r,10,1e2
r,101,-180.000,1e5,,1
r,102,-177.444,1e5,,1
r,103,-174.888,1e5,,1
r,104,-172.333,1e5,,1
r,105,-169.777,1e5,,1
r,106,-167.221,1e5,,1
r,107,-164.665,1e5,,1
r,108,-162.109,1e5,,1
r,109,-159.553,1e5,,1
r,110,-156.998,1e5,,1
r,111,-154.442,1e5,,1
r,112,-141.553,1e5,,1
r,113,-128.665,1e5,,1
r,114,-115.777,1e5,,1
r,115,-102.888,1e5,,1
r,116,-90.0000,1e5,,1
r,130,-102.000,1e5,,1
r,136,-77.1520,1e5,,1
r,137,-64.3041,1e5,,1
r,138,-51.4561,1e5,,1
r,139,-38.6081,1e5,,1
r,140,-25.7602,1e5,,1
r,141,-23.1841,1e5,,1
r,142,-20.6081,1e5,,1
r,143,-18.0321,1e5,,1
r,144,-15.4561,1e5,,1
r,145,-12.8801,1e5,,1
r,146,-10.3041,1e5,,1
r,147,-7.72805,1e5,,1
r,148,-5.15203,1e5,,1
r,149,-2.57602,1e5,,1
r,150,,1e5,,1
r,639,-58.7238,1e5,,1
r,640,-27.4476,1e5,,1
r,641,-24.7029,1e5,,1
r,642,-21.9581,1e5,,1
r,643,-19.2133,1e5,,1
r,644,-16.4686,1e5,,1
r,645,-13.7238,1e5,,1
r,646,-10.9790,1e5,,1
r,647,-8.23429,1e5,,1
r,648,-5.48952,1e5,,1
r,649,-2.74476,1e5,,1

! nodes for the lower seal flange
local,11,,38.24941495,50.051977923,,-12
n,1001
n,1005,.25
fill
n,1016,,.58677836
n,1020,.25,.58677836
fill
fill,1001,1016,2,1006,5,5,1
n,1026,,.896632635
local,12,,38.505,50
move,1026,11,0,999,0,12,-.065,999,0
fill,1016,1026,1,1021
local,11,1,39.12699808,50.47
n,1025,.5,148.5
n,1030,.5,129
n,1031,.5,109.5
n,1032,.5,90
csys,12
fill,1021,1025,3,1022,1,2,5
n,1033,.775,.97
n,1034,1.145,.97
n,1076,-.065,2.98
fill,1026,1076,8,1035,5
fill,1035,1076,7,1041,5
n,1060,.775,2.15593612
ngen,2,6,1033,1034,1,,.16
fill,1039,1060,3,1045,5
fill,1035,1039
fill,1041,1045,3,1042,1,4,5
n,1064,1.245,2.03
fill,1060,1064
n,1092,-.065,2.98
n,1096,.77960172,2.76
fill
n,1100,1.245,2.76
fill,1096,1100
fill,1056,1092,3,1065,9,9,1
ngen,3,9,1098,1100,1,,.26
n,1146,.14020351,4.4
fill,1092,1146,5,1101,9
n,1164,.14020351,4.98
fill,1146,1164,1,1155
local,11,,39.13520351,54.98,,-86.15
n,1168
n,1159,.3
ngen,3,-1,1159,1159,,,-.125
n,1148,.58,-.25
ngen,2,-18,1157,1159,1,.56
ngen,2,-9,1139,1141,1,.25
ngen,2,-27,1148,1148,,.81
ngen,2,-18,1130,1132,1,.56
fill,1096,1114,1,1105
csys,12
fill,1101,1105
fill,1110,1112,1,1111,,6,9
```

```
fill,1164,1168

! nodes for the upper seal flange
local,11,,38.405,52.81
n,2001,,5
n,2005,.25,5
fill
ngen,3,5,2001,2005,1,,-.25
n,2031,,3.45
n,2035,.91,3.45
fill
fill,2011,2031,3,2016,5,5,1
n,2051,,2.543442101
n,2055,.91,2.543442101
fill
fill,2031,2051,3,2036,5,4,1
n,2040,.91,3.29
fill,2040,2055,2,2045,5
n,2059,1.345,2.66
fill,2055,2059
n,2071,,2.17
n,2073,.21504507,2.17
fill
n,2077,.74504507,2.17
fill,2073,2077
fill,2051,2071,1,2060
fill,2054,2076,1,2065
fill,2060,2065
n,2081,1.345,2.17
fill,2077,2081
fill,2055,2077,1,2066,,5,1
n,2107,.85759646,.54
n,2109,1.10488343,.54
fill
n,2111,1.345,.54
fill,2109,2111
fill,2077,2107,5,2082,5,5,1
n,2117,.94488343
n,2119,1.10488343
fill
fill,2109,2119,1,2114
n,2112,.870715847,.35
fill,2112,2114
n,2120,1.345,3.45
n,2121,1.345,3.29
ngen,2,51,2071,2073,1,,-.305
ngen,2,3,2122,2124,1,,-.305

! nodes for the locking ring
local,11,,39.35,51.29
n,3001
n,3005,.435
fill
n,3009,.935
fill,3005,3009
n,3037,,.81
n,3041,.435,.693442101
fill
n,3045,.935,.693442101
fill,3041,3045
fill,3001,3037,3,3010,9,9,1
n,3145,,4.11
n,3149,.435,4.226557899
fill
n,3153,.935,4.226557899
fill,3149,3153
fill,3041,3149,11,3050,9,5,1
n,3181,,4.67
n,3185,.535,4.67
fill
n,3189,.935,4.67
fill,3185,3189
fill,3145,3181,3,3154,9,9,1

! nodes for the OCA inner shell (OCV)
local,11,1,,84.5
n,101,74.25,-90
n,111,74.25,-64.44174492
fill
local,12,1,28.3125,24.29659664
n,116,8.625
fill,111,116
csys
!n,117,36.9375,25.79659664
n,122,36.9375,43.95292590
fill,116,122
ngen,2,-879,1003,1003
fill,122,124
ngen,2,-1870,2003,2003
n,135,38.53,63.78649751
fill,133,135
local,12,1,29.905,63.78649751
n,140,8.625,64.23984399
fill,135,140
local,14,1,,1.8125
n,150,77.4375,90
fill,140,150

! nodes for the OCA outer shell
csys
n,601
n,613,47.0625
fill
n,622,47.0625,46.7775
fill,613,622
n,630,47.0625,47.6325
n,638,47.0625,75.3440689
fill,630,638
local,15,1,40.5625,75.3440689
n,640,6.5,62.55238078
fill,638,640
local,16,1,,-2.75
n,650,94.5,90
fill,640,650

! nodes for the polyurethane foam inner surface
csys
ngen,2,100,101,150,1
n,125,38.58338729,50.9
n,232,38.53,56.26

! nodes for the polyurethane foam outer surface
ngen,2,-100,601,650,1

! intermediate polyurethane foam nodes
fill,201,501,2,301,100,22,1
n,300,43.9375,50.9
n,331,41.5375,51.8825
n,332,41.5375,56.26
n,422,43.9375,46.7775
n,430,44.2375,47.6375
n,431,44.2375,51.8825
fill,222,422,1,322
fill,223,300,1,323
fill,332,532,1,432
fill,233,533,2,333,100,18,1

! nodes for the z-flanges
ngen,2,279,422,422,0
ngen,2,402,300,300,0
ngen,2,273,430,430,0
rp2,,,1,1
ngen,2,374,331,331,0
rp2,,,1,1

! elements for the lower seal flange
type,1
mat,1
real,1
e,1001,1002,1007,1006
rp4,1,1,1,1
egen,5,5,1,4,1
e,1026,1027,1036,1035
e,1027,1028,1036
e,1028,1029,1037,1036
e,1029,1030,1031,1037
e,1031,1032,1038,1037
rp3,1,1,1,1
e,1035,1036,1042,1041
rp4,1,1,1,1
e,1041,1042,1047,1046
rp4,1,1,1,1
egen,3,5,32,35,1
e,1056,1057,1066,1065
rp4,1,1,1,1
egen,4,9,44,47,1
mat,2
e,1060,1061,1070,1069
rp4,1,1,1,1
egen,4,9,60,63,1
egen,3,9,74,75,1
egen,3,9,56,59,1
```

```
egen,7,9,84,85,1
egen,3,1,99,99
egen,3,1,93,93

! elements for the upper seal flange
type,1
mat,1
real,1
e,2006,2007,2002,2001
rp4,1,1,1,1
egen,10,5,104,107,1
e,2040,2121,2120,2035
e,2060,2061,2052,2051
e,2061,2062,2052
e,2062,2063,2053,2052
e,2063,2064,2053
e,2064,2065,2054,2053
rp6,1,1,1,1
e,2071,2072,2061,2060
rp10,1,1,1,1
e,2122,2123,2072,2071
rp2,1,1,1,1
e,2125,2126,2123,2122
rp2,1,1,1,1
e,2082,2083,2078,2077
rp4,1,1,1,1
egen,6,5,169,172,1
egen,3,5,189,190,1

! elements for the locking ring
type,1
mat,2
real,1
e,3001,3002,3011,3010
rp4,1,1,1,1
egen,4,9,197,200,1
mat,1
e,3005,3006,3015,3014
rp4,1,1,1,1
egen,20,9,213,216,1
e,3145,3146,3155,3154
rp4,1,1,1,1
egen,4,9,293,296,1

! elements for the OCA inner shell (OCV)
type,2
mat,1
real,1
e,101,102
rp16,1,1
real,2
e,117,118
rp5,1,1
real,1
e,122,123
e,123,1003
e,2003,134
e,134,135
rp16,1,1

! elements for the OCA outer shell
real,1
e,601,602
rp18,1,1
real,3
e,619,620
rp3,1,1
e,630,631
rp8,1,1
real,1
e,638,639
rp12,1,1

! elements for the Z-flanges
real,4
e,622,701
e,701,702
e,702,1034
e,1034,1033
e,630,703
e,703,704
rp3,1,1
e,706,2120
e,2120,2035

! polyurethane foam elements
type,3
mat,3
real,1
e,201,301,302,202
rp22,1,1,1,1
e,224,223,323
e,301,401,402,302
rp21,1,1,1,1
e,322,422,300,323
e,300,125,224,323
e,401,501,502,402
rp21,1,1,1,1
e,333,233,232,332
e,233,333,334,234
rp17,1,1,1,1
e,331,431,432,332
rp19,1,1,1,1
e,430,530,531,431
rp20,1,1,1,1

! interface elements between the steel shells
!   and the polyurethane foam
type,5
mat,1
real,101
e,101,201
real,102
e,102,202
real,103
e,103,203
real,104
e,104,204
real,105
e,105,205
real,106
e,106,206
real,107
e,107,207
real,108
e,108,208
real,109
e,109,209
real,110
e,110,210
real,111
e,111,211
real,112
e,112,212
real,113
e,113,213
real,114
e,114,214
real,115
e,115,215
real,116
e,116,216
rp5,1,1
real,130
e,122,222
rp2,1,1
e,1003,224
real,101
e,702,300
e,701,422
e,622,522
real,150
e,706,332
e,705,331
e,704,431
e,703,430
e,630,530
real,116
e,300,702
e,422,701
e,706,332
e,705,331
e,704,431
e,703,430
e,2003,233
e,134,234
rp2,1,1
real,136
e,136,236
real,137
e,137,237
real,138
```

```
e,138,238
real,139
e,139,239
real,140
e,140,240
real,141
e,141,241
real,142
e,142,242
real,143
e,143,243
real,144
e,144,244
real,145
e,145,245
real,146
e,146,246
real,147
e,147,247
real,148
e,148,248
real,149
e,149,249
real,150
e,150,250
real,101
e,501,601
rp13,1,1
real,116
e,513,613
rp10,1,1
e,530,630
rp9,1,1
real,639
e,539,639
real,640
e,540,640
real,641
e,541,641
real,642
e,542,642
real,643
e,543,643
real,644
e,544,644
real,645
e,545,645
real,646
e,546,646
real,647
e,547,647
real,648
e,548,648
real,649
e,549,649
real,150
e,550,650

! interface elements between the lower seal flange
!   and the locking ring
type,4
mat,1
real,6
e,3038,1061
rp3,1,1

! interface elements between the upper seal flange
!   and the locking ring
type,4
mat,1
real,7
e,2056,3146
rp3,1,1

! interface elements between the lower seal flange
!   and the upper seal flange
type,5
mat,1
real,8
e,1164,2073
rp5,1,1

! couple the lower shell to the lower seal flange
type,6
mat,4
real,9
e,1001,1002
rp4,1,1

! couple the upper shell to the upper seal flange
type,6
mat,4
real,9
e,2001,2002
rp4,1,1

! springs between the lower seal flange
!   and the locking ring
type,7
mat,1
real,10
e,3038,1061
rp3,1,1

! springs between the upper seal flange
!   and the locking ring
type,7
mat,1
real,10
e,2056,3146
rp3,1,1

! springs between the lower seal flange
!   and the upper seal flange
type,7
mat,1
real,10
e,1164,2073
rp5,1,1


! displacement constraints
d,101,UX,0,,601,500,rotz
d,201,UX,0,,501,100
d,150,UX,0,,650,500,rotz
d,250,UX,0,,550,100
d,3099,UY,0
d,all,uz,0

! pressure loads
alls
pload=+(0.0-14.7)
p,101,102,pload,,122,1
p,123,1003,pload
p,1001,1006,pload,,1021,5
p,1026,1035,pload
p,1035,1041,pload
p,1041,1046,pload,,1051,5
p,1056,1065,pload,,1155,9
p,1164,1165,pload,,1167,1
p,1168,1159,pload
p,2077,2082,pload
p,2073,2074,pload,,2076,1
p,2127,2124,pload
p,2124,2073,pload
p,2125,2126,pload,,2126,1
p,2122,2125,pload
p,2071,2122,pload
p,2001,2006,pload,,2046,5
p,2051,2060,pload
p,2060,2071,pload
p,2003,134,pload
p,134,135,pload,,149,1

! delete unused nodes at seal flange interfaces
ndele,124
ndele,133

! solve the problem
fini
/solu
neqit,1000
alls
solv
fini
save

! post-process the problem
/post1
set
rsys,solu
ernorm,0
```

```
! table stress definitions for shell elements
nall
alls
esel,s,type,,2
etab,sit,nmisc,4
etab,sim,nmisc,9
etab,sib,nmisc,14

/com,
/com,
/com,
/com,++++++++++++++++++++
/com,+ lower seal flange +
/com,++++++++++++++++++++
/com,
/com,
nall
eall
nsel,s,node,,1000,1999,1
prns,prin

/com,
/com,
/com,
/com,++++++++++++++++++++
/com,+ upper seal flange +
/com,++++++++++++++++++++
/com,
/com,
nall
eall
nsel,s,node,,2000,2999,1
prns,prin

/com,
/com,
/com,
/com,+++++++++++++++++
/com,+ locking ring +
/com,+++++++++++++++++
/com,
/com,
nall
eall
nsel,s,node,,3000,3999,1
prns,prin

/com,
/com,
/com,
/com,++++++++++++++++++++++++++++++++++++
/com,+ OCV cylindrical and conical shells +
/com,++++++++++++++++++++++++++++++++++++
/com,
/com,
nall
eall
esel,s,elem,,324,331,1
pret

/com,
/com,
/com,++++++++++++++++++++++++++++++++++++
/com,+ OCV torispherical head crown shells +
/com,++++++++++++++++++++++++++++++++++++
/com,
/com,
nall
eall
esel,s,elem,,339,348,1    ! upper head
esel,a,elem,,309,318,1    ! lower head
pret

/com,
/com,
/com,
/com,++++++++++++++++++++++++++++++++++++++++
/com,+ OCV torispherical head knuckle shells +
/com,++++++++++++++++++++++++++++++++++++++++
/com,
/com,
nall
eall
esel,s,elem,,334,338,1    ! upper head
esel,a,elem,,319,323,1    ! lower head
pret

/com,
/com,
/com,
/com,++++++++++++++++++++++++++++++++++
/com,+ OCA outer shells and z-flanges +
/com,++++++++++++++++++++++++++++++++++
/com,
/com,
nall
eall
esel,s,elem,,349,399,1
pret

/com,
/com,
/com,
/com,++++++++++++++++++++++++++++++
/com,+ polyurethane foam elements +
/com,++++++++++++++++++++++++++++++
/com,
/com,
nall
eall
esel,s,elem,,415,559,1
prns,prin

! finalize ANSYS
nall
eall
save
/out,term
/eof
```

Table 2.10.1-5 – ANSYS® Input Listing for ICV Load Case 1

```
! initialize ANSYS
fini
/cle
/filename,icv_lc1,inp
/out,,txt

! start preprocessing the model
/prep7
/title, ICV Load Case 1: P=64.7/3.5 psia, T=160/160 F

! element types
et,1,42,,,1
et,2,51
et,3,12,,,,,,1
et,4,12,,,,,,1
et,5,3
et,6,14,,,2

! reference and uniform temperatures
tref,160
tunif,160

! material properties for non-slotted steel regions
ex,1,27.8e6
nuxy,1,.3
alpx,1,8.694e-6

! material properties for slotted steel regions
ex,2,13.9e6
ey,2,13.9e6
ez,2,1
nuxy,2,.3
nuyz,2,0
nuxz,2,0
alpx,2,8.694e-6
alpy,2,8.694e-6
alpz,2,8.694e-6

! material properties for the rigid coupling elements
ex,3,27.8e6
nuxy,3,.3
alpx,3,8.694e-6

! element real constants
r,1,.25
r,2,-15,1e9,-.036
r,3,15,1e9,-.036
r,4,0,1e9,-.01
r,5,1,1,1
r,10,1e2

! nodes for the lower seal ring
local,11,0,36.315,45.08954245
n,1001
n,1005,.25
fill
n,1016,,.575
n,1020,.25,.575
fill
fill,1001,1016,2,1006,5,5,1
n,1031,,1.48
n,1035,.84,1.48
fill
fill,1016,1031,2,1021,5,5,1
n,1046,,2.6759361
n,1050,.84,2.67593612
fill
fill,1031,1046,2,1036,5,5,1
n,1054,1.31,2.55
fill,1050,1054
n,1073,,3.5
n,1077,.844601720,3.28
fill
n,1079,1.095,3.28
fill,1077,1079
n,1081,1.31,3.28
fill,1079,1081
fill,1046,1073,2,1055,9,9,1
n,1127,.205,4.92
fill,1073,1127,5,1082,9
local,12,,37.01020351,50.58954246,,-86.15
n,1140,.3
n,1138,.3,-.25
fill
n,1122,.86
n,1120,.86,-.25
fill
n,1113,1.11
n,1111,1.11,-.25
fill
n,1095,1.67
n,1093,1.67,-.25
fill
csys,11
n,1145,.205,5.5
fill,1127,1145,1,1136
n,1149,.695,5.5
fill,1145,1149
fill,1120,1138,1,1129
fill,1093,1111,1,1102
fill,1077,1095,1,1086
fill,1091,1093,,,,6,9
fill,1073,1091,1,1082,,5,1
ngen,3,9,1079,1081,1,,.26

! nodes for the upper seal ring
n,2001,-.035,4.89
n,2003,.180045070,4.89
fill
n,2007,-0.035,5.5
n,2009,.180045070,5.5
fill
fill,2001,2007,1,2004,,3,1
n,2013,.710045070,5.5
fill,2009,2013
n,2017,1.31,5.5
fill,2013,2017
n,2040,-0.035,5.98
fill,2007,2040,2,2018,11
n,2035,0.875,5.873442101
fill,2029,2035
n,2039,1.31,5.99
fill,2035,2039
fill,2008,2030,1,2019,,10,1
n,2042,.245,5.98
fill,2040,2042
n,2043,.390419704,6.008925778
n,2044,.513700577,6.091299423
n,2049,.596074222,6.214580296
n,2054,.625,6.36
n,2058,.875,6.36
fill
fill,2035,2058,2,2048,5
fill,2044,2048
fill,2049,2053
ngen,5,5,2054,2058,1,,.1875
n,2104,.822596460,3.87
n,2106,1.07,3.87
fill
n,2116,1.07,3.33
fill,2106,2116,1,2111
n,2108,1.31,3.87
fill,2106,2108
fill,2013,2104,5,2079,5,5,1
n,2109,.835715950,3.68
fill,2109,2111
n,2114,.909883430,3.33
fill,2114,2116

! nodes for the locking ring
local,13,0,37.225,46.89954245
n,3001
n,3005,.435
fill
n,3008,.789412
fill,3005,3008
n,3037,,.81
n,3041,.435,.693442101
fill
n,3045,.935,.693442101
fill,3041,3045
fill,3001,3037,3,3010,9,8,1
n,3027,.935,.4
fill,3008,3027,1,3018
```

```
fill,3027,3045,1,3036
n,3101,,4.11
n,3105,.435,4.226557898
fill
n,3109,.935,4.226557899
fill,3105,3109
fill,3041,3105,11,3046,5,5,1
n,3137,,4.67
n,3141,.435,4.67
fill
n,3144,.789412,4.67
fill,3141,3144
fill,3101,3137,3,3110,9,8,1
fill,3109,3144,3,3118,9

! nodes for the lower shell
local,14,1,,73.25
n,4001,73.25,-90
n,4016,73.25,-64.50665929
fill
local,15,1,27.815,14.9171927
n,4025,8.625
fill,4016,4025
csys,0
n,4081,36.44,45.08954245
fill,4025,4081
n,4001,0,0

! nodes for the upper shell
local,16,1,,-5.75
n,5001,74.5,90
n,5016,74.5,64.42280563
fill
local,17,1,28.44,53.66954245
n,5025,8.625
fill,5016,5025
csys,0
n,5027,37.065,52.16954245
fill,5025,5027
n,5001,0,68.75

! elements for the lower seal ring
type,1
mat,1
real,1
e,1001,1002,1007,1006
rp4,1,1,1,1
egen,9,5,1,4,1
e,1046,1047,1056,1055
rp4,1,1,1,1
egen,5,9,37,40,1
egen,7,9,53,54,1
egen,3,27,55,56,1
mat,2
e,1050,1051,1060,1059
rp4,1,1,1,1
egen,3,9,73,76,1
egen,3,9,83,84,1

! elements for the upper seal ring
type,1
mat,1
real,1
e,2001,2002,2005,2004
rp2,1,1,1,1
egen,2,3,89,90,1
e,2007,2008,2019,2018
rp10,1,1,1,1
egen,2,11,93,102,1
egen,2,11,103,107,1
e,2046,2045,2034
rp2,1,1,0
e,2034,2035,2048,2047
e,2044,2045,2050,2049
rp4,1,1,1,1
egen,6,5,121,124,1
e,2079,2080,2014,2013
rp4,1,1,1,1
e,2084,2085,2080,2079
rp4,1,1,1,1
egen,5,5,149,152,1
egen,3,5,165,166,1

! elements for the locking ring
type,1
mat,2
real,1
e,3001,3002,3011,3010
rp4,1,1,1,1
egen,4,9,173,176,1
mat,1
e,3005,3006,3015,3014
rp3,1,1,1,1
e,3018,3017,3008
e,3014,3015,3024,3023
rp4,1,1,1,1
egen,3,9,193,196,1
e,3041,3042,3047,3046
rp4,1,1,1,1
egen,11,5,205,208,1
e,3096,3097,3106,3105
rp4,1,1,1,1
e,3101,3102,3111,3110
rp8,1,1,1,1
egen,4,9,253,259,1
e,3117,3118,3127,3126
e,3126,3127,3136,3135
e,3135,3136,3144,3144

! elements for the lower shell
type,2
mat,1
real,1
e,4001,4002
rp79,1,1
e,4080,1003

! elements for the upper shell
type,2
mat,1
real,1
e,2076,5026
e,5026,5025
rp25,-1,-1

! interface elements between the lower seal flange
!   and the locking ring
type,3
mat,1
real,2
e,3038,1051
rp3,1,1

! interface elements between the upper seal flange
!   and the locking ring
type,3
mat,1
real,3
e,2036,3102
rp3,1,1

! interface elements between the lower seal flange
!   and the upper seal flange
type,4
mat,1
real,4
e,1145,2009
rp5,1,1

! couple the lower shell to the lower seal flange
type,5
mat,3
real,5
e,1001,1002
rp4,1,1

! couple the upper shell to the upper seal flange
type,5
mat,3
real,5
e,2074,2075
rp4,1,1

! springs between the lower seal flange
!   and the locking ring
type,6
mat,1
real,10
e,3038,1051
rp3,1,1

! springs between the upper seal flange
```

```
!   and the locking ring
type,6
mat,1
real,10
e,2036,3102
rp3,1,1

! springs between the lower seal flange
!   and the upper seal flange
type,6
mat,1
real,10
e,1145,2009
rp5,1,1

! displacement constraints
d,4001,ux,0,,5001,1000,rotz
d,3075,uy,0

! pressure loads
pload=+(64.7-3.5)
alls
p,4001,4002,pload,,4079,1
p,4080,1003,pload
p,1001,1006,pload,,1041,5
p,1046,1055,pload,,1136,9
p,1145,1146,pload,,1148,9
p,1140,1149,pload
p,2001,2002,pload,,2002,1
p,2003,2006,pload,,2006,3
p,2009,2010,pload,,2012,1
p,2013,2079,pload
p,2001,2004,pload,,2004,3
p,2007,2018,pload,,2029,11
p,2040,2041,pload,,2043,1
p,2044,2049,pload,,2069,5
p,5001,5002,pload,,5025,1
p,5026,2076,pload

! solve the problem
fini
/solu
neqit,1000
alls
solv
fini
save

! post-process the problem
/post1
set
rsys,solu
ernorm,0

! table stress definitions for shell elements
nall
alls
esel,s,type,,2
etab,sit,nmisc,4
etab,sim,nmisc,9
etab,sib,nmisc,14

/com,
/com,
/com,
/com,++++++++++++++++++++
/com,+ lower seal flange +
/com,++++++++++++++++++++
/com,
/com,
nall
eall
nsel,s,node,,1000,1999,1
esln
prns,prin

/com,
/com,
/com,
/com,++++++++++++++++++++
/com,+ upper seal flange +
/com,++++++++++++++++++++
/com,
/com,
nall
eall
nsel,s,node,,2000,2999,1
esln
prns,prin

/com,
/com,
/com,
/com,+++++++++++++++++
/com,+ locking ring +
/com,+++++++++++++++++
/com,
/com,
nall
eall
nsel,s,node,,3000,3999,1
esln
prns,prin

/com,
/com,
/com,
/com,++++++++++++++++++++++
/com,+ cylindrical shells +
/com,++++++++++++++++++++++
/com,
/com,
esel,s,elem,,309,366,1
pret

/com,
/com,
/com,
/com,++++++++++++++++++++++++++++++++++
/com,+ torispherical head crown shells +
/com,++++++++++++++++++++++++++++++++++
/com,
/com,
esel,s,elem,,376,390,1    ! upper head
esel,a,elem,,285,299,1    ! lower head
pret

/com,
/com,
/com,
/com,++++++++++++++++++++++++++++++++++++
/com,+ torispherical head knuckle shells +
/com,++++++++++++++++++++++++++++++++++++
/com,
/com,
esel,s,elem,,367,375,1    ! upper head
esel,a,elem,,300,308,1    ! lower head
pret

! finalize ANSYS
nall
eall
save
/out,term
/eof
```

Table 2.10.1-6 – ANSYS® Input Listing for ICV Load Case 2

```
! initialize ANSYS
fini
/cle
/filename,icv_lc2,inp
/out,,txt

! start preprocessing the model
/prep7
/title, ICV Load Case 2: P=0.0/14.7 psia, T=70/70 F

! element types
et,1,42,,,1
et,2,51
et,3,12,,,,,,1
et,4,12,,,,,,1
et,5,3
et,6,14,,,2

! reference and uniform temperatures
tref,70
tunif,70

! material properties for non-slotted steel regions
ex,1,28.3e6
nuxy,1,.3
alpx,1,8.46e-6

! material properties for slotted steel regions
ex,2,14.15e6
ey,2,14.15e6
ez,2,1
nuxy,2,.3
nuyz,2,0
nuxz,2,0
alpx,2,8.46e-6
alpy,2,8.46e-6
alpz,2,8.46e-6

! material properties for the rigid coupling elements
ex,3,28.3e6
nuxy,3,.3
alpx,3,8.46e-6

! element real constants
r,1,.25
r,2,-15,1e9,-.036
r,3,15,1e9,-.036
r,4,0,1e9,-.01
r,5,1,1,1
r,10,1e2

! nodes for the lower seal ring
local,11,0,36.315,45.08954245
n,1001
n,1005,.25
fill
n,1016,,.575
n,1020,.25,.575
fill
fill,1001,1016,2,1006,5,5,1
n,1031,,1.48
n,1035,.84,1.48
fill
fill,1016,1031,2,1021,5,5,1
n,1046,,2.6759361
n,1050,.84,2.67593612
fill
fill,1031,1046,2,1036,5,5,1
n,1054,1.31,2.55
fill,1050,1054
n,1073,,3.5
n,1077,.844601720,3.28
fill
n,1079,1.095,3.28
fill,1077,1079
n,1081,1.31,3.28
fill,1079,1081
fill,1046,1073,2,1055,9,9,1
n,1127,.205,4.92
fill,1073,1127,5,1082,9
local,12,,37.01020351,50.58954246,,-86.15
n,1140,.3
n,1138,.3,-.25
fill
n,1122,.86
n,1120,.86,-.25
fill
n,1113,1.11
n,1111,1.11,-.25
fill
n,1095,1.67
n,1093,1.67,-.25
fill
csys,11
n,1145,.205,5.5
fill,1127,1145,1,1136
n,1149,.695,5.5
fill,1145,1149
fill,1120,1138,1,1129
fill,1093,1111,1,1102
fill,1077,1095,1,1086
fill,1091,1093,,,,6,9
fill,1073,1091,1,1082,,5,1
ngen,3,9,1079,1081,1,,.26

! nodes for the upper seal ring
n,2001,-.035,4.89
n,2003,.180045070,4.89
fill
n,2007,-0.035,5.5
n,2009,.180045070,5.5
fill
fill,2001,2007,1,2004,,3,1
n,2013,.710045070,5.5
fill,2009,2013
n,2017,1.31,5.5
fill,2013,2017
n,2040,-0.035,5.98
fill,2007,2040,2,2018,11
n,2035,0.875,5.873442101
fill,2029,2035
n,2039,1.31,5.99
fill,2035,2039
fill,2008,2030,1,2019,,10,1
n,2042,.245,5.98
fill,2040,2042
n,2043,.390419704,6.008925778
n,2044,.513700577,6.091299423
n,2049,.596074222,6.214580296
n,2054,.625,6.36
n,2058,.875,6.36
fill
fill,2035,2058,2,2048,5
fill,2044,2048
fill,2049,2053
ngen,5,5,2054,2058,1,,.1875
n,2104,.822596460,3.87
n,2106,1.07,3.87
fill
n,2116,1.07,3.33
fill,2106,2116,1,2111
n,2108,1.31,3.87
fill,2106,2108
fill,2013,2104,5,2079,5,5,1
n,2109,.835715950,3.68
fill,2109,2111
n,2114,.909883430,3.33
fill,2114,2116

! nodes for the locking ring
local,13,0,37.225,46.89954245
n,3001
n,3005,.435
fill
n,3008,.789412
fill,3005,3008
n,3037,,.81
n,3041,.435,.693442101
fill
n,3045,.935,.693442101
fill,3041,3045
fill,3001,3037,3,3010,9,8,1
n,3027,.935,.4
fill,3008,3027,1,3018
```

```
fill,3027,3045,1,3036
n,3101,,4.11
n,3105,.435,4.226557898
fill
n,3109,.935,4.226557899
fill,3105,3109
fill,3041,3105,11,3046,5,5,1
n,3137,,4.67
n,3141,.435,4.67
fill
n,3144,.789412,4.67
fill,3141,3144
fill,3101,3137,3,3110,9,8,1
fill,3109,3144,3,3118,9

! nodes for the lower shell
local,14,1,,73.25
n,4001,73.25,-90
n,4016,73.25,-64.50665929
fill
local,15,1,27.815,14.9171927
n,4025,8.625
fill,4016,4025
csys,0
n,4081,36.44,45.08954245
fill,4025,4081
n,4001,0,0

! nodes for the upper shell
local,16,1,,-5.75
n,5001,74.5,90
n,5016,74.5,64.42280563
fill
local,17,1,28.44,53.66954245
n,5025,8.625
fill,5016,5025
csys,0
n,5027,37.065,52.16954245
fill,5025,5027
n,5001,0,68.75

! elements for the lower seal ring
type,1
mat,1
real,1
e,1001,1002,1007,1006
rp4,1,1,1,1
egen,9,5,1,4,1
e,1046,1047,1056,1055
rp4,1,1,1,1
egen,5,9,37,40,1
egen,7,9,53,54,1
egen,3,27,55,56,1
mat,2
e,1050,1051,1060,1059
rp4,1,1,1,1
egen,3,9,73,76,1
egen,3,9,83,84,1

! elements for the upper seal ring
type,1
mat,1
real,1
e,2001,2002,2005,2004
rp2,1,1,1,1
egen,2,3,89,90,1
e,2007,2008,2019,2018
rp10,1,1,1,1
egen,2,11,93,102,1
egen,2,11,103,107,1
e,2046,2045,2034
rp2,1,1,0
e,2034,2035,2048,2047
e,2044,2045,2050,2049
rp4,1,1,1,1
egen,6,5,121,124,1
e,2079,2080,2014,2013
rp4,1,1,1,1
e,2084,2085,2080,2079
rp4,1,1,1,1
egen,5,5,149,152,1
egen,3,5,165,166,1

! elements for the locking ring
type,1
mat,2
real,1
e,3001,3002,3011,3010
rp4,1,1,1,1
egen,4,9,173,176,1
mat,1
e,3005,3006,3015,3014
rp3,1,1,1,1
e,3018,3017,3008
e,3014,3015,3024,3023
rp4,1,1,1,1
egen,3,9,193,196,1
e,3041,3042,3047,3046
rp4,1,1,1,1
egen,11,5,205,208,1
e,3096,3097,3106,3105
rp4,1,1,1,1
e,3101,3102,3111,3110
rp8,1,1,1,1
egen,4,9,253,259,1
e,3117,3118,3127,3126
e,3126,3127,3136,3135
e,3135,3136,3144,3144

! elements for the lower shell
type,2
mat,1
real,1
e,4001,4002
rp79,1,1
e,4080,1003

! elements for the upper shell
type,2
mat,1
real,1
e,2076,5026
e,5026,5025
rp25,-1,-1

! interface elements between the lower seal flange
!   and the locking ring
type,3
mat,1
real,2
e,3038,1051
rp3,1,1

! interface elements between the upper seal flange
!   and the locking ring
type,3
mat,1
real,3
e,2036,3102
rp3,1,1

! interface elements between the lower seal flange
!   and the upper seal flange
type,4
mat,1
real,4
e,1145,2009
rp5,1,1

! couple the lower shell to the lower seal flange
type,5
mat,3
real,5
e,1001,1002
rp4,1,1

! couple the upper shell to the upper seal flange
type,5
mat,3
real,5
e,2074,2075
rp4,1,1

! springs between the lower seal flange
!   and the locking ring
type,6
mat,1
real,10
e,3038,1051
rp3,1,1

! springs between the upper seal flange
```

```
!   and the locking ring
type,6
mat,1
real,10
e,2036,3102
rp3,1,1

! springs between the lower seal flange
!   and the upper seal flange
type,6
mat,1
real,10
e,1145,2009
rp5,1,1

! displacement constraints
d,4001,ux,0,,5001,1000,rotz
d,3075,uy,0

! pressure loads
pload=+(0.0-14.7)
alls
p,4001,4002,pload,,4079,1
p,4080,1003,pload
p,1001,1006,pload,,1041,5
p,1046,1055,pload,,1136,9
p,1145,1146,pload,,1148,9
p,1140,1149,pload
p,2001,2002,pload,,2002,1
p,2003,2006,pload,,2006,3
p,2009,2010,pload,,2012,1
p,2013,2079,pload
p,2001,2004,pload,,2004,3
p,2007,2018,pload,,2029,11
p,2040,2041,pload,,2043,1
p,2044,2049,pload,,2069,5
p,5001,5002,pload,,5025,1
p,5026,2076,pload

! solve the problem
fini
/solu
neqit,1000
alls
solv
fini
save

! post-process the problem
/post1
set
rsys,solu
ernorm,0

! table stress definitions for shell elements
nall
alls
esel,s,type,,2
etab,sit,nmisc,4
etab,sim,nmisc,9
etab,sib,nmisc,14

/com,
/com,
/com,
/com,++++++++++++++++++++
/com,+ lower seal flange +
/com,++++++++++++++++++++
/com,
/com,
nall
eall
nsel,s,node,,1000,1999,1
esln
prns,prin

/com,
/com,
/com,
/com,++++++++++++++++++++
/com,+ upper seal flange +
/com,++++++++++++++++++++
/com,
/com,
nall
eall
nsel,s,node,,2000,2999,1
esln
prns,prin

/com,
/com,
/com,
/com,+++++++++++++++++
/com,+ locking ring +
/com,+++++++++++++++++
/com,
/com,
nall
eall
nsel,s,node,,3000,3999,1
esln
prns,prin

/com,
/com,
/com,
/com,++++++++++++++++++++++
/com,+ cylindrical shells +
/com,++++++++++++++++++++++
/com,
/com,
esel,s,elem,,309,366,1
pret

/com,
/com,
/com,
/com,++++++++++++++++++++++++++++++++++
/com,+ torispherical head crown shells +
/com,++++++++++++++++++++++++++++++++++
/com,
/com,
esel,s,elem,,376,390,1    ! upper head
esel,a,elem,,285,299,1    ! lower head
pret

/com,
/com,
/com,
/com,++++++++++++++++++++++++++++++++++++++
/com,+ torispherical head knuckle shells +
/com,++++++++++++++++++++++++++++++++++++++
/com,
/com,
esel,s,elem,,367,375,1    ! upper head
esel,a,elem,,300,308,1    ! lower head
pret

! finalize ANSYS
nall
eall
save
/out,term
/eof
```

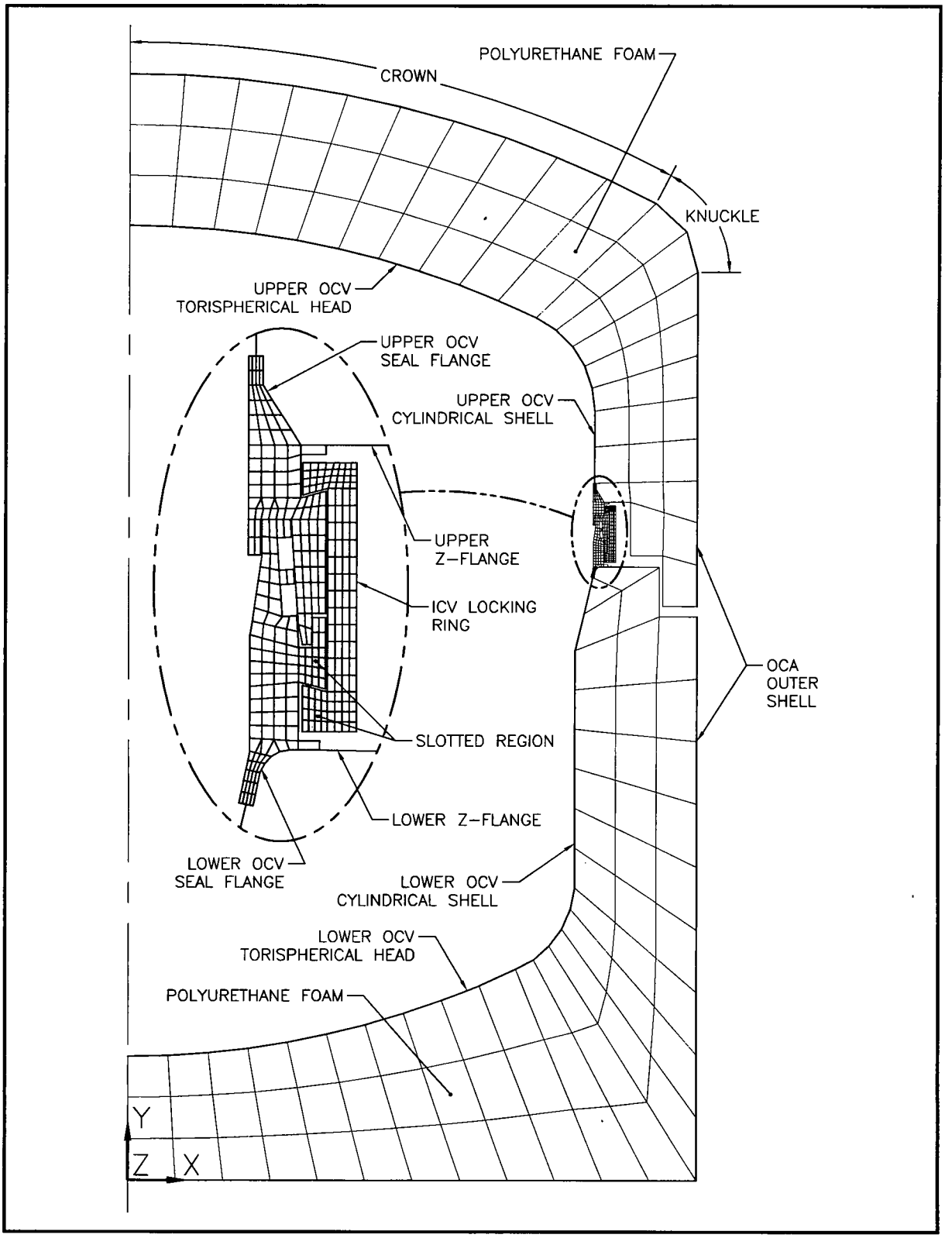

Figure 2.10.1-1 – OCA FEA Model Element Plot

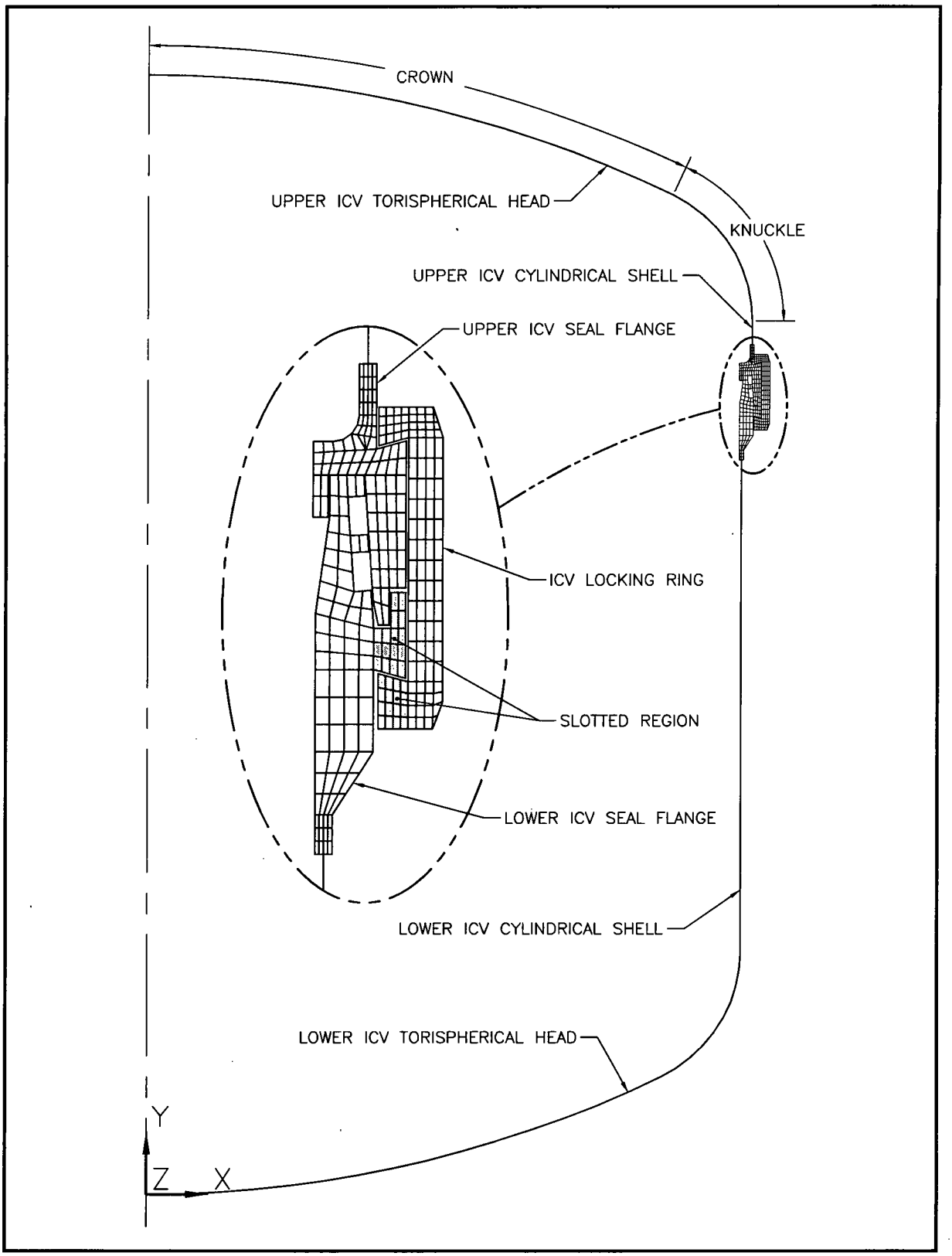

Figure 2.10.1-2 – ICV FEA Model Element Plot

2.10.2 Elastomer O-ring Seal Performance Tests

2.10.2.1 Introduction

Each containment O-ring seal material formulation shall be initially qualified for use in the HalfPACT packaging through the application of performance tests that demonstrate the material's ability to achieve and maintain a leaktight[1] seal at or beyond extremes for temperature, duration, minimum seal compression, and maximum seal compression change in a prototypical test fixture. The basis for formulation qualification test conditions applicable to the HalfPACT packaging is provided in Section 2.10.2.2, *Limits of O-ring Seal Compression and Temperature*. Section 2.10.2.3, *Formulation Qualification Test Fixture and Procedure*, defines the test fixture and test procedure for O-ring seal material qualification tests. Section 2.10.2.4, *Rainier Rubber R0405-70 Formulation Qualification Test Results,* summarizes the results of qualification testing successfully performed on Rainier Rubber[2] butyl rubber compound R0405-70.

Each batch of containment O-ring seal material shall additionally be required to satisfy the requirements of ASTM D2000[3] M4AA710 A13 B13 F17 F48 Z Trace Element. Section 2.10.2.5, *ASTM D2000 Standardized Batch Material Tests*, summarizes the industry standardized batch tests and correlates the ASTM D2000 designator to specific O-ring performance characteristics.

Additional information regarding past containment O-ring seal testing is presented in the report *Design Development and Certification Testing of the TRUPACT-II Package*[4].

2.10.2.2 Limits of O-ring Seal Compression and Temperature

2.10.2.2.1 Inner Containment Vessel Containment O-ring Seal Compression

The inner containment vessel (ICV) closure seal configuration consists of two O-ring seals, each located on a slightly different diameter in the ICV lid due to the tapered bore (see Appendix 1.3.1, *Packaging General Arrangement Drawings*, Sheets 5 and 6 of 12, for dimensional details). The upper O-ring seal is defined as the containment boundary, and the lower O-ring seal provides an annulus in which to establish a vacuum for leak testing.

In order to determine the minimum compression that may occur for the ICV containment O-ring seal, the worst-case tolerance stack-up on the lid flange, body flange, locking ring, and O-ring seal dimensions are utilized with the upper and lower seal flanges offset relative to each other. Figure 2.10.2-1 depicts the O-ring seal flange geometry for minimum ICV containment O-ring seal compression (note the reference datum for calculations).

---

[1] Leaktight is defined as leakage of 1×10^{-7} standard cubic centimeters per second (scc/sec), air, or less, per Section 5.4(3), *Reference Air Leakage Rate*, of ANSI N14.5-1997, *American National Standard for Radioactive Materials – Leakage Tests on Packages for Shipment,* American National Standards Institute, Inc. (ANSI).

[2] Rainier Rubber Company, Seattle, WA.

[3] ASTM D2000-08, *Standard Classification System for Rubber Products in Automotive Applications,* American Society for Testing and Materials, Philadelphia, PA, Volume 09.02, 2008.

[4] S. A. Porter, et al, *Design Development and Certification Testing of the TRUPACT-II Package*, 016-03-09, Portemus Engineering, Inc., Puyallup, Washington.

With reference to Figure 2.10.2-1, the following dimensions define the worst-case configuration for determining the minimum ICV containment O-ring seal compression:

a = 0.153 inches (maximum vertical gap; see Section 8.2.3.3.2.3, *Axial Play*)

b = 0.493 inches (minimum tab width; see Section 8.2.3.3.2.2, *Tab Widths*)

c = 0.561 inches (maximum groove width; see Section 8.2.3.3.2.1, *Groove Widths*)

d_L = 0.251 inches (maximum vertical offset (gage depth); see Figure 8.2-4)

d_U = 0.249 inches (minimum vertical offset (ball diameter); see Figure 8.2-1)

e = 0.330 inches (maximum seal groove offset; based on 0.300 ± 0.030)

f = 0.000 inches (minimum horizontal gap between upper and lower seal flange; closed)

r = 0.125 inches (nominal lower seal flange tab edge radius)

h = 0.253 inches (maximum O-ring seal groove depth; based on 0.250 ± 0.003)

w = 0.563 inches (maximum O-ring seal groove width; based on 0.560 ± 0.003)

α = 3.60° (minimum lower flange tab angle; based on 3.85° ± 0.25°)

β = 4.20° (maximum upper flange seal surface angle; based on 3.95° ± 0.25°)

θ = 3.60° (contact surfaces angle based on the average of angles α and β)

γ = 5.00° (maximum O-ring seal groove angle; based on 0° – 5°)

1. Worst-Case Location for the Center-Bottom of the O-ring Seal Groove

With reference to Figure 2.10.2-1, the worst-case location for the center-bottom of the O-ring seal groove is determined by finding the horizontal and vertical distance from the datum to the O-ring seal contact point on the lower seal flange, x_i and y_i, respectively:

$$x_i = f + b + \left[\left(e - \frac{d_L}{\cos(\alpha)}\right) + (h)\tan(\gamma) + \frac{w}{2}\right]\sin(\alpha) - (h)\cos(\alpha) = 0.264494 \text{ inches}$$

$$y_i = a + d_L + \left[\left(e - \frac{d_L}{\cos(\alpha)}\right) + (h)\tan(\gamma) + \frac{w}{2}\right]\cos(\alpha) + (h)\sin(\alpha) = 0.801270 \text{ inches}$$

2. Worst-Case Location for O-ring Seal Contact on the Upper Flange Sealing Surface

With reference to Figure 2.10.2-1, the worst-case location for O-ring seal contact on the upper seal flange sealing surface is determined by finding the horizontal and vertical distance from the datum to the O-ring seal contact point on the upper seal flange, x_o and y_o, respectively:

$$x_o = \frac{y_i + (x_i)\tan(\theta) + \frac{c}{\tan(\beta)} - d_U}{\frac{1}{\tan(\beta)} + \tan(\theta)} = 0.599877 \text{ inches}$$

$$y_o = d_U + \frac{x_o - c}{\tan(\beta)} = 0.778404 \text{ inches}$$

3. Maximum O-ring Seal Groove-to-Contact Surface Gap

The maximum O-ring seal groove-to-contact surface gap is determined by using the distance formula in two-dimensional Cartesian space:

$$g = \sqrt{(x_o - x_i)^2 + (y_o - y_i)^2} = 0.336162 \text{ inches}$$

4. Minimum O-ring Seal Cross-Sectional Diameter Due to Stretch

The minimum reduced O-ring seal cross-sectional diameter, d_{csr}, is determined by finding the maximum ICV containment O-ring seal groove diameter, D_g, calculating the O-ring seal stretch, s, and calculating the corresponding maximum reduction in O-ring seal cross-sectional diameter, r_{cs}, using worst-case dimensions.

Given a maximum lower seal flange control diameter, $D_L = 74.185$ inches (based on 74.155 ± 0.030), and a minimum lower seal flange control height, $H_L = 0.970$ inches (based on 1.000 ± 0.030), the maximum ICV containment O-ring seal groove diameter, D_g, is:

$$D_g = D_L - 2\left\{\left[H_L - \left(e + (h)\tan(\gamma) + \frac{w}{2}\right)\cos(\alpha)\right]\tan(\alpha) - (h)\cos(\alpha)\right\} = 73.637517 \text{ inches}$$

Given a minimum ICV containment O-ring seal inside diameter, $D_i = 70.070$ inches (based on $71.500 \pm 2\%$), the maximum ICV containment O-ring stretch, s, is

$$s = \frac{D_g - D_i}{D_i} = 5.09\%$$

The maximum reduction in O-ring seal cross-sectional diameter, r_{cs}, due to stretch (from Figure 3-3 of the *Parker O-ring Handbook*[5]) is calculated with the stretch, $s = 5.09$:

$$r_{cs} = 0.56 + 0.59s - 0.0046s^2 = 3.44\%$$

Given a minimum ICV containment O-ring seal cross-sectional diameter, $d_s = 0.390$ inches (based on 0.400 ± 0.010), the resulting reduced O-ring seal cross-sectional diameter, d_{csr}, is:

$$d_{csr} = d_s(1 - r_{cs}) = 0.376584 \text{ inches}$$

5. Minimum O-ring Seal Compression with an Offset Lid

The minimum ICV containment O-ring seal compression, ξ, is:

$$\xi = \frac{d_{csr} - g}{d_{csr}} = 10.73\%$$

The minimum O-ring seal compression is 10.73% with an offset lid. This is the worst case possible as a result of the HAC free drop.

[5] ORD 5700, *Parker O-ring Handbook*, 2007, Parker Hannifin Corporation, Cleveland, OH.

6. Minimum O-ring Seal Compression with a Centered Lid

With reference to Figure 2.10.2-1, the "centered" position for the lower seal flange relative to the upper seal flange occurs when point ① on the lower seal flange is moved to the midpoint between points ① and ②. Calculate the x-locations for points ① and ②:

$$x_1 = b - (d_L - r[1 - \sin(\alpha)])\tan(\alpha) = 0.484579 \text{ inches}$$

$$x_2 = c + (a + r[1 - \sin(\alpha)] - d_U)\tan(\beta) = 0.562553 \text{ inches}$$

Half the difference between the x_1 and x_2 values centers the lower seal flange tab within the upper seal flange groove (i.e., the ICV lid is centered in the ICV body). The "centered" horizontal offset, f_c, is:

$$f_c = \frac{x_1 - x_2}{2} = 0.038987 \text{ inches}$$

Recalculate the O-ring seal gap, g_c, based on the lid centered relative to the body:

$$x_{ci} = f_c + b + \left[\left(e - \frac{d_L}{\cos(\alpha)}\right) + (h)\tan(\gamma) + \frac{w}{2}\right]\sin(\alpha) - (h)\cos(\alpha) = 0.303481 \text{ inches}$$

$$y_{ci} = a + d_L + \left[\left(e - \frac{d_L}{\cos(\alpha)}\right) + (h)\tan(\gamma) + \frac{w}{2}\right]\cos(\alpha) + (h)\sin(\alpha) = 0.801270 \text{ inches}$$

$$x_{co} = \frac{y_{ci} + (x_{ci})\tan(\theta) + \frac{c}{\tan(\beta)} - d_U}{\frac{1}{\tan(\beta)} + \tan(\theta)} = 0.6000071 \text{ inches}$$

$$y_{co} = d_U + \frac{x_{co} - c}{\tan(\beta)} = 0.781046 \text{ inches}$$

$$g_c = \sqrt{(x_{co} - x_{ci})^2 + (y_{co} - y_{ci})^2} = 0.297279 \text{ inches}$$

Knowing that the ICV containment O-ring seal groove diameter, D_g, and correspondingly the O-ring seal stretch, s, and the reduced O-ring seal cross-sectional diameter, d_{csr}, are the same, the minimum ICV containment O-ring seal compression, ξ_c:

$$\xi_c = \frac{d_{csr} - g_c}{d_{csr}} = 21.06\%$$

The minimum O-ring seal compression is 21.06% with a centered lid. This is the normal, as-installed configuration, since the presence of the O-ring seal will inherently self-center the lid.

7. Maximum Change in O-ring Seal Compression from a Centered Lid to an Offset Lid

The maximum resulting change in compression, Δ, resulting in a minimally compressed ICV containment O-ring seal is:

$$\Delta = \xi_c - \xi = 10.33\%$$

This is the maximum change in compression of the O-ring seal as a result of the HAC free drop.

2.10.2.2.2 Containment O-ring Seal Qualification Temperature

Per Section 3.4.3, *Minimum Temperatures*, the minimum ICV containment O-ring seal temperature is -40 °F for normal conditions of transport (NCT) and -20 °F for hypothetical accident conditions (HAC). Per Table 3.4-1 in Section 3.4.2, *Maximum Temperatures*, the maximum ICV O-ring seal temperature for NCT is 150 °F. The duration of O-ring seal material exposure to elevated temperatures under NCT can conservatively be assumed as one year based on the replacement frequency of the O-ring seals. Per Section 3.5.3, *Package Temperatures*, the maximum ICV O-ring seal temperature for HAC is projected to be 290 °F. Time-history temperature data was not acquired during certification testing of the HalfPACT package. Based on their similarity, the time-history of the TRUPACT-II package OCV O-ring seal temperatures provided in Figure 3.5-6 for Certification Test Unit 1 (CTU-1) and Figure 3.5-10 for Certification Test Unit 2 (CTU-2) from the TRUPACT-II SAR[6] may be used. The duration of ICV O-ring seal material exposure to elevated temperatures within 90% of the reported 290 °F maximum is conservatively estimated to be less than 12 hours.

An Arrhenius correlation for butyl material with an activation energy of 80 kJ/mol for butyl rubber has been developed to account for diffusion limited oxidation effects.[7] Use of the Arrhenius correlation allows the effects of both NCT and HAC elevated temperature/duration conditions identified above to be conservatively enveloped by a single, 360 °F, 8-hour test.

Based on the above evaluations, the minimum O-ring seal qualification test parameters required for initial formulation testing of ICV containment O-ring seal materials is summarized in Table 2.10.2-1.

[6] U.S. Department of Energy (DOE), *Safety Analysis Report for the TRUPACT-II Shipping Package*, USNRC Certificate of Compliance 71-9218, U.S. Department of Energy, Carlsbad Field Office, Carlsbad, New Mexico.

[7] K. T. Gillen, C. Mathias, and M. R. Keenan, *Methods for Predicting More Confident Lifetimes of Seals in Air Environments*, SAND99-0553J, Sandia National Laboratories, March 1999.

Table 2.10.2-1 – Formulation Qualification Test O-ring Seal Compression Parameters

Simulated Condition	Required Compression (%)	Required Compression Change (%)	Required Temperature (°F)	Required Temperature Duration (hours)
NCT Cold	≤21.06	N/A	≤-40	N/A
HAC Free Drop	≤10.73	≥10.33	≤-20	N/A
HAC Fire		N/A	≥360	≥8

2.10.2.3 Formulation Qualification Test Fixture and Procedure

A bore-type test fixture shall be used to test the containment O-ring seal, representative of the bore seal configuration of the HalfPACT packaging. The fixture shall include an inner disk containing two, side-by-side O-ring seal grooves. An O-ring seal of prototypic cross-section for the ICV and butyl material, as delineated on the drawings in Appendix 1.3.1, *Packaging General Arrangement Drawings*, shall be placed into each seal groove, and the assembly then placed within a mating bore component. The test fixture shall employ jacking screws or equivalent devices to displace the disk radially relative to the bore, affecting the required O-ring compression on one side of the test fixture. Figure 2.10.2-2 conceptually illustrates the O-ring seal test fixture.

The sizes of all sealing components and O-ring seals utilized in the test fixture, including the amount of O-ring seal stretch, may be adjusted along with the amount of radial displacement to ensure that the parameters in Table 2.10.2-1 can be achieved. The test fixture's overall diameter may be reduced relative to a full-scale HalfPACT package to achieve a practical size for testing. A reduction in relative diameter is acceptable since the O-ring seal compression, compression change, and temperature are the parameters of primary importance relative to evaluating an O-ring material's ability to maintain a leaktight seal.

All test specimens may be coated lightly with vacuum grease prior to installation into the test fixture. The fully assembled test fixture shall be placed within an environmental test chamber for both heating and cooling with thermocouples attached to the fixture used to confirm the O-ring seal temperature.

The region between the two O-ring seals constitutes a test volume. To perform a leak test, the test volume shall be connected to a helium mass spectrometer leak detector, then evacuated to an appropriate level of vacuum and the outside of the test fixture surrounded with a contained and highly concentrated environment of helium gas, consistent with the guidelines of Appendix A, Section A.5.3, *Gas Filled Envelope – Gas Detector*, of ANSI N14.5[8]. An O-ring seal test shall be successful if the leakage between the seals is 1×10^{-7} standard cubic centimeters per second (scc/sec), air, or less (i.e., "leaktight").

[8] ANSI N14.5-1997, *American National Standard for Radioactive Materials – Leakage Tests on Packages for Shipment*, American National Standards Institute, Inc. (ANSI).

Test conditions shall be selected to simulate temperature/duration and minimum compression for the prototypic O-ring seals under NCT and HAC conditions. Each set of two test O-ring seals shall be subjected to an initial test at NCT Cold conditions with the inner disk offset as necessary to achieve the NCT required compression, to a second test at HAC Free Drop conditions with the inner disk initially positioned and then radially offset as necessary to achieve the HAC required compression and compression change magnitudes, to a third test at HAC Fire conditions after the required soak duration with the inner disk remaining offset, and to a fourth test at HAC Cold conditions with the inner disk remaining offset (see Table 2.10.2-1).

Helium leakage rate tests shall be performed at each cold temperature test configuration, either at -40 °F for the NCT Cold condition case, or at -20 °F for all other cases. Helium leakage rate testing is not practical at hot condition temperatures due to the rapid permeation and saturation of helium gas through the elastomeric material at high temperatures; a fully saturated O-ring seal test specimen results in a measured leakage in excess of 1×10^{-7} scc/sec, air. In lieu of leakage rate testing at the hot temperature test configuration, the ability to establish a rapid, hard vacuum between the O-ring seals shall be used as the basis for acceptance at elevated temperatures, with leaktightness proven subsequent to the elevated temperature phase by the final leakage rate test at -20 °F. The duration of each of the cold temperature phases of the test shall be defined by the time required to achieve the requisite cold temperatures whereas the duration of the hot phase shall be defined by the required elevated temperature and associated temperature duration given in Table 2.10.2-1.

2.10.2.3.1 Formulation Qualification Test Procedure

The process of formulation qualification leak testing O-ring seal material is given below.

1. Assemble the test fixture with two test O-ring seals.
2. Radially shift the disk inside the bore to establish reduced O-ring seal compression on one side of the test fixture, ensuring the NCT Cold compression requirements are met per Table 2.10.2-1.
3. Cool the test fixture to ≤-40 °F, continuing to restrain the disk in the NCT offset position relative to the bore.
4. Perform a helium leakage rate test with the test fixture temperature at ≤-40 °F.
5. Reposition the disk inside the bore to establish an appropriate starting position for the HAC Free Drop test with the test fixture temperature at ≤-20 °F.
6. Radially shift the disk inside the bore to establish a reduced O-ring seal compression on one side of the test fixture, ensuring the HAC Cold compression and compression change requirements are met per Table 2.10.2-1.
7. Perform a helium leakage rate test with the test fixture temperature at ≤-20 °F.
8. Warm the test fixture to the elevated test temperature (i.e., HAC Fire temperature per Table 2.10.2-1), continuing to restrain the disk in the HAC offset position relative to the bore.
9. Maintain the elevated temperature for ≥8-hour duration.

10. At the end of the elevated temperature duration, confirm that a rapid, hard vacuum can be achieved and maintained in the test volume between the two, test O-ring seals at the elevated temperature.
11. Cool the test fixture to ≤-20 °F, continuing to restrain the disk in the HAC offset position relative to the bore.
12. Perform a helium leakage rate test with the test fixture temperature at ≤-20 °F.

2.10.2.4 Rainier Rubber R0405-70 Formulation Qualification Test Results

Test results are summarized in Table 2.10.2-2, as referenced from GEN-REP-0001.[9] As shown in the table, the Rainier Rubber compound R0405-70 butyl rubber material is capable of maintaining a leaktight seal when subjected to worst-case seal compressions beyond the range of NCT and HAC cold and hot temperatures applicable to the HalfPACT package. For comparison, the minimum O-ring seal compression applicable for the NCT Cold condition (see Table 2.10.2-1) is 21.06% for the ICV. The NCT Cold tests summarized in Table 2.10.2-2 were conservatively performed with the disk in its full offset position, thus showing leaktight capability at NCT Cold conditions to as low as 10.38%. For the remaining tests, the applicable minimum compression is 10.73% for the ICV whereas the tests were all performed in the full offset position, thus showing leaktight capability to as low as 10.38%. For the HAC Free Drop test, the disk was initially centered and then shifted as much as 10.74%, which enveloped the applicable worst-case shift of 10.33% for the ICV. For the HAC Fire test, again per Table 2.10.2-1, a test temperature of at least 360 °F for at least 8 hours is applicable, whereas the actual test was conservatively performed at 400 °F for 8 hours, as noted in Table 2.10.2-2. Therefore, formulation qualification testing of Rainier Rubber compound R0405-70 bounds the minimum O-ring seal compressions for the HalfPACT package.

2.10.2.5 ASTM D2000 Standardized Batch Material Tests

Based on successfully demonstrating the ability to remain leaktight when subject to the formulation qualification tests, Rainier Rubber R0405-70 butyl rubber compound was selected to benchmark material performance parameters that can be evaluated using available industry standardized tests. Correlation of the R0405-70 butyl rubber compound performance to industry standard performance specifications establishes a standard quality and performance benchmark that is suitable for use in material batch testing. Note that a "formulation" represents a controlled chemical recipe and production process as defined by the material supplier, a "batch" represents the chemical compounding of a production quantity of material before vulcanizing, and a "lot" refers to the quantity of finished product made at any one time.

Qualification testing identified certain key parameters that are important to seal performance. Of these, two important parameters for this application are resistance to helium permeation and acceptable resiliency at cold temperatures. Butyl rubber performs very well resisting helium permeation, and the

[9] *Formulation Qualification Testing of Rainier Rubber Butyl Compound RR0405-70*, GEN-REP-0001, Rev. 0, Washington TRU Solutions, February 2010.

TR-10 test in ASTM D1329[10] provides an acceptable method for determining cold temperature material resiliency, with the properties of the R0405-70 acting as a baseline for the required resiliency.

The ability of the compound to withstand elevated temperatures while not having significant reduction in material properties is also required to maintain seal integrity after the hypothetical accident condition thermal event. Material properties in elastomers are reduced through the process of de-polymerization, an aging phenomenon. Elastomer aging can be accelerated by the application of energy (heat). The effect of aging can be quantified by measuring the reduction of physical properties after maintaining the seal material at an elevated temperature for a specific length of time. For the same amount of reduction in properties, a shorter time can be used at a higher temperature, or a longer time can be used at a lower temperature. ASTM D573[11] provides an acceptable method for determining the effects of temperature aging on elastomeric compounds.

ASTM D395[12] provides an acceptable method for determining the effects of compression set. R0405-70 butyl rubber compound uses an acceptance criteria of less than 25% compression set for 22 hours at an elevated temperature of 70 °C.

ASTM D2137[13] provides an acceptable method for determining an elastomeric material's ability to withstand cold temperatures and remain pliable. Although the TR-10 test in ASTM D1329 demonstrates the seal material's resiliency at a much lower temperature, this test verifies the seal material's lack of brittleness at the minimum regulatory temperature of -40 °C.

Hardness or durometer along with tensile strength and elongation are defined and checked to ensure durability of the seal material during operation. ASTM D2240[14] provides an acceptable method for determining the required 70 ±5 durometer, and ASTM D412[15] provides an acceptable method for determining the required minimum 10 MPa (1,450 psi) tensile strength and minimum 250% elongation, with the properties of the R0405-70 acting as a baseline for the required hardness, tensile strength, and elongation.

For proprietary seal materials that have fairly demanding requirements such as the R0405-70 butyl rubber compound, the compound is commonly specified by a company designator and subsequently checked against exacting performance standards. Specifying an elastomeric compound by its chemistry alone is difficult considering the sheer number of parameters that affect seal performance. However, by applying the above nationally recognized standards to a material batch, the important parameters are defined for verifying the performance of the seal material.

---

[10] ASTM D1329-88 (re-approved 1998), *Standard Test Method for Evaluating Rubber Property – Retraction at Lower Temperatures (TR Test),* American Society for Testing and Materials, Philadelphia, PA, Volume 09.01, 2001.

[11] ASTM D573-99, *Standard Test Method for Rubber – Deterioration in an Air Oven,* American Society for Testing and Materials, Philadelphia, PA, Volume 09.01, 2001.

[12] ASTM D395-01, *Standard Test Methods for Rubber Property – Compression Set,* American Society for Testing and Materials, Philadelphia, PA, Volume 09.01, 2001.

[13] ASTM D2137-94 (re-approved 2000), *Standard Test Methods for Rubber Property – Brittleness Point of Flexible Polymers and Coated Fabrics,* American Society for Testing and Materials, Philadelphia, PA, Volume 09.02, 2001.

[14] ASTM D2240-00, *Standard Test Method for Rubber Property – Durometer Hardness,* American Society for Testing and Materials, Philadelphia, PA, Volume 09.01, 2002.

[15] ASTM D412-98a, *Standard Test Methods for Vulcanized Rubber and Thermoplastic Rubbers and Thermoplastic Elastomers – Tension,* American Society for Testing and Materials, Philadelphia, PA, Volume 09.01, 2001.

ASTM D1414[16] is the standard method for testing O-ring seals, and covers most, but not all, of the required testing delineated above. However, due to the overall size of the O-ring seals and the additional testing specified, ASTM D2000[3] provides a better standard classification system.

Using the ASTM D2000 designator, O-ring seals with properties equivalent to R0405-70 butyl rubber material are classified as follows and summarized in the table below:

M4AA710 A13 B13 F17 F48 Z Trace Element

Designator	Condition
M	Metric units designator (default condition)
4	Grade 4 acceptance criteria for the tests specified
AA	Butyl rubber compound
7	70 Shore A durometer hardness per ASTM D2240
10	Tensile strength and elongation per ASTM D 412; acceptance criteria are a minimum 10 MPa (1,450 psi) tensile strength and a minimum 250% elongation
A13	Heat resistance test per ASTM D573; the acceptance criteria are a maximum 10 Shore A durometer hardness increase, a maximum reduction in tensile strength of 25%, and a maximum reduction in ultimate elongation of 25% at 70 °C
B13	Compression set per Method B of ASTM D395; acceptance criterion is a maximum 25% compression set after 22 hours at 70 °C
F17	Cold temperature resistance specifying low temperature brittleness per Method A, 9.3.2, of ASTM D2137; non-brittle after 3 minutes at -40 °C
F48	Cold temperature resiliency, where F is for cold temperature resistance, and 4 specifies testing to the TR-10 test of ASTM D1329; 8 indicates a TR-10 temperature of -50 °C (-58 °F), or less
Z Trace Element	Z designator allows specific notes to be added; "Z Trace Element" allows trace elements to be added to the elastomeric compound to meet the seal material requirements

[16] ASTM D1414-94 (re-approved 1999), *Standard Test Methods for Rubber O-Rings*, American Society for Testing and Materials, Philadelphia, PA, Volume 09.02, 2001.

Table 2.10.2-2 – Rainier Rubber R0405-70 Formulation Qualification O-ring Seal Test Results

Test Number①	O-ring Seal Number①	O-ring Seal Inside Diameter, D_s (in)	O-ring Seal Cross-Sectional Diameter, d_{cs} (in)		O-ring Seal Stretch, S (%)③	O-ring Seal Reduction in Cross-Sectional Diameter, R (%)④	Minimum O-ring Seal Cross-Sectional Diameter, d_{csr} (in)⑤	O-ring Seal Compression (%)⑥⑦			Temperature for "Leaktight" Leak Test (≤ 8.8 × 10^{-8} scc/sec, He)⑧			
			Max	Min				Center Disk	Offset Disk	Change	-40 °F	-20 °F	400 °F⑨	-20 °F
1	1	11.368	0.396	0.394	6.80	4.36	0.377	21.12	10.38	10.74	Yes	Yes	Yes	Yes
	4	11.500	0.396	0.392	5.58	3.71	0.377	21.12	10.38	10.74				
2	2	11.417	0.396	0.395	6.34	4.12	0.379	21.54	10.85	10.69	Yes	Yes	Yes	Yes
	3	11.465	0.395	0.394	5.90	3.88	0.379	21.54	10.85	10.69				

Notes:

① The test fixture's pertinent dimensions are taken in line with the direction of offset, which is also the position where the minimum cross-sectional diameter of the O-ring seals are placed: bore inside diameter, D_i = 12.736 inches; disk outside diameter, D_o = 12.655 inches; and the O-ring seal groove diameter, D_g = 12.14125 inches (based on the average of fixture measurements taken along the axis of offset). All tests are performed using WTS Test Fixture No. 4.

② Material for all O-ring seal test specimens is butyl rubber compound R0405-70, Rainier Rubber Co., Seattle, WA.

③ Given the O-ring seal inside diameter, D_s, the percent of O-ring seal stretch, $S = 100 \times (D_g - D_s)/D_s$.

④ From Figure 3-3 of the *Parker O-ring Handbook*[5] and based on the O-ring seal cross-sectional diameter, d_{cs}, the percent reduction in O-ring seal cross-sectional diameter, $R = -0.005 + 1.19S - 0.19S^2 - 0.001S^3 + 0.008S^4$ for $0 \le S \le 3\%$, and $R = 0.56 + 0.59S - 0.0046S^2$ for $3\% < S \le 25\%$.

⑤ The reduced O-ring seal cross-sectional diameter, $d_{csr} = d_{cs}(1 - R/100)$.

⑥ The percent O-ring seal compression with the disk *centered* is $100 \times [d_{csr} - \frac{1}{2}(D_i - D_g)]/d_{csr}$.

⑦ The percent O-ring seal compression with the disk *offset* is $100 \times [d_{csr} - (D_i - D_o) - \frac{1}{2}(D_o - D_g)]/d_{csr}$.

⑧ A "Yes" response indicates that helium leakage testing demonstrated that the leakage rate was ≤ 1.0×10^{-7} scc/sec, air (i.e., "leaktight" per ANSI N14.5). In all cases, measured leakage rates were ≤ 8.8×10^{-8} scc/sec, helium, for tests with a "Yes" response.

⑨ No helium leak tests were performed at elevated temperatures due to O-ring seal permeation and saturation by helium gas. The ability of the test fixture to establish a rapid, hard vacuum between the O-ring seals was used as the basis for leak test acceptance at elevated temperatures. A "Yes" response indicates that all tests rapidly developed a hard vacuum.

This page intentionally left blank.

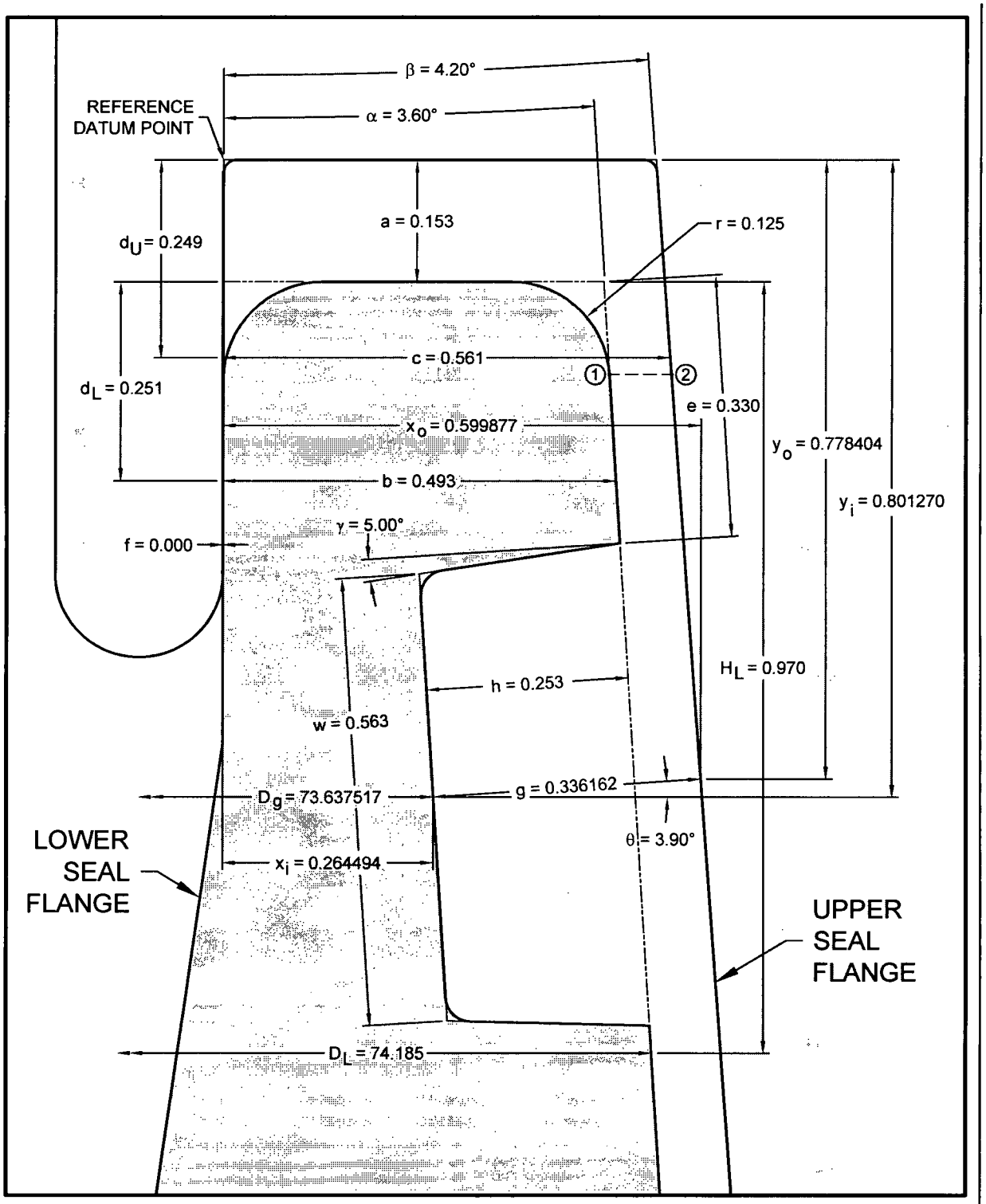

Figure 2.10.2-1 – Configuration for Minimum ICV O-ring Seal Compression

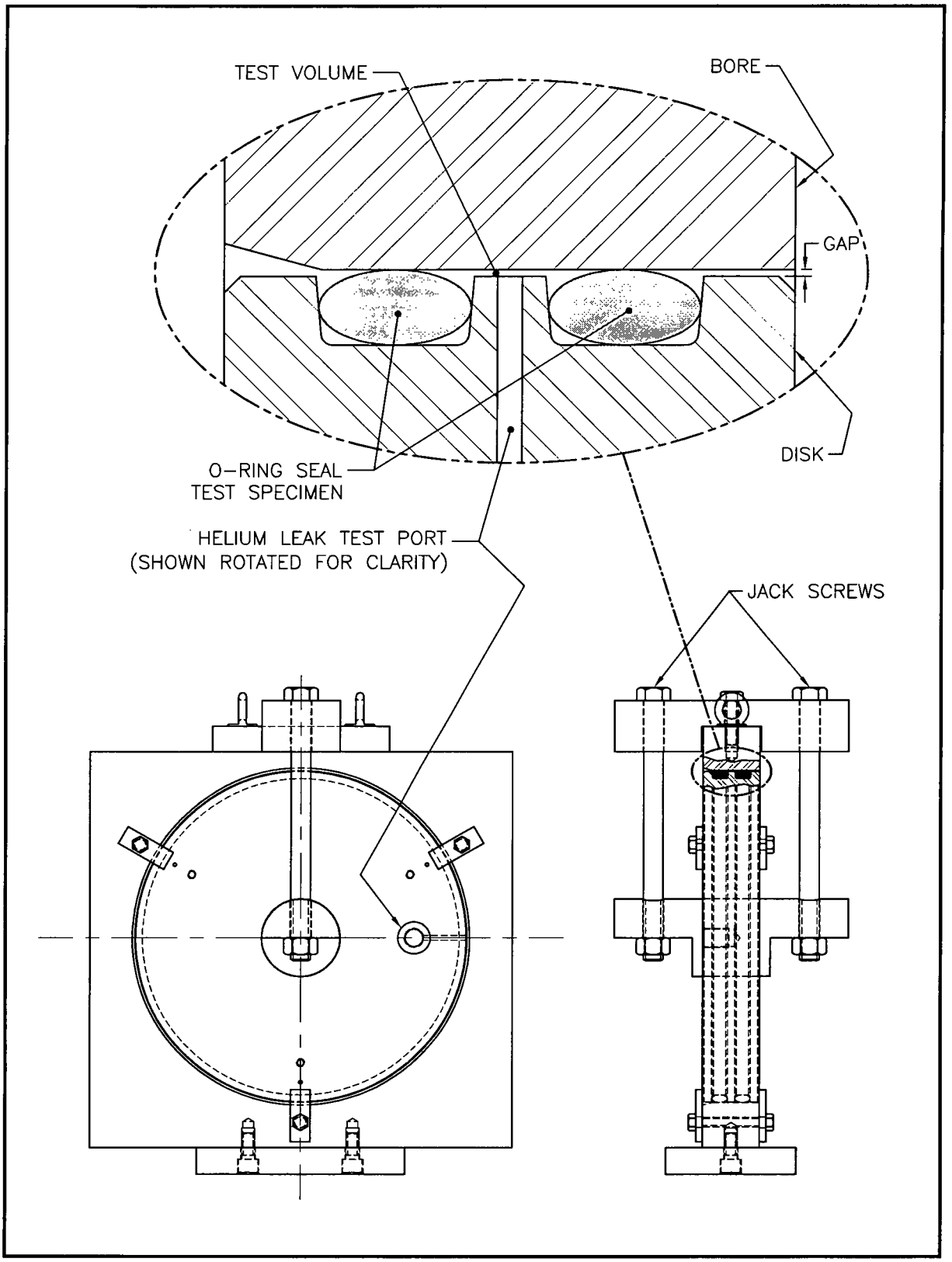

Figure 2.10.2-2 – Test Fixture for O-ring Seal Performance Testing

2.10.3 Certification Tests

Presented herein are the results of normal conditions of transport (NCT) and hypothetical accident condition (HAC) tests that address the free drop, puncture, and fire test performance requirements of 10 CFR 71[1]. This appendix summarizes the information presented in the test reports for the HalfPACT engineering test unit (ETU)[2] and certification test unit (CTU)[3]. The test units discussed in this section were configured for testing with two independent containment boundaries. All test results and conclusions with respect to the inner containment vessel (ICV) remain unchanged with the outer containment (now confinement) vessel (OCV) configured as secondary confinement boundary when its optional O-ring seals are utilized. The leaktight capability of the ICV and the structural response and ability of the outer containment (now confinement) assembly (OCA) to protect the ICV are unaffected by the OCV configuration using optional O-ring seals.

2.10.3.1 Introduction

The HalfPACT package, when subjected to the sequence of hypothetical accident condition (HAC) tests specified in 10 CFR §71.73, subsequent to the sequence of normal conditions of transport (NCT) tests specified in 10 CFR §71.71, is shown to meet the performance requirements specified in Subpart E of 10 CFR 71. As indicated in the introduction to Chapter 2.0, *Structural Evaluation*, with the exception of the immersion test, the primary proof of performance for the HAC tests is via the use of full scale testing. In particular, free drop, puncture, and fire testing of both a HalfPACT ETU and CTU confirmed that the ICV and OCV remained leaktight after a worst case HAC sequence. Observations from testing of the two test units also confirm the conservative nature of deformed geometry assumptions used in the criticality assessment provided in Chapter 6.0, *Criticality Evaluation.*

Since the HalfPACT package is essentially a "cut-down" version of the TRUPACT-II package, this appendix provides a number of comparative discussions between the HalfPACT and TRUPACT-II certification testing programs. Where appropriate, these comparisons are useful for providing an additional level of confidence in the HalfPACT testing programs by illustrating test results similar to the comprehensive TRUPACT-II certification testing program. As discussed in Appendix 2.10.3.5, *Technical Basis for Tests*, the selection of HalfPACT test conditions was determined based on the various TRUPACT-II certification tests.

2.10.3.2 Summary

As seen in the figures presented in Appendix 2.10.3.7, *Test Results*, successful testing of the ETU and CTU indicates that the various HalfPACT packaging design features are adequately designed to

---

[1] Title 10, Code of Federal Regulations, Part 71 (10 CFR 71), *Packaging and Transportation of Radioactive Material*, 01-01-12 Edition.

[2] Packaging Technology, Inc. (PacTec), *HalfPACT Packaging Engineering Prototype Test Report*, PacTec Engineering Document ED-019, Tacoma, Washington.

[3] S. A. Porter, et al, *Certification Test Report for the HalfPACT Package*, TR-001, Packaging Technology, Inc. (PacTec), Tacoma, Washington.

withstand the HAC tests specified in 10 CFR §71.73. The most important result of the testing program was the demonstrated ability of the OCV and ICV to remain leaktight[4].

Significant results of free drop testing common to both test units (ETU and CTU) are as follows:

- There was no evidence of buckling of either containment boundary shell. Modest damage to the inner containment vessel shells did occur, an amount somewhat in excess of what was reported in Appendix 2.10.3, *Certification Tests*, in the *TRUPACT-II package SAR*[5]. However, it is clear that the damage noted for the HalfPACT package corresponds to the much heavier payload drum's interaction with the packaging wall.
- No excessive distortion of the seal flange regions occurred for either the ICV or OCV, although some permanent deformation was noted.
- There was no rupture of the 3/8-inch thick, OCA outer shell.
- Observed permanent deformations of the HalfPACT packaging were less than those assumed for the criticality evaluation.

Significant results of puncture drop testing common to both test units (ETU and CTU) are as follows:

- Besides the obvious permanent damage to the OCA outer shell at the location of the various puncture bar impacts, there was evidence of some permanent deformation of the OCV shell. The most significant damage occurred at the OCV vent port fitting during testing of the CTU. The cumulative effects of the NCT and HAC free drops, and the subsequent puncture drop caused successively greater permanent deformation to the region adjacent to the vent port fitting. A crack was noted in the inner weld of the CTU's OCV vent port fitting, but not in the outer weld of the OCV vent port fitting. Subsequent helium leakage rate testing determined that OCV containment integrity was maintained. Although essentially identical in configuration, the ETU did not have a similarly cracked weld. See Appendix 2.10.3.7.2.8, *CTU Post-Test Disassembly*, for additional discussion regarding this result.
- Penetration of the OCA outer shell occurred below the 3/8-to-1/4-inch thick, OCA outer shell weld during testing of the ETU. The same test, repeated for certification testing, did not reproduce the hole. This result was due to lengthening the 3/8-inch thick, OCA outer shell from 12 to 18 inches, correspondingly changing the impact angle sufficiently to prevent penetration through the adjacent 1/4-inch thick shell.
- There was no rupture of the 3/8-inch thick, OCA outer shell. However, for both test units (ETU and CTU) a linear tear occurred along the weld at the 3/8-to-1/4-inch shell transition in the OCA body outer shell.

Significant results of fire testing common to both test units (ETU and CTU) are as follows:

- The fire tests met or exceeded the minimum flame temperature of 1,475 °F for 30 minutes as required by 10 CFR §71.73(c)(4).

---

[4] "Leaktight" is a leakage rate not exceeding 1×10^{-7} standard cubic centimeters per second (scc/sec), air, as defined in ANSI N14.5-1997, *American National Standard for Radioactive Materials – Leakage Tests on Packages for Shipment*, American National Standards Institute, Inc. (ANSI).

[5] U.S. Department of Energy (DOE), *Safety Analysis Report for the TRUPACT-II Shipping Package*, USNRC Docket No. 71-9218, U.S. Department of Energy, Carlsbad Field Office, Carlsbad, New Mexico.

- Gases formed by thermal degradation of the polyurethane foam were safely vented out the OCA fire vents located in the OCA lid and body.
- The polyurethane foam self-extinguished shortly after the end of the fire.
- The average residual thickness of unburned polyurethane foam in the OCA side wall was approximately five inches in regions undamaged by free drop tests, and approximately three inches in regions damaged by free drop tests. In regions of multiple free drop and puncture drop tests (e.g., at the OCV vent port), only charred foam and ceramic fiber paper remained.
- None of the containment seals sustained extensive degradation due to excessive temperature.

2.10.3.3 Test Facilities

Drop testing of the HalfPACT package prototype test unit was performed at Sandia National Laboratories' Coyote Canyon Aerial Cable Facility in Albuquerque, New Mexico. The drop test facility utilizes free fall and, if needed, rocket power to attain closely controlled impact velocities as defined by a particular testing program. The drop test facility consists of a 5,000-foot long wire cable suspended across a mountain canyon. The cable can support proportionally heavier package weights at lower elevations, with a package weight in excess of 50,000 pounds for the regulatory defined, hypothetical accident condition 30-foot free drop test. The "unyielding" target consists of a highly reinforced, armor steel plated concrete block as illustrated in Figure 2.10.3-1. The target is designed to accommodate test packages weighing up to 100 tons.

In accordance with the requirements of 10 CFR §71.73(c)(3), the puncture bar was fabricated from solid, six-inch diameter mild steel, approximately 36 inches long. The puncture bar was welded perpendicularly to a 1½-inch thick, mild steel plate having an outside diameter of approximately 24 inches. The top edge of the puncture bar was finished to a 1/4-inch radius. When utilized, the puncture bar was securely welded (mounted) to the impact surface.

Fire testing of the HalfPACT package prototype test unit was performed at Sandia National Laboratories' Lurance Canyon Burn Site in Albuquerque, New Mexico. The open pool fire facility can be adjusted to a maximum size of 30 by 60 feet for performing free-burning fires for a duration of 2 hours, maximum. Packages weighing up to 149 tons can be supported at heights up to a few meters above the pool surface. During fire testing, thermocouples and calorimeters that are strategically placed measure and record fire temperatures and heat flux, respectively. The pool is enclosed by a 20-foot high wind screen deployed in a nominal 50-foot radius from the pool center. The wind screen is constructed of chain link fencing fitted with aluminum slats resulting in a screen porosity of 50%. The wind screen demonstrates a 3-to-1 reduction in wind velocity in high wind conditions, and a 2-to-1 reduction in low wind conditions.

2.10.3.4 Test Unit Description

The HalfPACT package is essentially a 30-inch shorter version of the TRUPACT-II package, being identical in almost all respects, the few exceptions noted in later discussions. Both the HalfPACT and TRUPACT-II packages are designed to transport payloads of contact-handled transuranic (CH-TRU) waste. The HalfPACT package is designed to carry five different payload configurations: 1) seven 55-gallon drums, 2) one standard waste box (SWB), 3) four 85-gallon drums, 4) three 100-gallon drums, or 5) three shielded containers for its payload. The HalfPACT package height is based on the need to carry oversized 85-gallon drums used as overpacks for 55-gallon drums. Drums may weigh 1,000 pounds each, for a maximum weight of 7,000 pounds

for seven 55-gallon drums, 4,000 pounds for four 85-gallon drums, and 3,000 pounds for three 100-gallon drums. The maximum SWB weight is 4,000 pounds and the maximum weight of three shielded containers is 6,780 pounds.

For purposes of comparison, the primary design differences between the HalfPACT package and TRUPACT-II package are summarized as follows (see Figure 2.10.3-2 and Figure 2.10.3-3 for the differences between the packaging design and 55-gallon drum payload configuration for the TRUPACT-II and HalfPACT packages, respectively):

- maximum package weight: 18,100 pounds for HalfPACT; 19,250 pounds for TRUPACT-II,
- maximum payload assembly weight (including pallet, spacer, guide tubes, and slipsheets): 7,600 pounds for HalfPACT; 7,265 pounds for TRUPACT-II,
- payload assembly configurations (comparing current TRUPACT-II package certification):
  - 55-gallon drums: seven for HalfPACT; fourteen for TRUPACT-II (includes pipe overpacks),
  - SWBs: one for HalfPACT; two for TRUPACT-II,
  - 85-gallon drums: four for HalfPACT; eight for TRUPACT-II,
  - 100-gallon drums: three for the HalfPACT; six for the TRUPACT-II,
  - ten drum overpack (TDOP): none for HalfPACT; one for TRUPACT-II,
  - shielded containers: three for HalfPACT with radial and axial dunnage; none for TRUPACT-II
- overall height: 91½ inches for HalfPACT; 121½ inches for TRUPACT-II,
- ICV payload cavity length: 44 15/16 inches for HalfPACT; 74⅝ inches for TRUPACT-II,
- OCV cylindrical shell stiffening ring: removed for HalfPACT; included for TRUPACT-II,
- OCA body fire vent locations changed between HalfPACT and TRUPACT-II,
- OCA body, 3/8-inch thick outer shell length: 18 inches for HalfPACT; 12 inches for TRUPACT-II,
- Payload spacer: A payload spacer is used to reduce excess axial clearance for HalfPACT payloads consisting of 55-gallon drums, 100-gallon drums, short 85-gallon drums, and SWBs; no payload spacer is used for TRUPACT-II

The following sections expand on the individual details relating to the ETU and CTU configurations. Both HalfPACT packaging engineering test units were fabricated from TRUPACT-II packaging training units[6], as discussed below.

2.10.3.4.1 Engineering Test Unit (ETU)

The HalfPACT packaging engineering test unit (ETU) was fabricated from TRUPACT-II unit number 104, a TRUPACT-II packaging training unit. As illustrated in Figure 2.10.3-4, the OCA

[6] Early TRUPACT-II production units have shells of insufficient thickness per TRUPACT-II SAR requirements. Designated "training units", excessive grinding of some welds in localized regions reduced shell thicknesses below the minimum allowed by the TRUPACT-II (and HalfPACT) SAR packaging general arrangement drawings.

body for the HalfPACT ETU was created by removing 30 inches from the OCV cylindrical shell above the torispherical head, and 30 inches from the OCA outer shell below the 3/8-to-1/4-inch shell transition from TRUPACT-II unit number 104. All polyurethane foam and ceramic fiber paper below the parting line was removed. New ceramic fiber paper was installed, the shells welded closed, and new polyurethane foam installed. Polyurethane foam compressive strength properties were tested to be consistent with the requirements of Table 8.1-1 in Section 8.1.4.1, *Polyurethane Foam*. Similarly, as illustrated in Figure 2.10.3-5, the ICV body for the HalfPACT ETU was created by removing 30 inches of the cylindrical region above the torispherical head from TRUPACT-II unit number 104. Both the OCA and ICV lid assemblies remained unchanged.

Tested differences between the HalfPACT ETU and TRUPACT-II CTUs (i.e., components or parameters used during TRUPACT-II certification testing that were not used during HalfPACT certification testing) are summarized as follows:

- Seal flange O-ring seal region tolerances: carefully controlled fabrication procedures to arrive at worst case (minimum) O-ring seal compression and worst case (maximum) axial free play were used for the TRUPACT-II CTUs; the HalfPACT ETU used unmodified, as-built production unit tolerances,
- Loose debris outside the payload drums: additional cement and sand was used outside the payload drums for the TRUPACT-II CTUs, but not for the HalfPACT CTU (both test programs used additional loose sand inside the payload drums),
- Active and passive test instrumentation (e.g., thermocouples, accelerometers, pressure transducers, and/or temperature indicating labels): active and passive test instrumentation was used for the TRUPACT-II CTUs, but no instrumentation was used for the HalfPACT ETU,
- Internal pressure: pressurization of the containment vessels to the maximum normal operating pressure (MNOP) for some of the free drop, puncture drop, and fire tests was performed for the TRUPACT-II CTUs, but not for the HalfPACT ETU,
- Cooling before drop testing: cooling to -20 °F prior to some of the free drop and puncture drop tests was performed for the TRUPACT-II CTUs, but not for the HalfPACT ETU,
- Pre-heating before the fire test: pre-heating prior to fire testing was performed for the TRUPACT-II CTUs, but not for the HalfPACT ETU, and
- Cooling before leakage rate testing: cooling to -20 °F prior to post-test, helium leakage rate testing was performed for the TRUPACT-II CTUs, but not for the HalfPACT ETU.

In addition to the tested differences between the HalfPACT ETU and TRUPACT-II CTUs, the difference between the HalfPACT ETU and the HalfPACT packaging design depicted in Appendix 1.3.1, *Packaging General Arrangement Drawings*, are summarized as follows:

- Minimum shell material thickness: HalfPACT packaging design requires minimum shell material thicknesses per ASTM A480[7]; HalfPACT ETU was fabricated from a cut-down TRUPACT-II training unit (number 104) with localized regions not meeting ASTM A480 because of excessive grinding of some welds,

[7] ASTM A480/A480M, *Standard Specification for General Requirements for Flat-Rolled Stainless and Heat-Resisting Steel Plate, Sheet, and Strip*, American Society for Testing and Materials (ASTM), West Conshohocken, PA.

- OCA body, 3/8-inch thick outer shell length: HalfPACT packaging design is 18 inches long; HalfPACT ETU was 12 inches long,
- Painting of OCA exterior surfaces: HalfPACT packaging design allows optional painting; HalfPACT ETU was not painted,
- OCV vent and seal test port thermal plugs: HalfPACT packaging design specifies foam or ceramic fiber paper thermal plugs; HalfPACT ETU used polyurethane foam thermal plugs,
- Optional catalyst assembly recess in ICV aluminum honeycomb spacers: HalfPACT packaging design specifies Ø18 inches × 1½ inches deep; HalfPACT ETU used recesses Ø15 inches × 11/16 inches deep,
- Aluminum honeycomb spacer assembly attachment bracket: HalfPACT packaging design specifies right-angled brackets; HalfPACT ETU used obtuse-angled brackets,
- Locking ring stop tabs: HalfPACT packaging design specifies up to three stop tabs per locking ring; HalfPACT ETU used one stop tab per locking ring,
- OCA exterior welds: HalfPACT packaging design specifies 3/32-inch maximum weld reinforcement for OCA exterior welds; HalfPACT ETU used 3/32-inch maximum weld reinforcement only on new 3/8-to-1/4-inch, outer shell weld, and
- External handling features were added to the exterior surfaces of the HalfPACT ETU to facilitate lifting and handling the package during testing.

The following table summarizes a comparison of major component weights for the HalfPACT ETU and TRUPACT-II CTUs:

Packaging Component	TRUPACT-II Certification Test Units			HalfPACT ETU
	CTU No. 1	CTU No. 2	CTU No. 3	
Empty Package				
• ICV Assembly	2,614	2,773	2,570	2,025
• OCA Assembly	9,450	9,400	9,196	8,100
• Total	12,064	12,173	11,766	10,125
Payload				
• 55-Gallon Drums	7,000	7,000	7,000	7,350
• Pallet, Slipsheets, etc.	315	269	375	160
• Total	7,315	7,269	7,375	7,510
Loaded Package Total	19,379	19,442	19,141	17,635

2.10.3.4.2 Certification Test Unit (CTU)

Similar to the HalfPACT ETU, the HalfPACT packaging certification test unit (CTU) was fabricated from TRUPACT-II unit number 107, a TRUPACT-II packaging training unit. As illustrated in Figure 2.10.3-6, the OCA body for the HalfPACT CTU was created by removing 30 inches from the OCV cylindrical shell above the torispherical head, and 36 inches from the

OCA outer shell below the 3/8-to-1/4-inch shell transition from TRUPACT-II unit number 107. All polyurethane foam and ceramic fiber paper below the parting line was removed. Six inches of 3/8-inch thick, OCA outer shell was added below the existing 12-inch length to extend the shell length to 18 inches per the HalfPACT packaging design. New ceramic fiber paper was installed, the shells welded closed, and new polyurethane foam installed. Polyurethane foam compressive strength properties were tested to be consistent with the requirements of Table 8.1-1 in Section 8.1.4.1, *Polyurethane Foam*. Similarly, as illustrated in Figure 2.10.3-7, the ICV body for the HalfPACT CTU was created by removing 30 inches of the cylindrical region above the torispherical head from TRUPACT-II unit number 107. Both the OCA and ICV lid assemblies remained unchanged. All OCA exterior surfaces were painted gray.

Tested differences between the HalfPACT CTU and TRUPACT-II CTUs (i.e., components or parameters used during TRUPACT-II certification testing that were not used during HalfPACT certification testing) are summarized as follows:

- Seal flange O-ring seal region tolerances: carefully controlled fabrication procedures to arrive at worst case (minimum) O-ring seal compression and worst case (maximum) axial free play were used for the TRUPACT-II CTUs; the HalfPACT CTU used unmodified, as-built production unit tolerances,
- Loose debris outside the payload drums: additional cement and sand was used outside the payload drums for the TRUPACT-II CTUs, but not for the HalfPACT CTU (both test programs used additional loose sand inside the payload drums),
- Active and passive test instrumentation (e.g., thermocouples, accelerometers, pressure transducers, and/or temperature indicating labels): active and passive test instrumentation was used for the TRUPACT-II CTUs, but only temperature indicating labels were used for the HalfPACT CTU,
- Internal pressure: pressurization of the containment vessels to the maximum normal operating pressure (MNOP) for some of the free drop, puncture drop, and fire tests was performed for the TRUPACT-II CTUs, but not for the HalfPACT CTU,
- Cooling before drop testing: cooling to -20 °F prior to some of the free drop and puncture drop tests was performed for the TRUPACT-II CTUs, but not for the HalfPACT CTU,
- Pre-heating before the fire test: pre-heating prior to fire testing was performed for the TRUPACT-II CTUs, but not for the HalfPACT CTU, and
- Cooling before leakage rate testing: cooling to -20 °F prior to post-test, helium leakage rate testing was performed for the TRUPACT-II CTUs, but not for the HalfPACT CTU.

In addition to the tested differences between the HalfPACT CTU and TRUPACT-II CTUs, the difference between the HalfPACT CTU and the HalfPACT packaging design depicted in Appendix 1.3.1, *Packaging General Arrangement Drawings*, are summarized as follows:

- Minimum shell material thickness: HalfPACT packaging design requires minimum shell material thicknesses per ASTM A480; HalfPACT CTU was fabricated from a cut-down TRUPACT-II training unit (number 107) with localized regions not meeting ASTM A480 because of excessive grinding of some welds,

- Optional catalyst assembly recess in ICV aluminum honeycomb spacers: HalfPACT packaging design specifies Ø18 inches × 1½ inches deep; HalfPACT CTU used recesses Ø15 inches × 11/16 inches deep,
- Aluminum honeycomb spacer assembly attachment bracket: HalfPACT packaging design specifies right-angled brackets; HalfPACT CTU used obtuse-angled brackets,
- Locking ring stop tabs: HalfPACT packaging design specifies up to three stop tabs per locking ring; HalfPACT CTU used one stop tab per locking ring,
- OCA exterior welds: HalfPACT packaging design specifies 3/32-inch maximum weld reinforcement for OCA exterior welds; HalfPACT CTU used 3/32-inch maximum weld reinforcement only on new 3/8-to-3/8-inch and 3/8-to-1/4-inch, outer shell welds, and
- Payload Spacer: To accommodate a single layer of 55-gallon drums for the test payload, a 5-inch high wooden payload spacer was utilized,
- External handling features were added to the exterior surfaces of the HalfPACT CTU to facilitate lifting and handling the package during testing.
- The OCV was fabricated to the requirements of the ASME Boiler and Pressure Vessel Code, Section III, Division 1, Subsection NB (rather than Subsection NF).
- Some detailed dimensions for the OCV seal flanges, locking ring, and OCV upper main O-ring seal are slightly different from those delineated in Appendix 1.3.1, *Packaging General Arrangement Drawings.*
- Generic polymer may be used for the optional OCV containment (now confinement), test, and OCV vent port plug O-ring seals; all CTUs utilized butyl rubber for these seals.
- Butyl, neoprene, or ethylene propylene elastomers may be used for the ICV inner vent port plug O-ring seal, and the ICV seal test port plug O-ring seal; all CTUs used butyl rubber for these seals.
- Generic polymer may be used for the optional OCV vent port plug and cover handling O-ring seals, the OCV vent port cover O-ring seal, and the OCV seal test port plug O-ring seal; all CTUs used butyl rubber for these seals.
- Generic polymer may be used for the optional OCV guide plates; all CTUs used stainless steel for these plates.
- Aluminum honeycomb spacers may be constructed with one or two top sheet layers of aluminum; all CTUs used one top sheet layer.

The following table summarizes a comparison of major component weights for the HalfPACT ETU and CTU, and TRUPACT-II CTUs:

Packaging Component	TRUPACT-II			HalfPACT	
	CTU No. 1	CTU No. 2	CTU No. 3	ETU	CTU
Empty Package					
• ICV Assembly	2,614	2,773	2,570	2,025	2,120
• OCA Assembly	9,450	9,400	9,196	8,100	7,950
• Total	12,064	12,173	11,766	10,125	10,070
Payload					
• 55-Gallon Drums	7,000	7,000	7,000	7,350	7,410
• Pallet, Payload Spacer, etc.	315	269	375	160	590
• Total	7,315	7,269	7,375	7,510	8,000
Loaded Package Total	19,379	19,442	19,141	17,635	18,070

2.10.3.5 Technical Basis for Tests

The following sections supply the technical basis for the chosen test orientations and sequences for both the HalfPACT ETU and CTU as presented in Section 2.10.3.6, *Test Sequence for Selected Free Drop, Puncture Drop, and Fire Tests.*

2.10.3.5.1 Initial Test Conditions

2.10.3.5.1.1 Internal Pressure

Internal pressure could affect the certification test results in two ways. First, it imparts primary stress to the containment vessels, and second, it could affect the leaktight condition of the seals in a HAC fire. In the first case, containment vessel stress due to internal pressure is pr/t = 7,288 psi, where p, the internal design pressure, is 50 psi, the ICV mean radius, r, is 36.44 inches, and the thickness, t, is 0.25 inches. Per Regulatory Guide 7.6, this stress is compared to the design stress intensity, S_m = 20,000 psi at NCT temperatures. The result is that pressure-related membrane stress that is only 36% of the allowable stress. Pressure would normally be present only in the ICV, and due to the presence of the OCA, the polyurethane foam, and the OCV, the relative deformation of the ICV due to any free drop or puncture event is insignificant. Further, during TRUPACT-II testing, no pressure spikes as a result of impact were recorded. Thus, the addition of pressure membrane stress would be insignificant to the outcome of HalfPACT free drop and puncture drop testing.

In the second case, the pressure sealing capacity of the containment seals is significantly greater than the maximum normal operating pressure (MNOP) of 50 psig. For the HAC fire test, O-ring seal compression is expected to increase as a result of differential expansion between the seal and the surrounding metal, thus increasing the pressure capacity of the seal. Certification testing of the TRUPACT-II demonstrated that no pressure was lost for any of the fire tests. Therefore, as long as temperatures in the O-ring seal regions are similar to the temperatures measured during TRUPACT-II fire testing, pressurizing either the ICV or OCV is considered unnecessary for HalfPACT certification fire testing.

2.10.3.5.1.2 Temperature

Ambient temperature will be used at the time of HalfPACT certification testing. Results might differ if the two extremes (NCT maximum temperature, or minimum, -20 °F, temperature) were employed. However, it can be shown that these differences are not significant as follows.

As discussed in Section 2.7, *Hypothetical Accident Conditions*, polyurethane foam compressive strength at an NCT temperature of 160 °F is approximately 75% of the compressive strength at 75 °F, and at -20 °F is approximately 140% of the crush strength at 75 °F. In contrast, the minimum strength of the Type 304 stainless steel varies to a much lesser extent, decreasing from 35,000 psi at -20 °F[8] to 30,000 psi at 100 °F, and to 27,000 psi at 160 °F. Thus, for drop orientations where stresses in structural steel members are of concern, the worst case temperature is -20 °F since this is the temperature where the ratio of impact induced acceleration load to steel strength is the greatest. For drop orientations where deformations are of concern, elevated temperatures would result in a worst-case condition.

Deformations will be greater if the polyurethane foam is at NCT warm temperatures during free and puncture drops. The greater the deformation, the less residual foam thickness to protect the O-ring seals from thermal degradation in the subsequent fire. The elastomer seal material short-term temperature limit is 400 °F per Appendix 2.10.2, *Elastomer O-ring Seal Performance Tests*. Considering a maximum O-ring seal region temperature of 260 °F for TRUPACT-II fire testing and the relatively large amount of unburned foam following fire testing (~5 inches, average), the margin against O-ring seal failure is relatively large. In view of this, a reasonable limit for the average maximum O-ring seal region temperature for HalfPACT fire testing is 300 °F. In this case, the margin will be virtually as great as for the TRUPACT-II, and drop testing at warm temperatures is considered unnecessary.

Impact forces will be greater if the polyurethane foam is at NCT cold temperatures (-20 °F) during free and puncture drops. However, the bounding free drop where impact severity is a factor is a side slapdown. As discussed in Section 2.10.3.5.2.4, *Closure (Lid) Separation*, the results indicate that all HalfPACT slapdown drops are enveloped by TRUPACT-II slapdown drops. Therefore, reduction of the foam temperature would still not create a governing impact severity condition, and drop testing at cold temperatures is considered unnecessary.

2.10.3.5.2 Free Drop Tests

The HalfPACT package is qualified primarily by full scale testing, with the acceptance criterion being the ability to demonstrate leaktight containment for both the OCV and ICV.

Per 10 CFR §71.73(c)(1), the package is required to "strike an essentially unyielding surface *in a position for which maximum damage is expected.*" Therefore, for determining the drop orientations that satisfy the regulatory "maximum damage" requirement, attention is focused predominantly on the issue of containment. Loss of containment could potentially occur one of two ways: 1) directly, as a result of free drop impact damage, or 2) indirectly, as a result of normal conditions of transport (NCT) or hypothetical accident condition (HAC) impact damage that could lead to degradation of sealing capability in the subsequent puncture and/or fire events.

---

[8] For the purposes of this discussion, yield strength at -20 °F is extrapolated from data in Table 2.3-1 using a curve shape for Type 304 stainless steel in the -80 °F to 800 °F range in *Engineering Properties of Steel*, Philip D. Harvey, Editor, American Society for Metals, 1982.

Direct damage would take the form of one of the following:

1. Rupture of a containment vessel,
2. Buckling of a containment vessel,
3. Excessive deformation in the main O-ring sealing region resulting in the loss of a leaktight seal, and/or
4. Separation of one of the containment vessel lids from its corresponding body.

Indirect damage would require significant impact damage to the surrounding polyurethane foam leading to thermal degradation of the seal material. A significant reduction in polyurethane foam thickness or a gross exposure of the foam through splits or punctures in the OCA outer shell would have to occur near the main O-ring seal or vent port seal region. In a free drop event, such damage could occur as follows:

5. Deformation of the polyurethane foam due to impact could result in an inadequate remaining thickness to prevent seal thermal degradation in the fire event, and/or
6. Deformation of the OCA outer shell could lead to a fissure in the shell material or in a weld, or a puncture through the shell material, thereby exposing foam.

These six issues will now be discussed in detail in the following sections.

2.10.3.5.2.1 Containment Vessel Rupture

Rupture of a containment vessel as a result of the HAC free drop is not credible for the HalfPACT package. In comparison, the TRUPACT-II package was certified utilizing three different certification test packages that were subjected to a large number of 3-foot NCT free drops, and 30-foot HAC free drops. Post-test examination of the TRUPACT-II CTUs revealed no indication of impending rupture of either the OCV or ICV, either as a result of impact forces with the ground or as a result of interaction with the maximum-weight payload. The HalfPACT package is both 25% shorter and 6% lighter than the TRUPACT-II package. Otherwise, construction, including shell thicknesses and foam strength, is essentially identical[9]. Therefore, behavior of the HalfPACT package with regards to containment vessel rupture will be the same, and rupture will not occur as demonstrated during TRUPACT-II package certification testing.

2.10.3.5.2.2 Containment Vessel Buckling

Buckling of a containment vessel as a result of the HAC free drop is also not of concern. As mentioned above, the similar TRUPACT-II package was tested extensively as a part of its certification process. TRUPACT-II testing included a flat bottom impact with cold, -20 °F, polyurethane foam to impose maximum axial impact forces. In these drops, no indication of containment vessel buckling was observed. The HalfPACT package is, however, 6% less gross weight than the TRUPACT-II package, and the OCV body shell ring stiffener is not included. It will now be shown that these differences are insignificant relative to buckling.

Impact acceleration is a function of the crush force and of the package weight, as follows:

[9] With the exception of the overall reduction in packaging height of 30 inches, the HalfPACT and TRUPACT-II packages differ in only a few minor aspects. The two most notable aspects are removal of the OCV stiffener ring, and beneficially lengthening of the 3/8 inch thick portion of the OCA outer shell, just below the OCA closure joint.

$$g = \frac{F}{W}$$

where g is the impact level in units of gs, F is the crush force, and W is the package weight. If weight is reduced and the force is conservatively assumed to remain constant[10], it is possible to determine an impact level for a lighter package based on results for a heavier one. From the TRUPACT-II SAR, the impact for the governing, bottom-down drop, with -20 °F foam, was 385g. Using the above relation, the maximum bottom-down impact would therefore be $385g \times W_T / W_H = 409g$, where the TRUPACT-II package weight, W_T = 19,250 pounds, and the HalfPACT package weight, W_H = 18,100 pounds.

The compressive stress in the ICV shell is a function of both the impact load and the weight of the shell. The weight conservatively includes ICV assembly and upper aluminum honeycomb spacer assembly, but does not include the weight of the lower ICV torispherical head. Therefore, the total weight on the ICV shell is approximately 1,722 pounds, resulting in a corresponding compressive stress in the ICV shell of:

$$\sigma = \frac{P}{A} = \frac{Wg}{\pi dt} = \frac{(1{,}722)(409g)}{\pi(72.875)(0.25)} = 12{,}305 \text{ psi}$$

where the mean diameter of the ICV shell, d = 72.875 inches, and the shell thickness, t = 0.25 inches. Note that the stress calculated above is less than the equivalent value of 14,192 psi determined in the TRUPACT-II SAR. This result is because, even though the HalfPACT impact is 6% greater than the TRUPACT-II impact, the weight used is 18% less due to a 30-inch shorter OCV body shell length for the HalfPACT package. Therefore, since the governing stress in the HalfPACT ICV shells under worst case cold end drop conditions is lower than for the TRUPACT-II, buckling of the HalfPACT is not of concern.

Similarly, buckling of the OCV is not of concern. As for the TRUPACT-II, the HalfPACT OCV is surrounded by supporting polyurethane foam. And, even though the OCV body ring stiffener is not used on the HalfPACT package as for the TRUPACT-II package, the longest unsupported length for each package is almost identical. Therefore, buckling of the HalfPACT package OCV shell will not occur, and a cold, bottom end drop is not a bounding test.

2.10.3.5.2.3 Excessive Deformation in the Main O-ring Sealing Region

Excessive deformation in the main O-ring sealing region would be most likely to occur in a drop orientation where the seal region is in the impact zone. For the HalfPACT package, where the seal flanges are located approximately halfway along its length, the seal region can experience local impact only in a horizontal side drop. In addition, payload interaction forces between the payload and the ICV are maximized in a side drop since the entire payload inertia force must be carried through the ICV sidewall, and proportionally through the ICV seal region. Excessive deformation of the sealing surfaces could relieve O-ring seal compression and potentially affect leaktight containment. Therefore, a side drop orientation should be tested.

[10] This simplifying assumption is based on an equivalent impact "footprint" for the HalfPACT and TRUPACT-II packages. Due to lower deformation, strain hardening, and geometric considerations, the impact force is somewhat less for the lighter weight HalfPACT package, but is never greater than the TRUPACT-II package.

2.10.3.5.2.4 Closure (Lid) Separation

A lid could become partially separated from the body if tensile or moment forces on the lid are high enough to cause permanent deformation of the seal flanges or locking ring. Due to the shape of the HalfPACT package, direct tensile forces separating the lid from the body are not possible for primary impact in a free drop event. For the same reason, moment forces also do not occur at the joint in a horizontal side drop. However, in a near-horizontal orientation, it is possible for moment forces to occur at the lid joint for secondary impact in a slapdown event.

Since lid and closure design for both the TRUPACT-II and HalfPACT packages are identical, and since the TRUPACT-II package was subjected to two different slapdown drop orientations, the lid closure has previously been successfully subjected to such moment forces. It remains to be shown, however, that the moments experienced during TRUPACT-II package certification testing envelop or bound those of the HalfPACT package. Bounding analyses can be done using the methods outlined in NUREG/CR-3966[11].

Section 2.2 of NUREG/CR-3966 presents a method for evaluating the axial force, shear force, and bending moment in a package as it undergoes impact, including primary and secondary (slapdown) impacts. The analysis consists of two parts. First, the portion of the total energy that is absorbed by a given impact (say, primary) is determined. Realizing that this energy is equivalent to the area beneath the force-deflection curve for a given drop height and orientation, the maximum force acting on that end of the cask is established. Then, using this force and a quasi-static analysis, the axial, shear, and moment forces in the cask can be determined. These internal force distributions are plotted as a function of force, F, and cask length, L, in Figure 2.7 (primary impact) and Figure 2.10 (secondary impact) of NUREG/CR-3966. Using these relationships, the response of the TRUPACT-II and HalfPACT packages can be compared.

The relevant parameters of each package are defined as follows. The impact limiter in both cases is fully enveloping, and, for simplicity, the nose (primary) and tail (secondary) impact limiters are defined as meeting at the geometric center of the package. The length of the equivalent cask is defined in each case as equal to the length of the payload cavity, plus 2/3 of the length of each aluminum honeycomb spacer. The resulting length is 90.34 inches for the TRUPACT-II package model, and 60.34 inches for the HalfPACT package model, since the length of the HalfPACT package is 30 inches less than the TRUPACT-II package. In both cases, the package inside diameter is 73⅝ inches at the lower end is the OCV body, and is 76$^{13}/_{16}$ inches at the upper end is the OCV lid. In both cases, the outer diameter of the impact limiters is the outside diameter of the OCA outer shell, or 94⅜ inches. The weight (including the maximum weight payload) is 19,250 pounds for the TRUPACT-II package and 18,100 pounds for the HalfPACT package. The corresponding rotational mass moment of inertia is 89,487 in-lb-s^2 for the TRUPACT-II package and 59,239 in-lb-s^2 for the HalfPACT package.

The method described requires the use of impact limiter, force-deflection curves. These are generated by means of the Packaging Technology computer code, *CASKDROP*[12]. Once impact limiter geometry is defined, this program calculates crush force as a function of impact limiter

---

[11] T. A. Nelson, R. C. Chun, *Methods for Impact Analysis of Shipping Containers*, NUREG/CR-3966, UCID-20639, U.S. Nuclear Regulatory Commission, November 1987.

[12] S. A. Porter, *CASKDROP v2.31 – A Computer Program to Determine Cask Force-Deflection Response to a Free Drop*, Packaging Technology, Inc. (PacTec), Tacoma, Washington.

deformation using simple geometry and a foam stress-strain curve. A foam stress-strain curve is used that, for a horizontal side drop of 30 feet, gives the same deformation distance as for the TRUPACT-II certification tests (3⅝ inches for CTU No. 1, Test No. 2). An illustration of each package, along with the corresponding *CASKDROP* representation, is given in Figure 2.10.3-8. The forces and moments in the cask are evaluated at a distance "x" from the lid end, which is equivalent to the location of the axial center of the OCV locking ring, or 20.0 inches in each case. A drop height of 30 feet is used.

Given the package mass, rotational moment of inertia about its center of gravity, cask length, and angle of primary impact, the energy absorbed by the primary impact limiter can be found from Equation 2.2-10 of NUREG/CR-3966. From the force-deflection curve of the primary impact limiter at the same orientation the maximum force reached in the crush event can be found. Then, given the crush force and the distance, x, the resulting axial force, shear force, and bending moment in the cask at the location of interest (the OCV locking ring) can be found from Equations 2.2-1 through 2.2-3 of NUREG/CR-3966. Similarly, the forces and moments at the OCV locking ring due to the secondary impact can be found as follows: Equation 2.2-11 for the energy absorbed by the secondary impact limiter, the force-deflection curve for the secondary impact from *CASKDROP* (secondary impact is assumed to be horizontal), and Equations 2.2-12 and 2.2-13 for axial, shear, and moment forces. Note that the force-deflection curves are identical for TRUPACT-II and HalfPACT packages.

Since the lid force-deflection curves differ slightly from the body end force-deflection curves (because the cask diameter is 76 13/16 inches at the lid and 73⅝ inches at the body end), two complete sets of results are obtained for each package: one set is lid primary, body secondary, and the other is body primary, and lid secondary. Primary impact angles of 5°, 10°, and 15° are investigated, plus two special cases for the TRUPACT-II based on orientations used during actual testing. The results are summarized in Table 2.10.3-1. Also included in the table are lid primary impacts with the package's center of gravity over the impacted corner. Results are compared primarily based on shear and moment forces.

Note that for the TRUPACT-II, the forces due to the secondary impact are always greater than for the primary impact, whereas for the HalfPACT, this is not always the case. This outcome is a function of the different relationships between the cask length, L, and the locking ring location, x. Also, note that the worst overall case is for the TRUPACT-II, primary impact angle of 5°, body primary. The worst case actually tested (body primary, impact angle 18°) is within 2% of this maximum value. Importantly, note that none of the HalfPACT results approach these values. The worst case HalfPACT result (lid primary, impact angle 5°) has a shear load and moment of 7,431 pounds and $1.760(10)^7$ in-lb, respectively, which is much less than the actual TRUPACT-II certification test values (body primary, impact angle 18°; CTU No. 2, Test No. 1) of 477,148 pounds and $2.212(10)^7$ in-lb, respectively. Therefore, the worst case HalfPACT slapdown lid closure forces and moments are bounded by TRUPACT-II certification testing.

2.10.3.5.2.5 Insufficient Residual Foam Thickness for Fire Protection

The package deformations which result from free drop impacts will reduce the thickness of polyurethane foam in the region of damage, with a consequent reduction in the ability of the foam layer to insulate the seal regions during the fire event. If deformation is excessive, thermal degradation of the elastomeric O-rings could occur and the leaktightness of the ICV and/or OCV

could be affected. The worst case reduction in thermal resistance would occur where free drop and puncture damage are combined at the most vulnerable location on the package.

Of the two vessels, the OCV is most vulnerable, since as the outermost vessel it is nearest the fire. There are two penetrations in the OCV: the main closure (lid) and the vent port. Since the main seal flanges have considerably more thermal mass than the vent port fitting, the vent port fitting is the more critical location. Puncture damage is discussed in the next section, but for the purposes of choosing the most damaging free drop orientation relative to thermal degradation of the seals in the subsequent fire, the horizontal side drop, with the OCV vent port located in the center of the impact, is the worst case. The only other orientation in which greater local deformation might occur is at the lid knuckle, due to a center of gravity over corner drop. However, this location is relatively far from the sealing regions, and is therefore not as vulnerable in the subsequent fire.

2.10.3.5.2.6 OCA Outer Shell Fracture/Tearing

Deformation of the OCA shell, if it caused a fracture or tear in the base material or weld, would expose foam directly to the fire conditions. The polyurethane foam used in the HalfPACT is intumescent, such that relatively small holes or tears are filled with an expansive char under fire conditions. Depending on size, fractures or tears are therefore self-healing and do not result in significantly higher temperatures on the inside surface of the foam (i.e., in sealing regions). However, extensive testing of the TRUPACT-II certification packages exhibited no tendency to develop such openings, however, as a result of NCT or HAC free drops, regardless of orientation. This behavior is due to the highly ductile nature of Type 304 stainless steel and the use of full penetration welds for OCA shell construction. Therefore, substantial foam exposure as a result of a free drop is not credible.

2.10.3.5.3 Puncture Drop Tests

10 CFR §71.73(c)(3) requires a free drop of the specimen through a distance of 40 inches onto a puncture bar "in a position for which maximum damage is expected." As in Section 2.10.3.5.2, *Free Drop Tests*, the "maximum damage" criterion is evaluated primarily in terms of loss of containment. Loss of containment could occur directly, due to actual puncture bar impact on the package components, or indirectly, by inducing damage which might lead to degradation of sealing capability in the subsequent fire event.

Direct damage would take the form of one of the following:

1. Rupture of one of the containment vessels (ICV or OCV),
2. Separation of the OCV lid from its body,
3. Loss of leaktight capability of the OCV seals due to excessive local deformation of the sealing region, and/or
4. Loss of sealing capability of an ICV or OCV vent port plug.

For seal degradation to occur in a subsequent fire, significant exposure or loss of polyurethane foam would have to occur in the vicinity of the O-ring seals as a result of puncture damage. Such damage might occur as follows:

5. Deformation of the OCA shell due to puncture bar impact, when added to the deformation arising from the free drop, could result in inadequate remaining thickness to prevent local seal thermal degradation in the fire event, and/or
6. Puncture bar impact could result in a fissure in the OCA material or weld, exposing significant foam to the fire event.

These issues will now be discussed in detail in the following sections.

2.10.3.5.3.1 Containment Vessel Rupture

Rupture of one of the containment vessels is not a likely failure mode. The TRUPACT-II certification test packages were subjected to a number of puncture drops where the bar axis was aligned with the package center of gravity. The worst damage to the containment vessels was a relatively insignificant denting of the OCV in a region well removed from the seal regions. Due to its similar geometry but lighter weight, the HalfPACT package is slightly less susceptible to puncture bar damage than the TRUPACT-II. Therefore, direct rupture of the containment vessels will not occur for the HalfPACT.

2.10.3.5.3.2 Closure (Lid) Separation

Separation of the OCV lid due to puncture bar impact is extremely unlikely. To rip the OCV lid off of the OCV body would require failure of the OCV locking ring, which cannot occur due to puncture bar impact. The potential energy available in a 40-inch puncture drop is equal to $40/(12 \times 30) = 11.1\%$ of the energy available in the 30-foot free drop. As shown in Section 2.10.3.5.2.4, *Closure (Lid) Separation*, the greatest lid separation loads that are to be applied in the near-horizontal slapdown drop are not able to separate the OCV lid. Therefore, separation of the lid in a 40-inch puncture drop is not credible. To make such an event even more unlikely, the orientation of the puncture bar that is necessary to apply a separating load on the lid joint is such that it diverges from the package center of gravity, thus reducing the energy available to apply to the joint. Therefore, separation of the OCV lid due to puncture bar impact will not occur for the HalfPACT package. Local puncture bar damage is discussed below.

2.10.3.5.3.3 Loss of Lid Sealing Integrity

Loss of leaktight capability of the OCV seals due to local puncture bar deformation is not likely. This behavior is because, due to the presence of increased thickness (3/8 inch) OCA shells in the sealing region, of Z-flanges, and of polyurethane foam, virtually all of the puncture drop energy is absorbed before significant deformation of the OCV sealing area has taken place. This behavior was demonstrated during TRUPACT-II certification testing, by means of drops where the puncture bar axis was aligned with the OCV sealing area and the package center of gravity (TRUPACT-II CTU No. 2, Test No. 8, and CTU No. 3, Test No. 8). Therefore, loss of leaktight capability of the OCV seals due to local puncture bar deformation will not occur for the HalfPACT package. However, for reasons discussed below, a puncture bar impact is planned which will be located very near the OCV sealing area, with the axis passing through the package center of gravity, and which will simultaneously demonstrate the ability of the HalfPACT package to sustain such damage without loss of its leaktight capability.

2.10.3.5.3.4 Loss of Vent Port Sealing Integrity

Loss of sealing capability of an ICV or OCV vent port plug is unlikely for the same reasons cited in Section 2.10.3.5.3.3, *Loss of Lid Sealing Integrity*. Since deformation of the OCV in any puncture drop is minimal, only the OCV vent port plug could possibly be affected by a puncture impact. Due to the small size of the plug, and to protection by surrounding structure, deformations do not reach the level at which the seal could be affected. This behavior was well demonstrated during TRUPACT-II certification testing (CTU No. 1, Test No. 5; CTU No. 2, Test No. 7; and CTU No. 3, Test No. 7). Again, for reasons discussed below, a puncture bar impact is planned to occur directly over the OCV vent port, in alignment with the package center of gravity, and in combination with compounded NCT and HAC side drop damage. This test will amply demonstrate the ability of the HalfPACT package to sustain such damage without loss of OCV vent port leaktight capability.

2.10.3.5.3.5 Insufficient Residual Foam Thickness for Fire Protection

Deformation of the OCA shell due to puncture bar impact, when added to the deformation arising from the free drop, could result in inadequate remaining thickness to prevent local seal thermal degradation in the fire event. Therefore, a puncture drop is planned in which damage from free drop and puncture are combined, with the puncture located directly over the OCV vent port, as discussed above in Section 2.10.3.5.2, *Free Drop Tests*, and Section 2.10.3.5.3.4, *Loss of Vent Port Sealing Integrity*.

2.10.3.5.3.6 OCA Outer Shell Fracture/Tearing

Puncture bar impact could result in a fracture or tear of the OCA outer shell base material or weld, exposing significant foam to the fire event. The polyurethane foam used in the HalfPACT is intumescent, such that holes (such as puncture bar holes) or relatively small tears are filled with an expansive char under fire conditions. Depending on size, holes or tears are therefore self-healing and do not result in significantly higher temperatures on the inside surface of the foam, i.e., near sealing regions.

The likelihood of creating significant damage is increased by use of an oblique angle between the puncture bar and the package surface. It is also increased by the presence of a transition in package outer shell thickness. In the case of the HalfPACT package, the OCA outer shell experiences a transition in thickness from 1/4 inch to 3/8 inch, located approximately 19 inches below the lid-to-body interface joint. The 3/8-inch thickness is located above the transition. The angle of the package to the horizontal is approximately 20°. A puncture drop at this location is the most likely to produce relevant damage, since:

- a transition in shell thickness, including a full penetration weld, is located there,
- the puncture bar axis, aligned with the package center of gravity, has an oblique orientation to the package surface, increasing its likelihood to "bite" and rip the shell, and
- the location is close to the sealing region, relative to thermal degradation in the fire event.

Further down the package, even though the puncture bar orientation would be more oblique, there is no comparable shell thickness transition, and additionally, would be farther away from the vulnerable seal region. Farther up the package (closer to the lid-to-body joint), even though the puncture damage would be closer to the seals, the outer shell thickness has no transition, is

thicker (3/8 inch), and the puncture bar orientation is nearer to perpendicular to the package, thus minimizing its potential to "bite" and rip the shell. As described in the next section, in order to fully explore the potential of this puncture orientation, two separate puncture events are planned.

The circumferential location for the impact is chosen such that the worst-case damage at the OCV vent port and the worst case damage from one of the two punctures discussed here can both be simultaneously placed in the hottest part of the fire in the subsequent fire test. The hottest part of the fire is located approximately 1½ meters above the fuel surface[13]. Since the lowest part of the package is located one meter above the fuel surface (per 10 CFR §71.73(c)(4)), the damage must be 1/2 meter, or approximately 20 inches, above the lowest part of the package. If two damage locations are to be thus placed, they must be separated by approximately 110°, based on the HalfPACT package outside diameter. Thus, since either of the two puncture events discussed here most likely create the maximum damage in conjunction with the OCV vent port side drop/puncture drop damage, one is placed 110° counter-clockwise and the other 110° clockwise from the OCV vent port. In the fire, the OCV vent port damage, plus the worst one of the other two puncture damage sites, will therefore be placed in the hottest part of the fire.

2.10.3.5.4 Fire Test

At the conclusion of free drop and puncture drop testing, the HalfPACT test units will be subjected to a fully engulfing pool fire test in accordance with 10 CFR §71.73(c)(4). The package will be oriented horizontally in the flames and minimally supported to least impede the heat flow into the package. The combined damage due to the free and puncture drops on the OCV vent port region will be located in the hottest portion of the fire, i.e., 1½ meters above the fuel surface, i.e., 1/2 meter above the lowest part of the package. The damage due to other puncture drops will be evaluated, and the most damaging puncture test oriented similarly at 1/2 meter above the lowest part of the package.

Justification is provided in Section 2.10.3.5.1, *Initial Test Conditions*, for using ambient pressure and temperature in the HalfPACT test units. Temperature indicting labels will be used with the HalfPACT CTU to determine the maximum temperature in the O-ring seal region during the HAC fire test. Determination of the maximum O-ring seal region temperature must account for ambient temperature conditions starting below the HAC fire test initial temperatures predicted in Section 3.5.3, *Package Temperatures*. This will be accomplished by adding the temperature differential between the actual ambient temperature and the analytically predicted O-ring seal region starting temperature to the average measured O-ring seal region temperature. Although conservative, the result will be directly comparable to measured TRUPACT-II certification fire test temperatures in the O-ring seal regions. As discussed in Section 2.10.3.5.1, *Initial Test Conditions*, a maximum O-ring seal region temperature of 300 °F for HalfPACT fire testing shall be considered acceptable.

---

[13] M. E. Schneider and L. A. Kent, *Measurements of Gas Velocities and Temperatures in a Large Open Pool Fire*, Sandia National Laboratories (reprinted from *Heat and Mass Transfer in Fire*, A. K. Kulkarni and Y. Jaluria, Editors, HTD-Vol. 73 (Book No. H00392), American Society of Mechanical Engineers). Figure 3 shows that maximum temperatures occur at an elevation approximately 2.3 meters above the pool floor. The pool was initially filled with water and fuel to a level of 0.814 meters. The maximum temperatures therefore occur approximately 1½ meters above the level of the fuel, i.e., 1/2 meter above the lowest part of the package when set one meter above the fuel source per the requirements of 10 CFR §71.73(c)(4).

2.10.3.6 Test Sequence for Selected Free Drop, Puncture Drop, and Fire Tests

The following sections establish the selected free drop, puncture drop, and fire test sequence for both the HalfPACT engineering test unit (ETU) and HalfPACT certification test unit (CTU) based on the discussions provided in Section 2.10.3.5, *Technical Basis for Tests*. The test sequences are summarized in Table 2.10.3-2 and Table 2.10.3-3, and illustrated in Figure 2.10.3-9 and Figure 2.10.3-10 for the ETU and CTU, respectively.

2.10.3.6.1 Engineering Test Unit (ETU)

Free Drop No. 1 is a NCT free drop from a height of three feet, impacting horizontally on the ETU side, parallel to the forklift pockets, nearly opposite the OCV vent port. The 3-foot drop height is based on the requirements of 10 CFR §71.71(c)(7) for a package weight between 11,000 and 22,000 pounds. The purpose of this drop test is to demonstrate that the NCT free drop does not compromise the ability of the HalfPACT package to successfully sustain subsequent HAC test events in the same or other orientations.

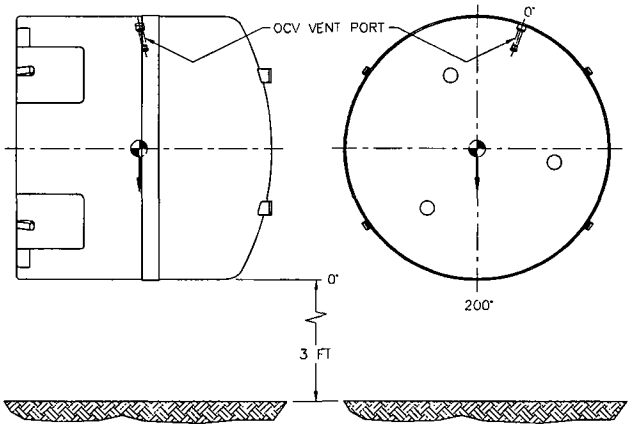

Free Drop No. 2 is a HAC free drop from a height of 30 feet, impacting horizontally on the ETU side, parallel to the forklift pockets, nearly opposite the OCV vent port. In this way, NCT and HAC free drop damage is cumulative. The 30-foot drop height is based on the requirements of 10 CFR §71.73(c)(1). The purpose of Free Drops Nos. 1 and 2, combined with Puncture Drop No. 7, is to create the greatest possible cumulative damage (i.e., the greatest reduction in foam thickness) in a region punctured through the OCA outer shell.

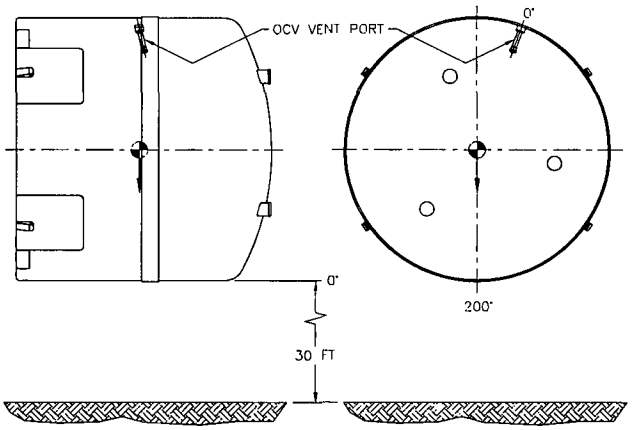

Free Drop No. 3 is a NCT free drop from a height of three feet, impacting horizontally on the ETU side, with the OCV vent port oriented downward. The 3-foot drop height is based on the requirements of 10 CFR §71.71(c)(7) for a package weight between 11,000 and 22,000 pounds. The purpose of this drop test is to demonstrate that the NCT free drop does not compromise the ability of the HalfPACT package to successfully sustain subsequent HAC test events in the same or other orientations.

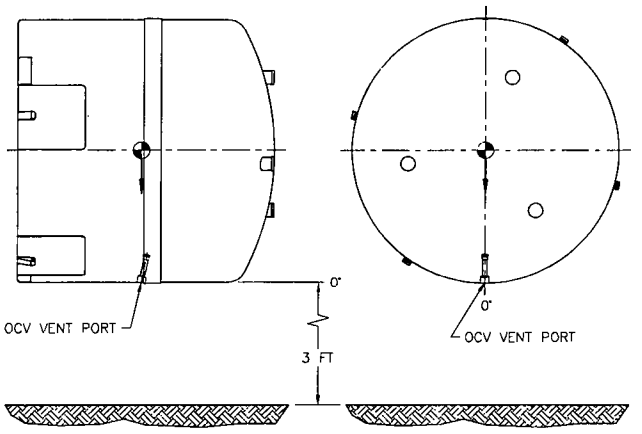

Free Drop No. 4 is a HAC free drop from a height of 30 feet, impacting horizontally on the ETU side, with the OCV vent port oriented downward. In this way, NCT and HAC free drop damage is cumulative. The 30-foot drop height is based on the requirements of 10 CFR §71.73(c)(1). The purpose of Free Drops Nos. 3 and 4, combined with Puncture Drop No. 8, is to create the greatest possible cumulative damage (i.e., the greatest reduction in foam thickness) over the OCV vent port.

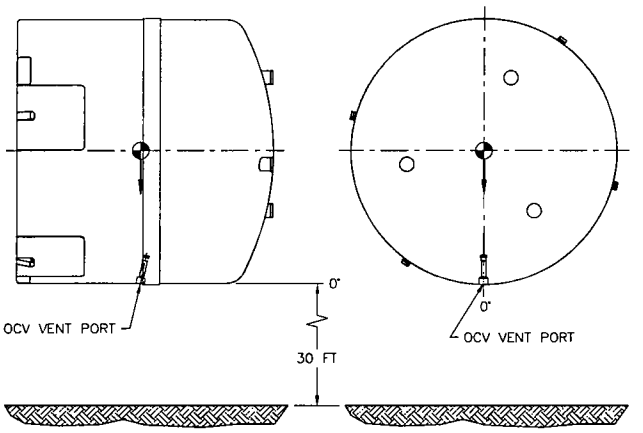

Free Drop No. 5 is a NCT free drop from a height of three feet, impacting the ETU bottom corner perpendicular to the forklift pockets, with the package's center of gravity over the impact point. The 3-foot drop height is based on the requirements of 10 CFR §71.71(c)(7) for a package weight between 11,000 and 22,000 pounds. The purpose of this drop test is to demonstrate that the NCT free drop does not compromise the ability of the HalfPACT package to successfully sustain subsequent HAC test events in the same or other orientations.

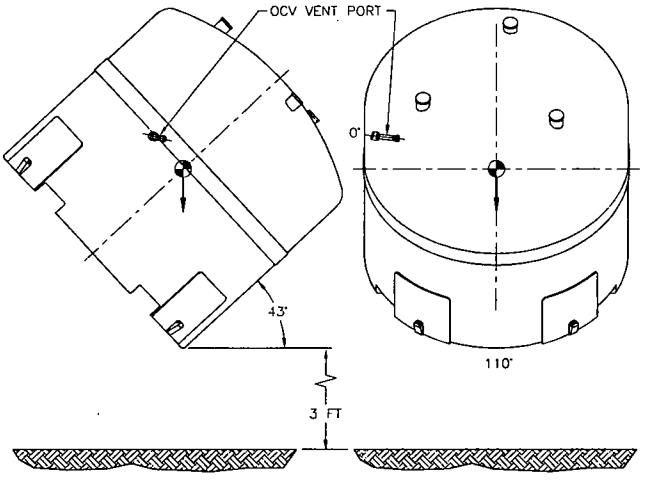

Free Drop No. 6 is a HAC free drop from a height of 30 feet, impacting the ETU bottom corner perpendicular to the forklift pockets, with the package's center of gravity over the impact point. In this way, NCT and HAC free drop damage is cumulative. The 30-foot drop height is based on the requirements of 10 CFR §71.73(c)(1). The purpose of Free Drops Nos. 5 and 6, combined with Puncture Drop No. 9, is to create the greatest possible cumulative damage in a region not tested during TRUPACT-II testing.

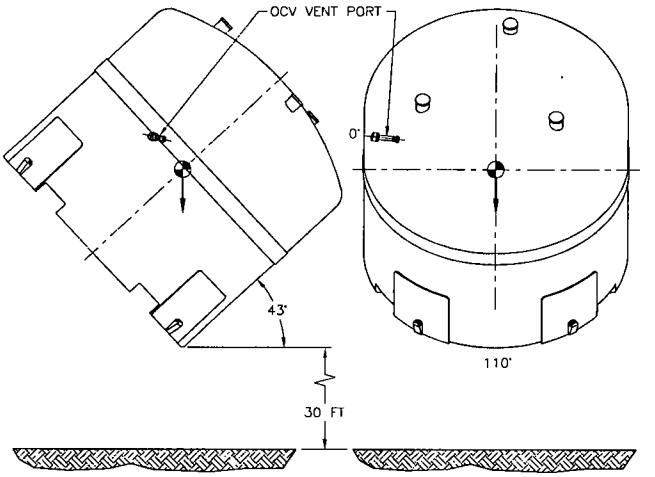

Puncture Drop No. 7 impacts directly onto the damage created by Free Drop Tests 1 and 2, directly below the 3/8-to-1/4-inch, OCA outer shell transition. The puncture drop height is based on the requirements of 10 CFR §71.73(c)(3). The purpose of Puncture Drop No. 7 is to breach the 1/4-inch thick OCA outer shell. Testing of this package region, when cumulatively damaged from the free drops, puncture drop, and fire testing demonstrate that containment integrity is maintained for the main OCV O-ring seal.

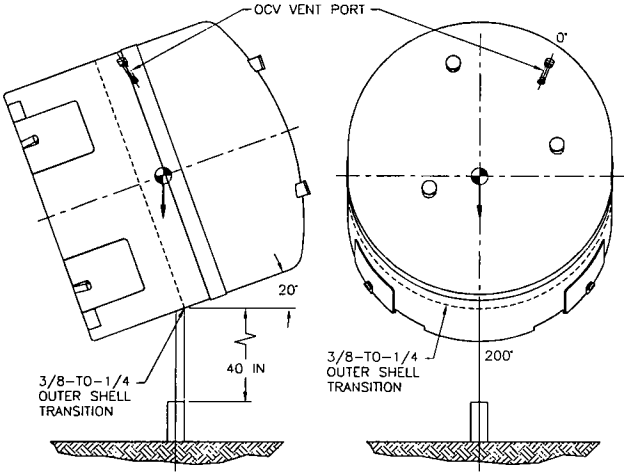

Puncture Drop No. 8 impacts directly onto the OCV vent port opening, compounding the cumulative damage created by Free Drop Tests 3 and 4. The puncture drop height is based on the requirements of 10 CFR §71.73(c)(3). The purpose of Puncture Drop No. 8 is to create the greatest cumulative damage (i.e., greatest reduction in foam thickness) over the OCV vent port region. Testing of this package region, when cumulatively damaged from the free drops, puncture drop, and fire testing, demonstrate that containment integrity is maintained for the OCV vent port O-ring seal.

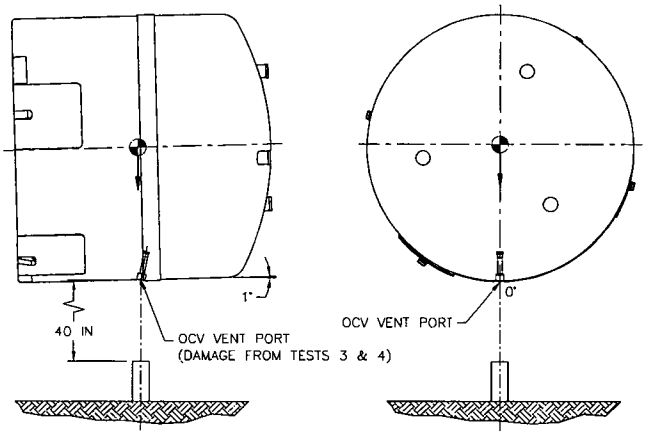

Puncture Drop No. 9 impacts directly onto the cumulative damage created by Free Drop Tests 5 and 6. The puncture drop height is based on the requirements of 10 CFR §71.73(c)(3). The purpose of Puncture Drop No. 9 is to create the greatest possible cumulative damage in a region not tested during TRUPACT-II testing. Testing of this package region, when cumulatively damaged from the free drops, puncture drop, and fire testing, demonstrates that containment integrity is maintained for the main OCV O-ring containment seal.

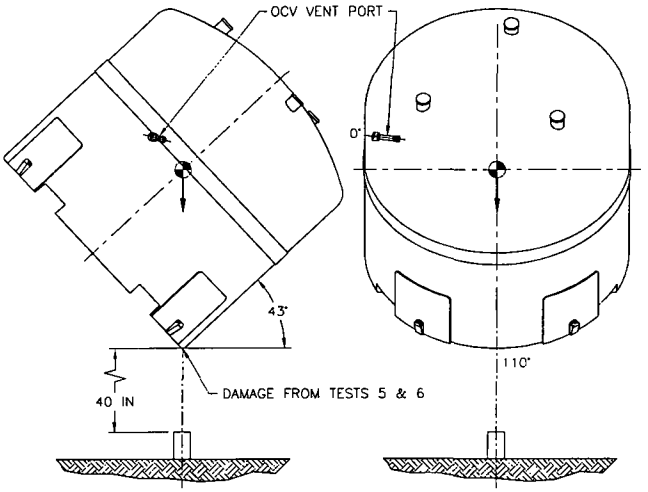

Puncture Drop No. 10 impacts directly above the 3/8-to-1/4-inch transition in the OCA body outer shell. The puncture drop height is based on the requirements of 10 CFR §71.73(c)(3). The purpose of Puncture Drop No. 10 is to attempt to break the circumferential weld at the 3/8-to-1/4-inch transition in the OCA body outer shell. Testing of this package region, when cumulatively damaged from the puncture drop and fire tests, demonstrates that containment integrity is maintained for the OCV vent port and main O-ring containment seals.

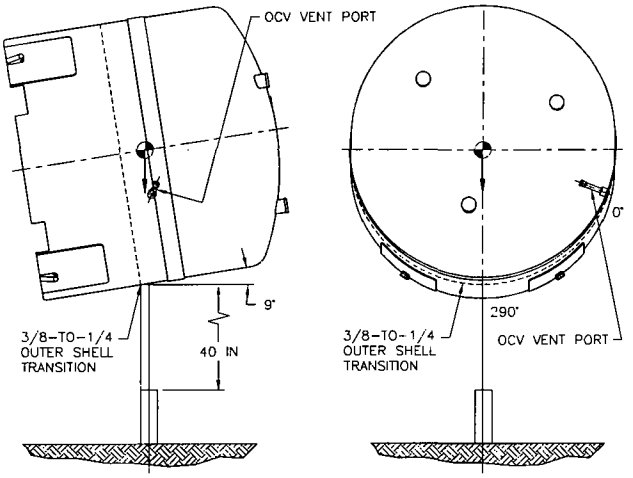

Fire No. 11 is performed by orienting the cumulative damage from Free Drop Tests 1 and 2, and Puncture Drop Test 7 at the hottest location in the fire (i.e., one meter above the fuel surface). The puncture damage from Puncture Drop No. 10 is oriented above the hole created by Puncture Drop No. 7 in an attempt to create a "chimney" through the foam cavity inside the OCA body.

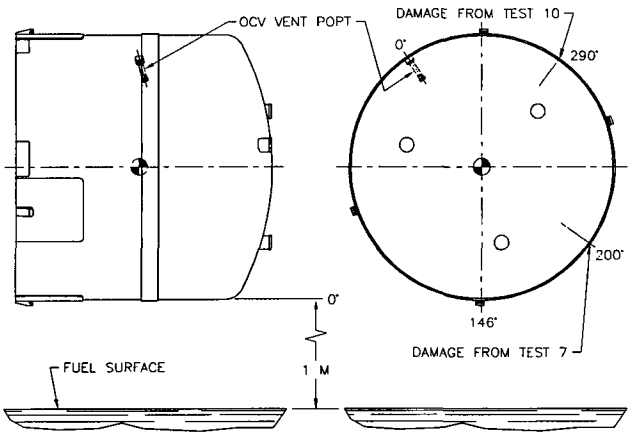

2.10.3.6.2 Certification Test Unit (CTU)

Free Drop No. 1 is a NCT free drop from a height of three feet, impacting horizontally on the CTU side, with the OCV vent port oriented downward. The 3-foot drop height is based on 10 CFR §71.71(c)(7) for a package weight between 11,000 and 22,000 pounds. The purpose of this drop test is to demonstrate that the NCT free drop does not compromise the ability of the HalfPACT package to successfully sustain the subsequent HAC test events in the same or other orientations.

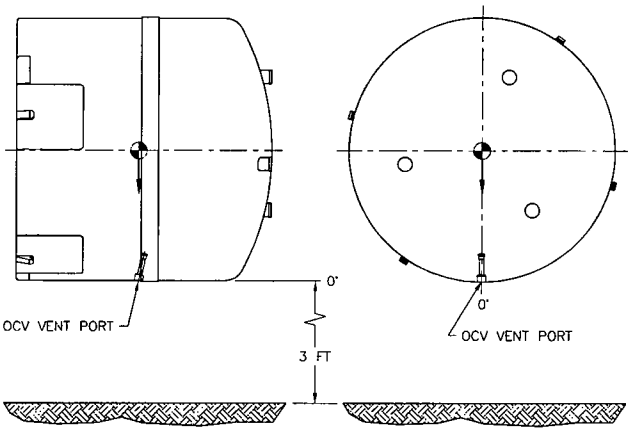

Free Drop No. 2 is a HAC free drop from a height of 30 feet, impacting horizontally on the CTU side, with the OCV vent port oriented downward. In this way, NCT and HAC free drop damage is cumulative. The 30-foot drop height is based on the requirements of 10 CFR §71.73(c)(1). The purpose of Free Drops Nos. 1 and 2, combined with Puncture Drop No. 4, is to create the greatest possible cumulative damage (i.e., the greatest reduction in foam thickness) over the OCV vent port.

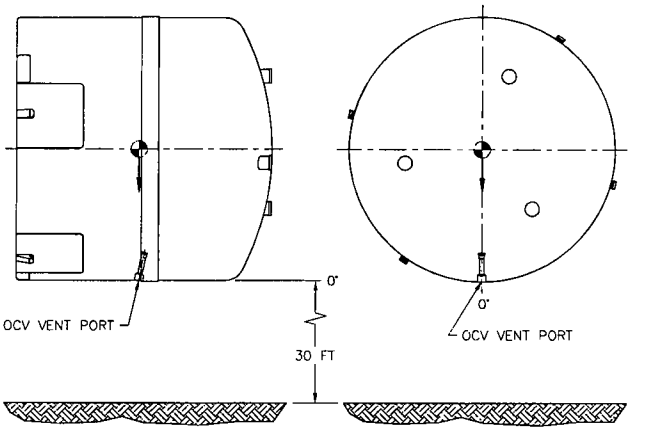

Free Drop No. 3 is a HAC free drop from a height of 30 feet, impacting 5° from horizontal with primary impact on the lid and secondary impact on a body tie-down lug. Although shown in Section 2.10.3.5.2.4, *Closure (Lid) Separation*, to be bounded by TRUPACT-II certification testing, the purpose of this drop is to apply the greatest separation forces to the closures. This test demonstrates retention of the lids, and that containment integrity is not compromised by this worst-case slapdown condition.

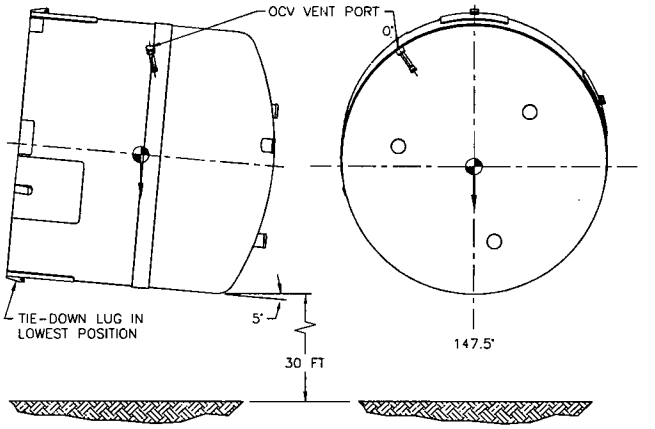

Puncture Drop No. 4 impacts directly onto the OCV vent port opening, compounding the damage created by Free Drop Tests 1 and 2. The puncture drop height is based on the requirements of 10 CFR §71.73(c)(3). The purpose of Puncture Drop No. 4 is to create the greatest cumulative damage (i.e., greatest reduction in foam thickness) over the OCV vent port region, thereby demonstrating that containment integrity is maintained for the OCV vent port O-ring seal.

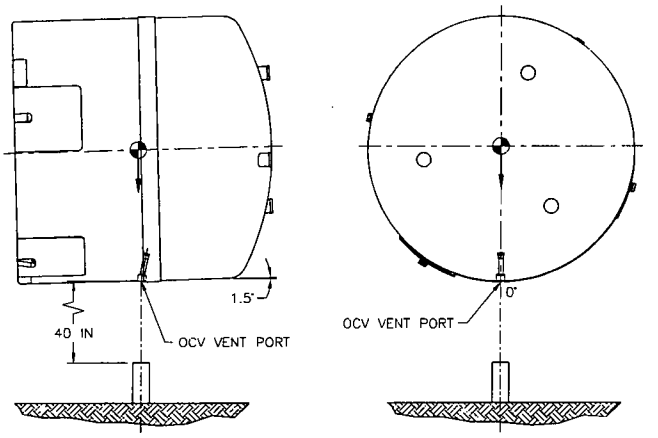

Puncture Drop No. 5 impacts directly above the 3/8-to-1/4-inch transition in the OCA body outer shell. The puncture drop height is based on the requirements of 10 CFR §71.73(c)(3). The purpose of Puncture Drop No. 5 is to attempt to break the circumferential weld at the 3/8-to-1/4-inch transition in the OCA body outer shell. Testing of this package region, when cumulatively damaged from the puncture drop and fire tests, demonstrates that containment integrity is maintained for the OCV vent port and main O-ring containment seals.

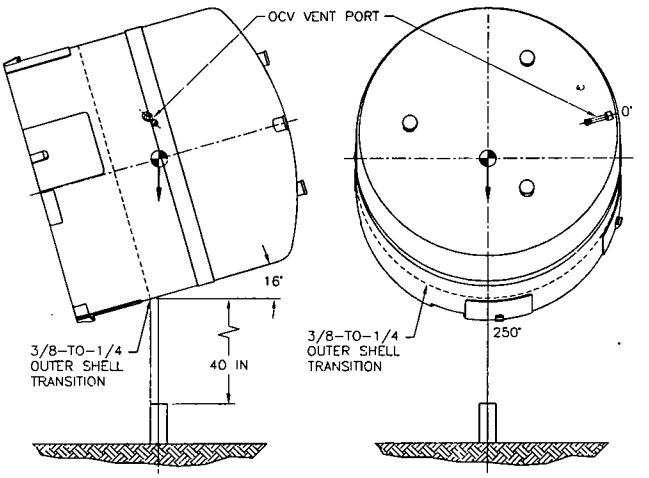

Puncture Drop No. 6 impacts directly onto the damage created by Free Drop Tests 1 and 2, directly below the 3/8-to-1/4-inch, OCA outer shell transition. The puncture drop height is based on the requirements of 10 CFR §71.73(c)(3). The purpose of Puncture Drop No. 6 is to breach the 1/4-inch thick OCA outer shell. Testing of this package region, when cumulatively damaged from the free drops, puncture drop, and fire testing demonstrate that containment integrity is maintained for the main OCV O-ring seal.

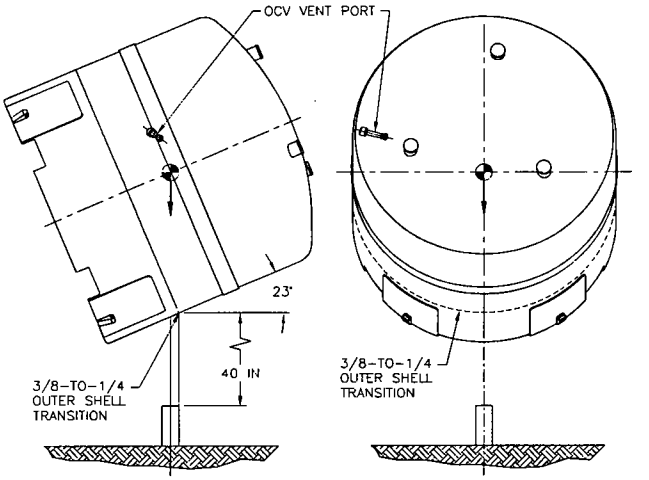

Fire No. 7 is performed by orienting the cumulative damage from Free Drop Tests 1 and 2, and Puncture Drop Test 4, at the hottest location in the fire (i.e., one meter above the fuel surface). In addition, the package is oriented to include the puncture damage from Puncture Drop No. 5 at the hottest location in the fire, directly opposite the damage from Free Drop Tests 1 and 2, and Puncture Drop Test 4.

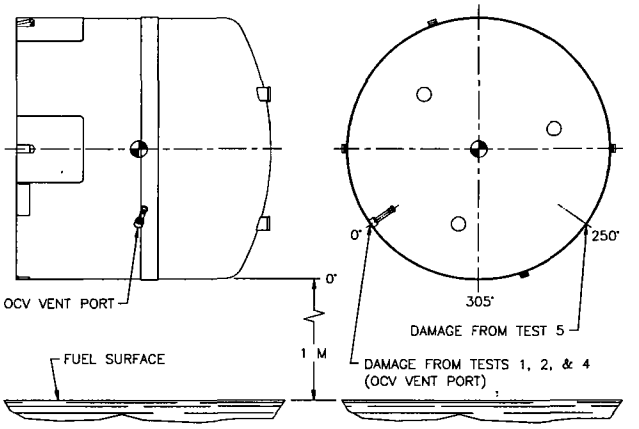

2.10.3.7 Test Results

The following sections report the results of free drop, puncture drop, and fire tests following the sequence provided in Section 2.10.3.6, *Test Sequence for Selected Free Drop, Puncture Drop, and Fire Tests*. Results are summarized in Table 2.10.3-2 and Table 2.10.3-3 for the ETU and CTU, respectively (also, see Figure 2.10.3-9 and Figure 2.10.3-10, respectively).

As can be seen in the subsequent sections, overall deformation and temperature results agree closely with those reported in the TRUPACT-II SAR.

Figure 2.10.3-12 through Figure 2.10.3-95 sequentially photo-document the engineering and certification testing process for the HalfPACT ETU and CTU, respectively.

2.10.3.7.1 Engineering Test Unit (ETU)

2.10.3.7.1.1 ETU Free Drop Test No. 1

Free Drop No. 1 was a NCT free drop from a height of three feet, impacting horizontally on the ETU side, parallel to the forklift pockets, nearly opposite the OCV vent port. As shown in Figure 2.10.3-9, the HalfPACT ETU was oriented horizontal to the impact surface (meridional angle (i.e., pitch) = 0°), and circumferentially aligned to impact 200° from the OCA vent port (between the tie-down lugs, with the forklift pockets oriented vertically). The following list summarizes the test parameters:

- verified meridional angle as 0° ±1°
- verified circumferential angle to be 200° ±1°
- verified free drop height as 3 feet, +1/-0 inches (actual drop height 3 feet, 1/2 inches)
- measured temperature at 53 °F at time of test
- conducted test at 9:54 a.m. on Tuesday, 2/18/97

A very slight rebound (bounce) occurred upon impact. The measured permanent deformations of the ETU were flats 16 inches wide at the OCA top, and 18 inches wide at the OCA bottom, corresponding to a crush depth of approximately 3/4 inches. In comparison, from the TRUPACT-II SAR for CTU No. 1, Test 1, the measured permanent deformations were flats 18 inches wide at both the OCA top and bottom.

2.10.3.7.1.2 ETU Free Drop Test No. 2

Free Drop No. 2 was a HAC free drop from a height of 30 feet, impacting horizontally on the ETU side, parallel to the forklift pockets, nearly opposite the OCV vent port. As shown in Figure 2.10.3-9, the HalfPACT ETU was oriented horizontal to the impact surface (meridional angle (i.e., pitch) = 0°), and circumferentially aligned to impact 200° from the OCA vent port (between the tie-down lugs, with the forklift pockets oriented vertically). The following list summarizes the test parameters:

- verified meridional angle as 0° ±1°
- verified circumferential angle to be 200° ±1°
- verified free drop height as 30 feet, +3/-0 inches (actual drop height 30 feet, 1 inch)
- measured temperature at 57 °F at time of test
- conducted test at 1:10 p.m. on Tuesday, 2/18/97

A small rebound (bounce) occurred upon impact. The measured permanent deformations of the ETU were flats 36 inches wide at the OCA top, and 33 inches wide at the OCA bottom, corresponding to a crush depth of approximately 3¼ inches. In comparison, from the TRUPACT-II SAR for CTU No. 1, Test 2, the measured permanent deformation were flats 37 inches wide at the OCA top, and 35 inches wide at the OCA bottom.

2.10.3.7.1.3 ETU Free Drop Test No. 3

Free Drop No. 3 was a NCT free drop from a height of three feet, impacting horizontally on the ETU side, with the OCV vent port oriented downward. As shown in Figure 2.10.3-9, the ETU was oriented horizontal to the impact surface (meridional angle (i.e., pitch) = 0°), and circumferentially aligned to impact directly onto the OCV vent port. The following list summarizes the test parameters:

- verified meridional angle as 0° ±1°
- verified circumferential angle to be 0° ±1°
- verified free drop height as 3 feet, +1/-0 inches (actual drop height 3 feet, 3/4 inches)
- measured temperature at 40 °F at time of test
- conducted test at 10:20 a.m. on Wednesday, 2/19/97

A very slight rebound (bounce) occurred upon impact. The measured permanent deformation of the ETU were flats 18 inches wide at both the OCA top and bottom, corresponding to a crush depth of approximately 3/4 inches. In comparison, from the TRUPACT-II SAR for CTU No. 1, Test 1, the measured permanent deformations were flats 18 inches wide at both the OCA top and bottom.

2.10.3.7.1.4 ETU Free Drop Test No. 4

Free Drop No. 4 was a HAC free drop from a height of 30 feet, impacting horizontally on the ETU side, with the OCV vent port oriented downward. As shown in Figure 2.10.3-9, the ETU was oriented horizontal to the impact surface (meridional angle (i.e., pitch) = 0°), and circumferentially aligned to impact directly onto the OCV vent port. The following list summarizes the test parameters:

- verified meridional angle as 0° ±1°
- verified circumferential angle to be 0° ±1°
- verified drop height as 30 feet, +3/-0 inches (actual drop height 30 feet, 2 inches)
- measured temperature at 48 °F at time of test
- conducted test at 1:47 p.m. on Wednesday, 2/19/97

A small rebound (bounce) occurred upon impact. The measured permanent deformations of the ETU were flats 34 inches wide at both the OCA top and bottom, corresponding to a crush depth of approximately 3¼ inches. In comparison, from the TRUPACT-II SAR for CTU No. 1, Test 2, the measured permanent deformation were flats 37 inches wide at the OCA top, and 35 inches wide at the OCA bottom.

2.10.3.7.1.5 ETU Free Drop Test No. 5

Free Drop No. 5 was a NCT free drop from a height of three feet, impacting the ETU bottom corner perpendicular to the forklift pockets, with the package's center of gravity over the impact point. As shown in Figure 2.10.3-9, the ETU was oriented at an angle 43° from horizontal relative to the impact surface (meridional angle (i.e., pitch) = 43°), and circumferentially aligned to impact 110° from the OCA vent port (between the tie-down lugs, with the forklift pockets oriented horizontally). The following list summarizes the test parameters:

- verified meridional angle as 43° ±1°
- verified circumferential angle to be 110° ±1°
- verified free drop height as 3 feet, +1/-0 inches (actual drop height 3 feet, 5/8 inches)
- measured temperature at 53 °F at time of test
- conducted test at 10:14 a.m. on Thursday, 2/20/97

A very slight rebound (bounce) occurred upon impact. The measured permanent deformation of the ETU was a flat 26 inches long and 5½ inches wide at the bottom corner, corresponding to a crush depth of approximately 1⅜ inches. No applicable comparison is available from the TRUPACT-II SAR.

2.10.3.7.1.6 ETU Free Drop Test No. 6

Free Drop No. 6 was a HAC free drop from a height of 30 feet, impacting the ETU bottom corner perpendicular to the forklift pockets, with the package's center of gravity over the impact point. As shown in Figure 2.10.3-9, the ETU was oriented at an angle 43° from horizontal relative to the impact surface (meridional angle (i.e., pitch) = 43°), and circumferentially aligned to impact 110° from the OCA vent port (between the tie-down lugs, with the forklift pockets oriented horizontally). The following list summarizes the test parameters:

- verified meridional angle as 43° ±1°
- verified circumferential angle to be 110° ±1°
- verified free drop height as 30 feet, +1/-0 inches (actual drop height 30 feet, 1 inch)
- measured temperature at 55 °F at time of test

- conducted test at 1:53 p.m. on Thursday, 2/20/97

A small rebound (bounce) occurred upon impact. The measured permanent deformation of the ETU was a flat 40 inches long and 12 inches wide at the bottom corner, corresponding to a crush depth of approximately 3¼ inches. In comparison, from the TRUPACT-II SAR for CTU No. 1, Test 3, the measured permanent deformation was a flat 53 inches long and 30 inches wide at the top corner (on the knuckle radius of the torispherical head), corresponding to a crush depth of approximately 3¾ inches.

2.10.3.7.1.7 ETU Puncture Drop Test No. 7

Puncture Drop No. 7 impacted directly onto the damage created by Free Drop Tests 1 and 2, directly below the 3/8-to-1/4-inch, OCA outer shell transition. As shown in Figure 2.10.3-9, the ETU was oriented at an angle 20° from horizontal relative to the impact surface (meridional angle (i.e., pitch) = 20°), and circumferentially aligned to impact 200° from the OCA vent port (between the tie-down lugs, with the forklift pockets oriented vertically). This orientation placed the puncture bar impact directly adjacent to and below the 3/8-to-1/4-inch thick transition in the OCA body outer shell (i.e., on the 1/4-inch thick shell). The following list summarizes the test parameters:

- verified meridional angle as 20° ±1°
- verified circumferential angle to be 200° ±1°
- verified puncture drop height as 40 +1/-0 inches (actual drop height 40¼ inches)
- measured temperature at 38 °F at time of test
- conducted test at 11:04 a.m. on Friday, 2/21/97

The puncture drop penetrated the OCA outer shell in the region damaged by Free Drop Tests 1 and 2. The measured permanent deformation of the ETU was a hole 10½ inches long and 11½ inches wide, measuring 8 inches deep radially and 11 inches deep along the axis of the puncture bar. Although no direct comparison is available, similar results may be obtained from the TRUPACT-II SAR. As shown in the TRUPACT-II SAR for CTU No. 1, Test 7, a similar hole occurred in the CTU body approximately 12 inches long. Further, as shown in the TRUPACT-II SAR for CTU No. 2, Test R, a similar hole occurred in the CTU body approximately 9½ inches deep along the axis of the puncture bar. From the TRUPACT-II SAR for CTU No. 2, Test 4, a similar hole occurred in the CTU head approximately 7 inches deep along the axis of the puncture bar. From the TRUPACT-II SAR for CTU No. 3, Test 4, a similar hole occurred in the CTU body approximately 8 inches deep along the axis of the puncture bar. Of final note, from the TRUPACT-II SAR for CTU No. 2, Test 4, similar puncture bar damage occurred at approximately the same distance from the main OCV containment O-ring seal as the damage produced on the HalfPACT ETU for this test.

2.10.3.7.1.8 ETU Puncture Drop Test No. 8

Puncture Drop No. 8 impacted directly onto the OCV vent port opening, compounding the cumulative damage created by Free Drop Tests 3 and 4. As shown in Figure 2.10.3-9, the ETU was oriented at an angle 1° from horizontal relative to the impact surface (meridional angle (i.e., pitch) = 1°), and circumferentially aligned to impact directly onto the OCV vent port. The following list summarizes the test parameters:

- verified meridional angle as 1° ±1° (i.e., package top-end slightly raised)
- verified circumferential angle to be 0° ±1°
- verified puncture drop height as 40 +1/-0 inches (actual drop height 40⅜ inches)
- measured temperature at 40 °F at time of test
- conducted test at 2:42 p.m. on Friday, 2/21/97

The puncture drop impacted the OCA outer shell in the region damaged by Free Drop Tests 3 and 4, and was offset approximately six inches from the OCV vent port due to high crosswinds. The measured permanent deformation of the ETU was a non-penetrating radial dent 2½ inches deep. In comparison, from the TRUPACT-II SAR for CTU No. 1, Test 5, the measured permanent deformation was a non-penetrating radial dent 3 inches deep.

2.10.3.7.1.9 ETU Puncture Drop Test No. 9

Puncture Drop No. 9 impacts directly onto the cumulative damage created by Free Drop Tests 5 and 6. As shown in Figure 2.10.3-9, the ETU was oriented at an angle 43° from horizontal relative to the impact surface (meridional angle (i.e., pitch) = 43°), and circumferentially aligned to impact 110° from the OCA vent port (between the tie-down lugs, with the forklift pockets oriented horizontally). This orientation placed the puncture bar impact directly over the OCA bottom corner onto the damage created by Free Drop Tests 5 and 6. The following list summarizes the test parameters:

- verified meridional angle as 43° ±1°
- verified circumferential angle to be 110° ±1°
- verified puncture drop height as 40 +1/-0 inches (actual drop height 40¼ inches)
- measured temperature at 28 °F at time of test
- conducted test at 12:26 p.m. on Monday, 2/24/97

The puncture drop impacted the OCA outer shell, centered on the corner drop damage created by drop tests 5 and 6. The measured permanent deformation of the ETU was a dent 3 inches deep along the axis of the puncture bar, with no penetration. In comparison, from the TRUPACT-II SAR for CTU No. 2, Test 5, resulted in a measured permanent deformation as a dent approximately 5 inches deep along the axis of the puncture bar.

2.10.3.7.1.10 ETU Puncture Drop Test No. 10

Puncture Drop No. 10 impacted directly above the 3/8-to-1/4-inch transition in the OCA body outer shell. As shown in Figure 2.10.3-9, the ETU was oriented at an angle 9° from horizontal relative to the impact surface (meridional angle (i.e., pitch) = 9°), and circumferentially aligned to impact 290° from the OCA vent port (between the tie-down lugs, with the forklift pockets oriented horizontally). This orientation placed the puncture bar impact directly adjacent to and above the 3/8-to-1/4 inch-thick transition in the OCA body outer shell (i.e., on the 3/8-inch thick shell). The following list summarizes the test parameters:

- verified meridional angle as 9° ±1°
- verified circumferential angle to be 290° ±1°

- verified puncture drop height as 40 +1/-0 inches (actual drop height 40¼ inches)
- measured temperature at 29 °F at time of test
- conducted test at 11:43 a.m. on Tuesday, 2/25/97

The puncture drop impacted the OCA outer shell in a region with no previous damage. The measured permanent deformation of the ETU was a circumferential tear along the 3/8-to-1/4 transition weld, approximately 27 inches long and 5½ inches deep radially. No applicable comparison is available from the TRUPACT-II SAR.

2.10.3.7.1.11 ETU Fire Test No. 11

Fire No. 11 was performed to demonstrate packaging compliance with the requirements of 10 CFR 71, and followed the guidelines set forth in IAEA Safety Series No. 37[14]. The following list summarizes the test parameters:

- Consistent with the TRUPACT-II SAR, the HalfPACT ETU was oriented on an insulated test stand (identical to the test stand used for TRUPACT-II fire testing) such that the most severe damage was approximately 1½ meters above the fuel surface. With a circumferential orientation of 146° (see Figure 2.10.3-9), the most severe damage was determined to be from the cumulative effects of free drop tests 1 and 2, and puncture drop test 7, followed by additional damage due to puncture drop test 10. Thus, the hole caused by puncture drop test 7 was located 1½ meters above the fuel surface, and the damage from puncture drop test 10 was located above the hole, approximately 3 meters above the fuel surface. Orienting the HalfPACT ETU this way maximized the potential for a "chimney"[15] to form between the penetrating damage from puncture drop tests 7 and 10.
- Consistent with Paragraph A-628.4 of IAEA Safety Series No. 37, the HalfPACT ETU was installed onto the insulated test stand at an elevation to place the lowest part of the package one meter above the fuel surface. The ETU was oriented horizontally on the test stand to maximize heat input.
- Consistent with Paragraph A-628.4 of IAEA Safety Series No. 37, requiring the test pool to extend 1 to 3 meters beyond the package edges, the test pool size extended approximately 1½ meters beyond each side of the ETU.
- Consistent with Paragraph A-628.5 of IAEA Safety Series No. 37, requiring wind speeds not to exceed 2 m/s (4.5 mph), a balloon was released that demonstrated both ground level and 1,000 feet altitude wind speeds under 5 mph. Weather conditions included a high altitude overcast, without precipitation for the duration of the fire test. Further, wind baffles were erected to surround the test pool to reduce the possible effects of wind gusts. The time-averaged wind speed during the fire test was approximately 1 mph both outside and inside the test area.
- Consistent with Paragraphs A-628.6 and A-628.8 of IAEA Safety Series No. 37, a JP4-type fuel was used for the fire test, and the amount of fuel was controlled to ensure the fire

[14] IAEA Safety Series No. 37, *Advisory Material for the IAEA Regulations for the Safe Transport of Radioactive Material (1985 Edition)*, Third Edition (As Amended 1990), International Atomic Energy Agency, Vienna, 1990.

[15] A "chimney" is characterized as a preferentially burning, convective flow channel from one opening to another. The formation of a chimney can cause severe erosion of the underlying insulating polyurethane foam thereby creating localized "hot spots" that could, in-turn, prevent the packaging from performing as intended.

duration exceeded 30 minutes. The fuel was floated on a pool of water approximately 1/2 meter deep to ensure even distribution during burning. The fire test lasted approximately 33 minutes, and burning continued for approximately 45 minutes after the end of the fire.

- Consistent with Paragraphs A-628.7 and A-628.9 of IAEA Safety Series No. 37, the test pool was instrumented to measure fire temperatures and heat fluxes at various locations around the ETU. Temperatures and heat fluxes were monitored before, during, and following the fire test until magnitudes stabilized back to ambient conditions. The average and standard deviation of the measured flame temperature was 1,575 ± 191 °F, and the average and standard deviation of the measured heat flux was 8.2 ± 3.8 Btu/ft^2-s.
- Consistent with Paragraph A-628.10 of IAEA Safety Series No. 37, the ETU containment O-ring seals were leakage rate tested following performance testing to verify containment integrity. Discussions regarding post-test leakage rate testing are provided in Section 2.10.3.7.1.12, *ETU Post-Test Disassembly*.
- Commenced fire testing (fire ignition) at 7:50 a.m. on Tuesday, 3/4/97. The ambient temperature was 43 °F at the start of the fire test.

Similar observations and results were noted in the TRUPACT-II SAR for fire testing. Since no instrumentation was utilized to measure HalfPACT ETU temperatures from fire testing, no direct comparison can be made to the reported TRUPACT-II CTU temperatures.

2.10.3.7.1.12 ETU Post-Test Disassembly

Post-test disassembly of the HalfPACT ETU was performed during the week of Monday, 3/10/97, through Friday, 3/14/97. Both abrasive cutting and gas plasma cutting methods were utilized, depending on their potential affect on subsequent post-test seal testing, to enable opening the ETU.

Upon removal of the OCA lid and body outer shells, the presence of several inches of very light density foam char that showed the intumescent behavior of the polyurethane foam. An average of 11 inches of undamaged foam was measured throughout the torispherical head region in the OCA lid. In regions remote from side drop damage, an average of 5 inches of undamaged foam was measured through the OCA lid side. In regions of side drop damage, an average of 3 inches of undamaged foam was measured through the OCA lid side. On a per-volume basis estimate, more than 80% of the polyurethane foam in the OCA lid remained undamaged.

Similarly, approximately 5 inches of undamaged foam was measured at the bottom center of the OCA body. In regions remote from side drop damage, an average of 6 inches of undamaged foam was measured through the OCA body side. In regions of side drop damage, an average of 3 inches of undamaged foam was measured through the OCA body side. On a per-volume basis estimate, more than 50% of the polyurethane foam in the OCA body remained undamaged.

In comparison, the TRUPACT-II packaging certification test units exhibited nearly identical amounts of undamaged polyurethane foam with a minimum of 5 inches remaining around the OCV except in localized regions damaged by free and puncture drops.

Upon removal of all the remaining polyurethane foam and ceramic fiber paper material, the OCV lid and body appeared lightly damaged. Some minor flattening was noted along the axes of the three sets of free drops (i.e., free drop tests 1 and 2, 3 and 4, and 5 and 6). Thus, damage to the OCV was mostly due to external application of force (i.e., due to the free drop and puncture drop tests). The ICV, however, appeared to have greater deformation coinciding with the axes of the

55-gallon payload drums. In contrast to the OCV, damage to the ICV was mostly due to an internal application of force caused by the greater weight capacity of the HalfPACT payload drums compared to that of the TRUPACT-II payload drums. The result was that the HalfPACT ETU ICV exhibited larger permanent deformation than compared to that of the TRUPACT-II CTUs. Several of the 55-gallon payload drums were distorted sufficiently to cause loss of their lids, as similarly noted for TRUPACT-II certification testing. Of final note, additional damage to the ETU ICV may have been caused by the 5+ inches of excess axial gap above the payload drums, since a payload spacer was not used for the HalfPACT ETU. This surplus axial gap could have allowed the non-immobilized payload drums to bounce excessively thereby compounding the effect of increased payload drum weight.

Demonstration of containment vessel leaktightness was accomplished by installing 3/8 NPT ports through the knuckle region of the OCV and ICV lid torispherical heads to allow evacuation and subsequent backfill of each corresponding containment vessel cavity with helium gas. This method ensured helium gas was present behind each containment seal, thereby validating the testing process. Although performed prior to beginning the ETU testing program, helium leakage rate testing was not performed on either of the metallic containment boundaries following testing of the ETU. Results of successful mass spectrometer helium leakage rate testing are summarized below:

Sealing Component	OCV	ICV
Main O-ring Seal	$<1.0 \times 10^{-8}$ cc/s, helium	7.8×10^{-8} cc/s, helium
Vent Port Plug O-ring Seal	3.6×10^{-8} cc/s, helium	3.0×10^{-8} cc/s, helium

When accounting for the conversion between air leakage (per ANSI N14.5) and helium leakage, a 2.6 factor applies for standard temperatures and pressures. Thus, a reported helium leakage rate of 7.8×10^{-8} cc/s, helium, is equivalently 3.9×10^{-8} cc/s, air, a magnitude well below the "leaktight" criterion of 1×10^{-7} cc/s, air, per ANSI N14.5.

The ICV wiper O-ring seal ring was damaged somewhat (buckled) in two locations due to failure of several adjacent drive screws. Thus, some of the payload drum filler material appeared to be forced into the region above the wiper O-ring seal. Both the damage to the wiper seal ring and presence of residual material in the wiper seal region were identically noted for the TRUPACT-II CTUs. As noted earlier, however, all containment O-ring seals successfully passed subsequent helium leakage rate testing thereby clearly demonstrating that containment integrity was maintained.

In conclusion, overall damage to the HalfPACT ETU paralleled the measured damage from TRUPACT-II certification testing. This was expected due to the close overall similarities between packages.

2.10.3.7.2 Certification Test Unit (CTU)

Performance testing in accordance with the requirements of 10 CFR §71.71 and §71.73 for free drops, puncture drops, and fire testing was performed based on a certification test plan prepared specifically for the HalfPACT certification testing program[16].

[16] S. A. Porter, et al, *Certification Test Plan for the HALFPACK Package*, TP-005, Rev. 1, March 6, 1998, Packaging Technology, Inc. (PacTec), Tacoma, Washington.

2.10.3.7.2.1 CTU Free Drop Test No. 1

Free Drop No. 1 was a NCT free drop from a height of three feet, impacting horizontally on the CTU side, with the OCV vent port oriented downward. As shown in Figure 2.10.3-10, the CTU was oriented horizontal to the impact surface (meridional angle (i.e., pitch) = 0°), and circumferentially aligned to impact directly onto the OCV vent port. The following list summarizes the test parameters:

- verified meridional angle as 0° ±1°
- verified circumferential angle to be 0° ±1°
- verified free drop height as 3 feet, +1/-0 inches (actual drop height 3 feet, 1/2 inches)
- measured temperature at 52 °F at time of test
- conducted test at 4:54 p.m. on Monday, 3/16/98

A very slight rebound (bounce) occurred upon impact. The measured permanent deformation of the CTU were flats 13 inches wide at both the OCA top and bottom, corresponding to a crush depth of approximately 1/2 inches. In comparison, from the TRUPACT-II SAR for CTU No. 1, Test 1, the measured permanent deformations were flats 18 inches wide at both the OCA top and bottom. Further, for HalfPACT ETU, Free Drop Test 1, presented in Table 2.10.3-2, the measured permanent deformations were flats 16 inches wide at the OCA top, and 18 inches wide at the OCA bottom. Finally, for HalfPACT ETU, Free Drop Test 3, also presented in Table 2.10.3-2, the measured permanent deformations were flats 18 inches wide at both the OCA top and bottom.

2.10.3.7.2.2 CTU Free Drop Test No. 2

Free Drop No. 2 was a HAC free drop from a height of 30 feet, impacting horizontally on the CTU side, with the OCV vent port oriented downward. As shown in Figure 2.10.3-10, the CTU was oriented horizontal to the impact surface (meridional angle (i.e., pitch) = 0°), and circumferentially aligned to impact directly onto the OCV vent port. The following list summarizes the test parameters:

- verified meridional angle as 0° ±1°
- verified circumferential angle to be 0° ±1°
- verified free drop height as 30 feet, +3/-0 inches (actual drop height 30 feet, 1 inch)
- measured temperature at 50 °F at time of test
- conducted test at 11:32 a.m. on Tuesday, 3/17/98

A small rebound (bounce) occurred upon impact. The measured permanent deformation of the CTU were flats 37 inches wide at both the OCA top and bottom, corresponding to a crush depth of approximately 3¾ inches. In comparison, from the TRUPACT-II SAR for CTU No. 1, Test 2, the measured permanent deformation were flats 37 inches wide at the OCA top, and 35 inches wide at the OCA bottom. Further, for HalfPACT ETU, Free Drop Test 2, presented in Table 2.10.3-2, the measured permanent deformations were flats 36 inches wide at the OCA top, and 33 inches wide at the OCA bottom. Finally, for HalfPACT ETU, Free Drop Test 3, also presented in Table 2.10.3-2, the measured permanent deformations were flats 34 inches wide at both the OCA top and bottom.

2.10.3.7.2.3 CTU Free Drop Test No. 3

Free Drop No. 4 was a HAC free drop from a height of 30 feet, impacting 5° from horizontal with primary impact on the lid and secondary impact on a body tie-down lug. As shown in Figure 2.10.3-10, the CTU was oriented at an angle 5° from horizontal relative to the impact surface (meridional angle (i.e., pitch) = 5°), and circumferentially aligned to impact 147½° from the OCA vent port (aligned with a tie-down lug). The following list summarizes the test parameters:

- verified meridional angle as 5° ±1°
- verified circumferential angle to be 147½° ±1°
- verified drop height as 30 feet, +3/-0 inches (actual drop height 30 feet, 1 inch)
- measured temperature at 41 °F at time of test
- conducted test at 11:50 a.m. on Wednesday, 3/18/98

A small rebound (bounce) occurred upon impact. The measured permanent deformation of the CTU was a flat 41½ inches wide at the OCA top, corresponding to a crush depth at the OCA lid of approximately 4¼ inches. In comparison, from the TRUPACT-II SAR for CTU No. 2, Test 1, the measured permanent deformation was a flat 45 inches wide at the OCA top. Also, from the TRUPACT-II SAR for CTU No. 3, Test 1, the measured permanent deformation was a flat 48 inches wide at the OCA top. Note that Tests 1 for TRUPACT-II CTU Nos. 2 and 3 were performed at cold temperature conditions (-20 °F). Had the TRUPACT-II slapdown drops been performed at ambient temperature conditions such as the case for HalfPACT CTU, Free Drop Test 3, the corresponding TRUPACT-II deformations would have been greater. These results correspond with the discussions from Section 2.10.3.5.2.4, *Closure (Lid) Separation*, where it is shown that TRUPACT-II slapdown drop testing bounds HalfPACT slapdown drop testing.

Of final note, approximately two inches of separation of the OCA Z-flanges was measured. The magnitude of this separation corresponds to the amount observed during TRUPACT-II slapdown testing. Regardless, the generous overlap of the OCA outer thermal shield provided sufficient protection of the OCA Z-flange gap for the subsequent fire test.

2.10.3.7.2.4 CTU Puncture Drop Test No. 4

Puncture Drop No. 4 impacted directly onto the OCV vent port opening, compounding the cumulative damage created by Free Drop Tests 1 and 2. As shown in Figure 2.10.3-10, the CTU was oriented at an angle 1½° from horizontal relative to the impact surface (meridional angle (i.e., pitch) = 1½°), and circumferentially aligned to impact directly onto the OCV vent port. The following list summarizes the test parameters:

- verified meridional angle as 1½° ±1° (i.e., package top-end slightly raised)
- verified circumferential angle to be 0° ±1°
- verified puncture drop height as 40 +1/-0 inches (actual drop height 40½ inches)
- measured temperature at 42 °F at time of test
- conducted test at 10:24 a.m. on Thursday, 3/19/98

The puncture drop impacted the OCA outer shell in the region damaged by Free Drop Tests 1 and 2, directly onto the OCV vent port. The measured permanent deformation of the CTU was a non-penetrating radial dent 3¾ inches deep. In comparison, from the TRUPACT-II SAR for CTU No. 1, Test 5, the measured permanent deformation was a non-penetrating radial dent 3 inches deep. Further, for HalfPACT ETU, Free Drop Test 8, presented in Table 2.10.3-2, the measured permanent deformation was a non-penetrating radial dent 2½ inches deep. Regardless of the greater radial deformation noted for the HalfPACT CTU, OCV vent port region, subsequent fire and helium leakage rate testing demonstrated that containment integrity was maintained.

2.10.3.7.2.5 CTU Puncture Drop Test No. 5

Puncture Drop No. 5 impacted directly above the 3/8-to-1/4-inch transition in the OCA body outer shell. As shown in Figure 2.10.3-10, the CTU was oriented at an angle 16° from horizontal relative to the impact surface (meridional angle (i.e., pitch) = 16°), and circumferentially aligned to impact 250° from the OCA vent port. This orientation placed the puncture bar impact directly adjacent to and above the 3/8-to-1/4-inch thick transition in the OCA body outer shell (i.e., on the 3/8-inch thick shell). The following list summarizes the test parameters:

- verified meridional angle as 16° ±1°
- verified circumferential angle to be 250° ±1°
- verified puncture drop height as 40 +1/-0 inches (actual drop height 40⅛ inches)
- measured temperature at 52 °F at time of test
- conducted test at 3:48 p.m. on Thursday, 3/19/98

The puncture drop impacted the OCA outer shell in a region with no previous damage. The measured permanent deformation of the CTU was a circumferential tear along the 3/8-to-1/4 transition weld, approximately 23 inches long and 4 inches deep radially. In comparison, the measured permanent deformation of the ETU was a circumferential tear along the 3/8-to-1/4 transition weld, approximately 27 inches long and 5½ inches deep radially. No applicable comparison is available from the TRUPACT-II SAR.

2.10.3.7.2.6 CTU Puncture Drop Test No. 6

Puncture Drop No. 6 impacted directly below the 3/8-to-1/4-inch transition in the OCA body outer shell. As shown in Figure 2.10.3-10, the CTU was oriented at an angle 23° from horizontal relative to the impact surface (meridional angle (i.e., pitch) = 23°), and circumferentially aligned to impact 110° from the OCA vent port (between the tie-down lugs, with the forklift pockets oriented horizontally). This orientation placed the puncture bar impact directly adjacent to and below the 3/8-to-1/4-inch thick transition in the OCA body outer shell (i.e., on the 1/4-inch thick shell). The following list summarizes the test parameters:

- verified meridional angle as 23° ±1°
- verified circumferential angle to be 110° ±1°
- verified puncture drop height as 40 +1/-0 inches (actual drop height 40¼ inches)
- measured temperature at 52 °F at time of test
- conducted test at 12:19 p.m. on Friday, 3/20/97

The puncture drop impacted the OCA outer shell in a region with no previous damage. The measured permanent deformation of the CTU was a non-penetrating radial dent 3½ inches deep. In comparison, the measured permanent deformation of the HalfPACT ETU was a hole 10½ inches long and 11½ inches wide, measuring 8 inches deep radially and 11 inches deep along the axis of the puncture bar. Rather than penetrating, the puncture bar slid on the surface of the OCA outer shell until sufficient offset was achieved to allow the HalfPACT CTU to roll off the puncture bar. This result was due to lengthening the 3/8-inch thick, OCA outer shell from 12 to 18 inches, correspondingly changing the impact angle sufficiently to prevent penetration through the adjacent 1/4-inch thick shell.

2.10.3.7.2.7 CTU Fire Test No. 7

Fire No. 7 was performed to demonstrate packaging compliance with the requirements of 10 CFR 71, and followed the guidelines set forth in IAEA Safety Series No. 37. The following list summarizes the test parameters:

- Consistent with the TRUPACT-II SAR and the HalfPACT ETU, the HalfPACT CTU was oriented on an insulated test stand (identical to the test stand used for TRUPACT-II and HalfPACT ETU fire testing) such that the most severe damage was approximately 1½ meters above the fuel surface. The most severe damage was determined to be from the cumulative effects of free drop tests 1 and 2, and puncture drop test 4, followed by additional damage due to puncture drop test 5. With a circumferential orientation of 305° (see Figure 2.10.3-10), the damage from the two sets of tests were located 1½ meters above the fuel surface.
- Consistent with Paragraph A-628.4 of IAEA Safety Series No. 37, the HalfPACT CTU was installed onto the insulated test stand at an elevation to place the lowest part of the package one meter above the fuel surface. The CTU was oriented horizontally on the test stand to maximize heat input.
- Consistent with Paragraph A-628.4 of IAEA Safety Series No. 37, requiring the test pool to extend 1 to 3 meters beyond the package edges, the test pool size extended approximately 1½ meters beyond each side of the CTU.
- Consistent with Paragraph A-628.5 of IAEA Safety Series No. 37, requiring wind speeds not to exceed 2 m/s (4.5 mph), a balloon was released that demonstrated both ground level and 1,000 feet altitude wind speeds under 5 mph at the start of the fire test. Weather conditions included relatively clear skies, without precipitation for the duration of the fire test. Further, wind baffles were erected to surround the test pool to reduce the possible effects of wind gusts. The time-averaged wind speed during the fire test was approximately 8 mph outside the test area, corresponding to approximately 4 mph inside the test area.
- Consistent with Paragraphs A-628.6 and A-628.8 of IAEA Safety Series No. 37, a JP4-type fuel was used for the fire test, and the amount of fuel was controlled to ensure the fire duration exceeded 30 minutes. The fuel was floated on a pool of water approximately 1/2 meter deep to ensure even distribution during burning. The fire test lasted approximately 33 minutes, and burning continued for approximately 30 minutes after the end of the fire.
- Consistent with Paragraphs A-628.7 and A-628.9 of IAEA Safety Series No. 37, the test pool was instrumented to measure fire temperatures and heat fluxes at various locations around the CTU. Temperatures and heat fluxes were monitored before, during, and following the

fire test until magnitudes stabilized back to ambient conditions. The average measured flame temperature was 1,486 °F.

- Consistent with Paragraph A-628.10 of IAEA Safety Series No. 37, the CTU containment O-ring seals were leakage rate tested following performance testing to verify containment integrity. Discussions regarding post-test leakage rate testing are provided in Section 2.10.3.7.2.8, *CTU Post-Test Disassembly*.
- Commenced fire testing (fire ignition) at 7:54 a.m. on Tuesday, 4/14/98. The ambient temperature was 51 °F at the start of the fire test.

No active temperature measuring devices were employed prior to, during, or following the HAC fire test. Further, measurement of the OCA outer shell temperature does not represent the OCV or ICV temperatures due to the large internal mass and thick, thermally insulating foam used within the OCA. As discussed in Section 3.1.1, *Packaging*, the temperatures of the OCV, ICV, and payload are effectively decoupled from the OCA outer shell and polyurethane foam for short term thermal transients. Instead, the initial temperature of the CTU may be estimated based on the ambient temperature of the Sandia National Laboratory testing facilities in the six weeks prior to the HAC fire test[17]. Climatological data for Albuquerque, New Mexico, during the month of March and first two weeks of April 1998 shows an average temperature of 48 °F for those six weeks. Thus, when adjusting for the elevation difference between the testing facilities and Albuquerque, the initial temperature for fire testing is taken as 43 °F.

As stated in Section 3.5.1.1, *Analytical Model*, the initial condition temperatures for the HAC fire test are presented in Table 3.5-1. Accordingly, the average temperature of the ICV wall and OCV wall is 133 °F and 131 °F, respectively. Therefore, the difference between the theoretical pre-fire package temperature and actual adjusted starting temperature is conservatively taken as 133 °F - 43 °F = 90 °F.

The CTU utilized passive, non-reversible temperature indicating labels at various locations near each containment vessel's seal flanges to record temperatures from the HAC fire test. Each set of temperature indicating labels recorded temperatures in 40 steps from 105 °F to 500 °F. As illustrated in Figure 2.10.3-11, some locations used redundant sets of temperature labels to ensure comprehensive results at critical regions.

A summary of temperature indicating label temperatures is presented in Table 2.10.3-4. The maximum measured OCV seal region temperature was 200 °F. Upwardly adjusting for the lower, pre-fire starting temperature by 90 °F results in a projected maximum OCV seal region temperature of 290 °F. The maximum measured ICV seal region temperature was 110 °F. Similarly adjusting for the lower, pre-fire starting temperature by 90 °F results in a projected maximum ICV seal region temperature of 200 °F. In comparison, certification testing of the TRUPACT-II package showed a maximum OCV seal region temperature of 260 °F, and a maximum ICV seal region temperature of 200 °F (see the TRUPACT-II SAR). As with the comparison of measurements of drop damage, fire temperatures between the two similar package designs agree very well.

[17] CTU was located at Sandia National Laboratories' Coyote Canyon drop test facility for the month of March, 1998, and the Lurance Canyon burn facility for the first two weeks of April, 1998. CTU was burned on April 14, 1998. The elevation difference between the two test facilities and the city of Albuquerque results in an average ambient temperature approximately 5 °F cooler than Albuquerque.

Two final observations are notable regarding fire testing. First, changing the OCV vent and seal test port thermal plugs from polyurethane foam to ceramic fiber paper material appears to have benefited the corresponding port plugs (compare ETU Figure 2.10.3-45, Figure 2.10.3-46, and Figure 2.10.3-47 to CTU Figure 2.10.3-84, Figure 2.10.3-86, and Figure 2.10.3-87). Second, with reference to Table 2.10.3-4, the temperature indicating labels (Nos. 3 and 7) at circumferential angle $\phi = 250°$ read substantially lower temperatures than all other OCV locations. The reason is not known since the 250° location was positioned in the hottest location in the fire (i.e., 1½ meters above the fuel surface).

2.10.3.7.2.8 CTU Post-Test Disassembly

Post-test disassembly of the HalfPACT CTU was performed during the week of Monday, 4/26/98, through Friday, 5/8/98. To limit potentially misleading peripheral damage to the CTU during post-test disassembly, only abrasive cutting methods were utilized.

As with the ETU, upon removal of the OCA lid and body outer shells, the presence of several inches of very light density foam char that showed the intumescent behavior of the polyurethane foam. Undamaged foam thicknesses in the OCA lid closely paralleled those measured for the HalfPACT ETU. An average of 11 inches of undamaged foam was measured throughout the crown region of the OCA lid torispherical head, and 9 inches of undamaged foam in the knuckle region. In regions remote from side drop damage, an average of 5 inches of undamaged foam was measured through the OCA lid side. In regions of side drop damage, an average of 3 inches of undamaged foam was measured through the OCA lid side. On a per-volume basis estimate, more than 80% of the polyurethane foam in the OCA lid remained undamaged.

Similarly, approximately 6½ inches of undamaged foam was measured at the bottom center of the OCA body. In regions remote from side drop damage, an average of 8 inches of undamaged foam was measured through the OCA body side. In regions of side drop damage, an average of 4½ inches of undamaged foam was measured through the OCA body side. On a per-volume basis estimate, more than 70% of the polyurethane foam in the OCA body remained undamaged. More undamaged foam remained in the OCA body for the CTU than for the ETU. This effect was most likely due to the presence of more wind during the CTU fire test, blowing from the package bottom toward the top. Regardless, the package closure region remained fully engulfed in the fire for the duration of the fire test.

In comparison, the TRUPACT-II packaging certification test units exhibited nearly identical amounts of undamaged polyurethane foam with a minimum of 5 inches remaining around the OCV except in localized regions damaged by free and puncture drops.

Upon removal of all the remaining polyurethane foam and ceramic fiber paper material, the OCV lid and body appeared lightly damaged. Some minor flattening was noted along the axes of the three free drops (i.e., free drop tests 1, 2, and 3). Thus, as with the ETU, damage to the OCV was mostly due to external application of force (i.e., due to the free drop and puncture drop tests). As with the ETU, the ICV, however, appeared to have greater deformation coinciding with the axes of the 55-gallon payload drums. In contrast to the OCV, damage to the ICV was mostly due to an internal application of force caused by the greater weight capacity of the HalfPACT payload drums compared to that of the TRUPACT-II payload drums. The result was that the HalfPACT CTU ICV exhibited larger permanent deformation than compared to that of

the TRUPACT-II CTUs. Several of the 55-gallon payload drums were distorted sufficiently to cause loss of their lids, as similarly noted for TRUPACT-II certification testing.

Demonstration of containment vessel leaktightness was accomplished by installing 1/2 NPT ports through the knuckle region of the OCV and ICV lid torispherical heads to allow evacuation and subsequent backfill of each corresponding containment vessel cavity with helium gas. This method ensured helium gas was present behind each containment seal, thereby validating the testing process. Helium leakage rate testing was also performed on the metallic containment boundaries following testing of the CTU. Helium leakage rate testing of each containment boundary was accomplished by welding each containment component (i.e., lid and body structure) to a flat steel plate. Each containment component was evacuated, tented with helium gas, and helium leakage rate tested to demonstrate containment integrity. Results of successful mass spectrometer helium leakage rate testing are summarized below:

Sealing Component	OCV	ICV
Main O-ring Seal	$<1.0 \times 10^{-8}$ cc/s, helium	$<1.0 \times 10^{-8}$ cc/s, helium
Vent Port Plug O-ring Seal	$<1.0 \times 10^{-8}$ cc/s, helium	$<1.0 \times 10^{-8}$ cc/s, helium
Lid Structure	3.5×10^{-8} cc/s, helium	$<1.0 \times 10^{-8}$ cc/s, helium
Body Structure	4.2×10^{-8} cc/s, helium	1.3×10^{-7} cc/s, helium

When accounting for the conversion between air leakage (per ANSI N14.5) and helium leakage, a 2.6 factor applies for standard temperatures and pressures. Thus, a reported helium leakage rate of 1.3×10^{-7} cc/s, helium, is equivalently 5×10^{-8} cc/s, air, a magnitude well below the "leaktight" criterion of 1×10^{-7} cc/s, air, per ANSI N14.5.

As with the ETU, the ICV wiper O-ring seal ring was damaged somewhat (buckled) in several locations due to failure of several drive screws. Thus, some of the payload drum filler material appeared to be forced into the region above the wiper O-ring seal. Both the damage to the wiper seal ring and presence of residual material in the wiper seal region were identically noted for the TRUPACT-II CTUs. As noted earlier, however, all containment O-ring seals successfully passed subsequent helium leakage rate testing due to the beneficial presence of the foam debris seal, thereby clearly demonstrating that containment integrity was maintained.

In general, damage to the CTU closely paralleled damage to the ETU. The only exception noted was for the OCV vent port region. Visual inspection of the OCV vent port fitting determined that the inner groove weld was cracked approximately 1/3 of its circumferential length. Upon closer visual inspection of the 5/16-inch inner groove weld, the weld size appeared below nominal size, possible due to excessive grinding of welded regions during fabrication. As noted earlier, both the ETU and CTU were fabricated from TRUPACT-II training units, i.e., production units with undersized welds in localized regions where excessive "flush" grinding sometimes significantly reduced the shell thickness. The only way to determine actual, as-tested, OCV vent port fitting weld sizes would be to "section" the fitting region, a process that was not performed. Of significance is that helium leakage rate testing determined that containment integrity was maintained due to the presence of the outer fillet weld. Therefore, although damaged during testing, the OCV vent port region nevertheless remained acceptably leaktight because of the double weld configuration.

In conclusion, with the aforementioned exception, overall damage to the HalfPACT CTU paralleled the measured damage from both HalfPACT ETU and TRUPACT-II certification testing, as expected.

Table 2.10.3-1 – TRUPACT-II / HalfPACT Comparison Using NUREG/CR-3966

Impact Angle (with respect to horizontal)	Axial, Shear, and Moment Forces at the OCV Locking Ring					
	Due to Primary Impact			Due to Secondary Impact		
	Axial Force, lb	Shear Force, lb	Moment, in-lb	Axial Force, lb	Shear Force, lb	Moment, in-lb
TRUPACT-II, Primary Impact on OCA Lid						
5°	121,225	465,347	$2.158(10)^7$	0	471,554	$2.186(10)^7$
10°	195,504	372,368	$1.727(10)^7$	0	471,036	$2.184(10)^7$
15°	251,344	315,030	$1.461(10)^7$	0	467,404	$2.167(10)^7$
20° (CTU Test, -20 °F)	302,679	279,288	$1.295(10)^7$	0	461,178	$2.138(10)^7$
47.7° (c.g. over corner)	738,279	223,251	$1.035(10)^7$			
TRUPACT-II, Primary Impact on OCA Body						
5°	118,730	455,768	$2.113(10)^7$	0	485,900	$2.253(10)^7$
10°	189,342	360,631	$1.672(10)^7$	0	485,275	$2.250(10)^7$
15°	244,441	306,378	$1.421(10)^7$	0	480,899	$2.230(10)^7$
18° (CTU Test, Ambient)	274,975	284,218	$1.318(10)^7$	0	477,148	$2.212(10)^7$
HalfPACT, Primary Impact on OCA Lid						
5°	115,380	7,431	$1.760(10)^7$	0	4,876	$1.157(10)^7$
10°	185,532	5,929	$1.407(10)^7$	0	4,866	$1.155(10)^7$
15°	235,898	4,961	$1.177(10)^7$	0	4,822	$1.144(10)^7$
37° (c.g. over corner)	451,020	3.373	$0.800(10)^7$			
HalfPACT, Primary Impact on OCA Body						
5°	112,409	7,240	$1.718\ (10)^7$	0	5,035	$1.195(10)^7$
10°	178,914	5,717	$1.357\ (10)^7$	0	5,022	$1.192(10)^7$
15°	227,810	4,791	$1.137\ (10)^7$	0	4,971	$1.180(10)^7$

Table 2.10.3-2 – Summary of HalfPACT ETU Test Results in Sequential Order①

Test No.	Test Description	Orientation		Test Temperature	Observations and Results
		θ②	ϕ③		
1	NCT 3' side drop opposite OCV vent port	0°	200°	53 °F	16"/18" flat at top/bottom; ~3/4" deep
2	HAC 30' side drop opposite OCV vent port	0°	200°	57 °F	36"/33" flat at top/bottom; ~3¼" deep
3	NCT 3' side drop on OCV vent port	0°	0°	40 °F	18"/18" flat at top/bottom; ~3/4" deep
4	HAC 30' side drop on OCV vent port	0°	0°	48 °F	34"/34" flat at top/bottom; ~3¼" deep
5	NCT 3' corner drop between tie-down lugs	43°	110°	53 °F	26" long × 5½" wide flat; ~1⅜ " deep
6	HAC 30' corner drop between tie-down lugs	43°	110°	55 °F	40" long × 12" wide flat; ~3¼" deep
7	Puncture drop below 3/8-to-1/4-inch transition	20°	200°	38 °F	10½" long × 11½" wide hole; ~8" deep
8	Puncture drop on OCV vent port	1°	0°	40 °F	~2½" deep dent
9	Puncture drop on damaged bottom corner	43°	110°	28 °F	~3" deep dent
10	Puncture drop above 3/8-to-1/4-inch transition	9°	290°	29 °F	~5½" deep dent; ~27" long weld tear
11	Fire with Test 1, 2, & 4 damage at hottest location	0°	146°	43 °F	~1,575 °F temperature; ~33 minutes

Notes:

① Tested 2/18/97 – 3/10/97.

② Meridional angle, θ, is relative to horizontal (i.e., side drop orientation).

③ Circumferential angle, ϕ, is relative to OCV vent port.

Table 2.10.3-3 – Summary of HalfPACT CTU Test Results in Sequential Order①

Test No.	Test Description	Orientation		Test Temperature	Observations and Results
		θ②	ϕ③		
1	NCT 3' side drop on OCV vent port	0°	0°	52 °F	13"/13" flat at top/bottom; ~1/2" deep
2	HAC 30' side drop on OCV vent port	0°	0°	50 °F	37"/37" flat at top/bottom; ~3¾" deep
3	HAC 30' slapdown drop on OCA lid/tie-down lug	5°	147½°	41 °F	41½" flat at top; ~4¾" deep at top
4	Puncture drop on OCV vent port	1½°	0°	42 °F	~3¾" deep dent
5	Puncture drop above 3/8-to-1/4-inch transition	16°	250°	52 °F	~4" deep dent; ~23" long weld tear
6	Puncture drop below 3/8-to-1/4-inch transition	23°	110°	52 °F	~3½" deep dent (no penetration)
7	Fire with Test 1, 2, & 4 damage at hottest location	0°	146°	43 °F	~1,485 °F temperature; ~33 minutes

Notes:

① Tested 3/16/98 – 4/14/98.

② Meridional angle, θ, is relative to horizontal (i.e., side drop orientation).

③ Circumferential angle, ϕ, is relative to OCV vent port.

Table 2.10.3-4 – Summary of HalfPACT CTU Temperature Indicating Label Readings

Temperature Indicating Label Location and Circumferential Angle, ϕ	Label Number	Temperature
OCV Conical Shell at 0° (OCV Vent Port Seal) – Free Drop Tests 1 & 2, and Puncture Drop Test 4	1a, 1b	180 °F, 170 °F
OCV Conical Shell at 110° – Puncture Drop Test 6	2	180 °F
OCV Conical Shell at 250° – Puncture Drop Test 5	3	130 °F
OCV Seal Flange at 0° (Main OCV Seals) – Free Drop Tests 1 & 2, and Puncture Drop Test 4	4a, 4b	200 °F, 200 °F
OCV Seal Flange at 110° (Main OCV Seals) – Puncture Drop Test 6	5	200 °F
OCV Seal Flange at 147½° (Main OCV Seals) – Free Drop Test 3	6	180 °F
OCV Seal Flange at 250° (Main OCV Seals) – Puncture Drop Test 5	7	140 °F
ICV Seal Flange at 0° (ICV Vent Port Seal) – Free Drop Tests 1 & 2, and Puncture Drop Test 4	8	105 °F
ICV Seal Flange at 0° (Main ICV Seals) – Free Drop Tests 1 & 2, and Puncture Drop Test 4	9	105 °F
ICV Seal Flange at 110° (Main ICV Seals) – Puncture Drop Test 6	10	105 °F
ICV Seal Flange at 147½° (Main ICV Seals) – Free Drop Test 3	11	110 °F
ICV Seal Flange at 250° (Main ICV Seals) – Puncture Drop Test 5	12	110 °F

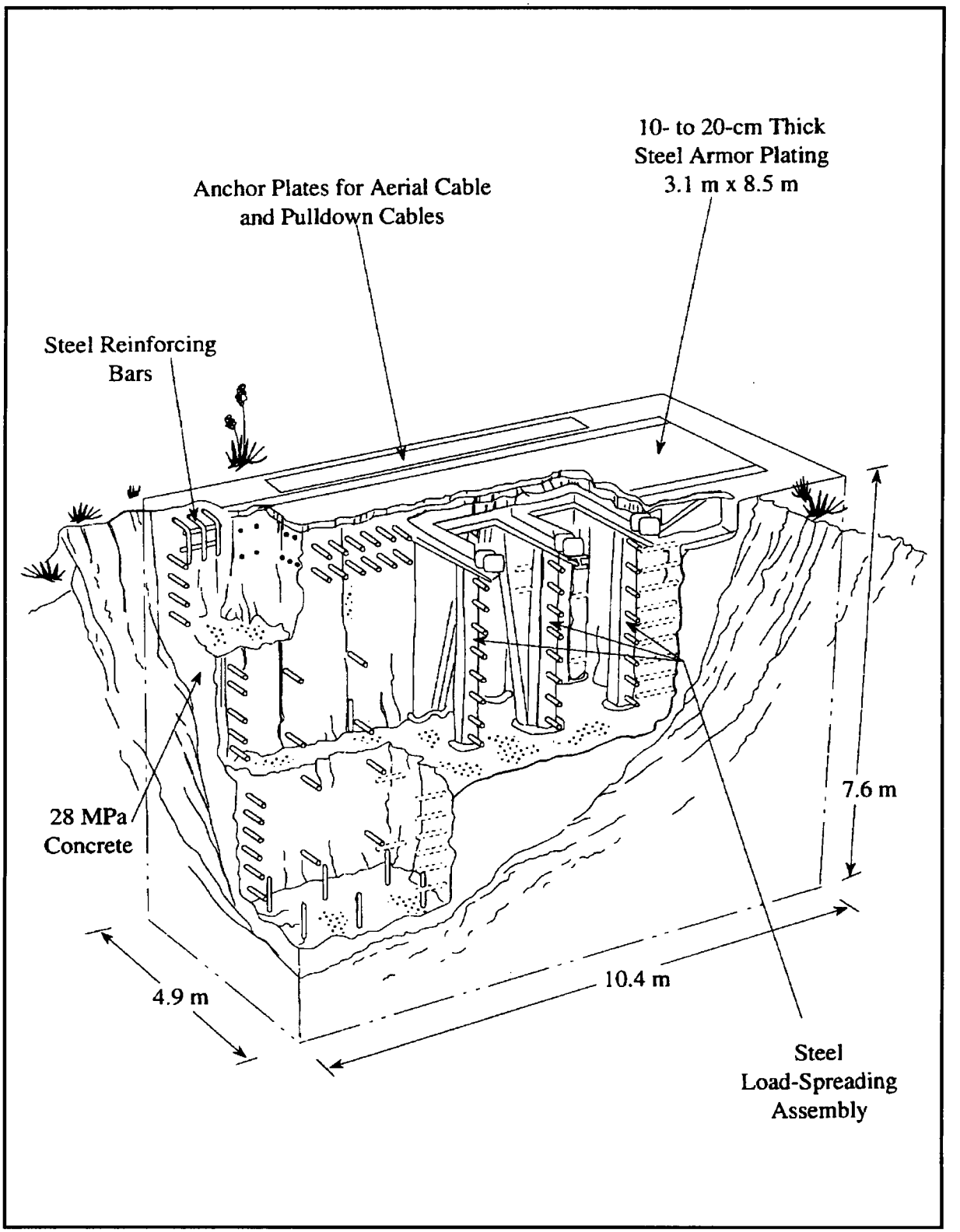

Figure 2.10.3-1 – Drop Pad at the Coyote Canyon Aerial Cable Facility

This page intentionally left blank.

Figure Withheld Under 10 CFR 2.390

Figure 2.10.3-2 – Design Comparison between a TRUPACT-II Packaging and a HalfPACT Packaging

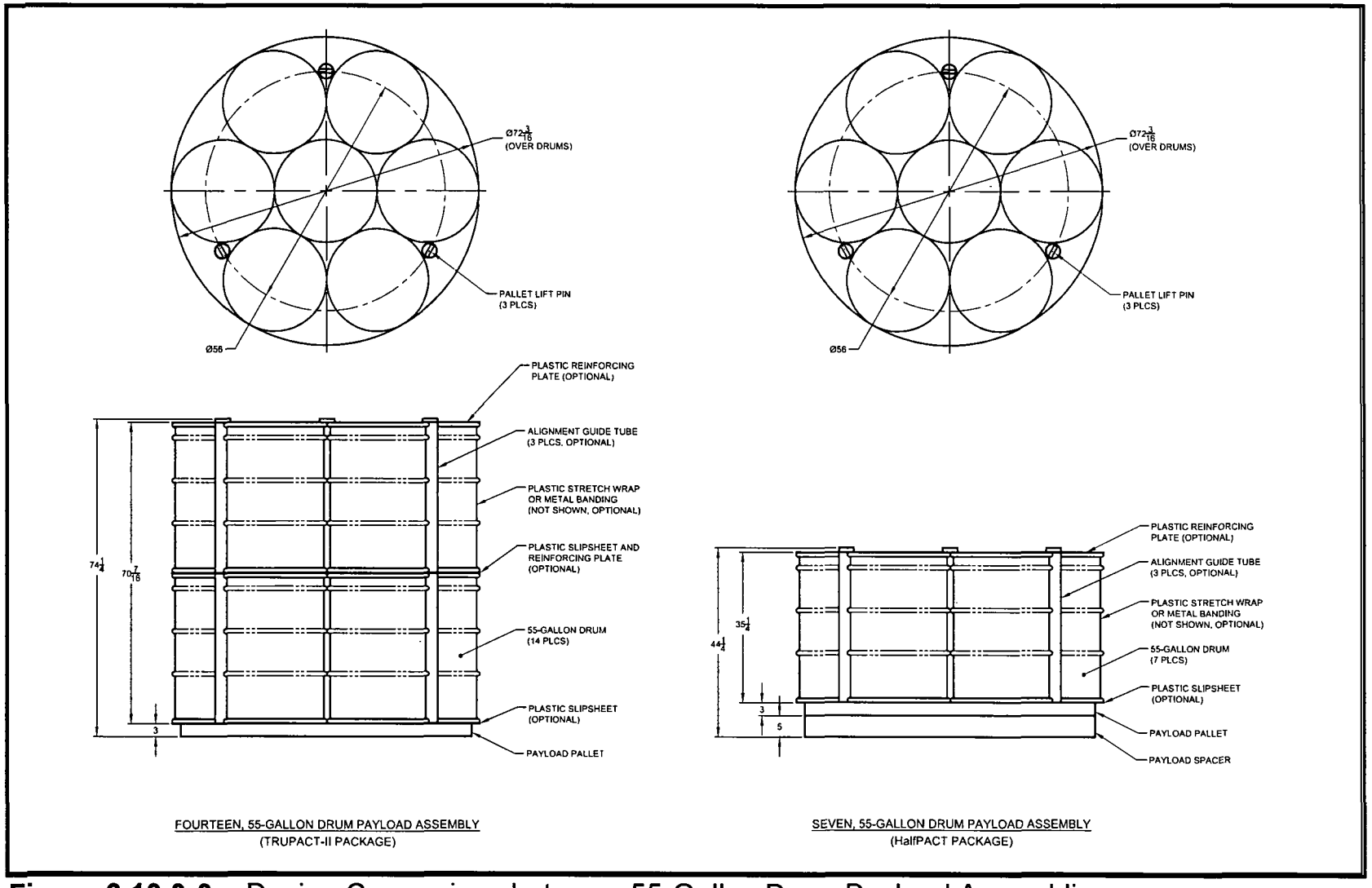

Figure 2.10.3-3 – Design Comparison between 55-Gallon Drum Payload Assemblies

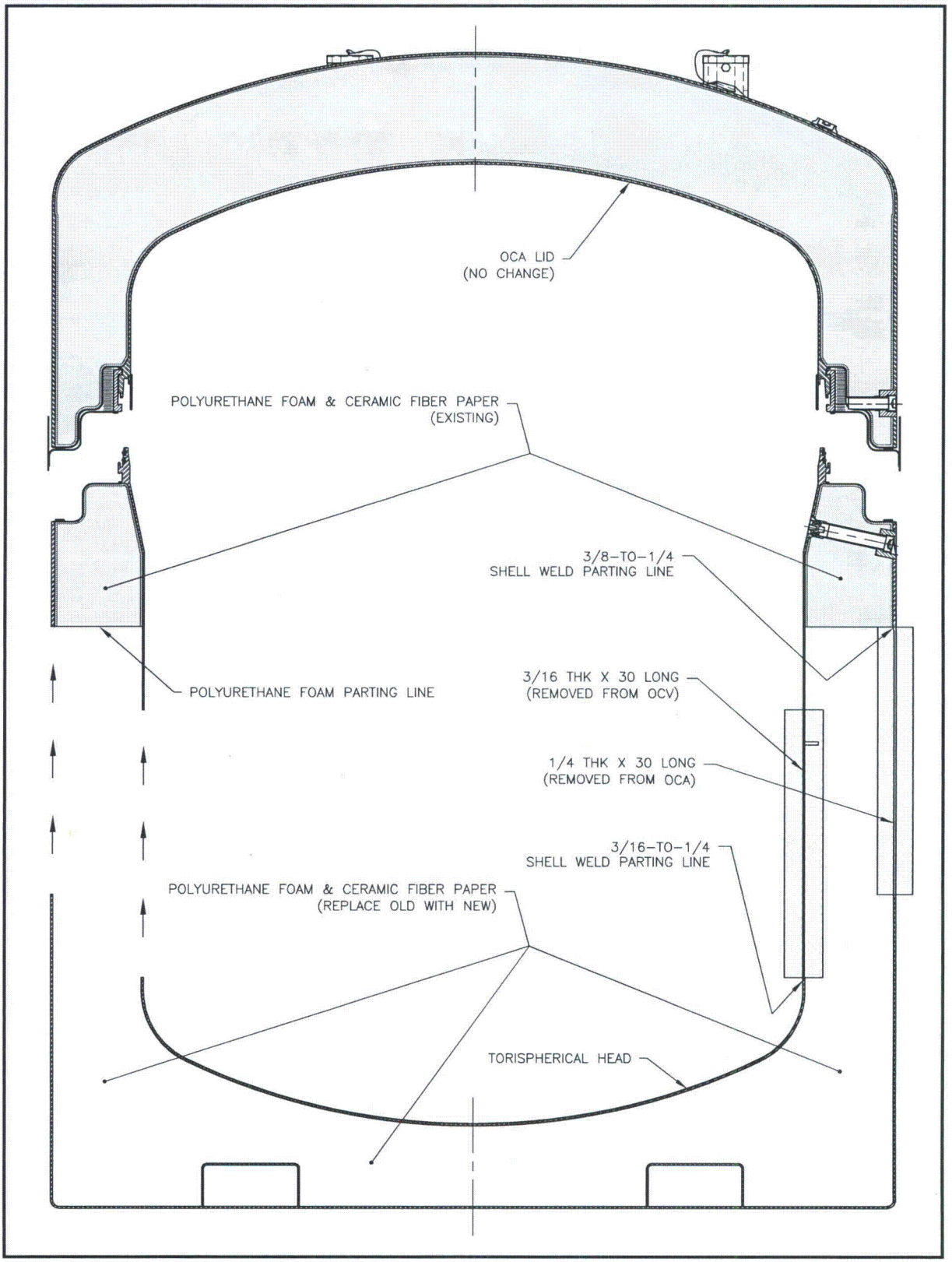

Figure 2.10.3-4 – Making the HalfPACT ETU OCA from TRUPACT-II Unit 104

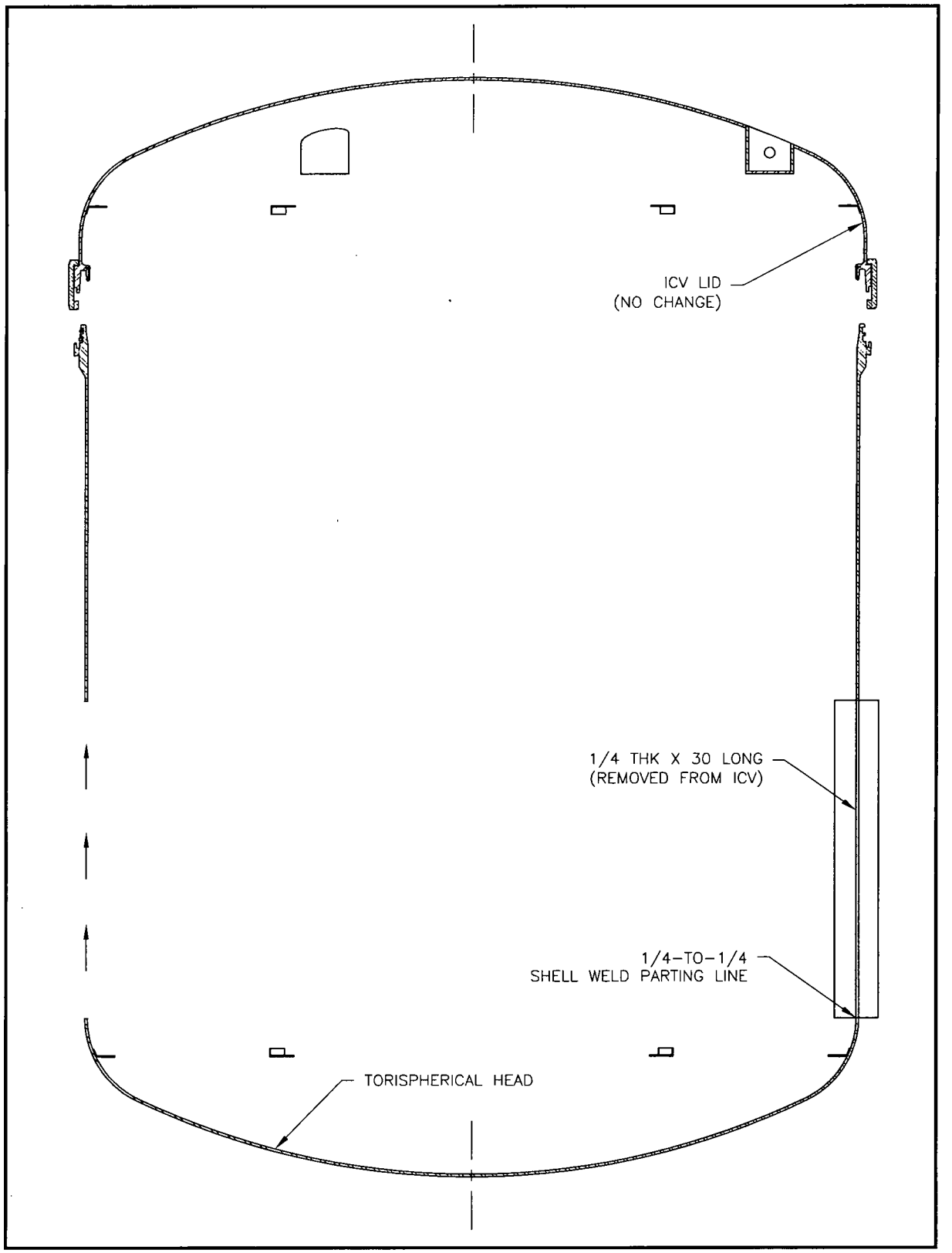

Figure 2.10.3-5 – Making the HalfPACT ETU OCA from TRUPACT-II Unit 104

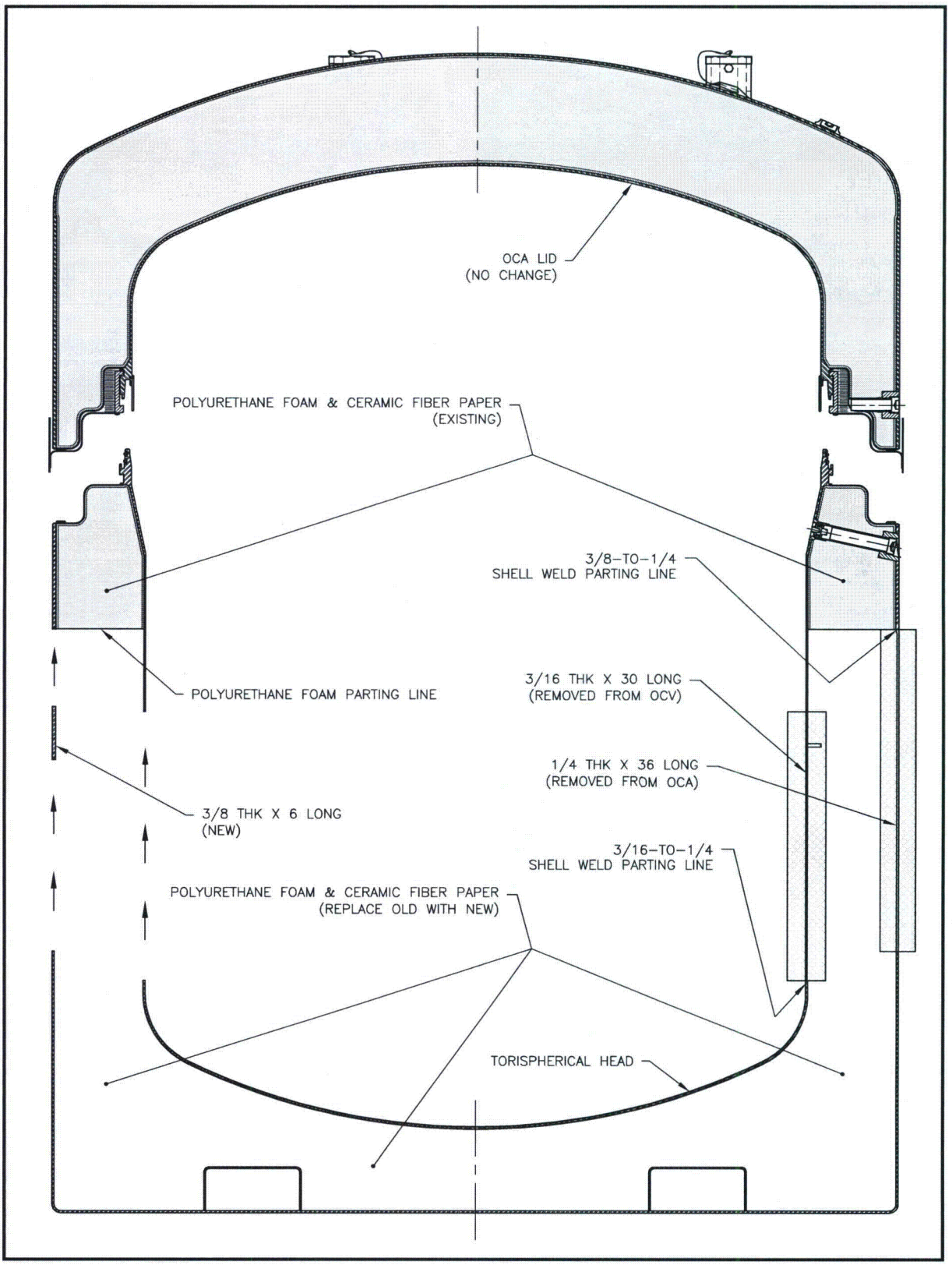

Figure 2.10.3-6 – Making the HalfPACT CTU OCA from TRUPACT-II Unit 107

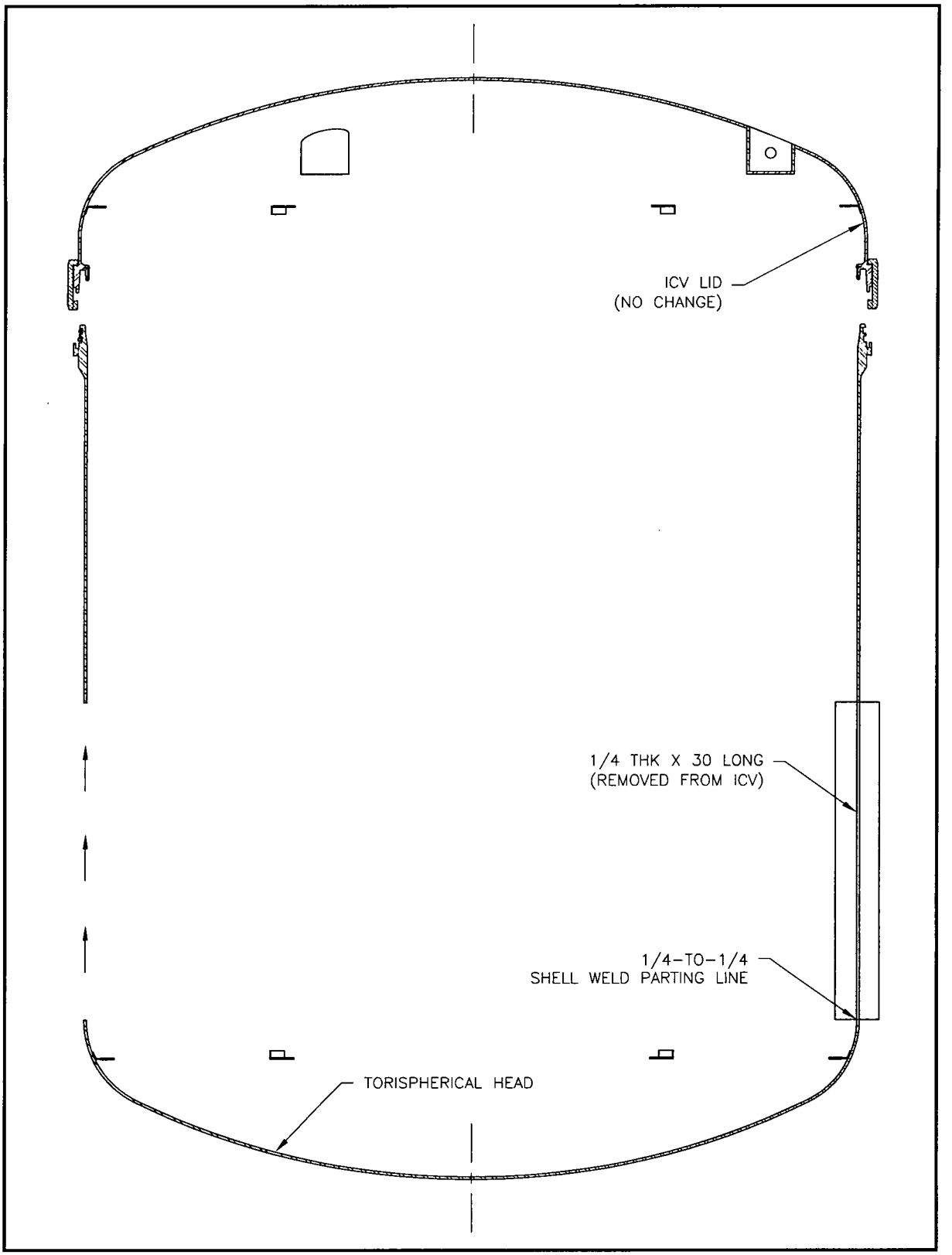

Figure 2.10.3-7 – Making the HalfPACT CTU ICV from TRUPACT-II Unit 107

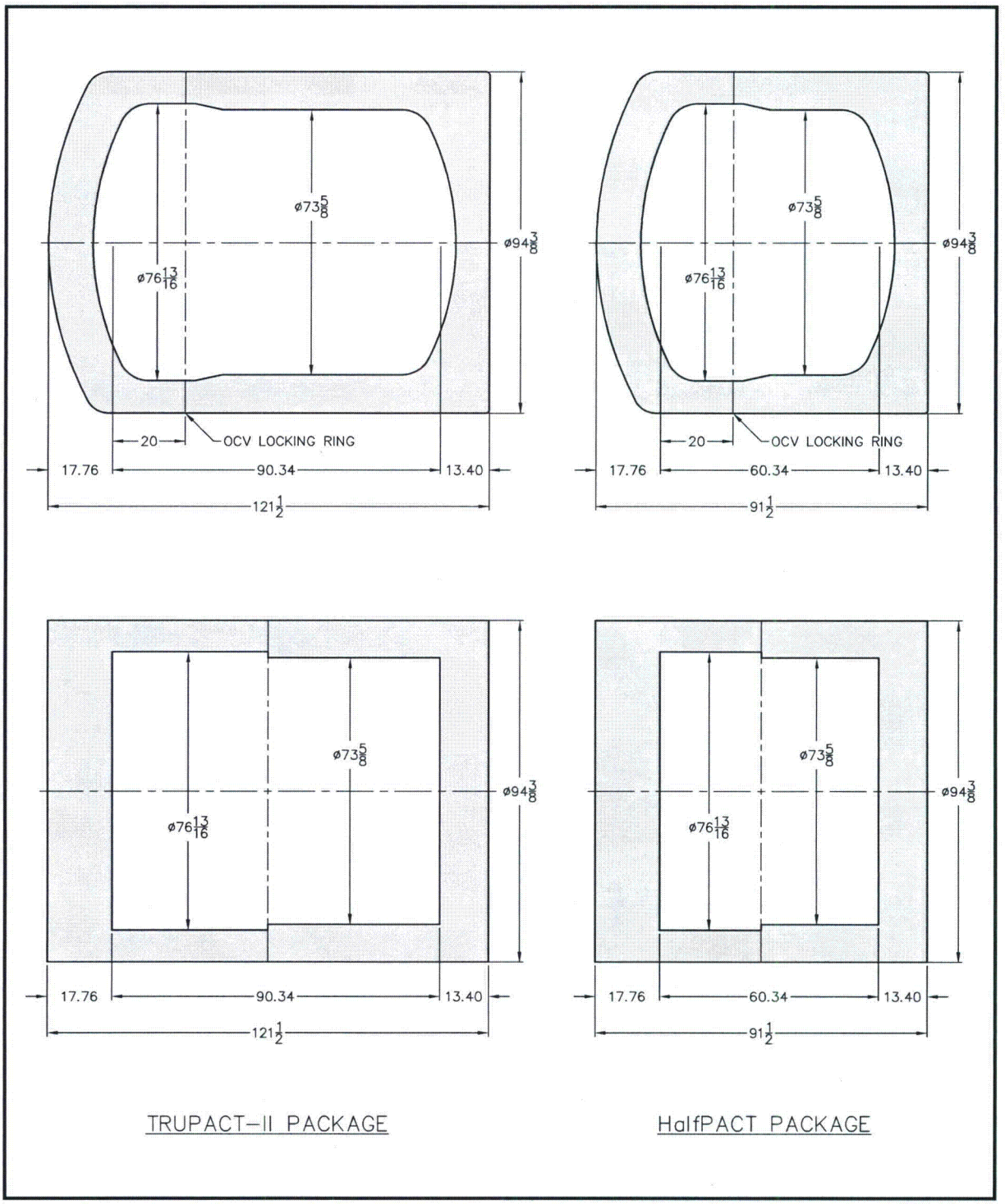

Figure 2.10.3-8 – Dimensional Comparison of TRUPACT-II and HalfPACT for NUREG/CR-3966 (Lower Figures are Simplifying Representations Used in *CASKDROP*)

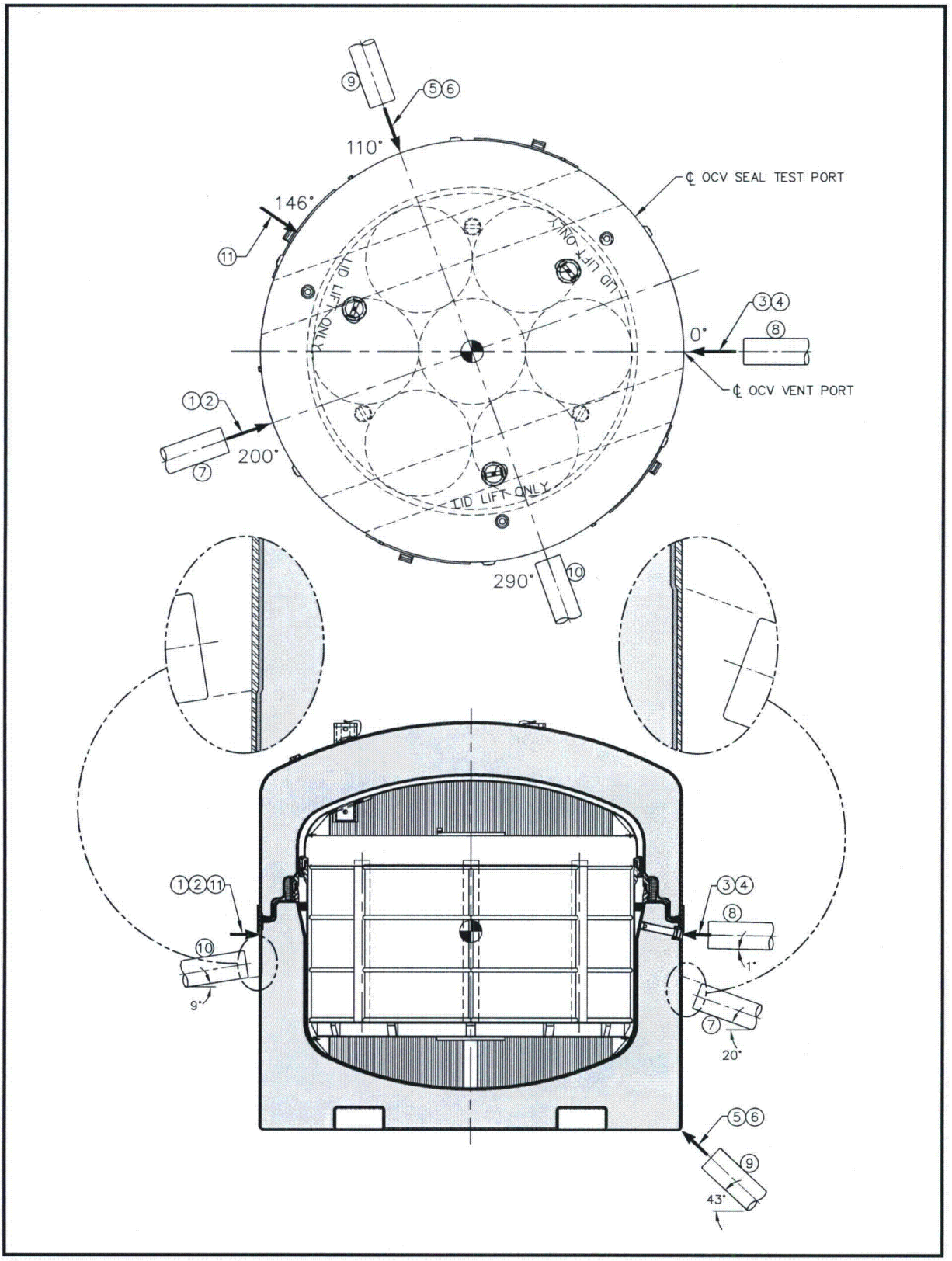

Figure 2.10.3-9 – Schematic of HalfPACT ETU Test Orientations

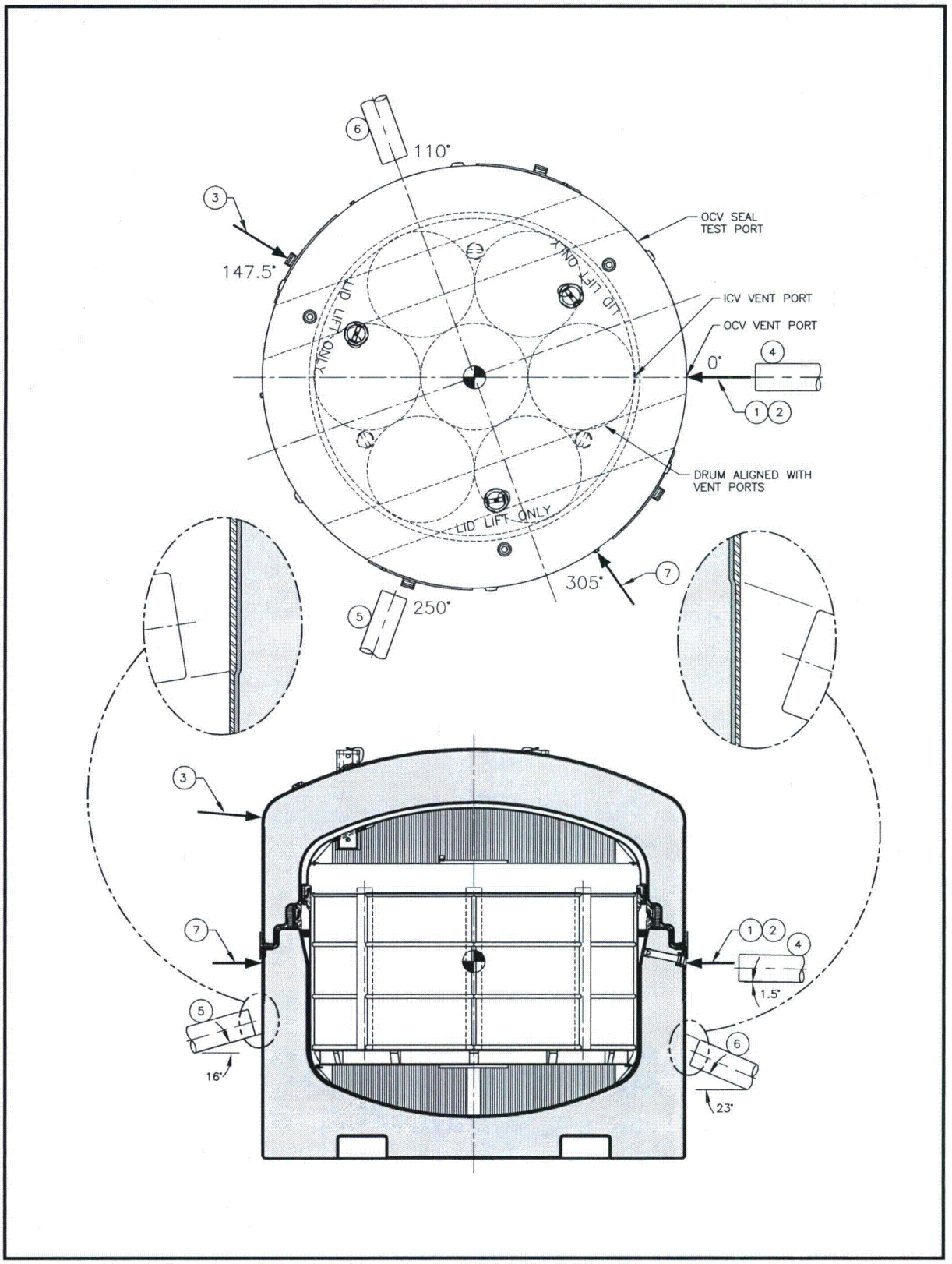

Figure 2.10.3-10 – Schematic of HalfPACT CTU Test Orientations

This page intentionally left blank.

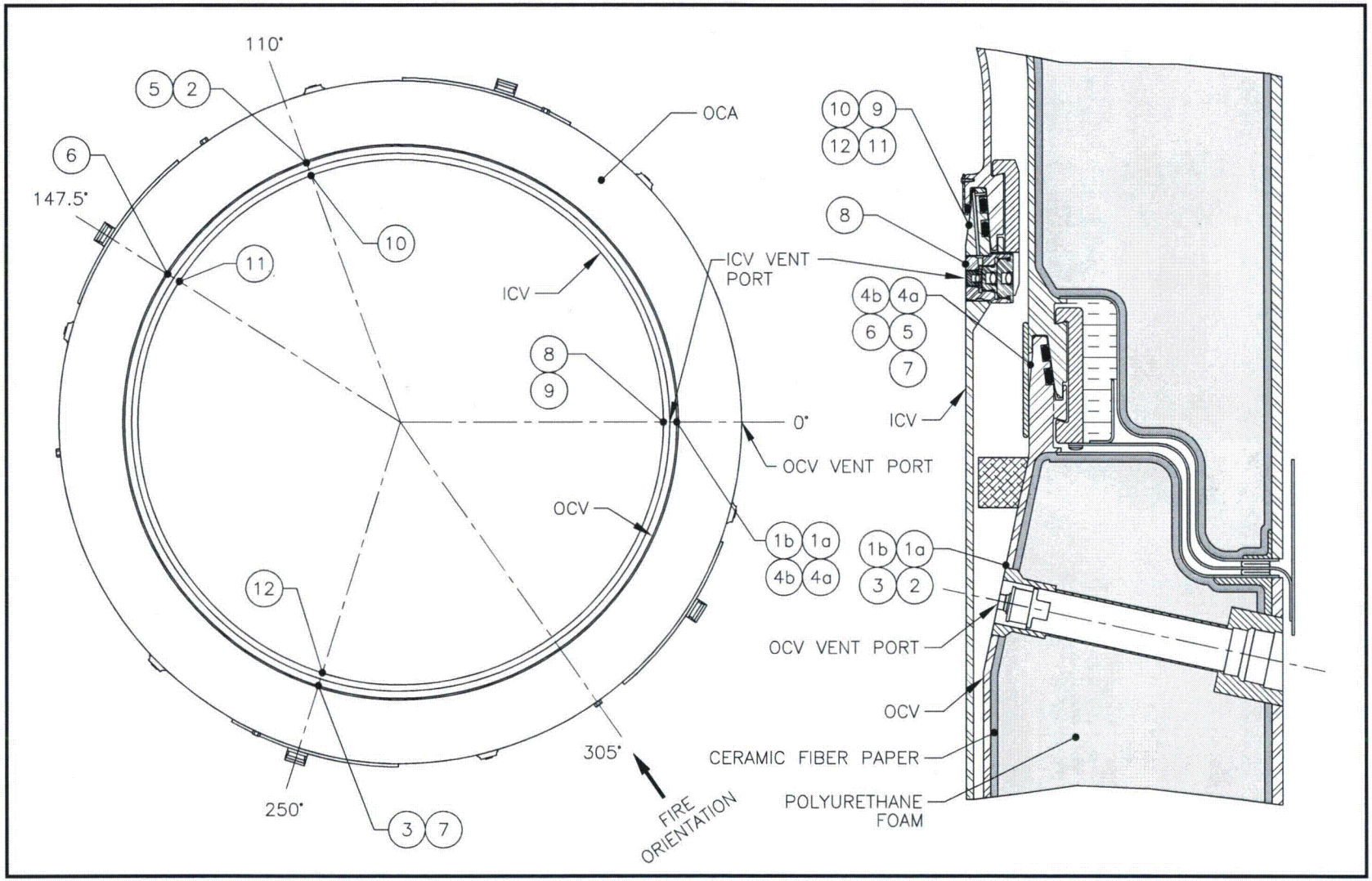

Figure 2.10.3-11 – Schematic of HalfPACT CTU Temperature Indicating Label Location

This page intentionally left blank.

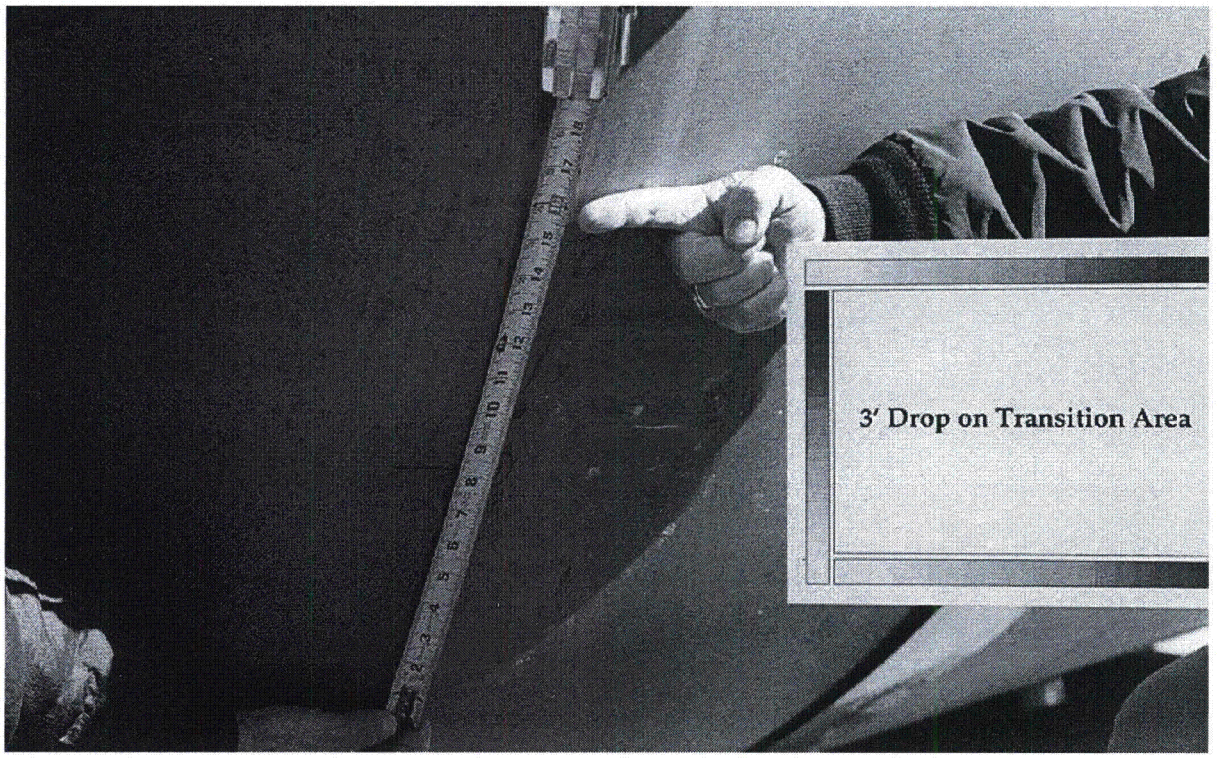

Figure 2.10.3-12 – ETU Free Drop Test 1; Top-End Damage; ~16" Wide Flat

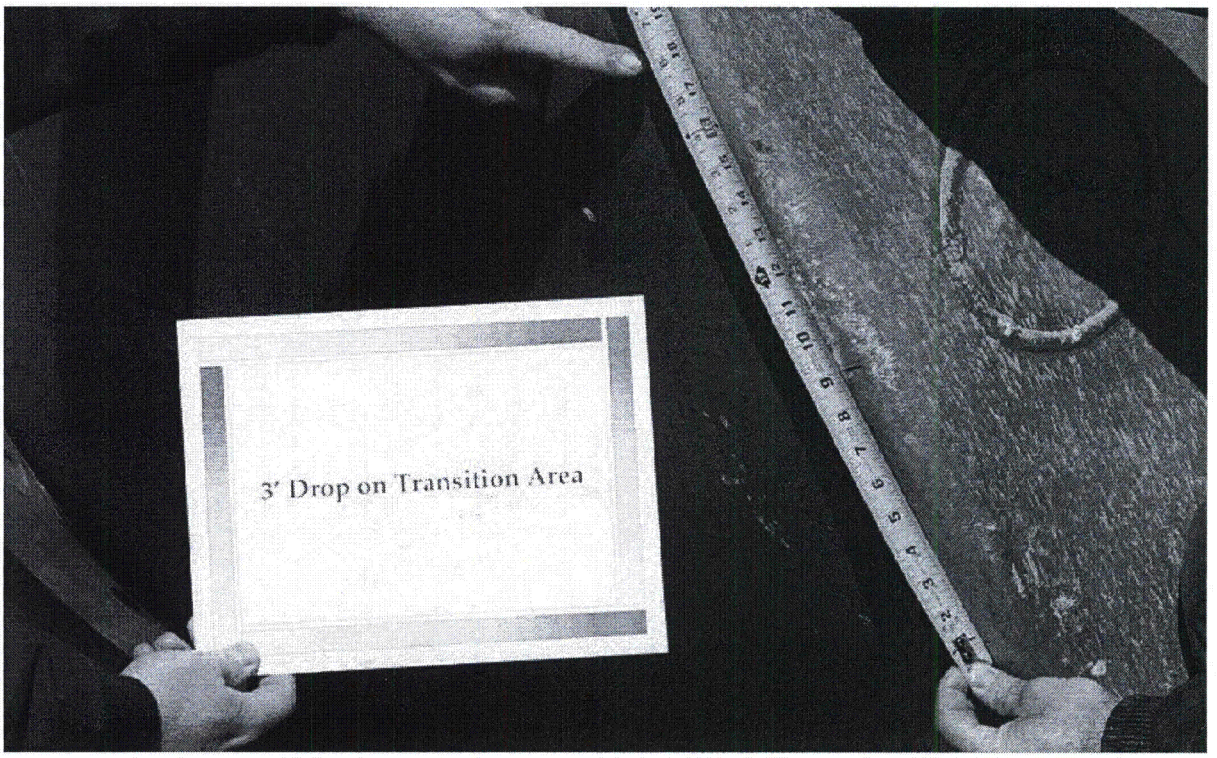

Figure 2.10.3-13 – ETU Free Drop Test 1; Bottom-End Damage; ~18" Wide Flat

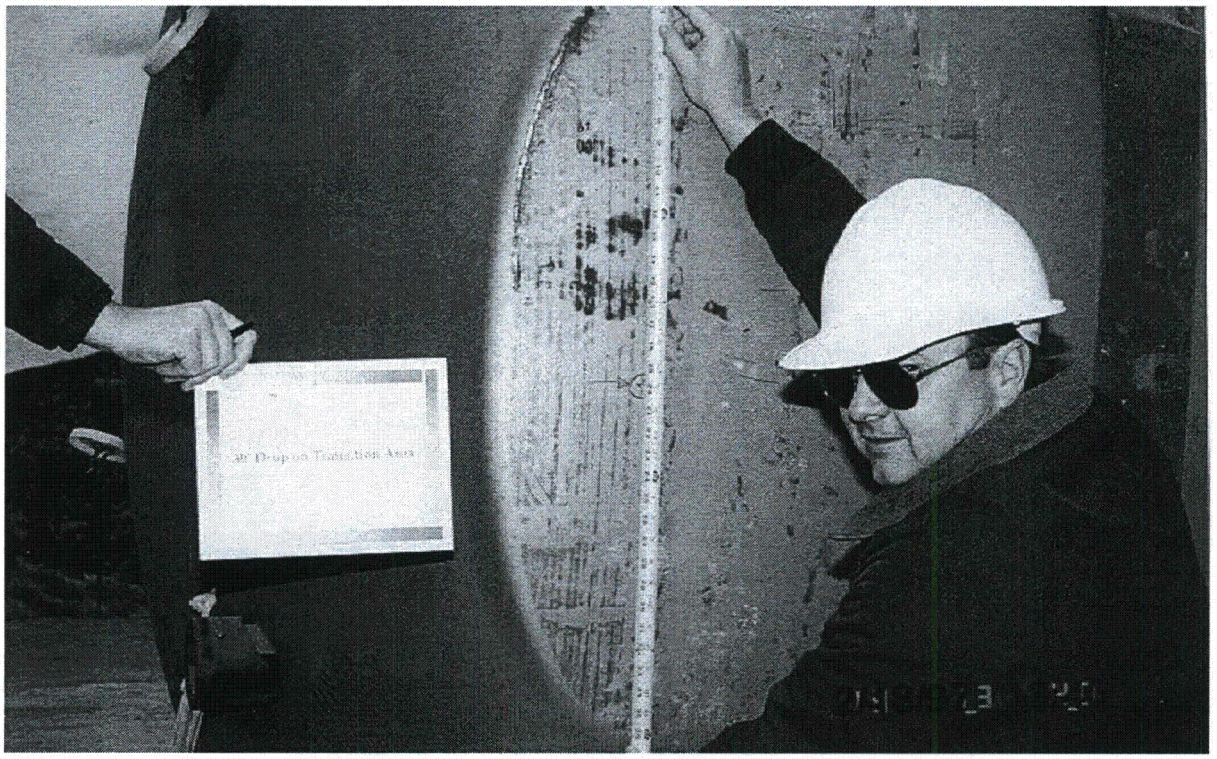

Figure 2.10.3-14 – ETU Free Drop Test 2; Top-End Damage; ~36" Wide Flat

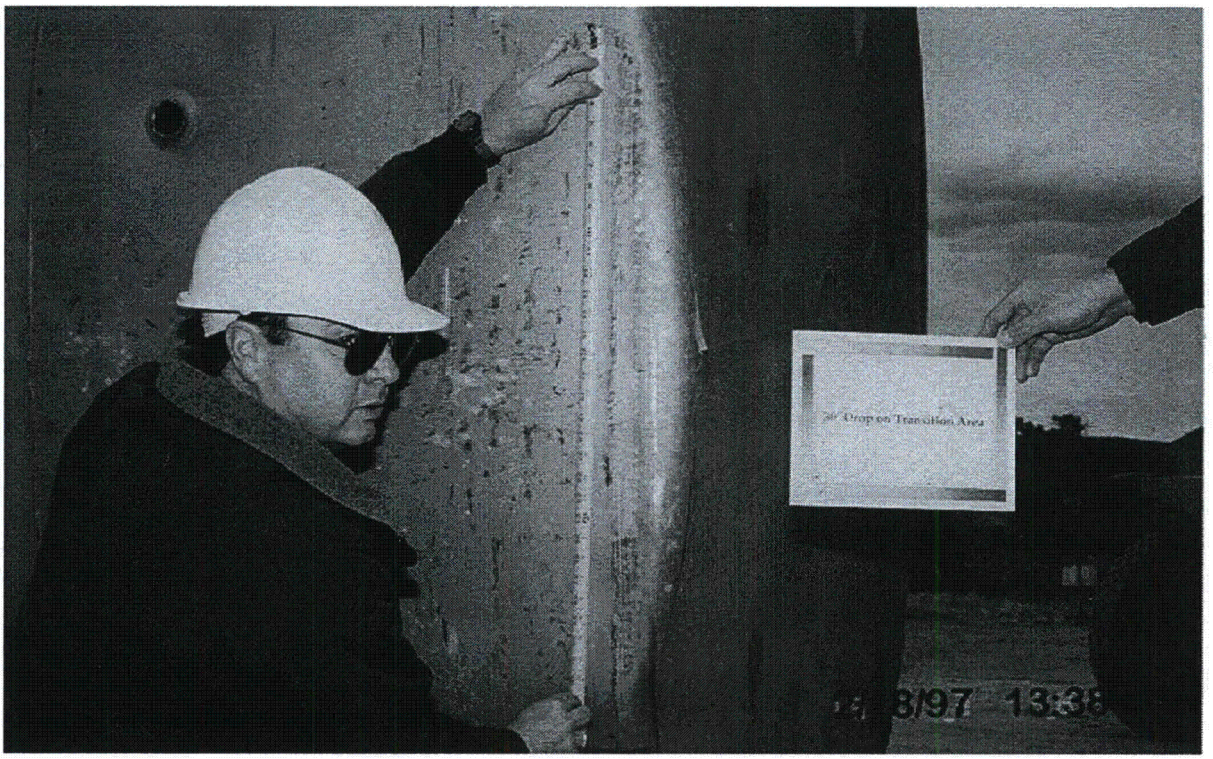

Figure 2.10.3-15 – ETU Free Drop Test 2; Bottom-End Damage; ~33" Wide Flat

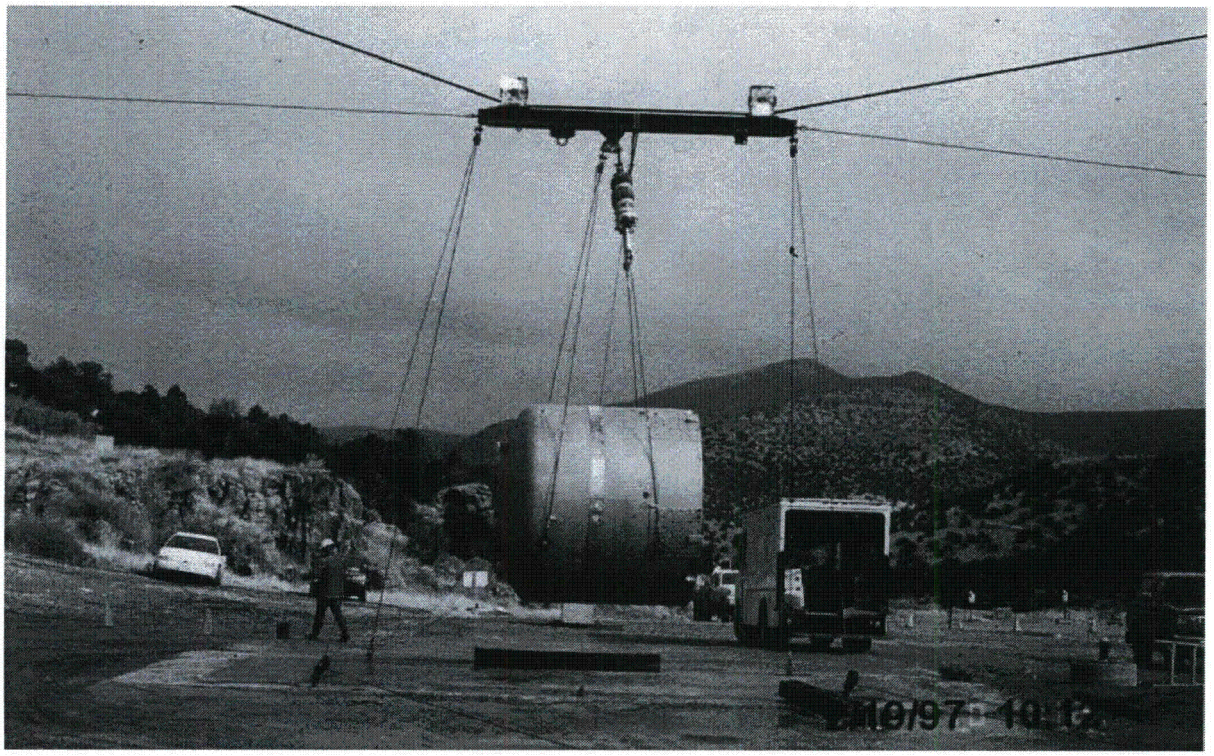

Figure 2.10.3-16 – ETU Free Drop Test 3; View Just Prior to NCT Free Drop Test

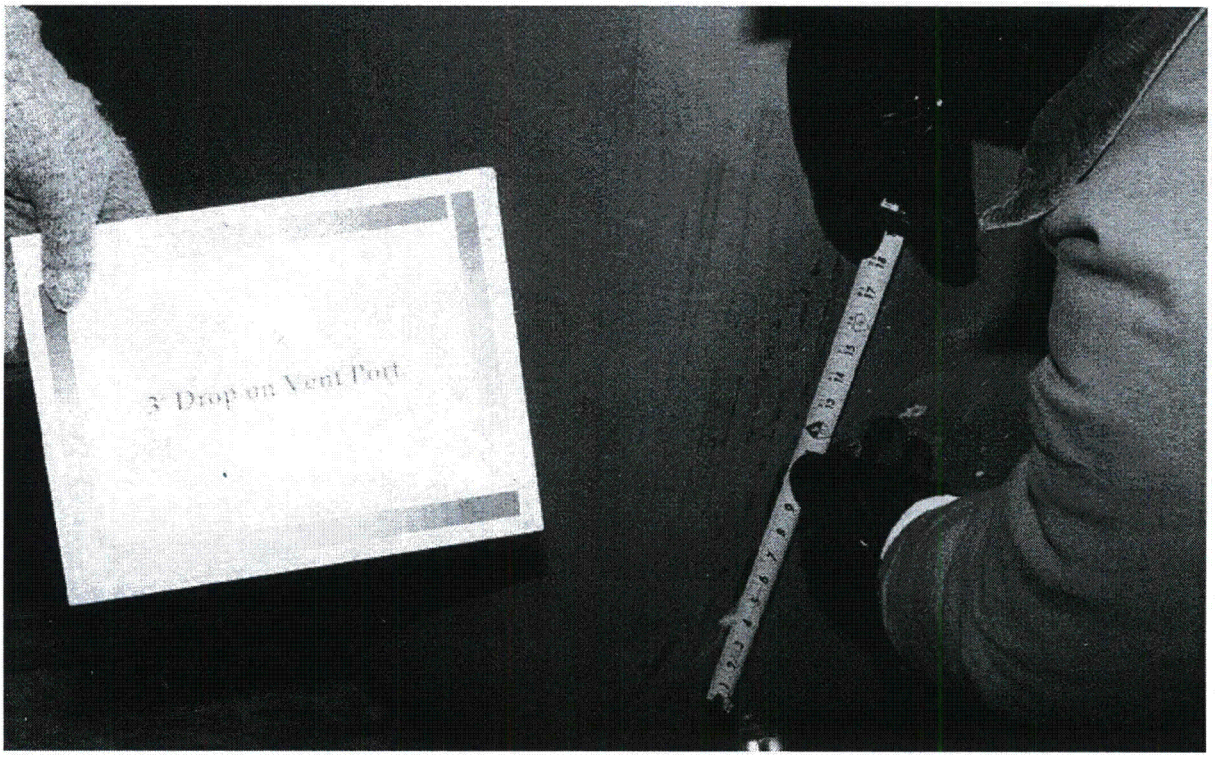

Figure 2.10.3-17 – ETU Free Drop Test 3; Top-End Damage; ~18" Wide Flat

Figure 2.10.3-18 – ETU Free Drop Test 4; Top-End Damage; ~34" Wide Flat

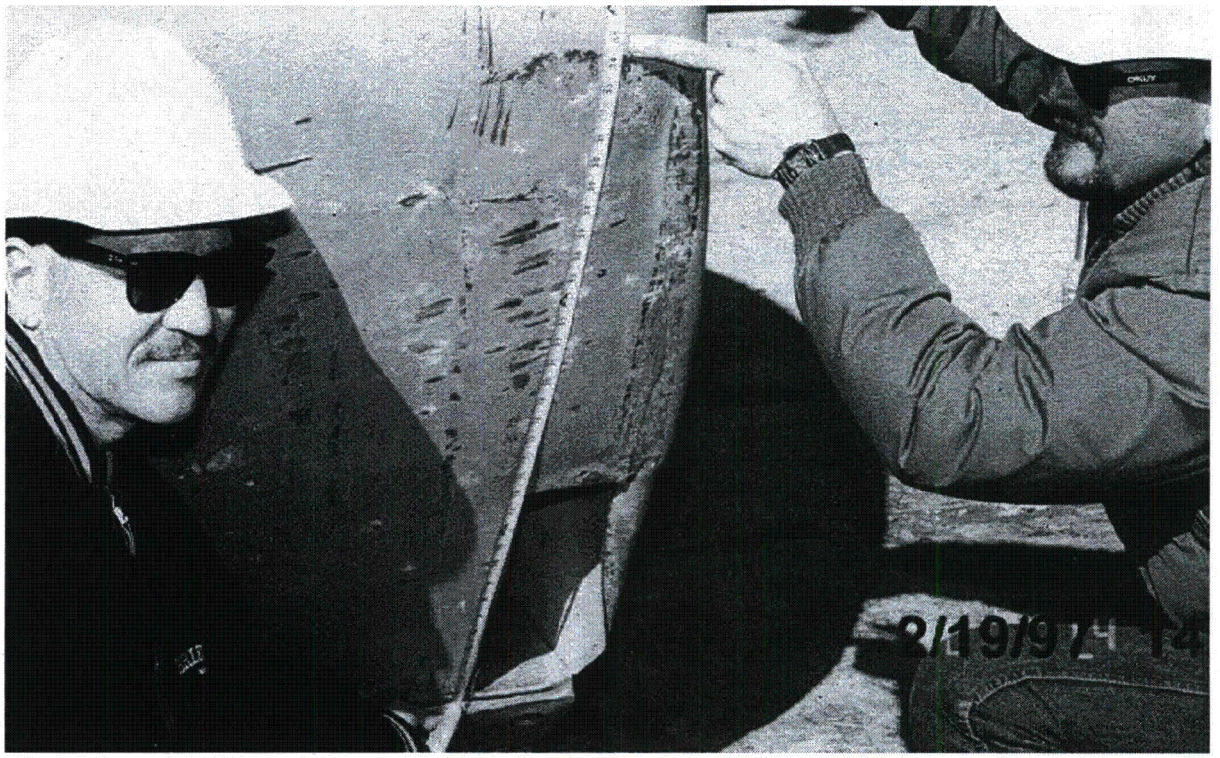

Figure 2.10.3-19 – ETU Free Drop Test 4; Bottom-End Damage; ~34" Wide Flat